Bioengineering Unit, Wolfson Centre

University of Strathclyde, Glasgow, United Kingdom

CARBON DIOXIDE TRANSFER IN MEMBRANE OXYGENATORS AND ASSOCIATED MEMBRANES

by

Peter Wong, B.Sc.,M.Sc.

Thesis submitted for the Degree of

Doctor of Philosophy in Bioengineering

October 1984

To my parents and nanny

ABSTRACT

A recently developed therapy for treatment of acute respiratory failure requires that the patient's metabolic carbon dioxide production be eliminated by a membrane oxygenator operated in an extracorporeal blood circuit. In conjunction with peripheral cannulation, the oxygenator should be optimised for CO_2 removal at low blood flow rates of 1.5 ℓ/min or less for adults. An extensive literature survey revealed that very few publications dealt with oxygenator CO_2 performance at low flow rates.

Two commercial devices, the Terumo CAPIOX II (1.6 m^2 and 3.3 m^2 membrane areas) hollow fibre oxygenator and the Travenol TMO (2.25 m^2 membrane area) parallel-plate oxygenator were evaluated in relation to the new therapy. A theoretical model describing carbon dioxide transfer in membrane oxygenators was used to correlate the experimental data. The Terumo CAPIOX II 3.3 m^2 unit was the only device capable of satisfying the carbon dioxide removal requirements necessary for the new therapy at the low blood flow rates stipulated.

Effects of blood and gas flow maldistribution were also studied in the TMO and CAPIOX II units respectively. Non-uniform blood flow was not a major factor contributing to the decline in CO_2 transfer performance compared with theory. This was confirmed in experiments with a modified TMO unit. Comparison with theory indicated that the membrane resistance was the controlling factor for CO_2 transfer in the CAPIOX II device.

A method was developed to assess the CO_2 transmission rate (G_{CO_2}) through oxygenator membranes under gas-membrane-liquid contact conditions. This forms the basis for the selection of suitable membrane materials for oxygenators. Although the G_{CO_2} values

for homogeneous silicone rubber membranes were consistent with the results of previous workers, significantly higher values were obtained for microporous polypropylene membranes. For microporous membranes under liquid contact conditions a 5-fold reduction in G_{CO_2} is obtained in this study compared to gas-membrane-gas tests, indicating that micropore wetting imposes a significant resistance to CO_2 transfer.

ACKNOWLEDGEMENTS

I wish to take this opportunity to convey my warmest thanks to the staff and members of the Bioengineering Unit who have helped in different ways during the course of this project.

In particular to:

DR. JOHN GAYLOR, my supervisor, for the considerable time and help he has given to me. His continual encouragement and guidance throughout this project is gratefully acknowledged.

MR. DAVID SMITH, for his assistance in the collection of blood required for the experiments.

MRS PAULINE TURNER and MRS GAIL CONNEL for the photographs taken in this study.

MR. GRAHAM PHILLIPS for the linear regression program acquired for the analysis of results contained in Chapter 5.

DR. PETER MAYES, DR. JAMES COURTNEY, MISS ZAHRA KOOCHAKI, MR. GUAN TAT KHOO, ALEXIS ROSS, JOAN WILSON and MONICA McCOLL for their ready help and friendship.

PROFESSOR JOHN P. PAUL for his support and providing the facilities for me to undertake this project.

Further I extend my gratitude and appreciation to:

MR. S. DENTON of Terumo Europe Inc., Belgium, for his generous supply of Terumo CAPIOX II hollow fibre oxygenators.

DR. MILLS of the Glasgow Royal Infirmary for the loan of the Van Slyke equipment.

MR. D. CRINGEAN of the Department of Natural Philosophy, University of Strathclyde for much of the glass repair work.

PROFESSOR CH.R.H. WILDEVUUR and DR. JAKOB ENNEMA of the University Hospital Groningen, The Netherlands, for making my visit to the Department of Experimental Surgery possible.

The Science and Engineering Research Council (SERC) for the two years funding of this project.

I am also extremely grateful to:
DR. LESLIE and MRS ROSE BARNARD for their understanding and kind assistance during the final stages of this project.
my PARENTS and NANNY: their encouragement and financial support given me during my studies away from home.

Finally, my special thanks to MRS LYNNE WESTWOOD for her competent and excellent typing of this thesis.

GLORIA ET HONOR DEO

CONTENTS

NOMENCLATURE

a	half-height of semi-infinite parallel plate channel
A	area of membrane
A'	constant in Arrhenius equation
C	concentration
C^*	concentration at equilibrium
C_{HB}	concentration of haemoglobin
C_T	total CO_2 content in blood
C_{Ti}	C_T at tube or channel inlet
C_{To}	C_T at tube or channel outlet
C_1	concentration of dissolved CO_2 in blood
$C_{1,i}$	C_1 at tube or channel inlet
C_2	concentration of reacted CO_2 in blood
D	diffusion coefficient
D_A	diffusion coefficient of CO_2 in NaOH solution
$D_{O_2,p}$	diffusion coefficient of O_2 in plasma
D_i	diffusion coefficient of specie i
D_m	diffusion coefficient of gas in the membrane
D_1	diffusion coefficient of dissolved CO_2 in blood
D_2	diffusion coefficient of reacted CO_2 in blood
G_{CO_2}	CO_2 transmission rate of membrane
H	haematocrit
J_o	flux of CO_2 out of pore
J_i	flux of specie i (or of CO_2 into pore)

k_1	forward rate constant for the reaction of CO_2 with OH^- ions
K	overall mass transfer coefficient
K_L	liquid phase mass transfer coefficient
K_1	equilibrium constant for the reaction of CO_2 with OH^- ions
K_2	equilibrium constant for the reaction of HCO_3^- with OH^- ions
N	number of tubes or channels
pCO_2	partial pressure of CO_2 in blood or gas phase
pH	$-\log_{10}$ [hydrogen ion concentration]
pk	$-\log_{10}$ [equilibrium constant]
P_{ATM}	barometric pressure
P_g	partial pressure of gas outside tube or channel
Pr	permeability of membrane
q_i	rate of reaction of specie i
Q	volumetric flow rate of blood or gas
r	radial co-ordinate
r*	dimensionless radius ($= r/R_i$)
R	gas constant ($= 8.314\ JK^{-1}\ mol^{-1}$)
R_i	tube inner radius
R_o	tube outer radius
R_O	overall resistance
R_M	membrane resistance
R_B	blood phase resistance
R_G	gas phase resistance
t	membrane thickness
T	temperature
$\vec{v}$	velocity vector
V	volume

V_z velocity in axial direction

$\dot{V}_i$ transfer rate of specie i

W channel width

y transverse co-ordinate (semi-infinite flat channel with two permeable walls)

z axial co-ordinate

z* dimensionless axial length ($= \frac{\pi D_l z}{2Q_B}$ for tube)

($= \frac{4 D_l Wz}{3 Q_B a}$ for parallel-plate)

Greek letters

α gas solubility in liquid

α_m gas solubility in membrane

α_l carbon dioxide solubility in blood

β buffer power

γ dimensionless wall resistance

θ_c fractional carbon dioxide removal, $\theta_c = (C_{Ti} - \bar{C}_{To})/C_{Ti}$

μ dynamic viscosity

μ_m membrane permeability

τ tortuosity factor

ϕ pore volume fraction or membrane porosity

ω empirical constant in equation 3.12

Subscripts

B blood

CO_2 carbon dioxide

g gas

Hb haemoglobin

k phase k

m	membrane
p	plasma
O_2	oxygen
w	at the wall
i	specie i or inlet
o	initial condition or outlet

1

INTRODUCTION

The first attempt to provide life support by oxygenating the lungs was described in a paper by Robert Hooke (1667) in which he wrote:

> "I propose to expose the blood of the animal to fresh air in a vessel and return the blood, to see if this will suffice for the life of the animal... and determine what benefit this may be to mankind."

This description was the forerunner to the concept of an artificial lung (or blood oxygenator), where the idea of a device used for blood-gas exchange outside the body was first suggested. Efforts to construct such a machine date back to 1885 when Von Frey and Grüber designed a device capable of supplying oxygenated blood to an isolated organ preparation. A successful heart-lung bypass on a dog was reported by Gibbon in 1937, and by the 1950's the use of lung devices for total support of adults during open-heart surgery was possible (Dennis et al. 1951; Gibbon et al. 1954).

Since that time numerous lung devices have been developed and can be classified into two main types: the bubble oxygenator with direct blood-gas contact, and the membrane oxygenator with separation of the blood from the gas by a membrane. Although the term "oxygenator" does not describe the CO_2 function of the artificial lung it will be used as a synonym in this thesis.

Essentially, oxygenators are blood-gas exchangers which temporarily replace or supplement the respiratory function of the natural lungs. Application of cardiopulmonary bypass (CPB)

procedures are required in two main areas of clinical medicine: firstly, they are used for open-heart surgery e.g. hole-in-the-heart congenital defects in the newborn, valve replacements and total heart-lung transplantation of the adult (Ionescu, 1981; Jamieson et al. 1983). The duration of CPB may range from 1 to 4 hours depending on the type and extent of the operation. The second area is for partial lung support e.g. acute respiratory failure. In this application the duration of partial bypass using an artificial lung may be from 8 hours to several days. Most of the short-term (1-4 hours) CPB's are conducted with bubble oxygenators because of their ease of operation. Although adequate for the short-term, progressive damage to blood is a limiting factor in long-term (8 hours or more) applications. Therefore, for long-term support membrane oxygenators are used exclusively.

In a typical CPB circuit for open-heartsurgery (Figure 1.1) blood is removed from the venae cavae of the patient and by cardiotomy suction from the heart chambers into a reservoir. As blood passes through the artificial lung, O_2 is added to and CO_2 is removed from the blood. A heat exchanger in the circuit enables normothermia ($37^{o}C$) or hypothermia ($20-30^{o}C$) to be employed during CPB. Online filters remove emboli in the circuit and circulation of the blood in the extracorporeal system is maintained by a roller pump. The main function of each bypass component is shown in Table 1.1. It should be noted that hypothermia lowers the patient's O_2 metabolism and hence the gas requirement of the artificial lung. This is a useful technique if haemodilution occurs due to priming of the CPB circuit with aqueous physiological solutions. Each year at least 100,000

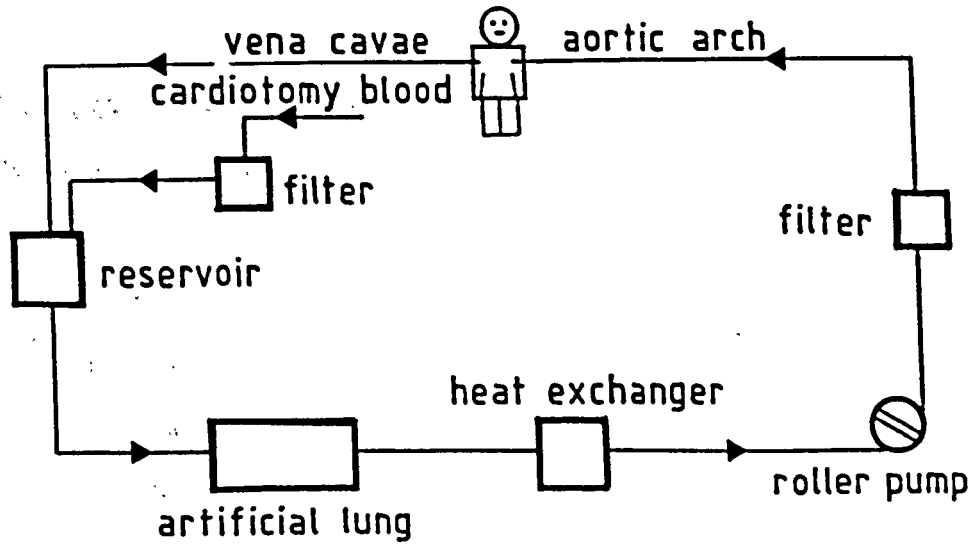

Figure 1.1 Total heart-lung bypass in open heart surgery.

Table 1.1 Main components and functions of the bypass circuit.

BYPASS COMPONENT	FUNCTION
Artificial lung	Oxygen uptake Carbon dioxide removal
Roller pump	Circulate blood
Heat exchanger	Control body temperature (hypothermia or normothermia)
Filters	Remove foreign particles

CPB operations are carried out in the USA, and between 200,000 and 250,000 worldwide (Galletti, 1980).

In the past ten years, application of long-term membrane oxygenator support for the treatment of acute respiratory failure (ARF) has been investigated (Zapol and Qvist, 1976; NIH Report, 1979). ARF is widespread and affects about 150,000 adults each year in the USA with an average mortality of 40%.

The aetiology of adult ARF is virtually unknown. However, the prominent feature of ARF is an increasingly inadequate oxygenation of the blood, often combined with a gradual accumulation of carbon dioxide. Therefore, a functional guideline based on blood gas levels has been adopted to define ARF, viz. when arterial pCO_2 is greater than 49 mmHg and/or when pO_2 is less than 60 mmHg and with the subject breathing air (Saunders, 1977).

Conventional mechanical ventilation therapy is the most common approach for ARF. However, in certain cases where all conservative methods of treatment have failed, membrane lung support may be warranted. Earlier therapies concentrated on supplying the body's oxygen needs and hence required relatively high blood flows (2.5 to 4.0 l/min for adults) through the membrane lung (Bartlett and Gazzaniga, 1978). These therapies were known collectively as extracorporeal membrane oxygenation (ECMO).

Multi-centre clinical trials were set up in the USA between the period 1973 to 1979 to assess ECMO support for the treatment of ARF. The trials aimed to compare patients treated by conventional therapy with the patients treated with a combination of conventional therapy and ECMO. The conventional therapy consisted of mechanical

ventilation with positive end-expiratory pressure (PEEP) and high inspired oxygen concentrations (FiO_2). The two patient groups were referred to as the "control treatment patients" and the "ECMO treatment patients" respectively. Of the 90 patients treated 42 were randomly allocated to the control group and the remainder to the ECMO group. The results of the trial were inconclusive with only 4 patients in each group surviving (NIH Report, 1979). In a review, Hill et al. (1978) stated that ECMO was highly effective in providing temporary long-term life support, and that ECMO patients lived an average of two days longer. However the value of ECMO therapy was not properly assessed since the ARF patients were in their terminal stage of the disease with an associated mortality of about 90%. Further work remains to define those groups of ARF patients who might benefit from ECMO therapy, particularly if applied at an earlier stage.

As an alternative to ECMO a new approach has been proposed by Kolobow (1977a). It is based on the hypothesis that the most conducive environment for recovery can be obtained by immobilising the natural lungs and improving the ventilation-perfusion mismatching using low ventilation rates. These conditions may be obtained by reducing the rate of spontaneous breathing through the extracorporeal removal of metabolic CO_2 with a membrane oxygenator together with low frequency positive pressure ventilation ($ECCO_2R$-LFPPV). Since CO_2 is present in high concentrations in blood its removal may be achieved with efficient membrane lungs operating at low bypass flow rates (0.5 to 1.5 l/min). The attendant advantage is a simplified cannulation technique compared

to that used for ECMO. To satisfy the patient's oxygen needs the natural lungs are supplied with 100% oxygen initially and the FiO_2 is progressively reduced with clinical improvement. As oxygen is absorbed by the natural lungs, the gas is replenished via a small catheter placed near the tracheal birfurcation (carina). The natural lungs are ventilated once or twice a minute, while at the same time kept almost immobilized in a neutral inflated state (Gattinoni et al. 1980). The advantages of $ECCO_2R$-LFPPV include a reduction in barotrauma and in haemodynamic disturbances compared with ECMO and conventional ventilation management.

The requirements of the new technique have initiated the optimisation of membrane lungs for carbon dioxide removal. In vitro evaluations are necessary together with theoretical models of the mass transfer process. Both are useful for design purposes. Oxygen transfer has been studied extensively in two of the most common membrane lung geometries; the parallel-plate and tubular configurations. The various models have been reviewed by Spaeth (1970), Colton (1976) and Eberhart et al. (1978). Relatively fewer studies have been reported in the literature on carbon dioxide transfer in membrane lungs. The carbon dioxide transfer models by Benn (1974) and Voorhees (1976) are the most comprehensive available and are reviewed in greater detail in Chapter 3.

This thesis is concerned with the CO_2 transfer evaluation of membrane oxygenators in relation to the new therapy. The experimental results will be compared with theoretical predictions obtained from Voorhees' model. As the CO_2 efficiency of these devices is partly dependent on the membrane CO_2 resistance, the thesis is also concerned with the evaluation of membrane transmission

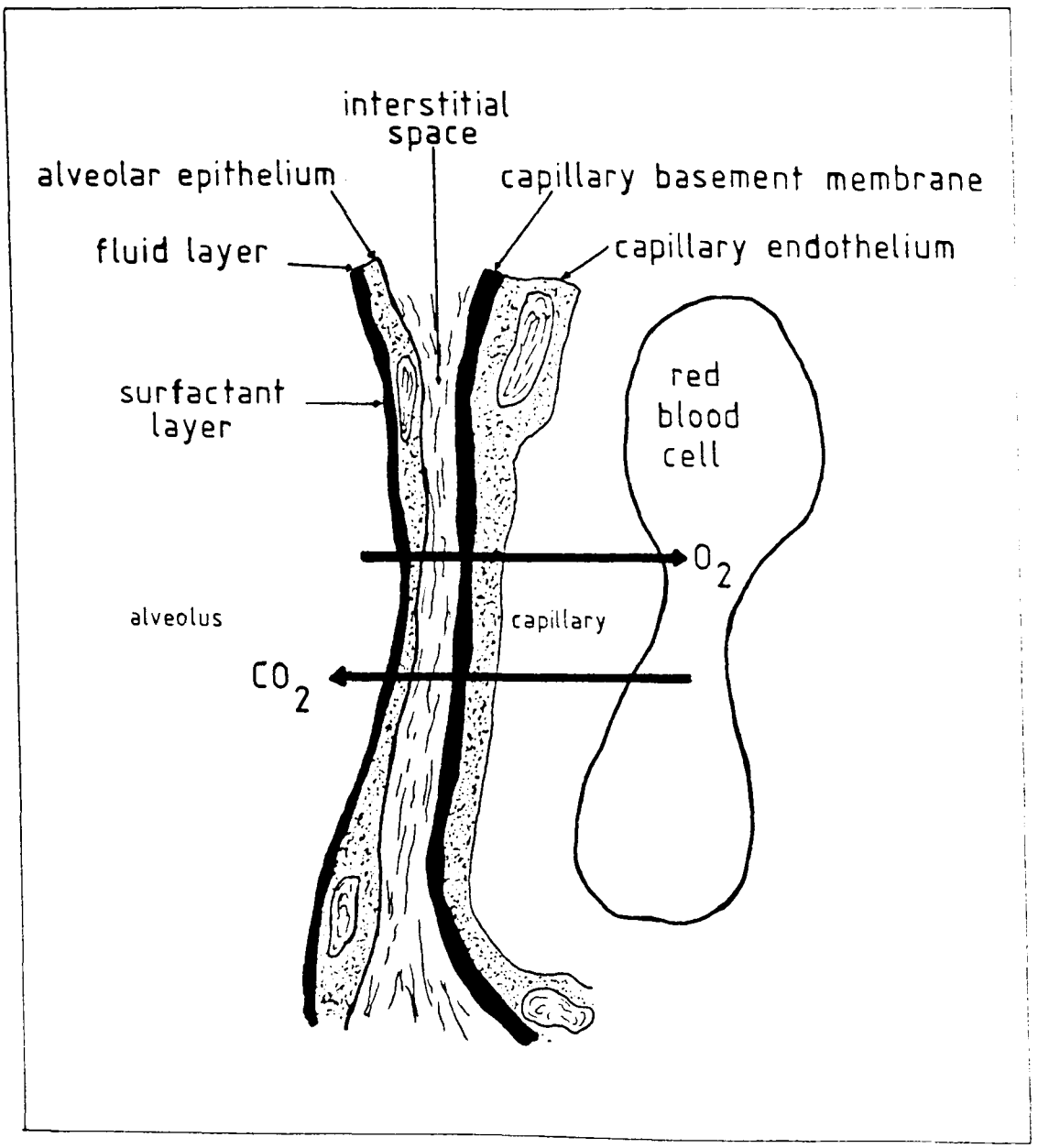

Figure 1.2 Ultrastructure of the respiratory membrane.

rates under liquid contact conditions.

To establish the basis for the analysis of membrane oxygenators for carbon dioxide transfer, descriptions of human lung function and gas transport in blood are given in sections 1.1 and 1.2 respectively. An overview of developments in extracorporeal carbon dioxide removal are presented in section 1.3. This chapter concludes with the objectives and layout of the thesis.

1.1 Human Lung Function

Detailed anatomy and physiology of the human lungs are described in many standard medical texts such as Bell et al. (1976) and Passmore and Robson (1968). Therefore, no attempt will be made to reproduce such detailed reviews in this thesis. Only the salient points, relevant to the development of artificial lungs will be mentioned. The human lungs contain about 700 million tiny sacs called alveoli. These are surrounded by a vast network of capillaries. Blood and air are separated by the endothelium of the capillaries and the very thin epithelium of the alveolar walls which comprise the respiratory membrane (Figure 1.2). The short diffusion distances (0.3 to 0.7 μm) and the large surface area (about 70 m^2) make the lungs highly effective gas exchangers. The narrow capillaries with an average diameter of 3 μm force the larger red blood cells to pass through in single file, creating good blood side mixing (Cooney, 1976; Folkow and Neil, 1971). This effect further assists gas exchange in the lungs.

The transfer of oxygen and carbon dioxide into and out of the blood is governed by the physical law of diffusion. One of the main factors that determines the rate at which the gas will diffuse through the respiratory membrane is the difference between the partial

pressure of the gas on the two sides of the membrane.

Carbon dioxide is about 20 times more soluble than oxygen in blood plasma and the flux is 20 times more rapid since the diffusion coefficients are similar. This advantage is partly offset by a smaller partial pressure difference from mixed venous blood to the alveolar air. As blood passes through the lungs, the partial pressure difference of carbon dioxide between venous blood and alveolar air is about 6 mmHg, while for oxygen the difference is 55 mmHg. In artificial lungs the partial pressure differences are considerably greater since pure oxygen may be used in the gas phase. For accurate representation of the exchange processes in membrane oxygenators it is important to take into account the various transport mechanisms of the respiratory gases in blood.

1.2 Blood Composition and Gas Transport

1.2.1 Physical properties

Blood is usually described as being a suspension of cellular elements in a faintly yellowish, transparent fluid known as the plasma. The plasma constitute about 55 per cent of the total blood volume. The cellular components of the blood are of three types:

Cell Type	Number (per mm^3)	Specific Function
Red blood cell	5,000,000	Gas transport
White blood cell	8,000	Anti-infection
Blood Platelets	300,000	Anti-bleeding

By far the most abundant are the red blood cells; often described as biconcave (doughnut-like) in shape and enclosed by a thin flexible membrane. Their diameter varies between 7 to 8 μm

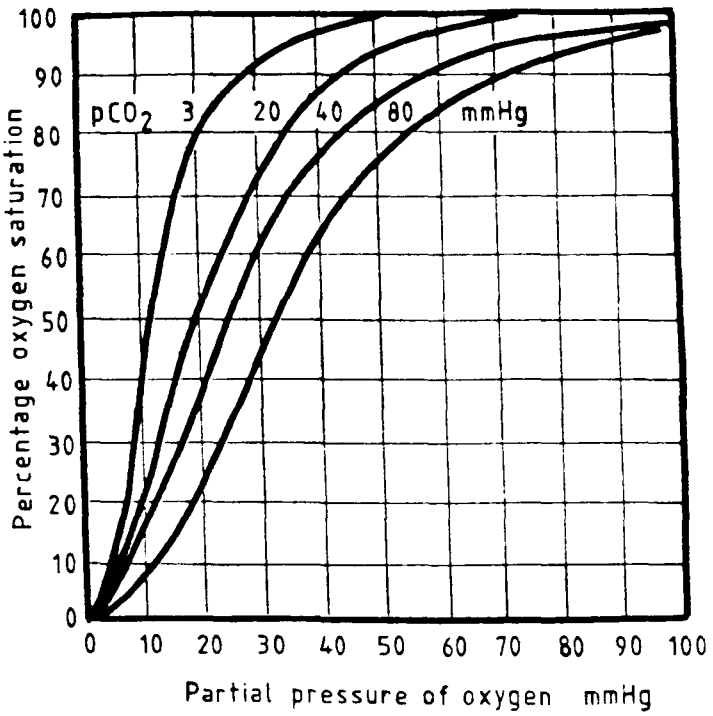

Figure 1.3 Oxygen dissociation curves of human blood at different partial pressures of carbon dioxide and 37 °C. (After Bock et al. 1924)

and are approximately 2 μm thick. Red blood cells contain a concentrated solution of an iron-containing protein, haemoglobin which is a major carrier for oxygen. The volume percentage of red blood cells in the blood is known as the haematocrit. This is approximately 40 to 45% in healthy adults.

The plasma is composed mainly of water (90 to 92 per cent) with various proteins such as serum albumin, serum globulin, fibrinogen, prothrombin and heparin. Mineral salts, nutrient materials, organic waste products, hormones, enzymes, antibodies and antitoxins, in addition to dissolved respiratory gases make up the remainder.

1.2.2 Oxygen transport

Oxygen is carried in blood mainly in the combined form as haemoglobin (Hb) to give a loose compound known as oxyhaemoglobin (HbO_2). This reaction in the blood can be represented simply as:

$$Hb + O_2 \rightleftharpoons HbO_2$$

The forward and reversible reactions are equally rapid, taking less than 0.01 seconds to complete, as compared to 0.3 to 0.75 seconds for the blood to traverse the lung capillaries (Yang, 1979).

The characteristics of the oxygen-haemoglobin combination vary with physiological conditions. Figure 1.3 show the non-linear equilibrium relationship between the bound and dissolved oxygen in blood which is called the oxygen dissociation curve. The curve shows the percentage saturation of haemoglobin at each oxygen pressure level in the physiological range, at different pCO_2 levels and at a temperature of $37^{\circ}C$. Oxygen combines with haemoglobin in the ratio of 1.34 ml O_2 (STPD) per gram of haemoglobin, while other

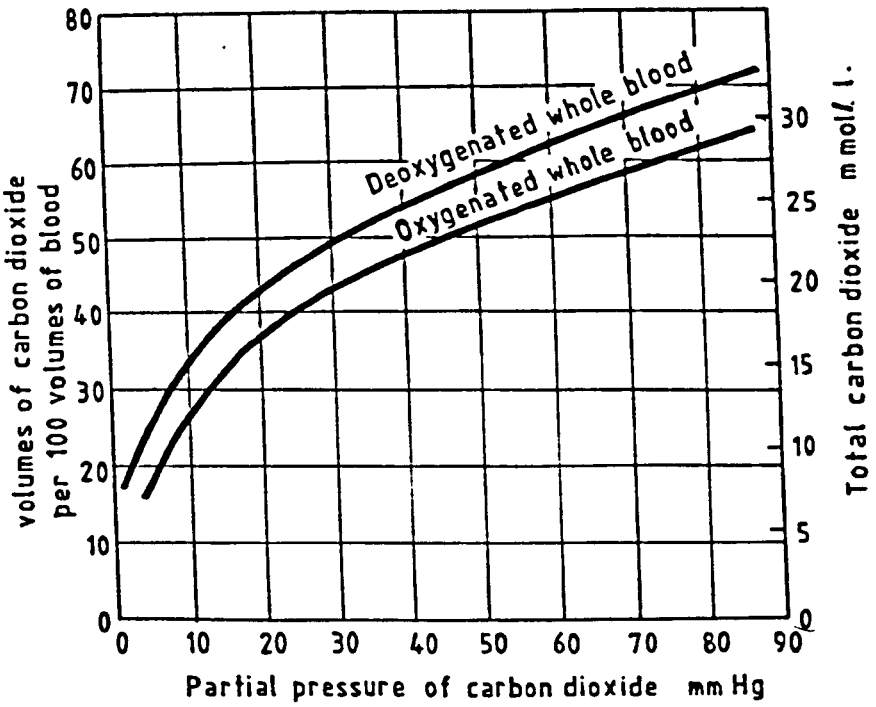

Figure 1.4 Carbon dioxide dissociation curves for deoxygenated and oxygenated blood. (after Bock et al. 1924).

investigators use 1.39 for the oxygen combining factor. The difference is due to the value taken for the molecular weight of haemoglobin (Kelman and Nunn, 1968).

Oxygen dissociation curves are affected by changes in temperature, pressure, pH, inorganic phosphates and pCO_2.

1.2.3 Carbon dioxide transport

Most of the carbon dioxide in blood is carried in the combined form as bicarbonate ions (HCO_3^-) and carbamino compounds (resulting from reactions with plasma proteins and haemoglobin). The remainder is in the form of dissolved CO_2. Table 1.2 shows the relative proportions of these forms in the plasma and in the red cells.

The equilibrium relationship between the dissolved and the total CO_2 is given by the carbon dioxide dissociation curve. These are shown for oxygenated and deoxygenated blood in Figure 1.4.

The plasma contains about 65 per cent and the red cells about 35 per cent of the total CO_2 content, in contrast to oxygen which is carried mainly as oxyhaemoglobin (typically 98 per cent).

The transport and elimination of carbon dioxide in membrane lungs are similar to the process that occurs in the natural lungs and follow the following sequence of events:

(a) Blood enters the membrane lung at the venous conditions such as those given in Table 1.2. As it passes through the membrane lung, carbon dioxide diffuses from the plasma, through the gas-permeable membrane and into the surrounding gas atmosphere. The carbon dioxide is continually released by the reversible reactions occuring in both the plasma [reaction (3)] and the red blood cell shown in Figure 1.5.

Table 1.2 Carbon dioxide carriage in blood (modified from Nunn, 1971).

Whole blood	Venous	Arterial
pH	7.367	7.40
pCO_2 mmHg	46.0	40.0
O_2 saturation %	70	95
Red cell concentration express as % of total blood content		
Bicarbonate ion	25.5	2.1
Carbamino-CO_2	7.3	27.3
Dissolved CO_2	2.2	5.1
Plasma		
Bicarbonate ion	61.8	62.4
Dissolved CO_2	3.2	3.1
Total CO_2 (all forms)		
Red cell	35	34.5
Plasma	65	65.5

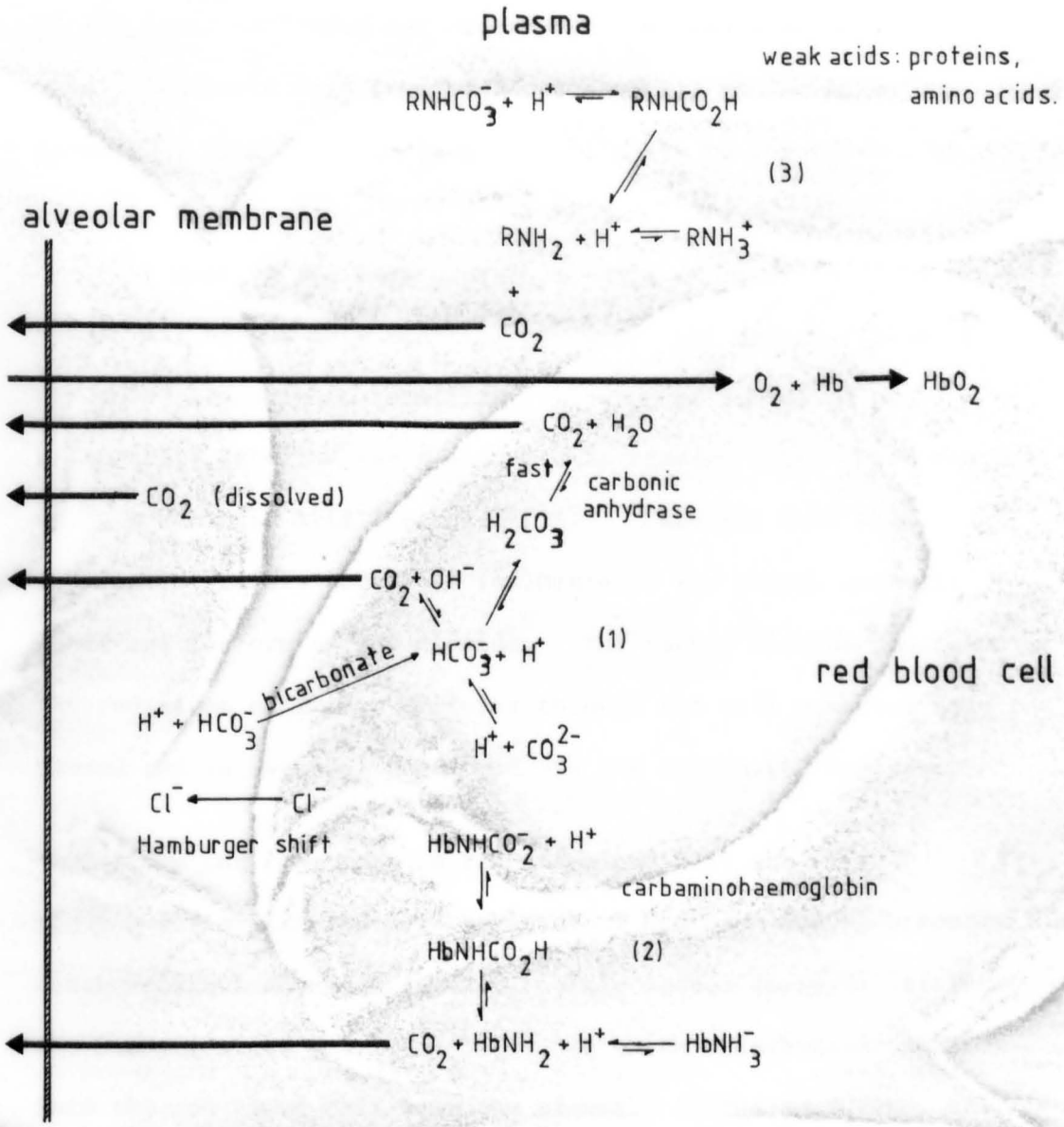

Figure 1.5 The major reactions which take place when gas exchange occurs between blood and alveolar gas.

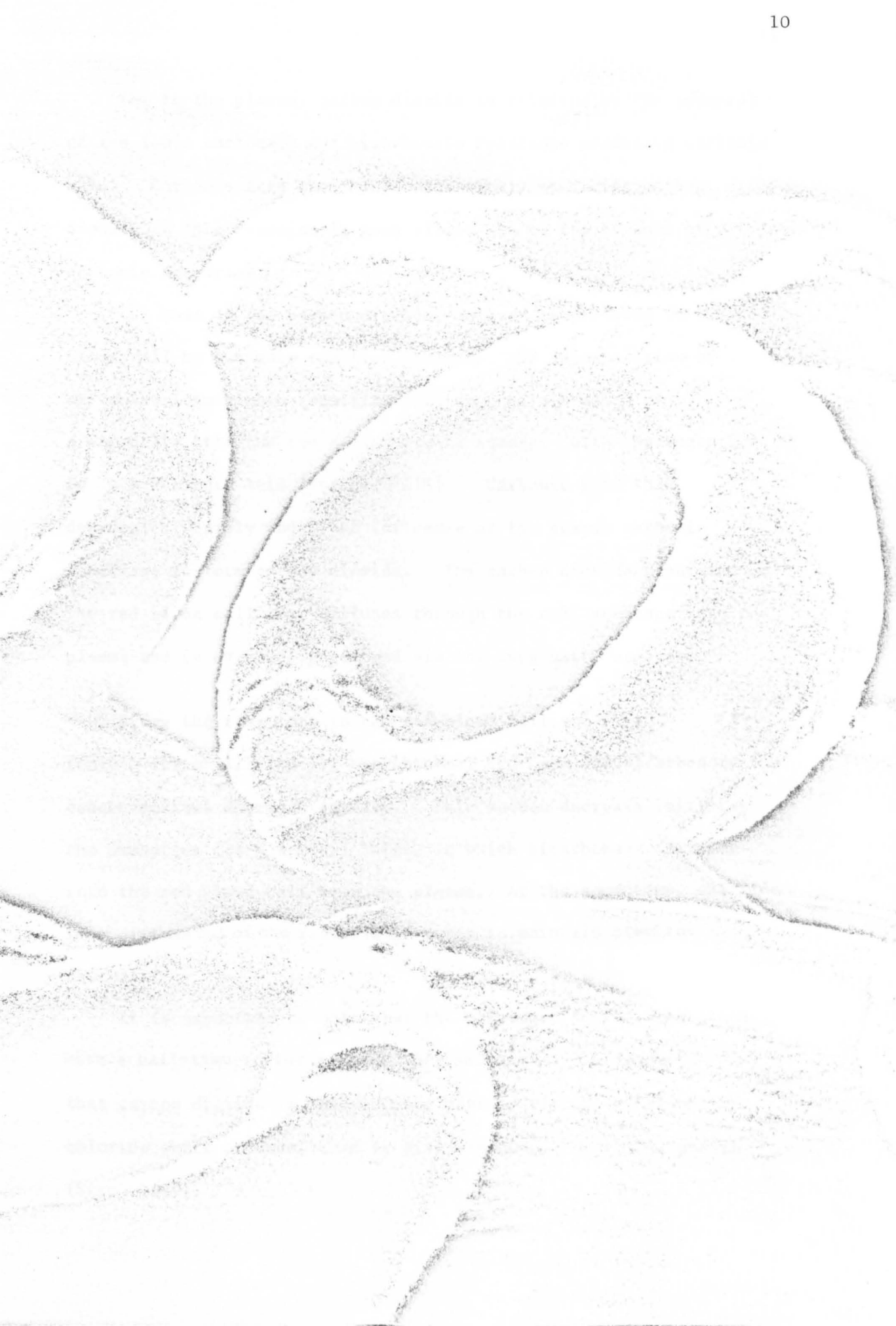

(b) In the plasma, carbon dioxide is released by the reversal of the ionic carbonate and bicarbonate reactions producing carbonic acid. Carbonic acid then dehydrates slowly producing carbon dioxide. This reaction is much slower due to the absence of carbonic anhydrase.

(c) Most of the carbon dioxide, however is produced in the red blood cell by two main reaction schemes: the decomposition of carbamino haemoglobin [reaction (2)] and the diffusion of bicarbonate into the red cell where it reacts with hydrogen ion to form carbonic acid [reaction (1)]. Carbonic acid then dehydrates rapidly under the influence of the enzyme carbonic anhydrase to form carbon dioxide. The carbon dioxide generated in the red blood cell then diffuses through the cell membrane into the plasma and is eventually removed via the oxygenator membrane.

Since the reactions in the red blood cell are fast (only a few milliseconds), the internal hydrogen and bicarbonate ion concentrations decrease rapidly. This sudden decrease initiates the Hamburger (or Chloride) Shift, in which bicarbonate diffuses into the red blood cell from the plasma. At the same time, chloride ions diffuse out of the red cell in order to maintain electro-neutrality.

It is important to note that the Hamburger Shift takes place with a half-time in the order of 0.1 seconds. This means that carbon dioxide is removed more rapidly via the bicarbonate-chloride shift process, than by direct dehydration in the plasma (Sirs, 1970).

As a result of carbon dioxide and oxygen exchange, two phenomena occur which lead to effects of carbon dioxide on oxygen transport and vice-versa. When carbon dioxide is removed, thus lowering the pCO_2, the haemoglobin has a greater affinity for oxygen uptake. This effect is known as the Bohr Shift. The decrease in pCO_2 causes a shift to the left of the dissociation curve (Figure 1.3). A more important phenomenon which promotes carbon dioxide release from the carbaminohaemoglobin is the Haldane Effect. This is the decreased affinity of haemoglobin for carbon dioxide due to oxygen uptake. Oxyhaemoglobin is a stronger acid than Hb. The increased acidity favours the conversion of more bicarbonate into carbonic acid, which then dissociates, releasing CO_2. The combined Bohr and Haldane Effects enhance transport rates of oxygen and carbon dioxide in the blood (Colton, 1976).

It is important also to identify the rate-limiting steps to carbon dioxide removal from blood. The chemical kinetics of the various CO_2 reactions and the rate of bicarbonate-chloride exchange have been studied (Calkins, 1971; Forster et al., 1980). Complete equilibrium of blood with CO_2 does not occur during the short residence time (0.1 to 1 s) in the natural lungs. On this premise, Calkins (1971) developed a non-equilibrium model for carbon dioxide transfer.

A review paper by Forster et al. (1980) on Cl^- and HCO_3^- movements across the red blood cell membrane indicates the half-times of the Hamburger Shift to be between 0.16 to 0.3 s. If the resistance offered by the red blood cell membrane to HCO_3^- ion and H^+ ion diffusion was substantial, a local equilibrium assumption

may be invalid for the analysis of CO_2 exchange in membrane oxygenators (Voorhees, 1976). However, the local equilibrium model may be used if the oxygenator membrane possesses a significant resistance to CO_2 transport, the changes in CO_2 content are small, and the residence times with oxygenators are large compared to the reaction times in blood.

It is important to note that carbon dioxide is not only removed via the lungs but also by the kidneys. The lungs being responsible for the volatile part (the CO_2 of carbonic acid) and the kidneys for the involatile part (the bicarbonate ions). Both the lungs and the kidneys work to maintain the blood gas and acid-base levels in man.

Comroe (1965) stated that the lungs are the most important organ in the body for acid excretion. In man at rest, the kidneys remove between 40 to 80 mEq per day and the lungs excrete about 13,000 mEq per day of CO_2. The equation which relates the blood acid-base levels in man is given by the Henderson-Hasselbalch relationship which is written as follows:

$$pH = pK + \log \frac{[base]}{[acid]} \qquad (1.1)$$

where pH is the negative logarithm of the hydrogen ion concentration.

pK is the negative logarithm of the dissociation constant of the acid.

In the case of the carbonic acid-bicarbonate system, equation 1.1 becomes:

$$pH = pK + \log \frac{[HCO_3^-]}{[H_2CO_3]} \qquad (1.2)$$

The case when $[HCO_3^-]$ equals $[H_2CO_3]$ is of interest because then the log term is zero. Since the pH of such a solution is 6.1 we have pH = pK = 6.1 for carbonic acid. In an actual sample of plasma, the pH is normally about 7.4, and hence pH - pK = 1.3. Therefore, the ratio of $[HCO_3^-]$ to $[H_2CO_3]$ is about 20 to 1 for plasma.

The fact that bicarbonate ions are by far the most abundant CO_2 species in blood has prompted some investigators to remove CO_2 by artificial kidneys as an alternative technique. This is discussed in section 1.3.2.

1.3 Overview of Extracorporeal CO_2 Removal

1.3.1 Membrane oxygenator technique

The early studies of using an extracorporeal membrane lung for carbon dioxide removal in order to control respiration have been developed to the stage of successful clinical application. The landmarks are highlighted below:

1977 - Kolobow et al. (1977a) proposed the concept of extracorporeal CO_2 removal with either an artificial kidney or membrane lung. Kolobow et al. (1977b) described a spiral coil membrane lung designed for efficient CO_2 removal. Two main areas investigated were (1) membrane envelope geometry to increase the CO_2 transfer and (2) selection of membranes with high CO_2 transfer properties.

1978 - Gattinoni et al.(1978) showed in animal studies that breathing could be arrested in the natural lung by removing all metabolic CO_2. The duration of bypass was about 24 hours during which good respiratory support was maintained.

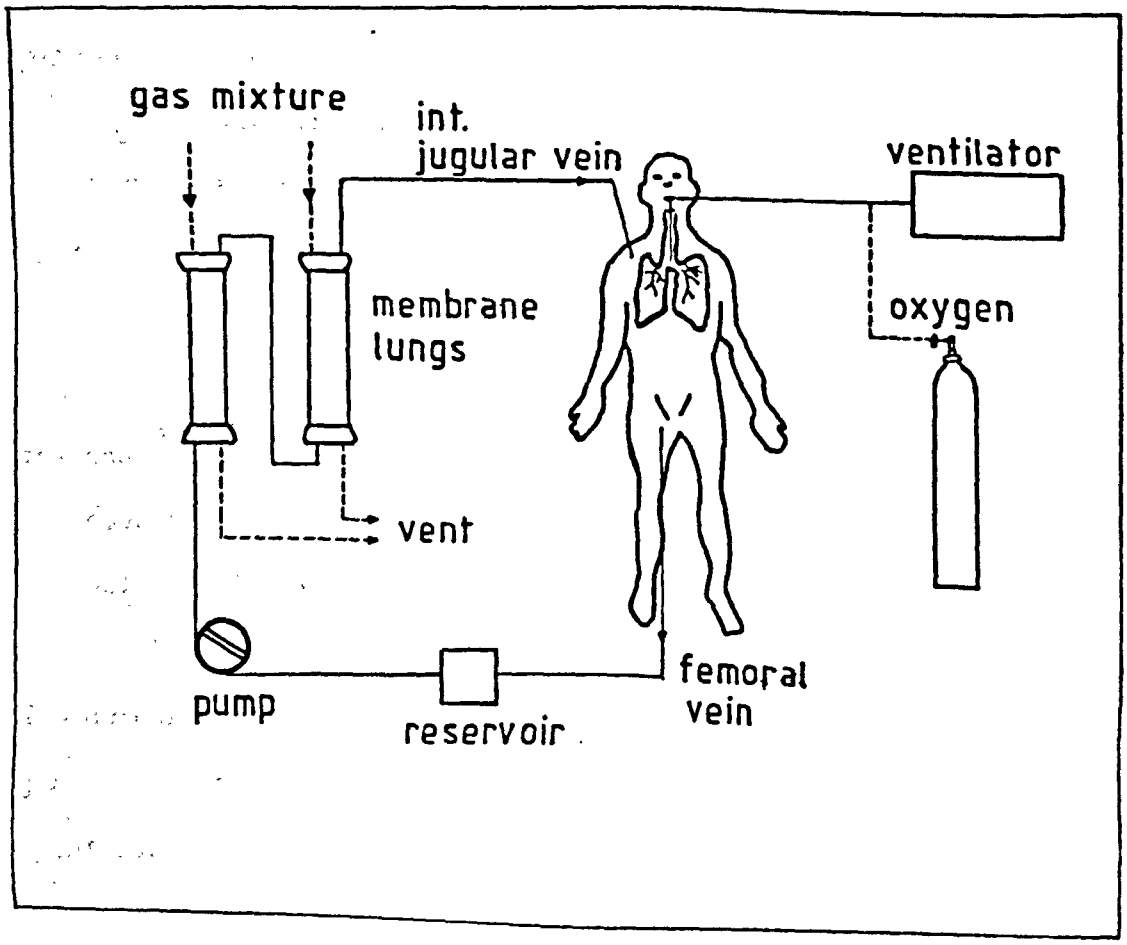

Figure 1.6 Extracorporeal carbon dioxide removal with low-frequency positive pressure ventilation [$ECCO_2R$-LFPPV].

1979 - Clinical trials were undertaken by Gattinoni et al. (1979) at the University of Milano, Italy.

It should be noted that two SCI-MED Kolobow membrane lungs (total membrane area of 7 m^2) were linked in series to provide adequate CO_2 removal at the low blood flows (1.0 to 1.4 l/min) obtained by veno-venous cannulation (Figure 1.6). The carbon dioxide removal by the membrane lungs ranged between 190 and 210 ml/min. About 20 per cent of the oxygen needs of the patient were supplied by the membrane lung and the rest was provided by LFPPV via the natural lungs at a ventilation rate of about 3 breaths/min.

1980 - Gattinoni et al. (1980) reported clinical results on three patients with terminal ARF. Two of these patients were successfully treated.

1981 - Further clinical trials were carried out by Gattinoni et al. (1981). In eleven patients with ARF, seven were treated successfully with $ECCO_2R$-LFPPV.

1982 - Presenti et al. (1982) reported the development of a double-lumen catheter to allow simpler blood access. The catheter was connected in veno-venous mode via the femoral vein. Blood flows of about 1.85 l/min were obtained which gave complete metabolic CO_2 removal while maintaining pCO_2 in the normal range of 35-45 mmHg.

- Barthelemy et al. (1982) reported CO_2 removal in a pumpless artery-to-vein perfusion circuit. A 2 m^2 HOSPAL M32 membrane oxygenator was used in the study.
- Peacock et al. (1982) evaluated CO_2 removal in a paediatric vortex-mixing membrane lung. The membrane surface area of

0.39 m^2 gave a CO_2 removal of 120 ml/min at a blood flow rate of 1.5 l/min. The CO_2 removal rate was reported to be sufficient for the treatment of ARF in children up to the age of 4 years.

1983 - Mook et al. (1983) reported CO_2 transfer characteristics of microporous polypropylene membrane lungs. The in vitro and in vivo studies were correlated with an existing CO_2 transfer theory in order to make performance predictions.

Schulte et al. (1983) applied $ECCO_2R$-LFPPV technique in two patients with ARF. Pulmonary support for ten days or more was demonstrated with one patient surviving.

1.3.2 Alternative techniques

The human lungs and kidneys are the two main organs which work together to maintain the blood gas and acid-base status of the body. The kidneys will maintain plasma bicarbonate concentration in the range of 25 to 28 mEq/ℓ. If plasma pCO_2 is altered as a result of impaired respiratory function, plasma bicarbonate concentration will be compensated by the kidneys to maintain the blood pH within normal range (about pH 7.4).

Therefore, artificial kidney devices operating on the haemodialysis principle have been investigated for extracorporeal CO_2 removal. It is well known that patients undergoing haemodialysis for renal failure experience a transient, mild hypoxemia. It has been suggested that the hypoxemia is the result of carbon dioxide removal during haemodialysis producing hypoventilation.

Kolobow et al. (1977a) have reported that artificial kidneys may be used to remove carbon dioxide, as bicarbonate ions (HCO_3^-).

However, in order to control breathing in man, the artificial kidney devices would have to be scaled up considerably.

Nevertheless, the application of haemodialysers for carbon dioxide removal has been pursued extensively. The well established haemodialysis technique and easy blood access with low blood flow (about 250 ml/min) makes the artificial kidney an attractive method for CO_2 removal. It is important to note that the bicarbonate-carbonate ions in blood act as buffers. The bicarbonate-carbonate system is the main buffer for excess hydrogen ions (H^+), hence maintaining normal blood pH (about 7.4). When the bicarbonate-carbonate system is used up, the other buffer systems in the body come into action, these are the phosphates (HPO_4^{2-}) and the various plasma proteins (such as $RNHCO_3^-$, $HbNHCO_3^-$). Therefore the main problem with using the artificial kidney for extracorporeal CO_2 removal via the HCO_3^- ions, is to buffer the excess H^+ ions.

To correct this imbalance in the artificial kidney approach, the dialysate has to be modified by adding an alkali. Updike and Schults (1973) reported the addition of sodium hydroxide and calcium hydroxide to buffer the excess hydrogen ions while others have tried acetate dialysis (Tolchin et al., 1978; Fleming et al., 1981a,1981b). Chang and Garella (1982) investigated the feasibility of systematic alkali infusion using sodium hydroxide together with dialysis in animal studies.

Another approach has been to use the artificial kidney and an artificial lung for metabolic CO_2 removal. In some patients with ARF the kidneys may also fail (Gattinoni et al., 1983; Martin, 1983). Hence, a combined artificial kidney and artificial lung system would

be helpful to provide long-term respiratory and metabolic support. The combined system would involve higher priming volume and an extra roller pump to be included in the extracorporeal circuit.

1.4 Thesis Objectives and Layout

In the previous developments, the artificial lungs used have been commercial devices which are designed for total CPB procedures.

As will be shown in the critical review of CO_2 removal of commercial membrane oxygenators (Chapter 2), little data exists for low blood flow operation pertinent to $ECCO_2R$-LFPPV therapy. Furthermore, there have been few attempts to relate the experimental CO_2 removal with theoretically predicted performance. One of the major difficulties in this context is the need to know a priori the membrane transmission rate for CO_2. At present no satisfactory method exists for determination of CO_2 gas transmission under gas-membrane-liquid conditions.

The objectives of the thesis are to:

(1) Evaluate in vitro two commercial membrane lungs in an oxygenator-deoxygenator closed-loop test circuit at low blood flow rates and venous input conditions appropriate to $ECCO_2R$-LFPPV therapy. The membrane lungs are:
   (a) Travenol TMO 2.25 m^2 parallel-plate membrane lung (Travenol Inc.)
   (b) Terumo CAPIOX II 1.6 m^2 and 3.3 m^2 hollow fibre oxygenator (Terumo Corp.)

It has been noted that blood flow maldistribution may occur in the Travenol TMO device at low blood flow rates (Bartlett et al. 1975). To investigate this effect several membrane lungs were

modified to reduce the number of parallel-connected blood paths (with consequent increase in path length). The details of the modification are reported in Chapter 4.

In the Terumo CAPIOX II membrane lungs, scaling (number of fibres) effects on carbon dioxide transfer were investigated. Gas flow maldistribution may occur in the full-size devices containing 20,000 and 38,000 fibres in the 1.6 m^2 and 3.3 m^2 membrane lungs respectively. To study the influence of scaling on carbon dioxide transfer, small test modules containing 35 or 70 fibres with an active length of 24 cm were evaluated.

(2) Compare the experimental data with the performance as predicted by a carbon dioxide transfer model. On the basis of the analysis, limiting parameters to gas transfer may be identified in membrane lungs.

(3) Develop a suitable gas-membrane-liquid test method to determine carbon dioxide gas transmission through microporous membranes in sheet form. Established gas-membrane-gas test conditions are not suitable for evaluation of microporous membranes. The presence of the blood-membrane interface alters the permeability characteristics of the membrane (Keller and Schultis, 1979; Schultis, 1980). Adjacent to the membrane is a liquid boundary layer, which offers an additional resistance to gas transfer. Therefore, in the test system, liquid boundary layer resistance must be reduced. The test method would also be suitable for nonporous membranes (silicone rubber). The data obtained may assist membrane selection for artificial lung applications.

Chapter 2 presents the review on CO_2 removal of commercial membrane oxygenators and associated membrane evaluations.

Chapter 3 gives the form of the comprehensive CO_2 transfer models developed by Benn (1974) and Voorhees (1976). The analysis of Voorhees was adopted for subsequent correlation with experimental data obtained in the thesis. Accordingly fuller details of this model are presented.

Chapters 4 and 5 contain the in vitro oxygenator and membrane evaluations respectively.

Chapter 6 presents conclusions and recommendations for further work.

CARBON DIOXIDE TRANSFER IN MEMBRANE OXYGENATORS AND ASSOCIATED MEMBRANES

"Of the artificial systems, the most attractive is that where, in imitation of the natural pulmonary anatomy, a membrane separates blood from gas"

(Melrose, D.G. 1959)

The use of a membrane to separate the blood and ventilating gas phases is a logical approach to artificial lung design because of its resemblance to the structure-function relationship in the human lungs. Although membrane oxygenators have been in use over the last thirty years, it has only been recently that efforts have been made to standardize the performance evaluation of such devices. An International Standards Organisation draft proposal (1981) gives requirements for gas exchange for total bypass. However, desirable values for such parameters as priming volume, flow resistance and level of blood trauma are not specified as these are largely dependent on the bypass application.

In this chapter, the protocol for evaluating membrane oxygenator performance is presented in relation to $ECCO_2R$-LFPPV. For this application the design criteria of the oxygenator and associated bypass circuit are based upon (1) optimal carbon dioxide exchange (2) low priming volume (3) low blood flow resistance for potential pumpless bypass and (4) maintenance of shear stresses below threshold values associated with blood trauma.

2.1 Membrane Oxygenator Requirements for $ECCO_2R$-LFPPV

2.1.1 Gas transfer

In man, oxygen and carbon dioxide gas exchange are dependent

on several factors. These include the patient's body surface area, temperature, age, haemoglobin content, and blood gas conditions of the venous blood (Gaylor, 1980, Melrose, 1976). The venous conditions may deviate considerably in the event of acute respiratory failure.

In the new therapy, metabolic CO_2 removal is the most important factor. The minimum metabolic CO_2 removal that is required of a membrane oxygenator can be calculated from Table 2.1 which shows typical blood gas conditions in an adult male under normothermic conditions and at rest. Assuming a cardiac output of 5 ℓ/min, the carbon dioxide removal rate is 200 mℓ(STPD)/min, while oxygen uptake is 250 mℓ(STPD)/min. These rates are obtained by multiplying the blood flow rate by the appropriate arterial-venous gas concentration difference.

On the basis of the physiological functions of the natural lung, Galletti et al. (1972) introduced the "rated flow" concept. This is defined as the flow rate of blood through the oxygenator which will raise the oxygen saturation from 65% at inlet to 95% at outlet when operated at a temperature of 37°C, blood haematocrit of 40% and base excess at zero. Simultaneously the partial pressure of carbon dioxide at outlet blood must be reduced to 40 mm Hg or less.

More recently, the "rated flow" concept has been superseded by the "oxygen reference blood flow rate" and the "carbon dioxide reference blood flow rate" specified in Draft Proposal DP7199 (International Standards Organisation, 1981). The oxygen reference blood flow rate is that which will result in an increase in oxygen content of 45 mℓ(STPD) per litre with passage through the oxygenator.

Similarly the carbon dioxide reference blood flow rate should result in a decrease in carbon dioxide content of 38 mℓ(STPD) per litre. These flow rates are obtained for reference blood inlet conditions as given in Table 2.2.

O_2 saturation	65 ± 5%
Hb content	12 ± 1 g%
pCO_2	45 ± 5 mmHg
base excess	0 ± 5 mEq/ℓ
temperature	37 ± 2°C

Table 2.2 Reference blood inlet conditions (mean ± tolerance).

Although the inlet conditions are similar to those proposed by Galletti et al. (1972) the main difference is the specification of the haemoglobin content which facilitates the calculation of O_2 transfer rates. The transfer rates obtained at the reference blood flows are similar to those achieved under normal physiological conditions. For a device with a reference blood flow rate of 5 ℓ/min the O_2 and CO_2 transfer rates are 225 and 190 mℓ(STPD)/min respectively. For routine CPB operations under normothermic conditions an extracorporeal blood flow rate of 2.4 ℓ/min per square metre of body surface area is considered adequate (Bartlett and Gazzaniga, 1981).

In the $ECCO_2R$-LFPPV therapy the oxygenator must be optimised for CO_2 removal as the bulk of the O_2 needs are met by apneic diffusion via the trachea. If the oxygenator were 100% efficient in CO_2 removal (i.e. outlet CO_2 content is zero) then the patient's

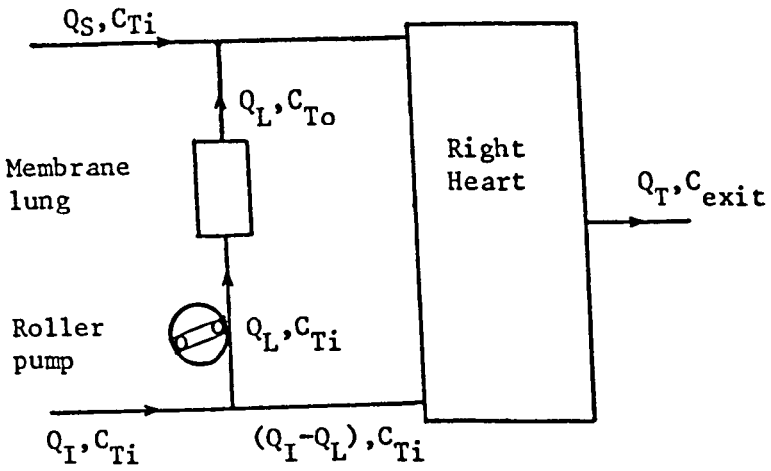

A mass balance at the right heart gives:

$$C_{exit} = \frac{(Q_S \cdot C_{Ti} + Q_L C_{To}) + (Q_I - Q_L) C_{Ti}}{Q_T}$$

If 100% efficient $C_{To} = 0$ and $Q_S + Q_I = Q_T$

$$C_{exit} = \frac{(Q_T - Q_L) C_{Ti}}{Q_T}$$

For C_{Ti} = 53 mℓ (STPD)/100 mℓ

Q_L = 0.38 ℓ/min

Q_T = 5.0 ℓ/min

$$C_{exit} = \frac{(5.0-0.38)}{5.0} \times 53 \text{ mℓ (STPD)/100 mℓ}$$

C_{exit} = 49.0 mℓ(STPD)/100 mℓ

where Q_S = blood flow rate in superior vena cava

Q_I = blood flow rate in inferior vena cava

Q_L = blood flow rate through membrane lung

Q_T = cardiac output

Figure 2.1 Concept of low flow veno-venous partial bypass in $ECCO_2R$-LFPPV therapy.

metabolic CO_2 may be eliminated at relatively low blood flow rates. Given an inlet CO_2 content of approximately 53 mℓ(STPD)/100 mℓ corresponding to the conditions listed in Table 2.1 a blood flow rate of 0.38 ℓ/min would be required to achieve a CO_2 transfer rate of 200 mℓ/min. It should be noted that when the blood from the oxygenator is admixed with the patient's venous blood the resultant CO_2 content leaving the right side of the heart will be at normal "arterial" values i.e. 49 mℓ(STPD)/100 mℓ for this case. The appropriate calculations are shown in Figure 2.1 for a cardiac output of 5.0 ℓ/min.

However, in practice, there are limiting factors to gas transfer which reduce the efficiency. The membrane and the adjacent blood side concentration boundary layer are the two main resistances, R_M and R_B respectively, to gas transfer. The gas side boundary layer resistance, R_G, can be considered negligible because the diffusion coefficients are approximately 10^4 greater in a gas phase compared to a liquid phase. However if water vapour from the blood phase condenses in the gas compartment of the oxygenator R_G may no longer be considered negligible. The overall resistance, R_O to gas transfer can be written as:

$$R_O = R_M + R_B + R_G \qquad (2.1)$$

In general, the CO_2 transfer for a given gas ventilation and blood flow rate is linearly related to the logarithmic mean pCO_2 difference (Murphy et al. 1979). Thus the higher the blood inlet pCO_2 the greater the CO_2 transfer rate. Because the inlet pCO_2 is normally about 45 mmHg high ventilation rates are essential to minimise build-up of CO_2 in the gas phase and hence maintain high log mean pCO_2 differences.

Table 2.1. Partial pressures, gas contents and pH for the blood of an adult male.

Parameters	Venous	Arterial
PO_2 mmHg*	40	95
O_2 content mℓ(STPD)/100 mℓ	15.5	20.5
O_2 saturation %	75	97.5
pH	7.376	7.400
pCO_2 mmHg	46.5	41.0
CO_2 content mℓ(STPD)/100 mℓ	53.0	49.0
mmoℓ/ℓ	23.81	22.01

STPD - Standard Temperature, Pressure, Dry.

*The SI unit for pressure is the Pascal (1 mmHg = 133.322 Pa).

2.1.2 Priming volume

In nearly all extracorporeal bypass circuits the oxygenator is operated with an in series blood reservoir. The purpose of the blood reservoir is twofold: (1) it permits collection of venous blood by gravity flow and (2) it accommodates changes in blood volume due to supply variations. The latter function provides an adequate operator reaction time in the event of cessation of venous delivery. Otherwise air emboli could be introduced to the patient's circulation. The reservoir volume is dependent on the bypass flowrate and, for adult CPB will range from 0.75 to 2.0 litres. The lower the blood flow rate the lower the reservoir volume required. Hence for the low flow rates used in $ECCO_2R$-LFPPV the reservoir volume may be kept quite low. In order to reduce the need for transfusion blood it is desirable to minimise the volume of blood in the rest of the circuit. This implies that the oxygenator should possess a low priming volume. Current priming volumes range from 80 to 180 mℓ per m^2 membrane area.

2.1.3 Resistance to blood flow

In contrast to bubble oxygenators, membrane devices are closed volume systems and hence it should be theoretically possible to overcome large pressure losses over the flow path by placing the blood pump at the inlet. However, if hydrophobic microporous membranes are employed (section 2.5) high trans-membrane pressures may promote plasma infiltration of the pores. For microporous membrane systems the pressure loss at the reference blood flow is typically 150 mmHg (Murphy et al. 1974; Suma et al. 1981). Clearly, lower pressure drops will result at the lower flowrates (relative to reference value) used in $ECCO_2R$-LFPPV therapy. Hence, it may be possible in certain

designs to utilise the natural arterio-venous pressure difference thereby eliminating the external blood pump (Barthelemy et al., 1982). Under these circumstances pressure drop would be limited to about 90 mmHg. Any pressure losses due to cannulae, connectors etc. will have to be taken into account.

2.1.4 Blood trauma

Many studies have been carried out on blood trauma and associated effects in extracorporeal circuits resulting from blood interactions with foreign materials, and these have been reviewed by Feijen (1977), Feijen et al. (1979) and Lindsay et al. (1980). With the present state of the art, the materials used in the bypass circuit are not truly antithrombogenic and hence anticoagulation therapy is necessary to prevent thrombus formation. Two factors contributing to blood trauma are contact with foreign surfaces and non-physiological flow conditions. When blood comes in contact with most foreign materials, protein absorption occurs resulting in a loss of platelets (thrombocytes). The phenomena has been related to platelet adhesion and is also influenced by other factors such as plasma composition, surface morphology of the material, surface charges, and flow conditions.

Non-physiological flows result in shearing forces or stresses which may damage blood elements. A threshold shear stress of about 15 N/m^2 has been shown to cause substantial platelet damage (Brown et al. 1975). This was measured by the amount of acid phosphatase or 5-hydroxytryptamine (serotonin) released by damaged platelets. According to Feijen (1977) the threshold shear stress for platelets is within laminar flow conditions. For red blood cells, greater

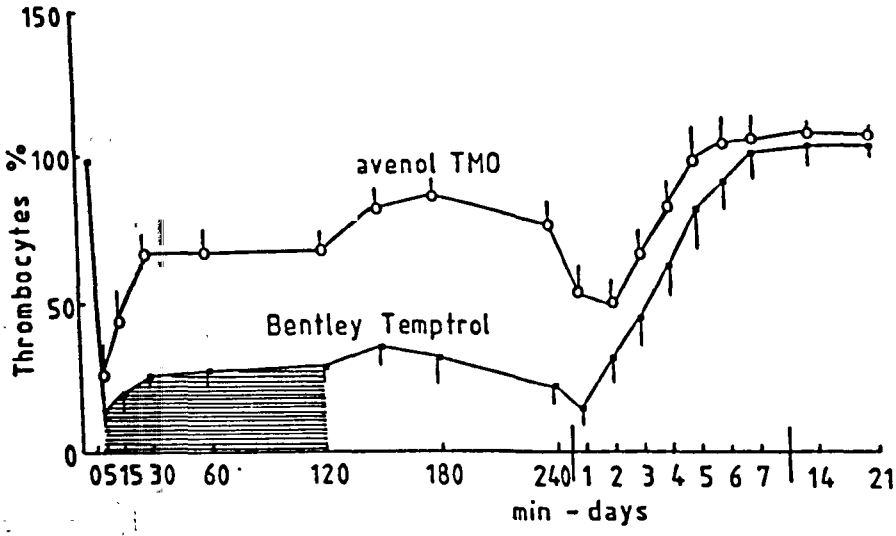

Figure 2.2 Changes in thrombocyte counts (percentage of initial values, mean ± SEM) during and after veno-arterial perfusion (3 l/min., during 2 h bypass, shaded area) in dogs, comparing the Travenol TMO membrane oxygenator with the Bentley Temptrol bubble oxygenator (Wildevuur, 1981).

shear stresses can be tolerated as the threshold is about 150 N/m^2 (Leverett et al. 1972) before haemolysis occurs. Although in vitro tests are useful to define the limits of cellular damage, it is difficult to know the extent of the blood damage due to flow under actual bypass conditions, as the cells are exposed to different shear-stress levels with each passage through the external circuit. On the other hand, the blood flow path within the oxygenator should not possess stagnant regions which promote the formation of red blood cell thrombus.

In short-term CPB, the contribution by the cardiotomy suction device to red cell damage (haemolysis) may completely mask the contribution by the oxygenator. De Jong et al. (1980) have shown that by carefully regulating cardiotomy suction, membrane oxygenators result in less haemolysis than bubble units. Furthermore these investigators demonstrated that membrane oxygenators maintained the number and function of thrombocytes more than bubble oxygenators during canine CPB procedures (Figure 2.2). In the study, the various contributions to blood trauma from priming solutions, tubings, pumps and cardiotomy suction were taken into account.

For long-term bypass applications (for example, acute respiratory failure), the risk of internal bleeding may become high due to the loss of platelets and to the anticoagulant therapy. Furthermore, it has been recognised that the effect of CO_2 removal results in extreme pH changes in blood emerging from the extra-corporeal device. Whether this is safe for long-term support is unclear. According to Kolobow et al. (1977), no detrimental effects from large pH variations were found in lambs undergoing CO_2 removal

therapy over a period of three days. However, studies by White et al. (1969) have shown in vitro that haemolysis occurs if the pH exceeds 7.8 and pCO_2 is low, but if blood was buffered by THAM to keep the pH at 7.4-7.5, no haemolysis occurred.

Although this thesis is not concerned with thrombogenesis in the bypass circuit for $ECCO_2R$-LFPPV therapy, it should be noted that protein adsorption and cellular deposition on the membrane may alter its transfer characteristics. This aspect is discussed in section 2.5.

2.2 Membrane Oxygenator Configuration

2.2.1 Tubular and parallel-plate devices.

Basically, membrane lungs fall into two design categories; the hollow fibre (tubular) and sheet-membrane (parallel-plate) designs. They are classified according to the geometry of the blood flow path.

The hollow fibre or tubular membrane oxygenator (also known as the capillary membrane oxygenator) is characterised by a large number of gas-permeable tubes arranged in parallel inside a jacket. Usually, blood flows inside the tubes and the ventilating gas (oxygen) flows counter-current outside the tubes. Several design factors have been examined in tubular units by Mockros and Gaylor (1975) in order to obtain adequate gas transfer rate per unit membrane area and low priming volumes for specified pressure drops. To produce such a unit, the flow-path length, tube spacing and the tube radius may be varied in any combination.

Gaylor and Mockros (1975) performed a similar analysis for sheet-membrane units. This type of geometry features a number of parallel-connected blood channels or layers. In this configuration

blood flows in thin films bounded by the opposing membrane walls with gas flowing countercurrent over the outer surfaces of the membranes. Generally, it is more difficult to achieve equi-distribution of blood to the flow paths in parallel-plate units than in hollow fibre designs. This is due to the difficulty in maintaining a uniform channel height over the area of each channel since the sheet membranes are compliant. As will be discussed in section 2.3.2 inflatable shims and plastic screens within the blood path have been used to promote more uniform distribution. For rectilinear laminar blood flow and with current membrane materials about 90-95% of the total resistance to O_2 transfer in hollow fibre or parallel-plate designs is due to the blood phase resistance R_B (Colton, 1976). Consequently numerous attempts have been made to design oxygenators which will reduce R_B by enhancing the diffusion process through convective mixing of the blood phase. These devices are known as secondary flow oxygenators.

2.2.2 Secondary flow devices

The term 'secondary flow' is used by engineers to denote convective transfer within a moving fluid at an angle or in a plane different from that of the main through-flow. Membrane oxygenators employing secondary flows can be subdivided into two types: active or passive mixing. Active devices are those in which there is energy input to achieve high shear rates or to create secondary flows. The Taylor-Vortex (Gaylor et al. 1973), the oscillating toroid (Drinker et al. 1969), the pulsed vortex-shedding (Bellhouse et al. 1973) and the rotating-disc (Hill et al. 1974) membrane oxygenators are examples of mixing types. In general, active type devices are more difficult to manufacture and may require ancillary components for their operation. Consequently, the only secondary flow device

that is currently available for clinical use is the pulsed vortex-shedding (Interpulse, Extracorporeal Inc.) oxygenator.

Passive devices, in contrast are those in which no energy input is needed except that required for steady blood flow. A common technique has been to place obstacles, for example screens, in the blood path to induce secondary flows or increase mixing. The Travenol TMO membrane oxygenator falls into this category. Another approach is to use flow geometries that naturally induce secondary flow, for example helically coiled tubes (Weissman and Mockros, 1969; Tanishita et al., 1975; Baurmeister et al., 1977). Detailed reviews of secondary flow devices are given by Colton (1976) and Drinker and Bartlett (1976).

2.3 Carbon Dioxide Transfer in Commercial Membrane Oxygenators.

It is well known that laminar flow membrane oxygenators designed on the basis of oxygen transfer have a sufficient capacity for carbon dioxide removal (Galletti, 1968; Voorhees, 1976). To obtain adequate oxygen transfer, blood flows of between 3 to 6 ℓ/min (for adults) are required. At these high blood flows, carbon dioxide transfer (between 250 to 340 mℓ(STPD)/min) is more than adequate. As the following review will show there are relatively few reports on CO_2 transfer rates of membrane oxygenators at low blood flows appropriate to $ECCO_2R$-LFPPV therapy. In addition, the measurement of the total CO_2 transfer rate is more difficult to perform than that for O_2 and consequently in some studies only changes in pCO_2 and pH are given. To further complicate the picture, some gas transfer evaluations have been carried out without control of (or at times without even recording) such factors as haematocrit, temperature, and inlet oxygen

saturation, all of which are important factors which alter the gas transfer function.

2.3.1. Sci-Med Kolobow

First described by Kolobow and Bowman (1963), the Sci-Med Kolobow oxygenator has been used extensively for long-term ECMO (Kolobow et al., 1971, 1975; Zapol et al. 1975), $ECCO_2R$-LFPPV (Gattinoni et al., 1980) and short-term CPB (Wheaton, 1978) procedures.

Physical description. The device is a variation of the sheet-membrane oxygenator, in which a spiral coil configuration is adopted (Figure 2.3). The core of the lung is a polycarbonate spool, onto which is tightly wound a membrane envelope. This envelope is composed of a pair of fabric-reinforced silicone rubber membranes separated by a polypropylene mesh spacer. Blood flows axially over the external surfaces of the envelope and the ventilating gas flows circumferentially in the envelope interior. The blood and gas streams are introduced or removed via ports situated on the end caps, and the entire assembly is encased by a tight-fitting silicone rubber sleeve. The oxygenator is available in various sizes ranging from 0.8 to 4.5 m^2 units with respective static priming volumes of 100 to 540 mℓ. Although high pressure drops (between 160-300 mmHg) are generated by these units at their reference blood flow rates, the reinforced membranes enable the device to be operated at transmembrane pressures up to 750 mmHg.

Gas transfer. Rawitscher et al. (1973) evaluated the 1.5 m^2 spiral coil membrane oxygenator with a rated flow of 1.4 ℓ/min at 37 ^{o}C and haematocrit of 40% in canine CPB. The carbon dioxide transfer rates obtained were 55.8, 73.6 and 70.1 mℓ/min at blood

flow rates of 1.0, 1.4 and 1.8 ℓ/min respectively. Carbon dioxide transfer was measured by analysis of exhaust gas. The exhaust gases from the oxygenator were collected for 1 minute in a Collins spirometer. CO_2 concentration of the exhaust gas was measured during the collection period with an infrared CO_2 analyser (Godart NV, type 146) and Beckman type R dynograph recorder (0 to 2.5% CO_2 = full scale). Continuous samples of exhaust gas were delivered to the CO_2 analyser and returned to the spirometer through ports in the gas collection system. The CO_2 transfer (mℓ/min) was calculated from the fraction of CO_2 in the exhaust gas multiplied by the volume of collected gas at STP.

Murphy et al. (1979) examined in ovine CPB the effects of: (1) membrane area and assembly techniques; (2) blood and gas phase pressures during operation and (3) blood flow rate, O_2 saturation and haemoglobin content on gas transfer performance in the spiral coil oxygenator. The effective membrane area of the unit was 4.55 m^2. The test conditions were: 38 ^oC temperature, 62 to 70% input O_2 saturation, 35 to 40% haematocrit, 40 to 50 mmHg inlet pCO_2 and an O_2 flow rate of 10 ℓ/min. The CO_2 transfer was calculated from the CO_2 concentration of output gas and gas flow rate. At the low blood rates of 0.89 and 1.80 ℓ/min, the corresponding CO_2 transfers were 111 and 139 mℓ/min respectively. Murphy et al. (1979) concluded from their studies that given a certain exchange area, and a constant rate of ventilation with oxygen, the CO_2 transfer rate is not markedly affected by blood flow rate, but rapidly approaches the limit set by the permeability characteristics of the membrane. The two main determinants of CO_2 transport are ventilation (i.e. O_2 flow rate) and blood pCO_2. At low O_2 flow rates, the CO_2 concentration in the

gas phase of the oxygenator can be high enough to exert a limiting effect on CO_2 transfer rate. Carbon dioxide transfer increases with blood pCO_2 and with ventilation, which both affect the partial pressure gradient which drives CO_2 across the membrane.

Kolobow et al. (1977b) reported a modification of the spiral coil oxygenator optimised for CO_2 removal. The major change involved an increased width of the membrane envelope to increase the length of the blood flow path. The modified spiral coil oxygenator had a membrane area of 1.4 m^2. At a blood inlet pCO_2 of 45 mmHg the CO_2 transfer rate was about 65.8, 77.0, 91.0 at blood flow rates of 0.4, 0.6 and 1.0 ℓ/min respectively. The membrane oxygenator performance was evaluated in lambs connected to a mechanical ventilator. An infrared CO_2 analyzer was used for the transfer measurements.

Gattinoni et al. (1980) used two 3.5 m^2 Sci-Med Kolobow membrane oxygenators arranged in series for $ECCO_2R$-LFPPV therapy to treat successfully three patients with terminal repiratory failure. Adequate CO_2 removal of between 200-300 mℓ/min was obtained at average blood and ventilating gas flow rates of 1.3 and 16 ℓ/min respectively.

2.3.2. Travenol TMO

The original design of the Travenol TMO was first described by Murphy et al. (1974) known as the STX-433 and STX-434 prototypes. Apart from the STX-434 model having a thicker blood manifold plate, the two models were essentially similar. The early designs incorporated microporous tetrafluoroethylene (PTFE or teflon) membranes of 30-50 μm thickness with a nominal pore diameter of 0.5 μm. Current Travenol TMO oxygenators use microporous poly-

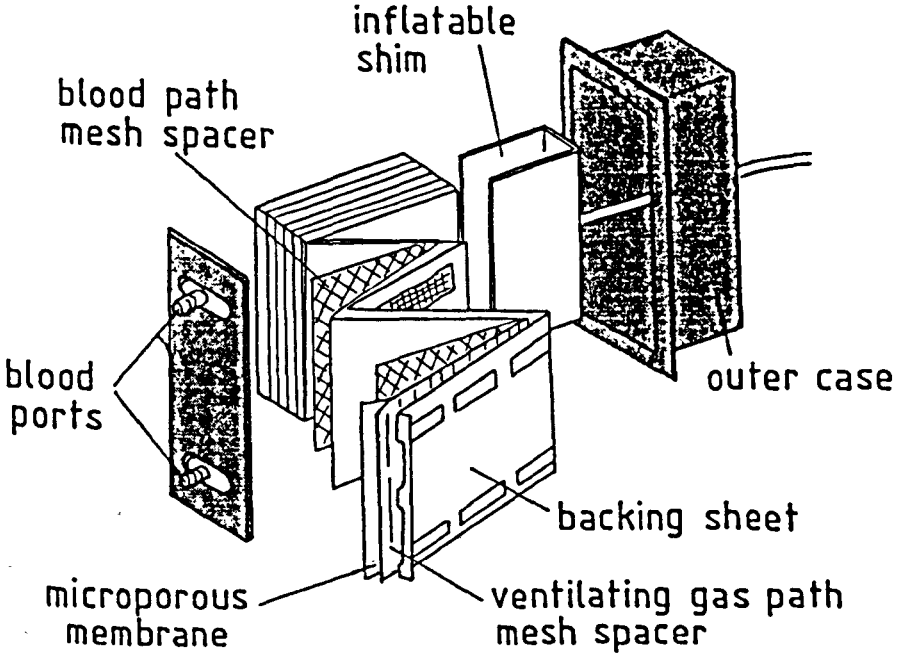

Figure 2.4 Exploded view of the Travenol TMO membrane oxygenator. (after Gaylor, 1980).

propylene membranes and are available in 2.25 m^2 and 1.12 m^2 surface areas for adult and paediatric CPB procedures respectively.

There are numerous publications describing its clinical application (e.g. Beall et al. 1976; Karlson et al. 1977). Data comparing its clinical performance with that of bubble oxygenators are also available (e.g. Liddicoat et al., 1975).

Physical description. The Travenol TMO membrane oxygenator for adult use is shown in Figure 2.4. It consists of a single module containing a 2-ply microporous polypropylene membrane (Celgard, Celanese Corp.) folded in an accordion fashion to form 30 parallel-connected blood channels separated by gas paths. Integrity of the blood and gas paths is provided by supporting screens. The screen in the blood phase is made of nylon monofilaments (0.3 mm diameter) which are oriented at 45^{o} to the direction of blood flow in the envelope . On the gas side an open-weave square mesh of polyvinyl chloride-coated fibreglass strands (0.3 mm diameter) runs parallel to the gas flow direction. The total membrane area is 2.25 m^2, but the effective exchange area is somewhat reduced by the masking effect of the strands of the screens in the blood and gas phases. Co-current blood and gas flow is the normal recommended operation. An inflatable bag surrounding the blood- and gas-path assembly acts as a shim. The shim is inflated to a desired pressure (normally 200 mmHg) to regulate the thickness of the blood-phase envelopes. Since the oxygenator is housed in a deformable plastic case the whole assembly is further enclosed in a rigid metal holder. A relatively high pressure drop (about 120 mmHg) results from this configuration with the high rated flow (6 ℓ/min). The maximum

inlet blood pressure at the oxygenator should not exceed 300 mmHg. To avoid deformation of the membrane and possible plasma exudation due to high blood pressures, venous and arterial pumps are necessary for operation in the bypass circuit. As the porosity of the membrane allows a substantial flux of water vapour from the blood phase which can condense in the gas paths giving an additional resistance to transfer, a gas heater module is supplied to reduce this effect. At the present time, the TMO total bypass oxygenator with polypropylene membrane is not recommended for long term support of respiratory failure (Travenol laboratories, Inc. 1976).

Gas exchange. Karlson et al. (1974) reported data on CO_2 removal in the prototype model STX-434 (surface area 2.25 m^2). The studies were performed with ovine CPB and with the following blood input conditions: PCO_2 36 to 65 mmHg, O_2 flow rate 10 to 15 ℓ/min and shim pressure 150 to 300 mmHg. For these rather variable conditions the CO_2 transfer ($\dot{V}_{CO_2}$, mℓ/min) was expressed as a function of blood flow rate (Q_B, ℓ/min) through the following empirical relationship:

$$\dot{V}_{CO_2} = 134.0\ Q_B - 28.0\ Q_B^2 + 1.98\ Q_B^3 \qquad (2.2)$$

(correlation coefficient, $r = 0.676$)

Equation 2.2 predicts $\dot{V}_{CO_2}$ ranging from 60.2 to 144.7 mℓ/min corresponding to a blood flow rate range of 0.5 to 1.5 ℓ/min appropriate to CO_2 removal therapy.

A relationship for the carbon dioxide transfer as a function of oxygen flow rate was also derived. An increase of ventilation

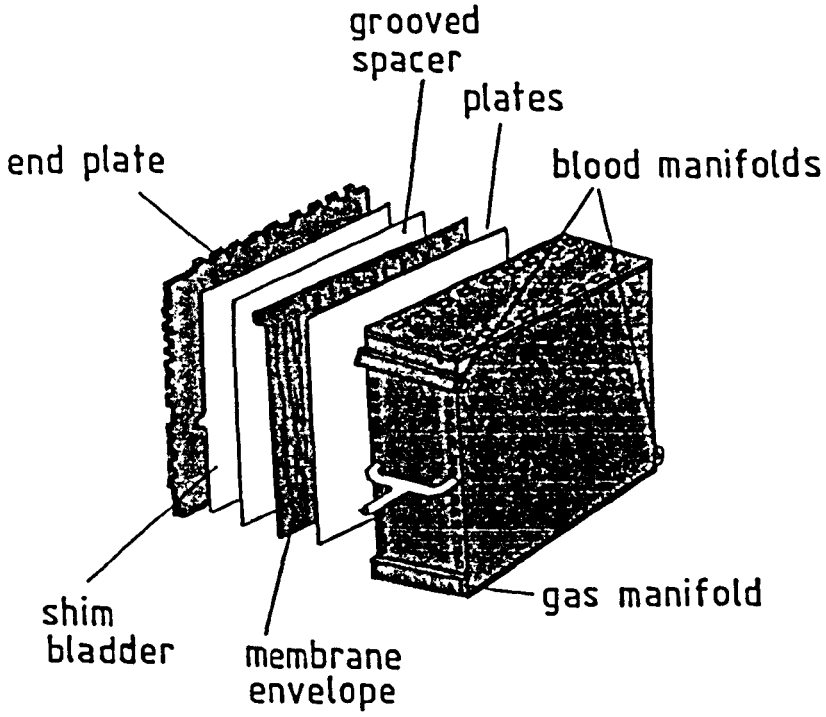

Figure 2.5 Exploded view of the Hospal M32 membrane oxygenator. (after Barthelemy et al.,1982)

($\dot{V}_E$, ℓ/min) leads to a notable increase in carbon dioxide transfer rate and for input pCO_2 = 37 mmHg and Q_B = 4.0 ℓ/min may be represented by:

$$\dot{V}_{CO_2} = 37.5\ \dot{V}_E - 3.12\ \dot{V}_E^2 + 0.0944\ \dot{V}_E^3 \qquad (2.3)$$
$$(r = 0.956)$$

Finally, the CO_2 transfer rate is a function of blood input pCO_2. For an oxygen flow rate of 15 ℓ/min and Q_B = 4.0 ℓ/min, the relation between the CO_2 transfer rate and the input blood pCO_2 (mmHg) was given empirically by:

$$\dot{V}_{CO_2} = 4.52\ pCO_2 - 8.87 \times 10^{-3}\ pCO_2^2 - 1.62 \times 10^{-5}\ pCO_2^3 \qquad (2.4)$$
$$(r = 0.944)$$

CO_2 transfer rate measurements were as reported by Galletti et al. (1971) and calculated from the CO_2 concentration of output gas and gas flow rate. Karlson et al. (1974) also noted that CO_2 transfer decreased if the pressure in the "shim" exceeded the blood pressure at the input port of the oxygenator and if water vapour condensation occurred in the gas phase. Therefore, the oxygenator was operated at a "shim" pressure equal to the input blood pressure and dry, heated oxygen was used to ventilate the oxygenator.

2.3.3. Hospal M32

The Hospal M32 was first reported by Barthelemy et al. (1982) and was evaluated for carbon dioxide removal at low blood flow operating conditions in a pumpless artery-to-vein circuit.

Physical description. The Hospal M32 oxygenator is a parallel-plate unit with 2.0 m^2 microporous membrane (Figure 2.5). The silicone-coated polynodosic cellulose membrane is arranged into 22

blood envelopes which are fed and drained by individual silicone rubber ports. The stack of envelopes and spacers is enclosed in a rigid housing with blood and gas inlet and outlet manifolds at each corner. Blood layer thickness is controlled by an inflatable shim similar to that in the Travenol TMO. The oxygenator has a resistance to blood flow of about 30 mmHg per ℓ/min of blood flow without the shim and about 45 mmHg with the shim inflated to a pressure exceeding the blood inlet pressure.

Gas exchange. The CO_2 transfer removal is greater with the shim than without the shim. In the absence of the shim and with an input pCO_2 of 50 mmHg, the CO_2 transfer is in the order of 100 mℓ/min at a blood flow rate of 1.0 ℓ/min, and 125 mℓ/min at a blood flow rate of 2.0 ℓ/min. If the shim is inflated at a pressure exceeding the blood inflow pressure, the CO_2 transfer rate is in the order of 130 mℓ/min at a blood flow rate of 1.0 ℓ/min and 180 mℓ/min at a blood flow rate of 2.0 ℓ/min (Barthelemy et al. 1982). In an arterio-venous circuit the mean arterial pressure determines the blood flow rate through the devices, which in turn can be modulated by shim pressure. In the study of Barthelemy et al. (1982) using a pumpless, artery-to-vein bypass in two apneic sheep for a period of 5 hours, the arterial pCO_2 stabilized at a value around 62 mmHg. A mean arterial blood pressure of about 100 mmHg provided an extra-corporeal blood flow rate varying between 1.2 and 1.4 ℓ/min. This allowed a CO_2 transfer rate between 120 and 155 mℓ/min, accompanied by a pCO_2 drop of 24 to 30 mmHg in the transit through the oxygenator. Further evaluations over a period of 24 hours showed that the oxy-genator exhibited some thrombosis which impaired blood flow through the exchange paths, and a new oxygenator replacement was necessary at

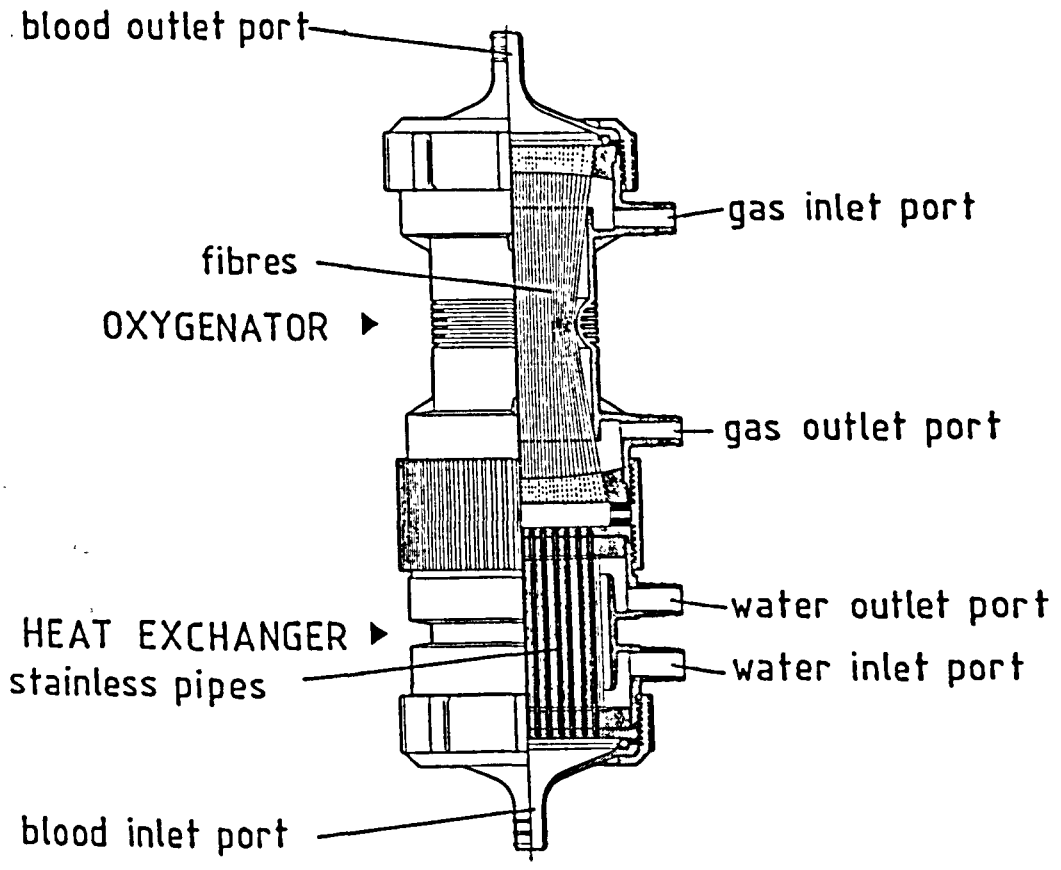

Figure 2.6 Cross section of the Terumo CAPIOX II hollow fibre membrane oxygenator.

12 hours. The extracorporeal blood flow rate allowed adequate CO_2 removal (in relation to the animal) hence allowing a pumpless operation. This simplified the extracorporeal circuit and reduced blood trauma. An oxygen flow rate of 10 ℓ/min was employed in the long-term evaluation being well in excess of the maximum ventilation (4 ℓ/min) required by the oxygenator. Barthelemy et al. (1982) suggested that for CO_2 removal in the adult human, a 3 m^2 model may be necessary.

2.3.4 Terumo CAPIOX II.

A new hollow fibre oxygenator using microporous polypropylene membranes has been developed recently by Terumo Corporation of Japan. (Tsuji et al. 1981.) An integral heat exchanger was not available in the original design but was incorporated later. Both animal and clinical evaluations have been carried out extensively with the oxygenator (Meserko et al. 1981; Suma et al., 1981; Sinkewich et al. 1982, Riley et al. 1983).

Physical description. The CAPIOX II consists of a bundle of microporous polypropylene hollow fibres oriented axially within a cylindrical transparent casing made of acrylonitrile - styrene copolymer (Figure 2.6). The hollow fibres have an internal diameter of 200 μm and a wall thickness of 25 μm. The fibre withstands a transmembrane pressure of 1,000 mmHg. The pores size averages 700 Å and the fibre porosity is 50%. The ends of the 130-140 mm long fibres are secured in a polyurethane material. Incorporated at one end of the device is a heat exchanger.

Blood is introduced into the heat exchanger via a conical polycarbonate inlet port. After passage through the heat exchanger,

the blood enters the fibre lumens and is discharged through a conical outlet port. The ventilating gas is circulated countercurrent to the blood flow via ports located on the lateral surface of the transparent housing. To prevent shunting of the gas flow, the outer casing is "waisted" at it's midpoint. The unit is ethylene oxide sterilized and disposable. It is available in four sizes with physical specifications as shown in Table 2.3.

	HFO-16	HFO-33	HFO-43	HFO-54
Effective membrane area (m^2)	1.6	3.3	4.3	5.4
Effective fibre length (mm)	130	140	130	140
Number of fibres	2.0×10^4	3.8×10^4	5.3×10^4	6.0×10^4
Priming volume (mℓ)	200	420	550	700
Maximum blood flow rate (ℓ/min)	2.0	4.0	5.2	6.5

Table 2.3. CAPIOX II Specifications

Gas exchange. Tsuji et al. (1981) reported gas transfer data for prototype Terumo hollow fibre units without the integral heat exchanger. Devices of 1.8 and 3.3 m^2 surface areas were evaluated in vitro with bovine blood of 12 g% haemoglobin and 50 mmHg inlet pCO_2. Carbon dioxide transfer rates were recorded at different oxygen flow rates. The carbon dioxide transfer rates at the maximum oxygen flow rate operated are shown in Table 2.4.

Surface area m^2	blood flow rate ℓ/min	Oxygen flow rate ℓ/min	$\dot{V}_{CO_2}$ mℓ/min
1.8	0.9	2.7	86.4
	1.62	2.7	111.6
	1.80	2.7	115.2
3.3	1.65	4.95	158.4
	1.98	4.95	171.6

Table 2.4. Carbon Dioxide Transfer in the 1.8 and 3.3 m^2 units.

Carbon dioxide transfer rates were also evaluated in a canine partial bypass circuit. A 1.0 m^2 oxygenator was perfused with venous blood of haematocrit 31 $\pm$ 2%, O_2 saturation 62 $\pm$ 10%, pO_2 36 $\pm$ 7 mmHg and pCO_2 46 $\pm$ 7 mmHg. The blood and oxygen flow rates to the oxygenator were 0.97 $\pm$ 0.16 ℓ/min and 1.0 ℓ/min respectively and at a temperature of 37°C. Carbon dioxide transfer rate averaged 43 $\pm$ 2 mℓ/min. The carbon dioxide transfer rates were calculated from the measurement of CO_2 concentration in the exhaust gas by gas chromatography.

Riley et al. (1983) presented results of the Terumo CAPIOX II 4.3 m^2 membrane oxygenator for adult CPB. Although CO_2 transfer rates of about 300 mℓ/min were obtained at 22% haematocrit, 47 mmHg inlet pCO_2 and ventilation rate of 5.6 ℓ/min, the blood flow rate of 5.6 ℓ/min is far in excess of that for the CO_2 therapy application. Carbon dioxide transfer parameters were calculated from the ventilating gas flow values and mass spectrometer measurements as reported by Riley (1982).

Terumo Corporation (1983) presented CO_2 transfer rate data for the CAPIOX II 1.6 m^2 oxygenator. The tests were performed in an in vitro circuit using bovine blood and at ISO reference blood input conditions. At blood flow rates of 1.0 ℓ/min and 2.0 ℓ/min the carbon dioxide transfer rates were 95 mℓ/min and 110 mℓ/min respectively. The oxygen flow rate was 3 ℓ/min. For the CAPIOX II 3.3 m^2 oxygenator at a blood flow rate of 2 ℓ/min and oxygen flow rate of 5.5 ℓ/min, the carbon dioxide transfer rate was 180 mℓ/min. The transfer rates quoted were estimated by the author from the manufacturers' data sheets in which the relationship $\dot{V}_{CO_2}$ and O_2 flow rate is given graphically. The values should be regarded with caution as the manufacturer neither states the number of units evaluated nor the experimental variation in $\dot{V}_{CO_2}$ measurement. Higher O_2 flow rates were not tested by the manufacturer although his graphs suggest that further increases in $\dot{V}_{CO_2}$ could be expected with increased ventilation.

2.3.5 Interpulse oxygenator

Studies of the fluid mechanics of the aortic valve (Bellhouse and Bellhouse, 1969) have shown that strong vortices formed in the aortic sinuses behind each valve cusp, and that considerable mixing occurred between the blood in the sinuses and that in the aorta. The principle of creating good mixing in the blood phase to enhance oxygen gas transfer led to the development of the Oxford-Bellhouse membrane oxygenator (Bellhouse et al. 1973). This secondary flow type oxygenator was progressively developed to a commercially available design known as the Interpulse Membrane Oxygenator (Extracorporeal Inc.)

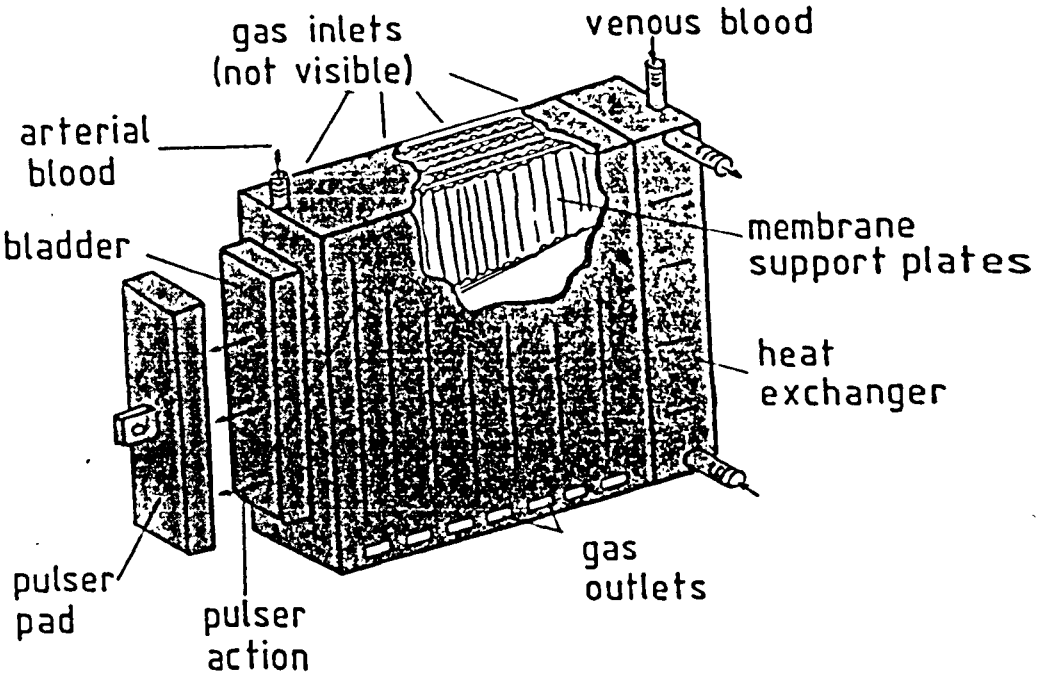

Figure 2.7 Diagram of the Oxford Interpulse membrane oxygenator.

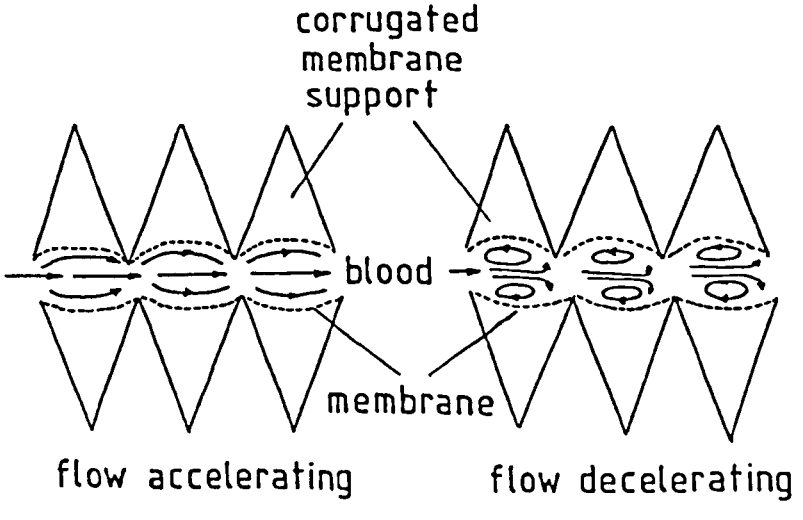

Figure 2.8 Secondary flow phenomenon occurring in the Oxford oxygenator.

Physical description. The Interpulse system consists of a membrane oxygenator and a pulser module (Figure 2.7). The oxygenator is a disposable microporous gas-exchange device with an integral heat exchanger. A notable feature of the adult oxygenator is the active membrane surface area of 0.8 m^2, which is considerably less than most membrane oxygenators currently available. It has seven blood channels, the microporous polyhetrafluoroethylene (PTFE or Teflon) membrane is supported over plastic plates to form longitudinal furrows, normal to the blood flow direction. Moulded plastic manifolds with inlet and outlet ports for blood tubing connections are located on each side of the oxygenator. Gas inlets and outlets are on each exterior plate. Oxygen flows in the channels between the support plates and membrane and blood is channelled between the membrane barriers. Flexible diaphragms at both ends of the oxygenator allow a pulse to be transmitted to the blood phase.

The effect of the pulser is to generate secondary vortices (Figure 2.8) in the membrane furrows. Consequently O_2 enriched blood is brought from the membrane surface to the mainstream of the flow, thus enhancing gas exchange efficiency. The blood is pulsed through the oxygenator with a mean pressure gradient of only 15 mmHg across the oxygenator and heat exchanger. Oxygen transfer can be varied by altering the pulse rate and the carbon dioxide transfer can be altered by changing the gas flow rate.

More recently, a smaller version of the oxygenator with a membrane area of 0.39 m^2 has been evaluated for paediatric application. The paediatric unit is not yet available commercially.

Gas exchange. The Interpulse oxygenator has been evaluated in vitro and in clinical CPB. (Spratt et al. 1981). The oxygen and carbon dioxide reference blood flow is in excess of 6 ℓ/min as determined in accordance with the ISO reference conditions. The carbon dioxide transfer reported at a blood flow rate of 2.2 ℓ/min, pulse rate of 250 pulses/min and oxygen flow rate of 15 ℓ/min is about 205 mℓ/min. Bovine blood was used for the gas transfer evaluations.

Peacock et al. (1983) reported data on the paediatric unit using human blood in an in vitro oxygenator-deoxygenator test circuit. For ISO standard conditions carbon dioxide gas transfer was about 120 mℓ/min at a blood flow rate of 1.5 ℓ/min. Carbon dioxide concentrations of the gas were analysed by an infrared Beckman LB-2 analyser. Peacock et al. (1983) suggested that the device would be capable of removing the total CO_2 production of a 20 kg child if the device were used solely for CO_2 removal in the treatment of acute respiratory failure.

2.4 Summary of CO_2 Transfer in Membrane Oxygenators

A comparative analysis of available gas transfer data is difficult, because of differing test conditions. Furthermore, the fragile and changing characteristics of blood when circulated outside the body are well known (Feijen, 1977). In vitro and in vivo comparisons are useful in addition to these, mathematical models can also help in the validation of gas transfer studies. In studies where CO_2 content of whole blood is not measured, an estimate of the total CO_2 content could be obtained through pH, pCO_2 and haemoglobin data and the use of nomograms. However errors are compounded in this approach and the transfer rates so obtained may be grossly inaccurate

Symbol in Figure 2.9	oxygenator	A m^2	Q_B ℓ/min	$\dot{V}_{CO_2}$ mℓ(STPD)/min	reference
●	Sci-Med. (modified)	1.4	0.4 0.6 1.0	65.8 77.0 91.0	Kolobow et al. 1977b
○	Sci-Med.	1.5	1.0 1.4 1.8	55.8 73.6 70.1	Rawitscher et al. 1973
⊙	Sci-Med.	4.55	0.89 1.8	111.0 139.0	Murphy et al. 1979
ø	Two Sci-Med.	7.0	1.0-1.4	190-210	Gattinoni et al. 1979
◆	Travenol STX-434	2.25	0.5 1.5	60.2 144.7	Karlson et al. 1974
◇	Travenol TMO (PTFE)	2.25	1.0 2.0	90.0 160.0	Birnbaum and Bücherl, 1974
★	Hospal M32	2.0	1.0 2.0	130.0 180.0	Barthelemy et al. 1982
⊡	Terumo CAPIOX II (modified)	1.8 3.3	0.9 1.62 1.8 1.65 1.98	86.4 111.6 115.2 158.4 171.6	Tsuji et al. 1981
■	Terumo CAPIOX II	1.6	1.0 2.0	95.0 110.0	Terumo Corp. 1983
X		3.3	2.0	180.0	

Symbol in Figure 2.9	oxygenator	A m^2	Q_B ℓ/min	$\dot{V}_{CO_2}$ mℓ(STPD)/min	reference
▲	Pulsed-vortex * Paediatric unit	0.39	0.484 0.995 1.488 2.006	84.0 111.6 118.7 131.3	Peacock et al. 1983
▼	Pulsed vortex Paediatric unit	0.39	0.518 1.011 1.505 1.955	76.4 88.1 92.6 116.5	Bellhouse et al. 1981
△	Interpulse	0.8	2.2	205.0	Spratt et al. 1981

Table 2.5. CO_2 transfer performance data for membrane oxygenators under low blood flow conditions.
(*Frequency = 0.8-4.0 Hz, Stroke volume = 9 mℓ)

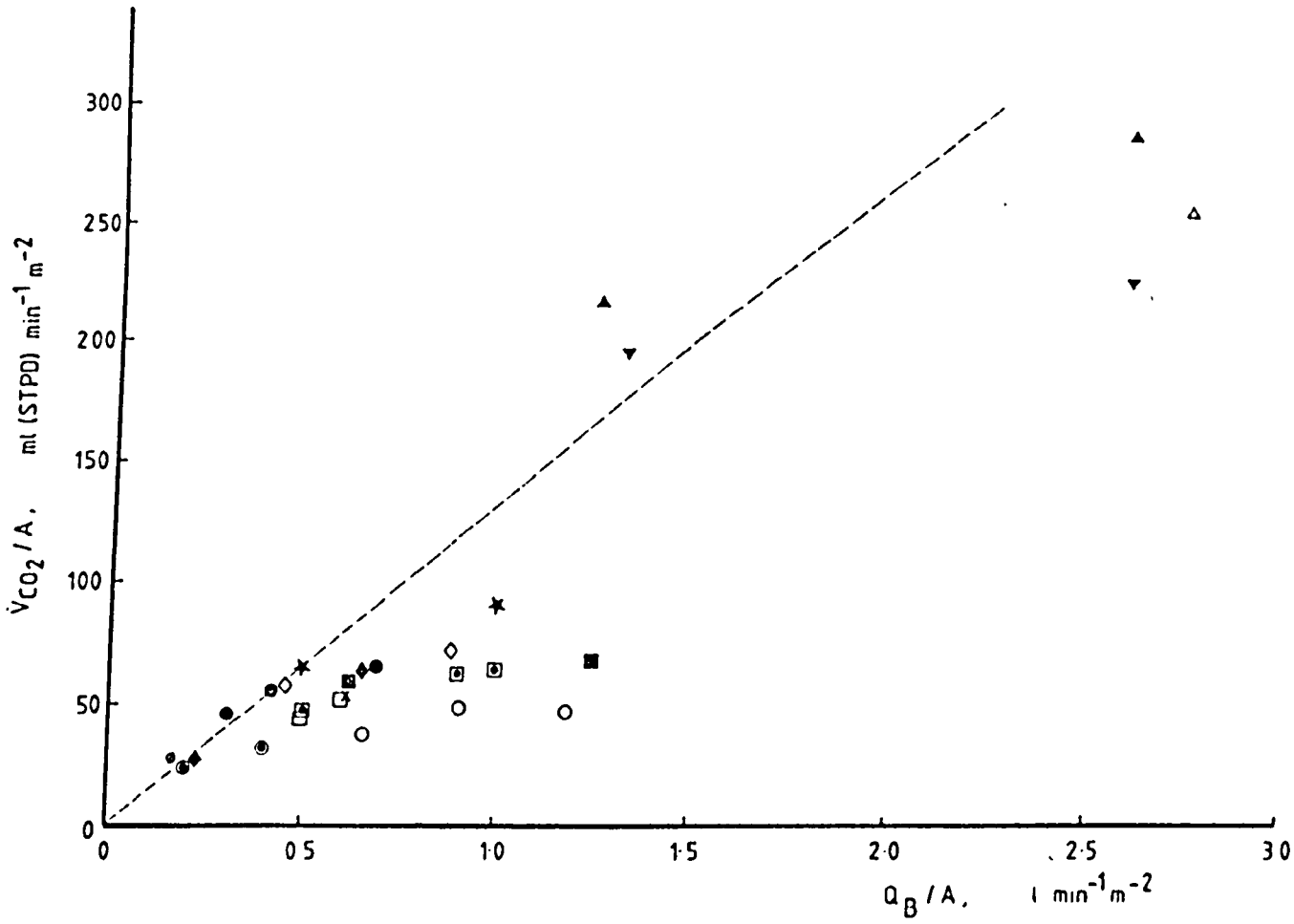

Figure 2.9. Normalised CO_2 transfer performance.

compared to more direct methods i.e. of the exhaust gas CO_2 fraction or actual measurement of blood CO_2 (Galletti et al. 1972). The foregoing review has not dealt with publications in which only pH and pCO_2 data have been reported.

A summary of the CO_2 transfer performance in membrane oxygenators under low blood flow rate conditions is presented in Table 2.5.

Normalized CO_2 transfer performance. Despite the variations in experimental test conditions and in some cases less than optimal ventilation rates, the laminar flow devices show remarkably similar performance characteristics. As the Q_B/A ratio increases, asymptotic $\dot{V}_{CO_2}/A$ values are obtained with laminar flow designs. In the case of the Sci-Med Kolobow design, relatively small increases in $\dot{V}_{CO_2}$ with increasing Q_B have been attributed to membrane permeability limitations (Murphy et al. 1979). Although membrane limited performance may be observed with homogeneous type membranes (Sci-Med), the performance of laminar flow devices with microporous membranes may be influenced by appreciable blood phase CO_2 resistance to transfer. This is clearly demonstrated by the much higher normalized values obtained with the pulsed-vortex secondary flow oxygenator.

It is interesting to predict the required membrane area in order to satisfy CO_2 transfer requirements for low flow $ECCO_2R$-LFPPV therapy. The broken line (Figure 2.9) represents the normalized performance at a CO_2 transfer rate of 200 mℓ(STPD)/min and at a blood flow rate of 1.5 ℓ/min. It would appear that some of the laminar flow devices are capable of achieving the CO_2 removal requirements but only at Q_B/A ratios of $\leq 0.5\ \ell\ min^{-1}m^{-2}$. At this Q_B/A ratio, membrane areas of $\geq 3\ m^2$ would be required. In contrast, for the

secondary flow pulsed-vortex device a Q_B/A ratio of about 1.7 $\ell\,min^{-1}m^{-2}$ and a membrane area of only 0.9 m^2 would be necessary.

2.5 Membrane Permeability

The purpose of the membrane in a blood oxygenator is to separate the blood and gas compartments, yet, at the same time, allow for high oxygen and carbon dioxide gas exchange rates through the membrane. For this reason, the membrane must be made thin enough so diffusion distances for the gases are short, yet mechanically strong enough to prevent rupture under imposed transmembrane pressure gradients.

Materials currently used in membrane oxygenators are classified into two main categories : (1) homogeneous (nonporous) and (2) microporous type membranes. The mechanism of gas transport differs in the two membrane types. In homogeneous membranes, gas transport occurs by diffusion and solution of the gas in the polymer. For microporous membranes, gas transport is primarily that of diffusive and convective flow through the pores. Both membrane types are commonly used in oxygenators. A third category, viz. composite or hybrid membranes has been evaluated as potential materials for membrane oxygenators (Ketteringham et al. 1975, Keller and Shultis, 1979). Two composite membranes which have reached commercial application are the polysulfone membrane (Dohi et al. 1981) and the silicone-coated polyrodosic cellulose membrane (Barthelemy et al. 1982). Table 2.6 lists various membrane materials and types used in oxygenators.

MEMBRANE TYPE	POLYMER MATERIAL
Homogeneous	Polydimethyl siloxane (silicone rubber)
	Polydimethyl siloxane-polycarbonate copolymer
Microporous	Polypropylene
	Polytetrafluoroethylene (PTFE)
Composites	Silicone-coated polynodosic cellulose
	Polysulfone

Table 2.6 Oxygenator membranes

Various factors affect the gas transport properties through the membrane. These factors are external experimental conditions, such as pressure and temperature and on internal polymer structures (Robb, 1968; Rogers, 1971). In the actual oxygenator application, the permeability characteristics of the membrane may be affected by blood contact (Keller and Shultis, 1979). In studies with microporous membranes, fluid migration into the pores (Keller and Shultis, 1979) or formation of a protein layer on the surface of the membrane (Bartlett et al. 1975; Longmore, 1981) indicate an appreciable reduction in gas permeation through the membranes.

2.5.1 Theory

Homogeneous membranes. The transfer rates of a gas, i, through a homogeneous membrane is a function of two properties: the diffusivity, $D_{i,m}$ ($m^2 s^{-1}$), and the solubility, $S_{i,m}$ (mol m^{-3} kPa^{-1}), of the gas in the polymer. If the gas flux, J_i, across a sheet membrane in the direction x is given by Fick's first law, then:

$$J_i = -D_{i,m} \frac{dC_{i,m}}{dx} \quad \frac{mol}{m^2 s} \tag{2.5}$$

where $c_{i,m}$ is the molar concentration of the gas in the membrane mol m^{-3}.

If the membrane is of thickness, t_m and C_1 and C_2 are the gas concentrations at the membrane surfaces then:

$$- \frac{dC_{i,m}}{dx} = \frac{C_1 - C_2}{t_m} \tag{2.6}$$

Assuming $C_{i,m} = S_{i,m}.P_{i,m}$ according to Henry's Law with P_i being the partial pressure of the gas then:

$$J_i = \frac{D_{i,m}.S_{i,m}}{t_m} (P_1 - P_2) \tag{2.7}$$

The product $D_{i,m}$ $S_{i,m}$ is known as the membrane permeability, Pr_i, and is useful in explaining the selectivity of homogeneous membranes to various gases. For example, the high solubility of CO_2 in silicone rubber accounts for the five times greater CO_2 permeability than that for O_2 since the gases have similar diffusivities in the polymer (Robb, 1968).

The permeability is an intrinsic property of the material. It is convenient when comparing different membranes of varying thicknesses to consider the gas transmission rate, G_i, which is defined as the gas flux per unit partial pressure difference across the membrane i.e. $J_i/(P_1-P_2)$. Thus for homogeneous membranes:

$$G_i = \frac{Pr_i}{t_m} \quad \frac{mol}{m^2 s.kPa} \tag{2.8}$$

Usually G_i is expressed in units of cm^3(STPD)/(cm^2.s.cmHg) for oxygenator membranes and for other membrane applications reported in the literature.

Microporous membranes. A similar gas flux expression can be stated for microporous membranes assuming the flux to be uniform across each pore diameter and in the absence of convective flow the diffusive flux, J_i is given by:

$$J_i = \frac{\phi D_{i,g} \tau}{t_m} (P_1 - P_2) \qquad (2.9)$$

where ϕ is the pore volume fraction

$D_{i,g}$ is the diffusivity of the gas, i within the gas phase inside the pore (cm^2/s)

τ is the tortuosity factor to account for the convoluted pores with the membrane structure.

Comparing equation (2.9) with equation (2.7) the gas transmission rate, G_i for microporous membranes gives:

$$G_i = \frac{\phi D_{i,g} \tau}{t_m} \qquad (2.10)$$

Convective flow through the pores occurs if an absolute pressure differential across the membrane exists (Yasuda and Lamaze, 1971). To avoid convective effects in gas-membrane-gas tests, isobaric conditions are necessary (Gaylor et al. 1975). In this situation diffusion will be influenced by the molecular diameter of the diffusing gases. As the molecular diameter of CO_2 (0.46 nm) is slightly greater than O_2 (0.30 nm), the permeability of CO_2 in microporous membranes will be less than for O_2. This would seem consistent with a permeability ratio Pr_{CO_2}/Pr_{O_2} of 0.89 reported by Gaylor et al. (1975) for microporous polypropylene (Celgard 2400, Celanese Corp.).

In the oxygenator application the gas phase total pressure

should not exceed that in the blood phase otherwise gaseous emboli would be introduced into the blood by convective flow through the membrane pores. The gas transfer will consequently be that of diffusion, however the dependency on molecular diameter may no longer apply if for example plasma migration occurs into the pores.

2.5.2 Review of literature

In principle gas permeability methods are of the same basic form. The permeant gas of interest passes from a source to a sink through the membrane which is the controlling resistance. The permeability of the gas is measured by the rate of depletion in the source or by the rate of appearance of permeant in the sink. The sink may be in the gas or liquid phase. For membrane oxygenator applications it is more useful to carry out gas permeability tests under gas- membrane-liquid contact conditions which better simulate the in vivo conditions of the oxygenator device.

The main obstacle in measuring gas permeabilities through the membrane under liquid contact experimental conditions is an associated liquid boundary layer resistance adjacent to the membrane. High speed stirring of the fluid (Katoh and Yoshida, 1978) combined with rapid chemical reaction to absorb the permeant gas (Keller and Shultis, 1979) or the use of open-pore cellular foam support to create mixing next to the membrane (Grimsrud and Babb, 1966) are reported techniques for reducing liquid boundary layer resistance. Furthermore, there are numerous methods for measuring the permeant gas in the liquid phase of the test system. Although a brief review will examine some of the techniques for measuring O_2 and CO_2 gas permeability through oxygenator membranes, particular reference will

be made to gas-membrane-liquid test methods for carbon dioxide transmission rates.

Esmond and Dibelius (1965) described a vertical rotating (100 r.p.m.) diffusion chamber for determining gas transmission rates of silicone rubber membranes. The blood volume in the chamber was 117 cm^3 and mixing to reduce the boundary layer effects was accomplished by a pool of mercury at the bottom of the blood chamber which mixed the blood during the rotation phase. Oxygen permeability was measured by flowing oxygen at 1 ℓ/min into a chamber opposite the blood compartment. The rotating chamber was stopped briefly at regular intervals to remove blood samples for testing.

Lautier et al. (1970) designed an experimental set up to determine gas transfer rates under gas-membrane-blood test conditions. The CO_2 was measured in the gas phase by a titration method. This was achieved by collecting the gas mixture from the test unit and bubbling the gas through an aqueous alkaline perchlorate solution (50 g/ℓ distilled water) which precipitated the carbon dioxide as barium carbonate and liberated H^+. The pH of the solution was kept constant at 10.0 by the addition of a solution of 0.1 or 1.0 M barium hydroxide, $Ba(OH)_2$ of a known titre. The amounts of added $Ba(OH)_2$ were recorded as a function of time. The titrating reagent was an 0.1 M hydrated barium hydroxide solution to which 50 g of barium perchlorate and 50 cm^3 of isopropanol were added per litre of solution. This reagent was filtered before use to remove barium carbonate formed during preparation.

The recording of the barium hydroxide solution volume as a function of time enabled the CO_2 transfer rate ($\dot{V}_{CO_2}$) to be calculated by the formula:

$$\dot{V}_{CO_2} = K.T.P \qquad (2.11)$$

where P is the slope of the volume-time curve

K is a constant depending upon the chart speed and the burette capacity

T is the titre of the barium hydroxide reagent.

All measurements were performed when a "steady state" was achieved, which results in a linear portion of the recorded curve. Lautier et al. (1970) also studied the effects of blood and oxygen flow rates and blood mixing on carbon dioxide transfer. All these factors resulted in a substantial increase of CO_2 as well as O_2 transfer rates. Although the intrinsic permeability of the membrane was not measured, the technique for determining CO_2 transfer is worth noting.

Ketteringham et al. (1975) carried out an extensive study of oxygen and carbon dioxide gas transmission rates of membranes used in blood oxygenators. The blood-membrane-gas tests were performed in a spiral channel cell of diameter 12.5 cm exposing a membrane test area of 98.3 cm^2. Outdated human bank blood was used and adjusted to pH 7.4. The blood pressure drop across the channel was 76 mmHg at 10 mℓ/min flow rate. The CO_2 transfer rate through the membrane was calculated from the carbon dioxide fraction of the ventilation gas at exit using an infra-red CO_2 analyser and the gas flow rate. CO_2 transmission rate (G_{CO_2}) was obtained from the transfer rate and the appropriate logarithmic mean pCO_2 difference.

The flow dependence of G_{CO_2} indicates that the transfer resistance is a function of the membrane resistance and an apparent "blood film" resistance. Ketteringham et al. (1975) investigated

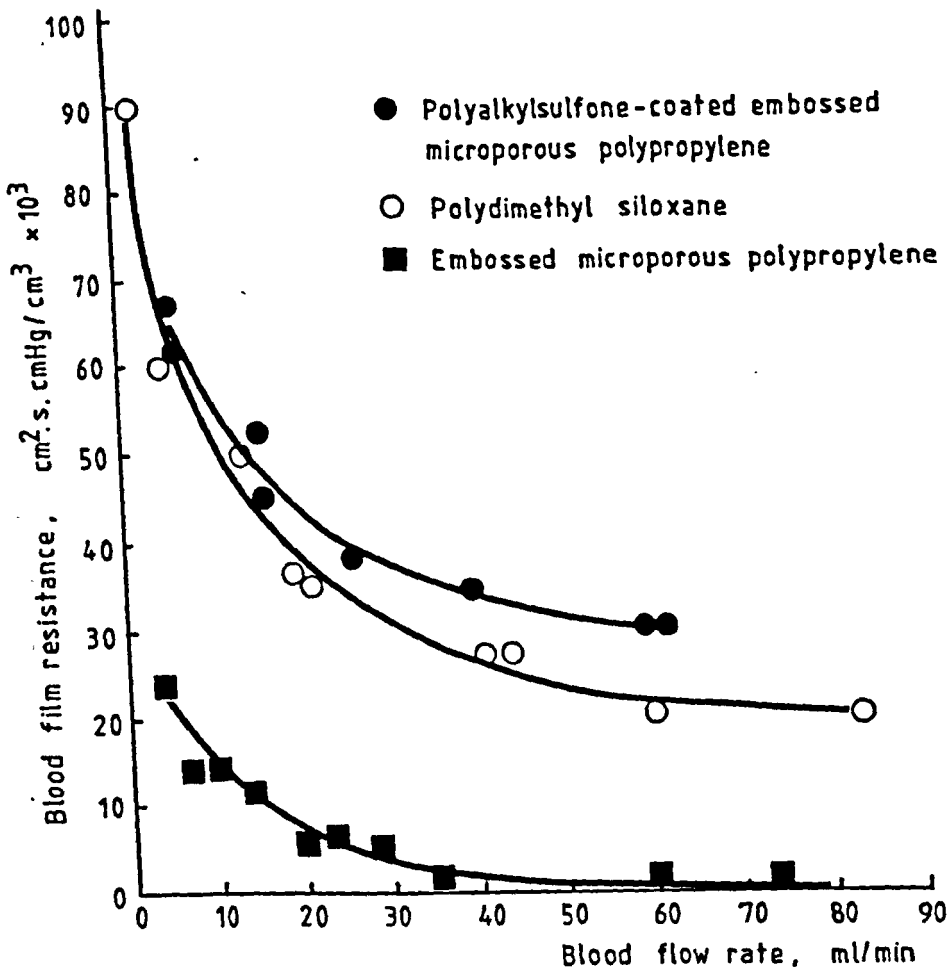

Figure 2.10 Carbon dioxide transfer dependence on "blood film" resistance and blood flow rate (from Ketteringham et al. 1975).

this by measuring the G_{CO_2} of the membrane in the spiral cell under a gas-membrane-gas test condition and calculating the value of the "blood film" resistance as a function of blood flow rate according to:

$$\text{Blood film resistance} = \frac{1}{\text{overall permeability}} - \frac{1}{\text{membrane permeability}} \quad (2.12)$$

Although equation 2.12 is valid for homogeneous membranes, it is not necessarily true for microporous membranes since gas-membrane-liquid test conditions may alter their permeability characteristics.

The values obtained for polyalkylsulfone (PAS) - coated embossed microporous polypropylene, polydimethyl siloxane and embossed microporous polypropylene at 24°C are shown in Figure 2.10. Ketteringham and coworkers showed that the carbon dioxide transfer rates are 6-10 times greater than oxygen transfer for the microporous PAS-coated polypropylene than for polydimethyl siloxane membrane at comparable flow rates. Therefore, in a device with secondary flow, blood film resistances are reduced and higher oxygen and carbon dioxide transfer in PAS membranes can be taken advantage of. Data was also presented for the G_{CO_2} of PAS-coated and uncoated microporous polypropylene, and a polydimethyl siloxane/polycarbonate copolymer under blood-to-gas test conditions as shown in Table 2.7.

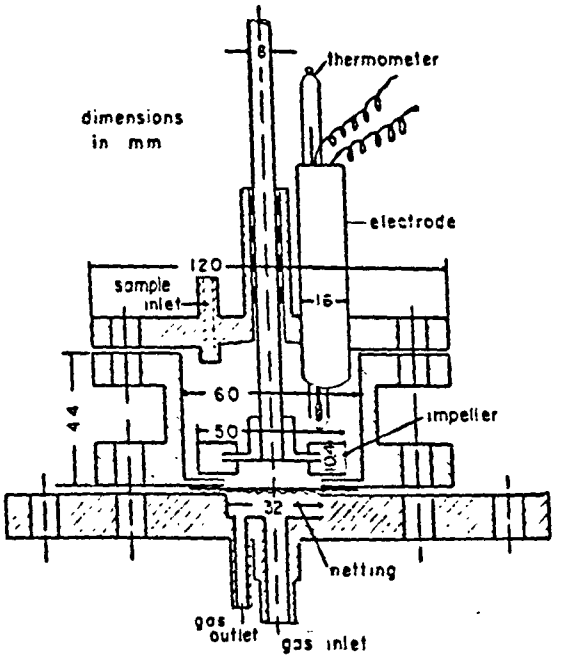

Figure 2.11 Experimental absorber (from Katoh and Yoshida, 1972).

	Normalised blood flow rate ($\frac{cm^3}{min\ m^2}$)		
Membrane	500	1000	2500
PAS on microporous polypropylene	6.0×10^{-5}	7.8×10^{-5}	1.09×10^{-4}
Uncoated microporous polypropylene	5.85×10^{-5}	8.51×10^{-5}	1.45×10^{-4}
Polydimethyl siloxane/ polycarbonate copolymer	-	8.99×10^{-6}	1.49×10^{-5}

Table 2.7 Blood-to-gas carbon dioxide transmission rates in cm^3 (STPD)/(cm^2.s.cmHg) at 37°C.

Katoh and Yoshida (1972) studied the rate of absorption of oxygen into deoxygenated blood through four types of membranes. The test absorber (Figure 2.11) was equipped with a stainless steel variable speed stirrer. In the centre base of the vessel the test membrane is supported by a wire mesh over a 3.2 cm diameter opening. Gases were passed in the bottom cover beneath the membrane. A thermometer and an oxygen electrode were inserted through the top cover of the vessel. The membranes evaluated in the system were Teflon (25 μm thick), "Phycon", (Fuji Polymer Industries Ltd) a silicone rubber membrane reinforced with nylon mesh (approximately 150 μm thick), "Phycon Non-woven", a silicone rubber membrane reinforced with non-woven fabric (approximately 70 μm thick) and "Silastic" 500-1 (125 μm thick, Dow Corning Inc.). In addition to blood, other liquids were used as absorbents for oxygen.

An analysis of the results was obtained from an oxygen mass balance:

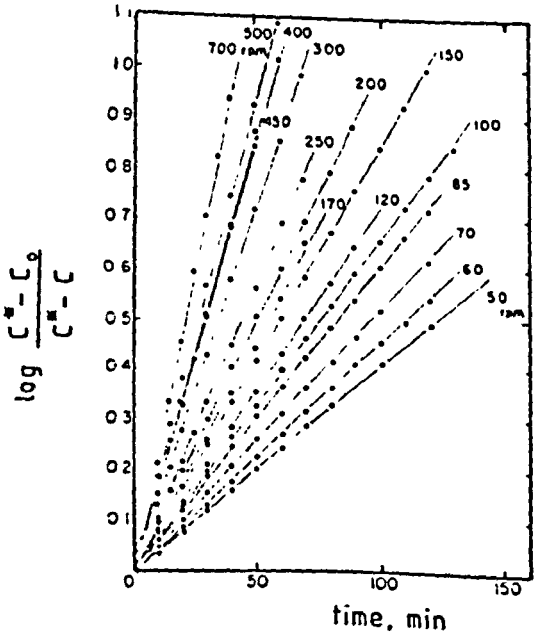

Figure 2.12 Plots for evaluation of K_L, oxygen absorption into water through Phycon membrane at 36.5 °C.

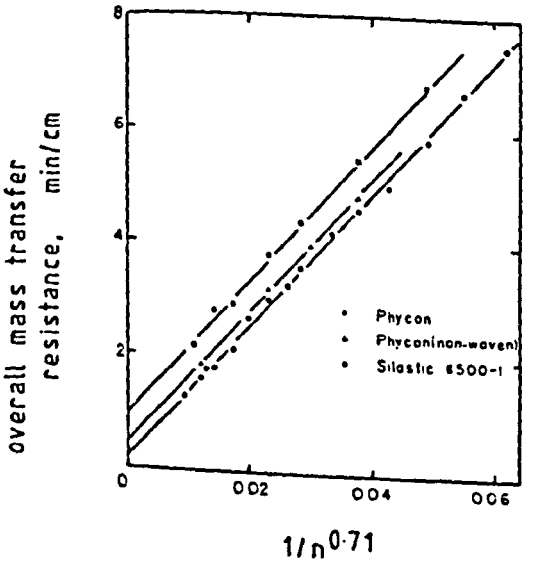

Figure 2.13 Wilson plots to determine membrane resistance.

$$V \frac{dc}{dt} = KA(C^*-C) \qquad (2.13)$$

Integration gives

$$\log\left[\frac{C^*-C_o}{C^*-C}\right] = \frac{KA}{2.303V} t \qquad (2.14)$$

For a given value of K, a plot of the left-hand side of equation (2.13) against the time t from the start of run should give a straight line passing through the origin, from the slope of which K can be evaluated. Figure 2.12 shows the plots of liquid phase mass transfer coefficient (K_L) variation with stirrer speed (n) for the runs with the Phycon membrane at 36.5 ^oC. Figure 2.13 shows the Wilson plots for oxygen absorption into water with three types of membranes. The overall resistance to transfer is plotted as a function of n^{-a} (where a is arbitrarily selected to give a linear relationship). From the linear fit, one can conclude that the liquid phase mass transfer coefficient K_L varies in proportion to the stirrer speed n to the power of a (a = 0.71). Extrapolation back to the intercept at the ordinate gives the membrane resistance (as $n^{-a} \to 0$, when $n \to \infty$, i.e. zero resistance is assumed at infinite stirrer speed). The membrane resistances thus obtained can be deducted from the overall resistance to give the liquid phase resistance.

Using the above test system and a similar analysis Katoh and Yoshida (1978) determined the CO_2 permeability of a silicone rubber (100 μm thick, Fuji Systems Co., Japan) and the microporous polypropylene (20 μm thick, Celanese Corp., USA.) membranes. The values obtained were 3.4 x 10^{-5} cm^3 (STPD)/(cm^2s cmHg) for the

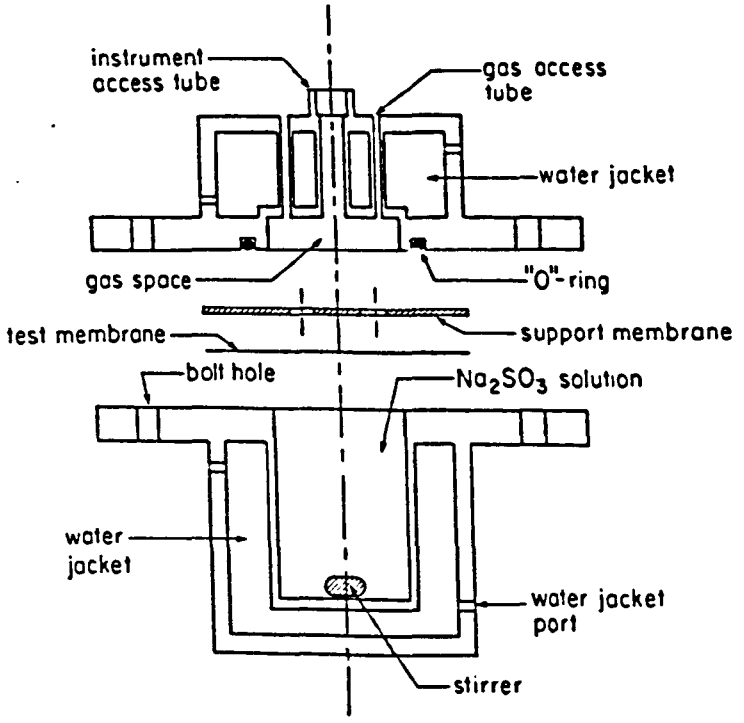

Figure 2.14 Schematic diagram of apparatus used to measure membrane oxygen permeability (Keller and Shultis, 1979).

silicone rubber, and 4.1 x 10^{-4} cm^3 (STPD)/(cm^2 s.cmHg) for the microporous polypropylene membrane.

Keller and Shultis (1979) developed a test system for measuring oxygen transmission rates (G_{O_2}) through membranes in the gas-membrane-liquid transfer mode in which the liquid phase transport resistance is reduced to a negligible level. This was achieved by a chemical reaction on the liquid side which reacts rapidly and irreversibly with the oxygen crossing the membrane. Sodium sulphite (Na_2SO_3) was chosen as the "oxygen" sink for the reaction. Na_2SO_3 combines irreversibly with O_2 to give sodium sulphate. This reaction is catalysed by cobaltous nitrate. The kinetics of the reaction is discussed in more detail by Shultis (1980).

The permeability test cell (Figure 2.14) consists of lower and upper chambers, between which the test membrane is securely held. Instrumentation ports for monitoring oxygen partial pressures are located in the upper chamber. Na_2SO_3 solution is placed in the lower chamber and the test membrane is sealed in place. Humidified oxygen is introduced through the upper chamber and isolated. The decrease in oxygen pressure is measured as a function of time for about 10 minutes and the permeability is determined from the data. In the same study, the effect of 3 hours exposure of the membrane to blood on permeability was assessed, after which the permeability measurement was carried out, the membrane was rinsed and once again exposed to the blood fraction. The process was repeated after 6, 12 and 24 hr of exposure.

Several membranes were studied; Celgard microporous polypropylene, silicone rubber and PS-200 (a single ply celgard micro-

porous membrane coated on one side with a 1.5 μ polysulphone-polysiloxane copolymer film). A smooth and a rough side permeability value was reported by Keller and Shultis (1979) for the Celgard microporous membrane. Based on the oxygen permeability results of these membranes (Table 2.8) it was postulated that the main resistance to gas transfer through microporous membranes is the liquid migration into the pores so that gas transfer is limited by the rate of oxygen diffusion through the stagnant liquid in the pores.

membrane	G_{O_2}, $\frac{cm^3(STPD)}{cm^2\ s\ cmHg}$
Celgard microporous polypropylene	
- "smooth" side	$1.45 \pm 0.15 \times 10^{-5}$
- "rough" side	$2.30 \pm 0.2 \times 10^{-5}$
Sci-Med 2.5 μm silicone rubber	$2.2 \pm 0.3 \times 10^{-5}$
PS-200	$1.6 \pm 0.25 \times 10^{-4}$

Table 2.8 Oxygen permeabilities of tested membranes at 37 °C.

The higher permeability of the PS-200 membrane seems to be consistent with this hypothesis, since the film coating the liquid-contacting side of this membrane prevents liquid from entering the pores.

The effect of long-term blood contact on the membrane has been shown to cause a reduction in permeability. Keller and Shultis (1979) also tried to differentiate the blood components which may affect permeability, by exposing the membrane to serum and plasma, in order

to examine the effects of fibrinogen adsorption. The PS-200 membrane was the only one showing no loss of permeability following 24 hours exposure to serum.

Dohi et al (1981) measured a polysulfone membrane permeability in a 50cm^2 test cell under gas-membrane-liquid test condition. The 1.0ℓ of water was deoxygenated by bubbling nitrogen gas and circulated at a high flow rate of 500 mℓ/min in the circuit, while O_2 or CO_2 was absorbed through the test cell. During the test procedure, pO_2 or pCO_2 in the water was measured at regular intervals. The boundary layer resistance on the water side was reduced by circulating the water at a high flow rate. In spite of high flow rate operation similar to Ketteringham et al. (1975), the validity of reducing boundary layer resistance to a negligible level was not demonstrated in this experimental circuit.

2.5.3 Summary.

Reported literature values on gas permeabilities through membranes show substantial variations depending on the test conditions used. Typical carbon dioxide gas transmission rates are at least 5 times greater under gas-membrane-gas compared to gas-membrane-liquid test conditions for the Celgard microporous polypropylene and the polydimethyl siloxane membranes (Gaylor et al. 1975; Katoh and Yoshida, 1978). Table 2.9 gives the summary of CO_2 gas transmission rates reported in the literature, together with O_2 gas transmission rates for comparison.

For the liquid phase, human blood (Ketteringham et al. 1975), bovine blood, aqueous solutions of haemaglobin as well as distilled water have been used. (Katoh and Yoshida, 1978). Moreover,

Membrane	Test condition	$G^*_{CO_2}$	$G^*_{O_2}$	Reference
Celgard microporous polypropylene 2400	gas-to-gas	6.2×10^{-3}	7.0×10^{-3}	Gaylor et al. 1975
Silicone rubber		8.26×10^{-4}	1.58×10^{-4}	
Celgard microporous Polypropylene	gas-to-Na_2SO_2			
-smooth side		-	1.45×10^{-5}	Keller and Shultis 1979
-rough side			2.3×10^{-5}	
Sci-Med silicone rubber		-	2.2×10^{-5}	
PS-200		-	16.0×10^{-5}	
Celgard microporous Polypropylene	water-to-gas	4.1×10^{-4}	-	Katoh and Yoshida 1978
Silicone rubber		3.4×10^{-5}	-	
Microporous polypropylene	blood-to-gas	1.45×10^{-4}	-	Ketteringham et al. 1975
Silicone rubber		3.0×10^{-5}	-	

*Gas transmission rate (G) is in units of $\frac{cm^3(STPD)}{cm^2 \text{ s cmHg}}$.

Table 2.9 Comparison of CO_2 and O_2 gas transmission rates through oxygenator membranes.

different analytical methods are reported for CO_2 measurements depending on whether CO_2 is determined in the gas or liquid phase. In CO_2 desorption evaluations where CO_2 is measured in the gas phase, infra-red CO_2 analyser (Katoh and Yoshida, 1978; Ketteringham et al. 1975), titration method using $Ba(OH)_2$ (Lautier et al. 1970) and manometric method (Shultis, 1980) have been reported. Where CO_2 measurements are carried out in the liquid phase, pCO_2 electrodes are commonly used to monitor the CO_2 content change. Mechanical stirring or the use of porous support structures are used to reduce the liquid boundary layer resistance. Chemical reactions in the liquid phase can also reduce boundary layer resistances (Shultis, 1980).

A test method for determining gas permeabilities through membranes under gas-membrane-liquid test conditions must be able to reduce the liquid boundary layer resistances to a negligible level. Moreover a suitable method of CO_2 determination is also necessary. pCO_2 electrodes are subject to response time errors (Adams and Hahn, 1982) thus a more accurate method is desirable.

A test system which takes into account liquid boundary layer resistance and a chemical reaction which rapidly combines with the CO_2 as it crosses the membrane is described in Chapter five.

The CO_2 measurements were performed using the Corning carbon dioxide analyser (Corning Medical Ltd., England) available for the oxygenator evaluations.

CARBON DIOXIDE TRANSFER MODELS

Mathematical modelling of biological systems has become an important tool to aid the design of medical engineering devices. For example in membrane lungs, the basic problem is that of mass transfer between the blood and gas separated by a semi-permeable membrane. Models to describe oxygen and carbon dioxide transfer in membrane lung channels with laminar flow present major problems. Gross simplifications must be made, and the justification of these assumptions often lies in the effectiveness of the final model. It is always essential to verify the model by comparing the predicted behaviour with that determined experimentally. Once the model has proven to give an accurate simulation, the model can be used to alter major parameters with relative ease. For example, the effect of blood flow rate or length of flow path on mass transfer, can be studied and design parameters can be determined without resorting to an extensive experimental programme.

This chapter presents briefly the basis of mass transport, the convective-diffusion equation for the theoretical analyses applicable to membrane lungs, and the various carbon dioxide models reported in literature. The comprehensive model developed by Voorhees (1976) was selected as appropriate for correlation with experimental work as carried out in the thesis. Numerical solution was performed utilising a computational package developed by Dr. P.J.D. Mayes of the Department of Mathematics, Strathclyde University. Results from the mathematical model are presented for tubular and parallel plate geometries. For reference input conditions the influence of membrane resistance and gas phase pCO_2 are examined.

3.1 Mass Transport

The mass transport mechanism of interest in membrane lungs is that of molecular diffusion. This is the movement of a chemical species from a region of higher concentration to one of lower concentration and is termed ordinary diffusion. The term "ordinary" is used to distinguish this mode of transfer from diffusion as a result of thermal or pressure gradients or external forces. Usually for the physical conditions existing in the membrane lung, we need only consider ordinary diffusion, which will be referred to simply as diffusion in this chapter unless otherwise stated.

When diffusion is coupled with fluid motion due to external means, we have convective mass transfer. Other higher order mass transfer modes are active transport and facilitated transport, both of which are of physiological interest. Basically, facilitated transport is diffusion aided by a carrier, while active transport goes against concentration gradients, with energy provided by such means as biological or biochemical reactions.

3.2 Convective-Diffusion Equation

Mass transfer problems in blood flowing in membrane lung channels or tubes are described by the general form of the convective-diffusion equation as follows:

$$\frac{DC_{i,k}}{Dt} = -\nabla J_{i,k} + q_{i,k} \qquad (3.1)$$

Rate of accumulation of specie i in phase k.	Net diffusional flux of specie i in phase k.	Rate of chemical production of specie i in phase k.

The equation accounts for the convection, diffusion and chemical reaction of species i, in a homogeneous and isotropic phase k. With further assumptions of steady-state, constant total mass density conditions and applying Fick's Law, equation (3.1) in vector notation becomes:

$$\text{div}(\vec{V} C_{i,k}) = \nabla \cdot D_{i,k} \nabla C_{i,k} + q_{i,k} \qquad (3.2)$$

Where $\vec{V}$ is the velocity vector and $D_{i,k}$ is the diffusional coefficient of specie i in phase k. Equation (3.2) is the basic equation for the theoretical analysis of oxygen and carbon dioxide transfer in membrane lungs. To simplify the problem, the majority of published analyses assume that:

(a) Blood is a homogeneous, incompressible, Newtonian fluid

(b) Fully developed laminar flow exists at entry into the mass transfer section of the tube or channel

(c) Convection occurs only in the axial direction

(d) Diffusion occurs only in the direction perpendicular to the tube or channel wall

(e) Diffusion coefficient of specie i is constant

(f) Local chemical equilibrium exists throughout the phase.

Since the tube or channel dimensions (> 150 μm) in membrane oxygenators are much greater than the size of the red blood cell (about 8 μm), it is reasonable to assume the blood to be homogeneous and a continuum approach is valid. Furthermore, as blood is a heterogeneous fluid on a microscopic level, the simple Fick's Law relationship employing molecular diffusivities cannot be used directly (Spaeth, 1970). The usual procedure is to introduce an effective diffusivity for dissolved gas diffusing through blood.

Effective diffusion coefficients are dependent on the haematocrit, the relative permeabilities of the continuous (plasma) and suspended (red cells) phases, as well as temperature and viscosity. Consequently, it has been difficult to obtain reliable diffusivity data for carbon dioxide species in blood. Similar problems are encountered for the determination of oxygen diffusivity in blood.

Local chemical equilibrium can be assumed if the red cell membrane resistance to bicarbonate ions is negligible compared with the oxygenator membrane resistance and the changes in CO_2 content are small. Voorhees (1976) stated that the local equilibrium assumption may be valid for low blood flow conditions and large channel dimensions typical of commercial membrane oxygenators.

Given the local equilibrium the continuum assumption, equation 3.2 may be summed for the three CO_2 species that exist in blood i.e. dissolved, bicarbonate and carbamino forms. With the other assumptions listed in section 3.2 one obtains for a tubular geometry with radial and axial co-ordinates r and z respectively:-

$$V_z \frac{\partial C_T}{\partial z} = \frac{1}{r} \frac{\partial}{\partial r} \left[r\left(D_d \frac{\partial C_d}{\partial r} + D_b \frac{\partial C_b}{\partial r} + D_c \frac{\partial C_c}{\partial r}\right)\right] \qquad (3.3)$$

where the total CO_2 concentration C_T is the sum of the dissolved CO_2 (C_d), bicarbonate (C_b) and carbamino CO_2 (C_c) concentrations:

$$C_T = C_d + C_b + C_c \qquad (3.4)$$

D_d, D_b and D_c are the respective diffusivities and V_z is the axial velocity which is a function of r only.

The majority of CO_2 transfer models reported in the literature are based on equation 3.3 and differ in the relations for C_T and in the treatment of the individual diffusion terms. Most models assume Newtonian fluid behaviour for blood and hence the axial velocity

profile V_z is parabolic.

Equation 3.3 is solved in conjunction with a set of boundary conditions appropriate to the problem. All models assume uniform concentration at inlet to the transfer section and axisymmetric transfer. At the membrane wall either constant concentration or flux matching conditions may be taken. The flux matching condition is the more general case and allows for a finite wall resistance to gas transfer whereas the constant concentration at the wall implies zero wall resistance.

3.3. Review of CO_2 Transfer Models

A comprehensive review of existing CO_2 transfer models in membrane oxygenators has been compiled by Voorhees (1976) and Colton (1976). Therefore only a brief résumé of CO_2 transfer models is presented below with the most complete CO_2 transport models of Benn (1974) and Voorhees (1976) described in greater detail. The most common membrane oxygenator geometry investigated is the tubular type.

Weissman and Mockros (1967) proposed a model to theoretically predict carbon dioxide removal in a permeable tube. The total carbon dioxide content, C_T was taken to be a linear function of the dissolved CO_2 concentration, C_d:-

$$C_T = 1.14 \times 10^{-2} + 10.00 C_d \qquad (3.5)$$

where C_T and C_d are in mmol/ℓ.

Since C_T is a function of C_d only then the term $\partial C_T/\partial z$ in equation 3.3 may be written as

$$\frac{\partial C_T}{\partial z} = \frac{dC_T}{dC_d} \cdot \frac{\partial C_d}{\partial z} = 10 \frac{\partial C_d}{\partial z} . \qquad (3.6)$$

For the assumption of Newtonian behaviour for blood

$$V_z = 2\bar{V}\left[1 - \left(\frac{r}{R_1}\right)^2\right] \tag{3.7}$$

where $\bar{V}$ is the mean velocity in the tube and R_i is the tube internal radius.

Weissman and Mockros considered the diffusion of HCO_3^- and carbamino CO_2 to be negligible and hence with equations 3.6 and 3.7, equation 3.3 becomes:-

$$2O\bar{V}\left[1 - \left(\frac{r}{R_i}\right)^2\right]\frac{\partial C_d}{\partial z} = D_d\left[\frac{1}{r}\frac{\partial}{\partial r}\left(r\frac{\partial C_d}{\partial r}\right)\right] \tag{3.8}$$

which is a linear partial differential equation (PDE).

The PDE was solved with the following boundary conditions:

Uniform inlet concentration

$$C_d = C_{d,in} \quad \text{at} \quad z = 0, \quad 0 \leq r \leq R_i$$

Axisymmetry

$$\frac{\partial C_d}{\partial r} = 0 \quad \text{at} \quad r = 0, \quad z \geq 0$$

constant wall concentration (zero wall resistance)

$$C_d = C_{d,w} \quad \text{at} \quad r = R_i, \quad z \geq 0 \tag{3.9}$$

Defining the following dimensionless variables:-

$$r^* = \frac{r}{R_i}\ ; \quad z^* = \frac{D_d z}{2O\bar{V}R_i^2}\ ; \quad C^* = \frac{C_d - C_{d,in}}{C_{d,w} - C_{d,in}}$$

then equation 3.8 can be expressed in dimensionless form as:

$$(1-r^{*2})\frac{\partial C^*}{\partial z^*} = \frac{1}{r^*}\frac{\partial}{\partial r^*}\left(r^*\frac{\partial C^*}{\partial r^*}\right) \tag{3.10}$$

with boundary conditions:

$$\left.\begin{array}{llll} C^* = 0 & \text{at} & z^* = 0, & 0 \leq r^* \leq 1 \\ \dfrac{\partial C^*}{\partial r^*} = 0 & \text{at} & r^* = 0, & z^* \geq 0 \\ C^* = 1 & \text{at} & r^* = 1, & z^* \geq 0 \end{array}\right\} \qquad (3.11)$$

Equation 3.10 and boundary conditions constitute the classical Graetz problem for convective heat transfer in which an analytical solution may be obtained (e.g. Sellars et al., 1956). Weissman and Mockros offered no experimental data to validate their transfer model. Comparison with an analysis for oxygen transfer showed that for laminar flow the length of tubing needed to eliminate CO_2 is less than the length needed for oxygen uptake.

Villarroel et al. (1970) modelled CO_2 transfer in a tubular geometry for laminar and shear-augmented diffusion. The same relationship as Weissman and Mockros (1967) was used to approximate the total carbon dioxide content (equation 3.5). Thus the convective-diffusion equation was solved neglecting bicarbonate and carbamino diffusion terms. By assuming bicarbonate concentration constant through the tube, pH profiles were generated from C_d (or pCO_2) profiles via the Henderson-Hasselbalch equation. An improvement over the previous model was the incorporation of a flux matching wall condition to account for a finite wall resistance. In a comparison with the oxygen transfer analysis, similar conclusions as Weissman and Mockros (1967) were obtained. Villarroel et al. (1970) concluded that the wall resistance parameter is significant for the transport of oxygen and carbon dioxide and must be considered in the mathematical analysis, especially in the case of carbon dioxide. No experimental data were reported to verify the CO_2 transfer model.

In a further paper experimental data were obtained for comparison with the CO_2 theoretical model (Villarroel and Lanham, 1973). pCO_2

data obtained compared well with the theory, but this agreement was attributed to the wall limited nature of their experimental devices (Voorhees, 1976). Total CO_2 transfer rates were not reported.

Harris et al. (1970) formulated the convective-diffusion equation for tube flow by assuming the following non-linear relationship between C_T and pCO_2:

$$C_T - C_d = \frac{\omega pCO_2}{1+\omega pCO_2} \qquad (3.12)$$

where C_T, C_d is in mol/ℓ

pCO_2 is in mmHg

and ω is an empirical constant.

A value of $\omega = 0.02386$ was found to give the best data fit over the range $0 \leq pCO_2 \leq 140$ to the CO_2 dissociation curve reported by Guyton (1966). In the CO_2 model, only diffusion of dissolved CO_2 was considered and a non-Newtonian velocity profile was incorporated in the equation. No indication was given by the authors as to whether they had solved their CO_2 transfer theory hence no conclusion can be drawn from their study as to the validity of the model. Experimental data were not reported in this study for comparison purposes.

Bradley and Pike (1971) considered carbon dioxide removal as dependent on the simultaneous oxygen uptake. The model was derived by simplifying the general convective-diffusion equation for steady-state, isothermal flow of blood in a permeable tube. The diffusion of the bicarbonate ion and carbamino CO_2 was neglected and the only diffusing specie considered was dissolved CO_2. Since the carbon dioxide dissociation curve is influenced by pO_2 or oxygen saturation,

a linear relationship between C_T and pCO_2 in blood was modified to include an oxygen saturation term (S) given by:

$$C_T = 16.8 - 3.36S + 0.205pCO_2 \qquad (3.13)$$

where C_T is in mmol/ℓ

S is the fractional O_2 saturation of haemoglobin

pCO_2 is in mmHg

The modified convective-diffusion equation was solved numerically with an oxygen saturation term included:

$$V_z \left[\frac{0.205}{\alpha_d}\frac{\partial C_d}{\partial z} - 3.36\frac{\partial S}{\partial z}\right] = D_d \frac{1}{r}\frac{\partial}{\partial r}\left(r\frac{\partial C_d}{\partial r}\right) \qquad (3.14)$$

where α_d is the solubility coefficient of dissolved CO_2 in blood with boundary condition:

$$\left.\begin{aligned} C_d &= C_{d,in} \quad \text{at} \quad z = 0, \quad 0 \leq r \leq R_i \\ \frac{\partial C_d}{\partial r} &= 0 \quad \text{at} \quad r = 0, \quad z \geq 0 \\ C_d &= C_{d,w} \quad \text{at} \quad r = R_i, \quad z \geq 0 \end{aligned}\right\} \qquad (3.15)$$

The theoretical model underpredicted carbon dioxide transfer compared to that found experimentally. The discrepancy between the theory and experimental data is due to the limitations of the model. The carbon dioxide model was taken to be independent of pH, but CO_2 removal is a function of pH via the bicarbonate ion and carbamino CO_2. Hence taking into account bicarbonate ion and carbamino CO_2 as important diffusion species may give a more reliable CO_2 transfer model.

3.3.1 Benn's weak acid model

Benn (1974) postulated that a weak acid solution containing CO_2, HCO_3^- and carbonic anhydrase would be similar to blood in its CO_2

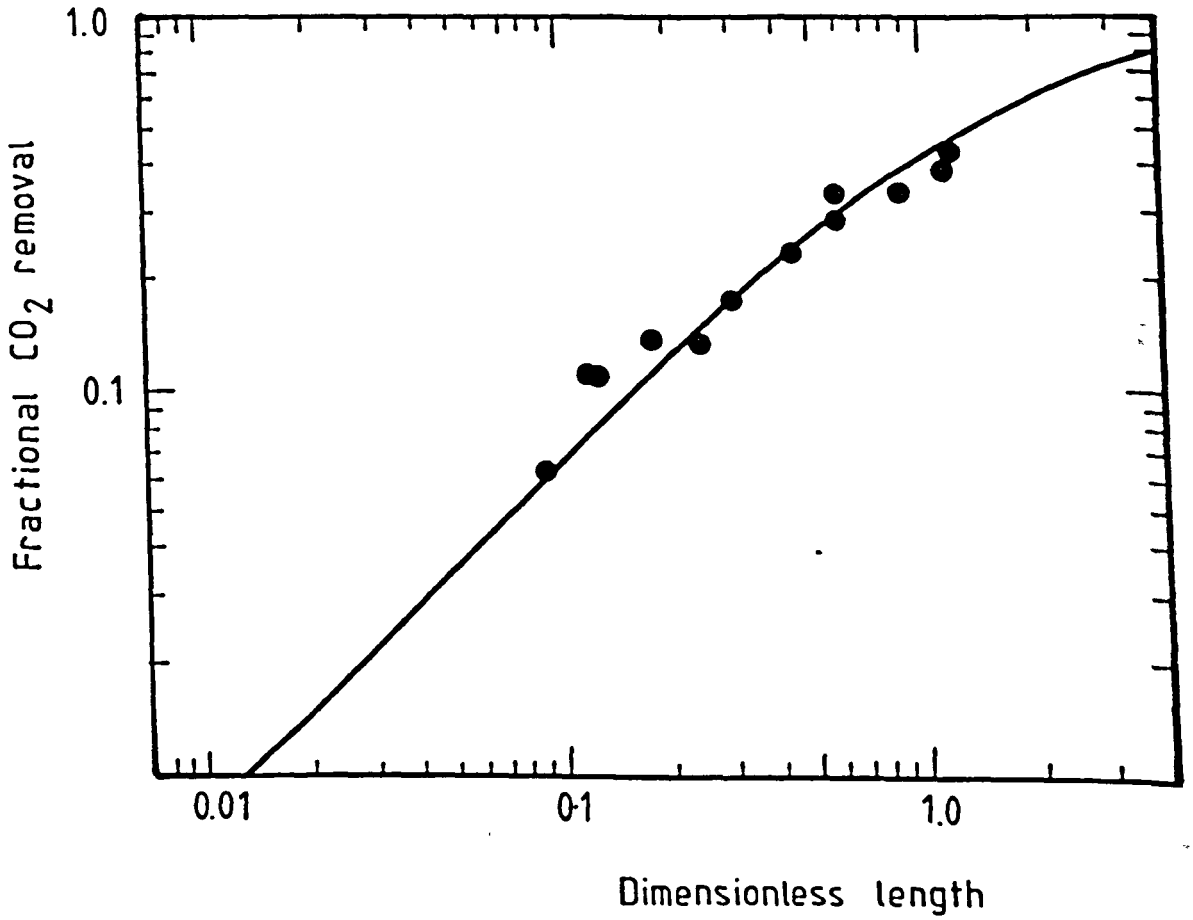

Figure 3.1 Theory and data for fractional CO_2 removal for blood flowing in a permeable tube. The dimensionless reaction rate (R) is $\geq$ 500 and f(HHb) = 0.45 (after Benn 1974).

transfer characteristics. He showed that weak acid diffusion has an important role in the transfer of the CO_2 species. In a weak acid phosphate (H_3PO_4) buffer solution and pH range of 7.0 to 7.6, only HCO_3^- and dissolved CO_2 are the main species to be considered in the general convective-diffusion equation. An overall buffering behaviour of the weak acids was assumed in the model.

An extension of the weak acid model was considered for CO_2 transfer in blood. The modified version takes into account the effect of CO_2 released from haemoglobin during oxygenation. Benn also included facilitation of CO_2 transport by HCO_3^-, the kinetics of carbonic anhydrase (assumed to be uniformly distributed throughout the blood) and the effects of weak acids (for example, haemoglobin, globulins, albumins and phosphates) in the blood.

Blood was assumed to be a homogeneous fluid and the convective-diffusion equation was written for dissolved CO_2 and HCO_3^-. Carbamino CO_2 was incorporated into the dissolved CO_2 in the tube. The resulting transfer equations were non-dimensionalized and solved numerically. Details of the equations can be referred to in Benn's Ph.D. thesis (Benn, 1974).

To validate the theoretical model blood experiments were carried out. In the experiments with fresh whole blood a good agreement between theory and experimental data was obtained (figure 3.1). This was only valid if the O_2 related effects denoted by f(HHb) were minimal and the CO_2-bicarbonate reaction rate (R) was chosen such that equilibrium transfer conditions existed in the blood channel. The boundary condition at the tube wall for all species except dissolved CO_2 is zero flux. The fractional CO_2 removal, θ_c, is related to the uniform inlet CO_2 content C_{Ti}, and the cup-mixed outlet CO_2 content $\bar{C}_{To}$ by:

$$\theta_c = (C_{Ti} - \bar{C}_{To})/C_{Ti} \qquad (3.16)$$

and the dimensionless tube length, which is equal to $(D_d z)/(4R_i^2\bar{V})$.

Benn used a value of 1.92×10^{-5} cm^2/s for D_d and 1.18×10^{-5} cm^2/s for D_b. Using these values a ratio of D_b/D_d of 0.615 was calculated. At $R \geq 500$ and f(HHb) = 0.45, CO_2 and HCO_3^- was considered to be at "equilibrium" throughout the CO_2 transfer process. The blood inlet conditions used were: 21.0 mmHg pCO_2, 18.0 mmHg pO_2, 7.62 pH, 27.5 O_2 saturation, 16.0 g% Hb and 24°C temperature. The CO_2 total content determinations were performed using the Van Slyke apparatus.

3.3.2 Voorhees' model

Voorhees (1976) described a theoretical model to account for the different CO_2 diffusing species in blood flowing in macrochannel devices with tubular and parallel plate geometries. The model was a development from his initial CO_2 transfer theory (Dorson and Voorhees, 1974) which assumed that the total CO_2 content and bicarbonate ion were a linear function of dissolved CO_2. This approximation however did not give a good agreement with experimental data and was abandoned in favour of the present theoretical CO_2 model. In this model, several assumptions are made. Blood is treated as a homogeneous fluid, under steady state and local chemical equilibrium conditions. Bicarbonate ion is considered to be an important diffusing specie and a simple equilibrium relationship was derived for the concentration of dissolved CO_2 (denoted by C_1) in terms of the concentration of reacted CO_2 (denoted by C_2). The CO_2 dissociation curve is approximated by the equation

$$C_1 = \frac{C_2}{K'} 10^{C_2/\beta} \qquad (3.17)$$

(a) Permeable tube

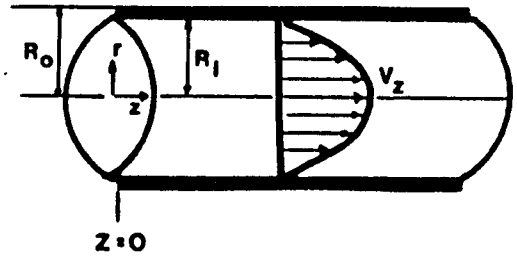

(b) Semi-infinite parallel plate with two permeable walls

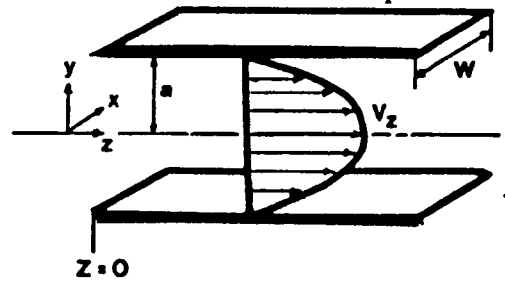

	(a)	(b)
V_z :	$2\bar{V}(1 - \left[\frac{r}{R_i}\right]^2)$	$\frac{3}{2}\bar{V}(1 - \left[\frac{y}{a}\right]^2)$
Z^* :	$\frac{\pi N D Z}{2Q}$	$\frac{4\ NWD\ Z}{3Qa}$
γ :	$\frac{D_1\alpha_1\ \ell n R_o/R_i}{D_m\alpha_m}$	$\frac{D_1\alpha_1 t}{D_m\alpha_m a}$

Figure 3.2 Comparison of velocity profiles and dimensionless parameters for parallel plate and tubular geometries.

where K' (dimensionless) and β (mmoℓ/ℓ) are constants.

The total CO_2 content (C_T) is the sum of the dissolved and reacted forms given by:

$$C_T = C_1 + C_2 \tag{3.18}$$

where C_2 is the sum of the concentrations of bicarbonate and carbamino species. To simplify the development, the reacted CO_2 species were assumed to diffuse at the same rate. If the dissolved species C_1 has a diffusion coefficient D_1 and the reacted species C_2 has a diffusion coefficient D_2, then the convective-diffusion equation 3.3 for a Newtonian fluid flowing in a tube [Figure 3.2(a)] becomes:

$$2\bar{V}\left(1 - \frac{r^2}{R_1^2}\right) \frac{\partial}{\partial z} (C_1+C_2) = D_1 \frac{1}{r} \frac{\partial}{\partial r} \left(r \frac{\partial C_1}{\partial r}\right) + D_2 \frac{1}{r} \frac{\partial}{\partial r} \left(r \frac{\partial C_2}{\partial r}\right) \tag{3.19}$$

Nondimensionalising with $r^* = r/R_i$; $z^* = (D_1 z)/(2\bar{V}R_i^2)$, equation (3.19) becomes:

$$(1-r^{*2}) \frac{\partial}{\partial z^*} (C_1+C_2) = \frac{1}{r^*} \frac{\partial}{\partial r^*} \left[r^* \frac{\partial}{\partial r^*} \left(C_1 + \frac{D_2}{D_1} C_2\right)\right] \tag{3.20}$$

It is important to note that C_1 and C_2 have not been non-dimensionalised. Since the flow rate through the tube, Q is given by $Q = \pi R_i^2 \bar{V}$ then z^* can be expressed as:

$$z^* = \frac{\pi D_1 z}{2Q} \tag{3.21}$$

Equation 3.20 is solved with the following boundary conditions:

$$\left.\begin{aligned} &C_1 + C_2 = C_{Ti} && \text{at } z^* = 0,\ 0 \le r^* \le 1 \\ &\frac{\partial}{\partial r^*}(C_1+C_2) = 0 && \text{at } r^* = 0,\ z^* \ge 0, \\ &\frac{\partial}{\partial r^*}\left(C_1 + \frac{D_2}{D_1} C_2\right) = \frac{1}{\gamma}(\alpha P_g - C_1) && \text{at } r^* = 1,\ z^* \ge 0, \end{aligned}\right\} \quad (3.22)$$

where α_1 is the solubility of dissolved CO_2 in blood.

γ is the dimensionless wall resistance parameter defined as:

$$\gamma = \frac{D_1 \alpha_1 \ln R_o/R_i}{D_m \alpha_m} \quad (3.23)$$

where $D_m\alpha_m$ is defined as the membrane permeability (μ_m) and R_o is the tube outer radius. For the wall condition, it should be noted that dissolved and reacted CO_2 species in the blood may diffuse to the membrane boundary. γ may be considered to represent the resistance of the membrane wall relative to that of the blood phase. For $\gamma = 0$ the boundary condition reduces to that of constant concentration i.e. wall resistance is zero.

Voorhees also considered the CO_2 transfer in a semi-infinite parallel plate channel with two permeable walls of half-height, a, and width, W [Figure 3.2(b)] . The corresponding dimensionless convection-diffusion equation was:

$$(1-y^{*2}) \frac{\partial}{\partial z^*}(C_1+C_2) = \frac{\partial^2}{\partial y^{*2}}\left(C_1 + \frac{D_2}{D_1} C_2\right) \quad (3.24)$$

where

$$y^* = \frac{y}{a}\ ; \quad z^* = \frac{4WD_1 z}{3Qa}$$

and the concentration C_T was considered to be a function of only the transverse (y) and the axial (z) directions, and independent of the lateral direction (x)

The boundary conditions for the parallel plate (equation 3.24) are given below:

$$\left.\begin{aligned} C_1 + C_2 &= C_{Ti} && \text{at } z^* = 0,\ -1 \leq y^* \leq 1 \\ \frac{\partial}{\partial y^*}(C_1+C_2) &= 0 && \text{at } z^* \geq 0,\ y^* = 0 \\ \frac{\partial}{\partial y^*}\left(C_1 + \frac{D_2}{D_1} C_2\right) &= \frac{1}{\gamma}(\alpha_1 P_g - C_1) && \text{at } z^* \geq 0,\ y^* = \pm 1 \end{aligned}\right\} \quad (3.25)$$

γ is the dimensionless wall resistance defined as:

$$\gamma = \frac{D_1\ \alpha_1\ t}{D_m \alpha_m a} \quad (3.26)$$

where t is the membrane thickness.

Comparison of the relevant dimensionless parameters for the permeable tube and parallel-plate with two permeable walls are summarized in Figure 3.2(a) and 3.2(b) respectively.

3.4 CO_2 Transfer Theory - Predictions

Solutions to the tubular and parallel-plate equations (3.20 and 3.24 respectively) were obtained using computer programs developed by Dr. P.J.D. Mayes, Dept. of Mathematics, University of Strathclyde. The programs use the NAG routine D03PBF (Dew and Walsh, 1981) which is based on the Method of Lines (Madsen and Sincovec, 1974). Using this technique good agreement has been found with analytical (Graetz) solutions and with O_2 transfer (analogous to CO_2 transfer) results obtained independently by Colton and Drake (1971). Also excellent agreement has been found with the solution obtained independently by Khoo (1984) to the CO_2 transfer equations using a Crank-Nicolson finite difference scheme.

3.4.1 Input parameter selection

The numerical analysis solves for the reacted CO_2 concentration, C_2, at any r*, z* location within the tube. Dissolved CO_2 concentrations, C_1 are calculated via the dissociation curve

Table 3.1 Input parameters for the CO_2 transfer model (ISO reference conditions).

Specified			Derived		
C_{Ti}	:	23.36 mmol/ℓ	H	:	36%
$pCO_{2,in}$	:	45.0 mmHg	β	:	25.449 mmol/ℓ (T = 37°C)
C_{Hb}	:	12.0 g%	K'	:	122.07
D_2/D_1	:	0.6	α_1	:	0.02945 mmol/ℓ.mmHg
γ	:	0.0,0.01,0.05, 0.1,0.2 or 0.5	$C_{1,i}$	:	1.3253 mmol/ℓ
P_g	:	0,5,10 or 15 mmHg			

relationship given by equation 3.17.

$$C_1 = \frac{C_2}{K'} 10^{C_2/\beta} \qquad (3.17)$$

$C_2(r^*,z^*)$ also depends on the following blood input, membrane and gas phase conditions:

C_{Ti}	:	total CO_2 concentration at inlet ($z^* = 0$)
$pCO_{2,in}$	:	inlet blood pCO_2
C_{Hb}	:	haemoglobin concentration
D_2/D_1	:	CO_2 diffusivity ratio (reacted/dissolved)
γ	:	membrane resistance
P_g	:	gas phase pCO_2
α_1	:	CO_2 solubility in blood

The constants β and K' in equation 3.17 may be determined from the specified C_{Ti}, $pCO_{2,in}$, α_1 and C_{Hb} as shown in Appendix A for ISO reference input conditions. Diffusivities and solubilities are dependent on haematocrit and temperature. The relevant relationships are given in Appendix A for the estimation of these quantities. Voorhees (1976) found that his experimental data was best correlated with theory if a D_2/D_1 ratio was taken. This value is in good agreement with Benn (1974) who used a D_2/D_1 ratio of 0.615.

3.4.2 Effect of gas phase pCO_2 and wall resistance on CO_2 transfer

For ISO reference input conditions (Table 2.2) the CO_2 removal in tube and parallel plate geometries were computed for various combinations of P_g and γ. The input data sets (derived parameters are calculated in Appendix A) are shown in Table 3.1.

Practical application of the theory may be made if the fractional CO_2 removal, θ_c is plotted as a function of z^*. θ_c is defined in equation 3.16:

$$\theta_c = \frac{C_{Ti} - \bar{C}_{To}}{C_{Ti}} \tag{3.16}$$

The velocity-weighted average CO_2 content (cup-mixed), $\bar{C}_{To}$, is, in the tubular case, given by:

$$\bar{C}_{To} = \frac{\int_0^1 C_1(1-r^{*2})r^*dr^* + \int_0^1 C_2(1-r^{*2})r^*dr^*}{\int_0^1 (1-r^{*2})r^*dr^*} \tag{3.27}$$

Experimentally, θ_c may be determined readily since blood samples taken from outlet of the oxygenator are equivalent to cup-mixed values.

Figure 3.3 shows θ_c as a function of z^* for zero gas phase pCO_2 ($P_g = 0$) and for the range of wall resistances quoted in Table 3.2. In Figure 3.4 the influence of finite P_g values for wall resistances of 0.0, 0.1 and 0.5 are displayed. These figures are for the tube configuration; corresponding plots for parallel plates are given in Figures 3.5 and 3.6. The influence of gas phase and wall conditions on CO_2 removal will be discussed with reference to transfer in tubes. Similar effects may be observed in parallel plate systems.

It may be seen from Figure 3.3 that the wall resistance parameter, γ has a profound effect on CO_2 removal even under optimal gas phase conditions i.e. $P_g = 0$ mmHg. Compared to the infinitely permeable wall, $\gamma = 0$ a wall resistance of 0.2 will require about a 10-15 fold increase in tube length in order to achieve the same CO_2 removal rate. As will be presented in Chapter 4 evaluation of a commercial hollow fibre oxygenator has indicated γ values of about 0.4. Thus considerable improvement in performance could be attained if γ were to be reduced. Since γ is proportional to $\ell n(R_o/R_i)$

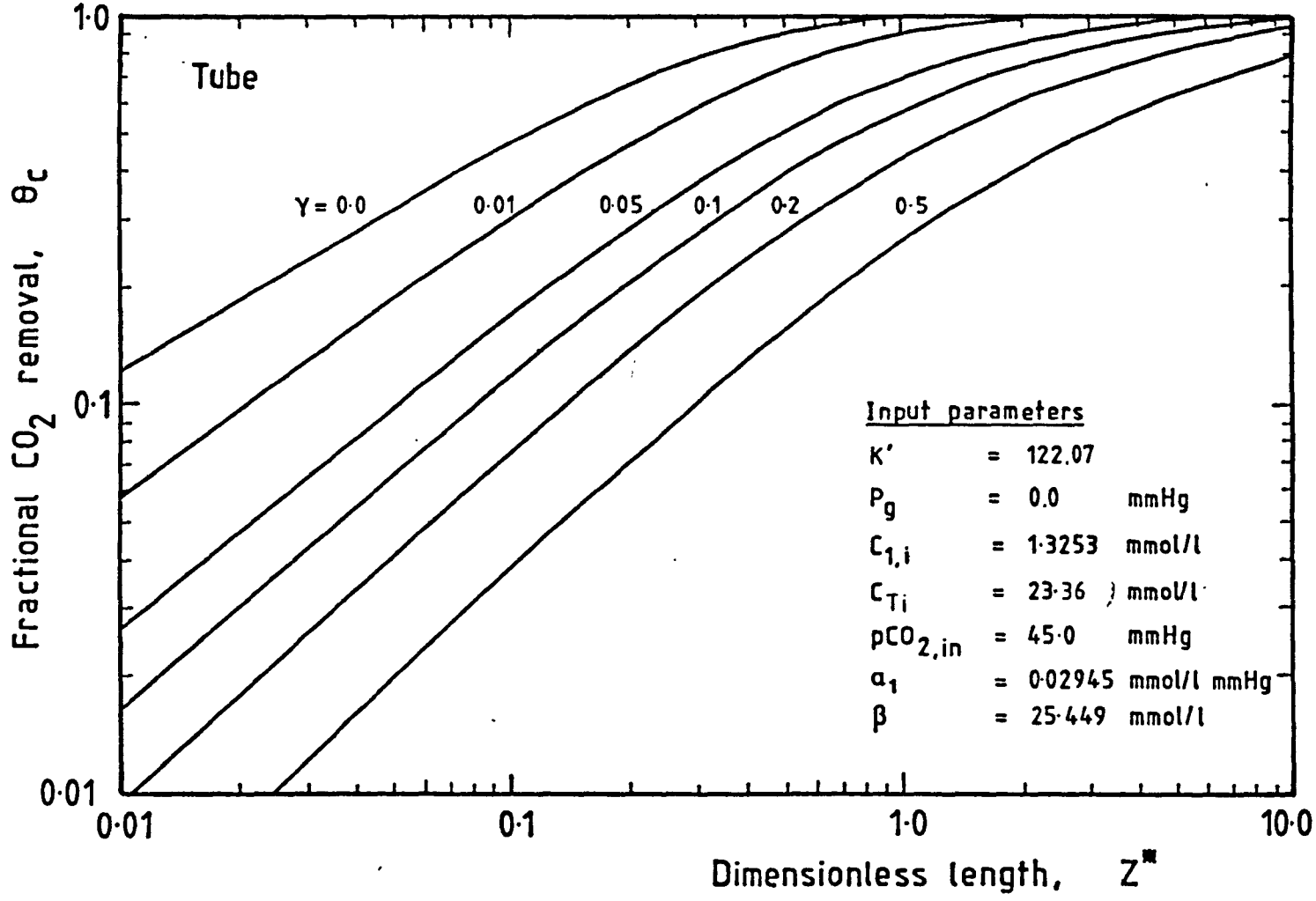

Figure 3.3 Theoretical CO_2 transfer in tubular geometry - Effect of wall resistance.

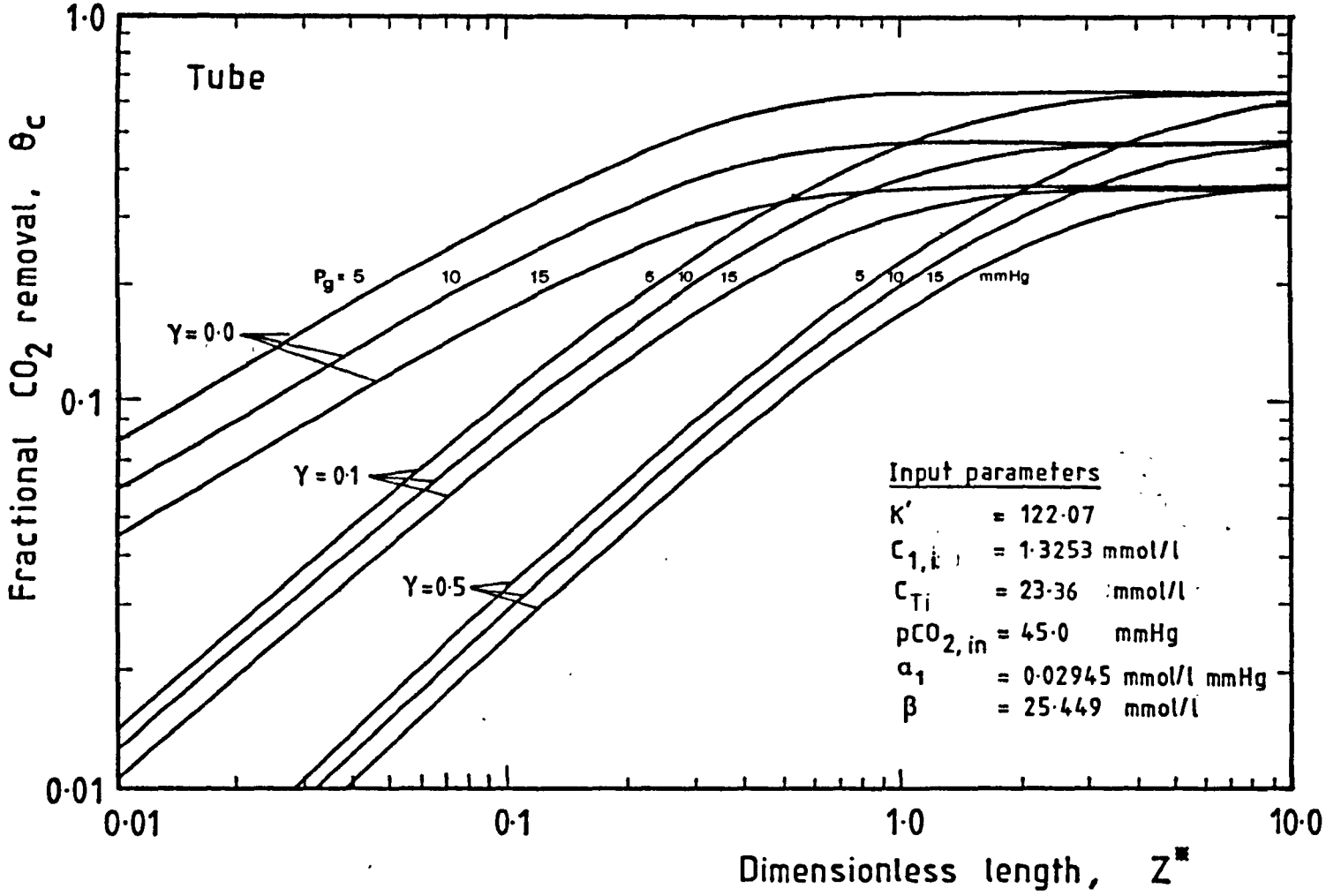

Figure 3.4 Theoretical CO_2 transfer in tubular geometry - Effect of various P_g.

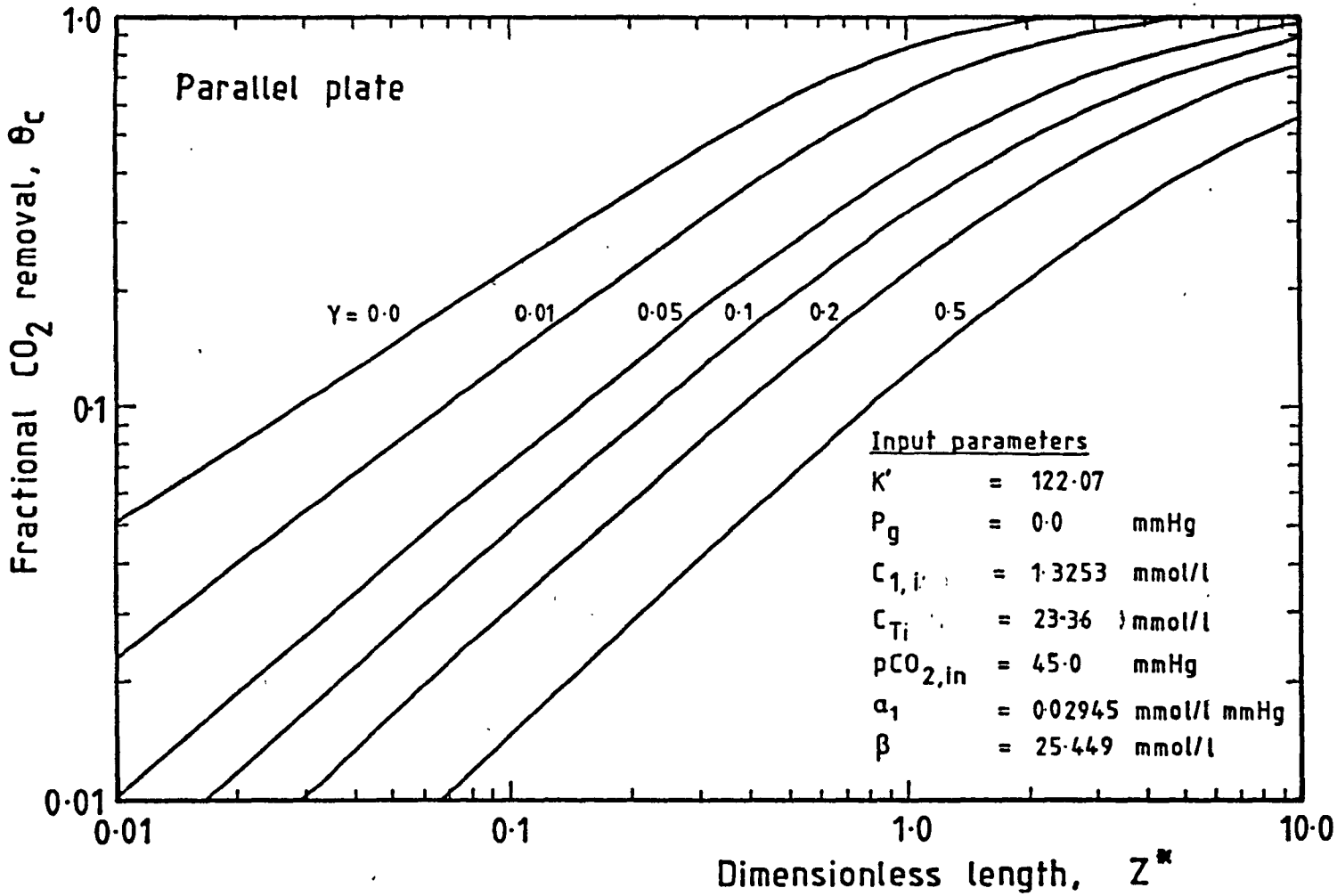

Figure 3.5 Theoretical CO_2 transfer in parallel plate geometry - Effect of wall resistance.

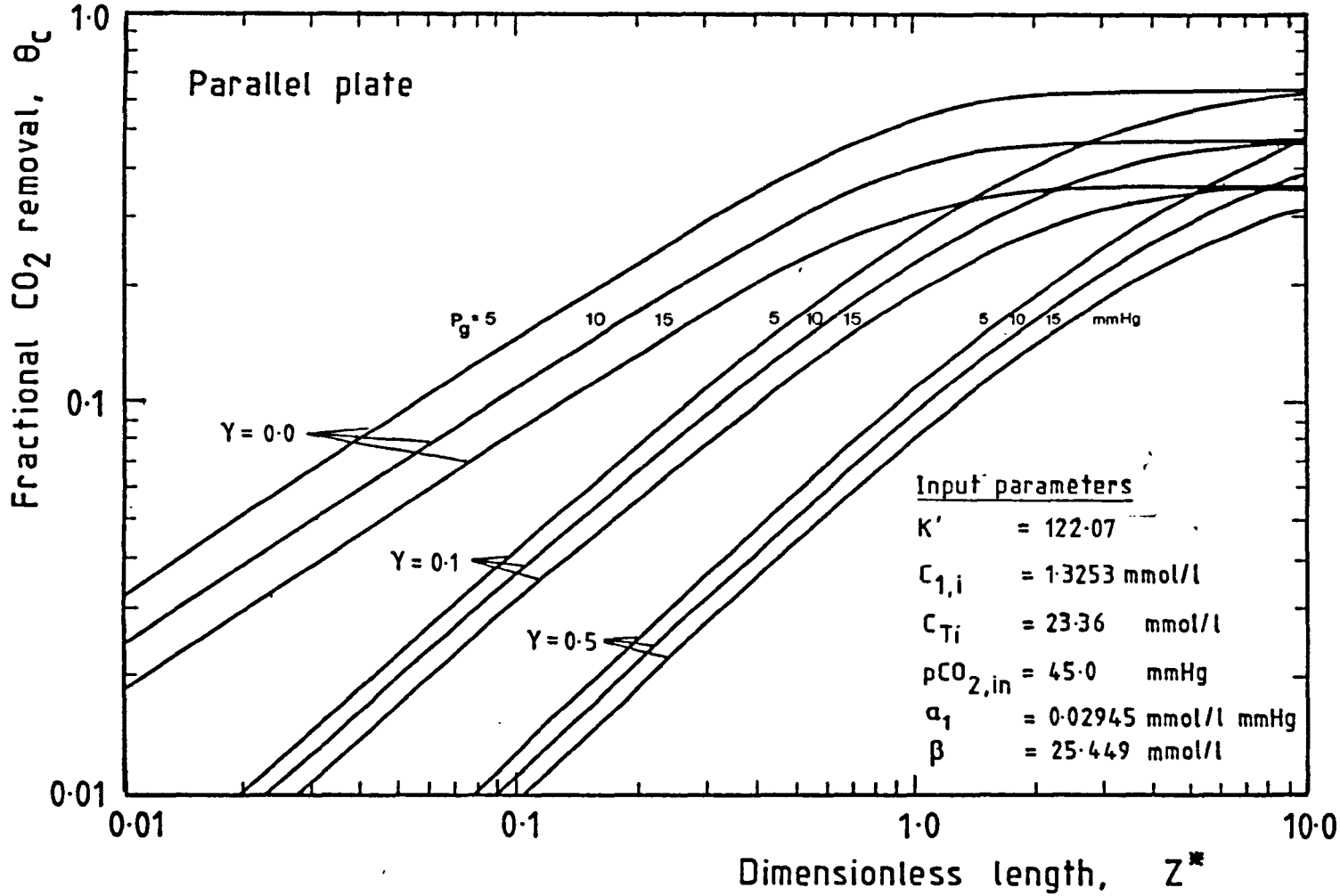

Figure 3.6 Theoretical CO_2 transfer in parallel plate geometry - Effect of various P_g.

and inversely proportional to $D_m\alpha_m$ (i.e. membrane permeability) as defined in equation 3.23, a reduction in the tube wall thickness or an increase in the membrane permeability will result in a reduction in the wall resistance parameter. Although it could be argued that an increase in the tube inner radius, R_i, could bring about a reduction in γ, the priming volume of the oxygenator would be increased (proportional to R_i^2).

As the partial pressure driving force for CO_2 transfer is relatively small (pCO_2 = 45 mmHg for reference input conditions and P_g = 0.0 mmHg) any finite gas phase pCO_2 will be expected to reduce the CO_2 removal at a fixed z*. This effect is shown clearly in Figure 3.4. The relative increase in tube length required for a given θ_c as P_g is increased is greater for lower wall resistances. For example if θ_c = 0.2 the tube length would have to be increased about 2.6 times as P_g is raised from 5 to 15 mmHg (assuming γ = 0.0). If γ = 0.5 the corresponding tube length increase would be about 1.6 times.

Voorhees (1976) carried out CO_2 transfer experiments in a single tube system and presented theoretical predictions for P_g = 0. This is readily justified since high ventilation rates were used in his experimental system thus one could assume that P_g = 0. However, no theory predictions were presented to study the effect of finite gas phase, P_g on CO_2 transfer.

In practice, an oxygenator with a countercurrent flow system will exhibit a finite P_g at gas phase outlet as the CO_2 concentration builds up along the length of the ventilation compartment. The magnitude of P_g at outlet can be calculated from measurement of the inlet ventilation flow rate, $Q_{g,i}$, the total CO_2 transfer and the total O_2 uptake by the blood.

The theory predictions for finite P_g are however based on the assumption that the gas phase pCO_2 is constant along the length of the tube or parallel-plate. A more suitable analysis would be to solve simultaneously the transport equations for blood and gas phases. However this more complex analysis is outwith the scope of this thesis. The present predictions for finite P_g will be used as first order approximation for oxygenator performance under conditions of reduced ventilation rates. One way in which this can be done is to use an average arithmetic mean P_g based on the inlet gas phase pCO_2 (usually 0 mmHg) and the outlet pCO_2 which can be determined as previously mentioned. This mean P_g can then be used as input data for the theoretical model.

The theory predictions illustrate that CO_2 removal in clinical membrane oxygenators may be controlled by alteration in ventilation flow rate (analogous to the human lung), i.e. the higher the $Q_{g,i}$ the smaller the outlet P_g and hence the greater the CO_2 removal.

3.4.3 Design predictions for $ECCO_2R$-LFPPV

From section 2.4 it has been suggested that suitable removal criteria would be a $\dot{V}_{CO_2}$ of 200 mℓ(STPD)/min at a blood flow rate, Q_B of 1.5 ℓ/min, giving a $\dot{V}_{CO_2}/Q_B$ ratio of about 130 mℓ CO_2 (STPD)/ℓ. This corresponds to a $\dot{V}_{CO_2}/Q_B$ ratio of 6.0 mmol CO_2 (STPD)/ℓ. Design predictions for $ECCO_2R$-LFPPV at the given $\dot{V}_{CO_2}/Q_B$ ratio can be derived given the following relationship:

$$\dot{V}_{CO_2} = Q_B(C_{Ti} - \bar{C}_{To}) \qquad (3.27)$$

Since $\theta_c = (C_{Ti} - \bar{C}_{To})/C_{Ti}$, equation 3.27 can be rearranged to give:

$$\dot{V}_{CO_2} = Q_B\theta_C C_{Ti} \qquad (3.28)$$

and

$$\frac{\dot{V}_{CO_2}}{Q_B} = \theta_C C_{Ti} \tag{3.29}$$

For the ISO Standard condition C_{Ti} = 23.36 mmol/ℓ, and for $\dot{V}_{CO_2}/Q_B$ = 6.0 mmol CO_2 (STPD)/ , θ_C = 0.26. At this θ_C value, the dimensionless length z* required may be determined from Figure 3.3 assuming maximal ventilation (i.e. P_g = 0.0 mmHg). From equation 3.21, z* = $(\pi D_1 z)/(2Q)$ which is applicable for a single tube. For a hollow fibre oxygenator with N parallel-connected tubes and a total blood flow rate, Q_B:

$$z^* = \frac{\pi D_1 N z}{2Q_B} \tag{3.30}$$

Therefore, since Q_B is known, then Nz may be determined to meet the removal criteria, which will depend also on the wall resistance. It should be noted that Nz is the product of the total number of tubes and the length of each tube. The selection of tube length is dependent on the pressure drop criteria and manufacturing constraints in a manner similar to that analysed for O_2 transfer requirements by Mockros and Gaylor (1975).

4

IN VITRO EVALUATION OF MEMBRANE OXYGENATORS

4.1 Introduction

The gas transfer tests were performed in a closed-circuit system using bovine blood. Two types of membrane oxygenators both incorporating microporous polypropylene membranes were evaluated; the Travenol TMO (2.25 m^2-adult unit) parallel-plate membrane oxygenator and the Terumo CAPIOX II (1.6m^2 and 3.3m^2 units) hollow fibre oxygenators.

At low blood flow rates, it has been noted that blood flow maldistribution may occur in the Travenol TMO device (Bartlett et al. 1975). Therefore, modifications to the Travenol device were undertaken to investigate this effect (section 4.2.1). Theoretical predictions were used to correlate with the experimental results.

Since the partial pressure driving force (blood pCO_2 - gas phase pCO_2) available for CO_2 transfer in membrane oxygenators is relatively small, build up of CO_2 in the gas phase may impede CO_2 transfer unless the oxygenator is adequately ventilated. This effect may be prominent in hollow fibre membrane lungs which have tightly-packed fibre bundles. To study this effect small scale hollow fibre test modules were built with uniformly spaced fibre bundles. The details and test procedure for the evaluation of these modules are given in section 4.2.2. Data from these experiments were correlated with theory.

For the clinical $ECCO_2R$-LFPPV therapy, the membrane oxygenators should possess a high carbon dioxide transfer rate to blood flow rate ratio ($\dot{V}_{CO_2}/Q_B$) and a low flow resistance. Typically, a $\dot{V}_{CO_2}/Q_B$ of 120-140 mℓ CO_2 (STPD)/ℓ will be required in the treatment of an adult if Q_B is limited to 1.5 ℓ/min.

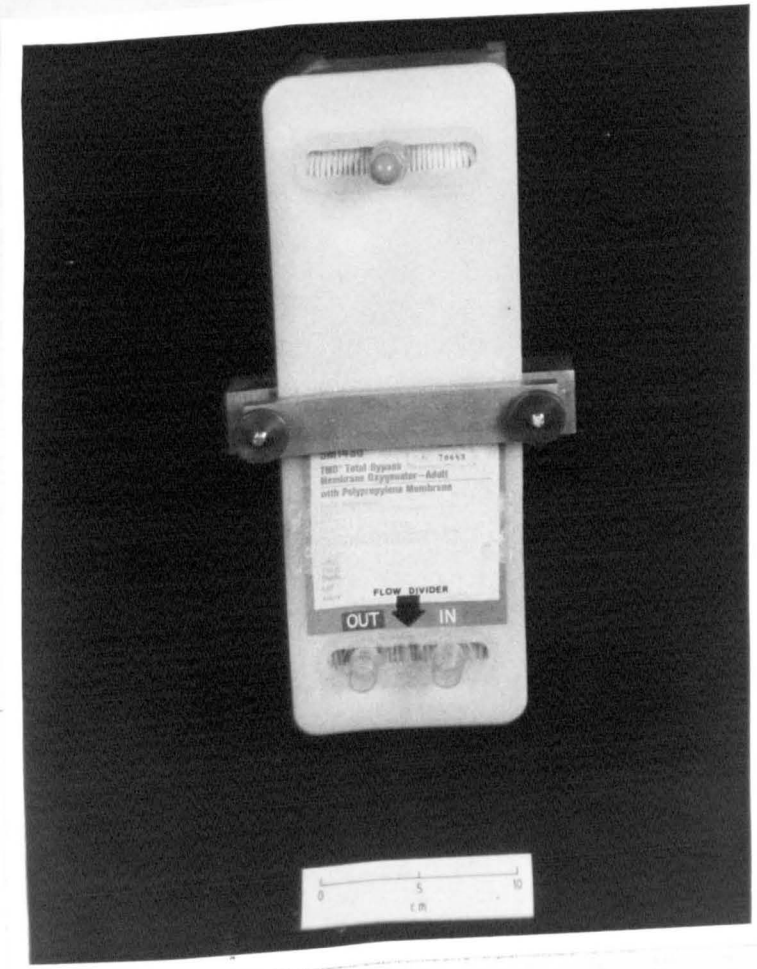

(a) Modified Travenol TMO

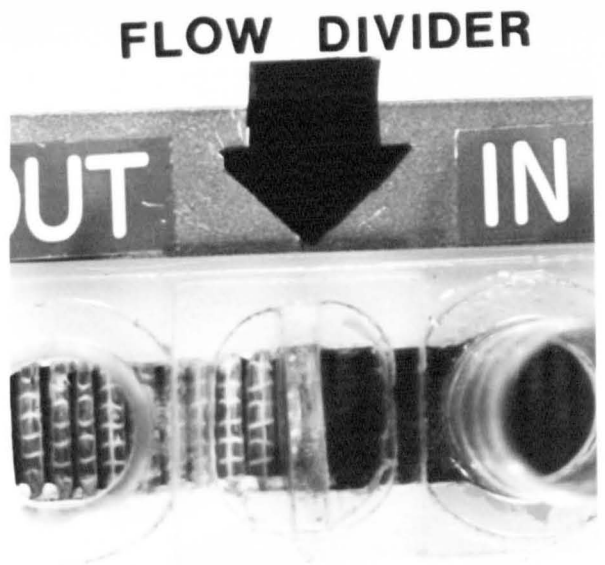

(b) Close-up view of flow divider

Figure 4.1

4.2 Membrane Oxygenators - Modifications and Test Modules

Descriptions of the modified TMO and hollow fibre test modules are given below. The reader is referred to sections 2.3.2 and 2.3.4 for specifications of the standard Travenol TMO and Terumo CAPIOX II oxygenators.

4.2.1 Travenol TMO modification

The Travenol TMO device was modified in such a way as to divide the membrane stack into two sections (each containing 15 blood paths) connected in series. Thus, the inlet blood flow need only be distributed into 15 parallel paths instead of 30 as in the original design. The modification is shown in figure 4.1a, in which the original inlet blood port is replaced by two ports. Shunting of the blood between the ports is prevented by the internal flow divider (Figure 4.1b). In operation blood enters one of these ports and flows upwards through one-half of the membrane stack and, by blocking off the original outlet port, the flow is directed downwards through the other half. It can be seen that for a given blood flowrate the mean velocity and total path length are doubled for the modified device as compared with the standard oxygenator.

4.2.2 Hollow fibre test modules

Small test modules (Figure 4.2), containing 35 or 70 hollow fibres of the same type as used in the CAPIOX II membrane lungs were constructed. The construction method which has been described by Leong (1983) enables the fibres to be uniformly spaced apart within the fibre bundle. In the present modules, the fibres are separated by a distance of approximately 2mm (i.e. 8 x fibre O.D.) to ensure complete ventilation by the gas phase. Moreover any blockage within individual fibres may be readily observed and due allowance made when

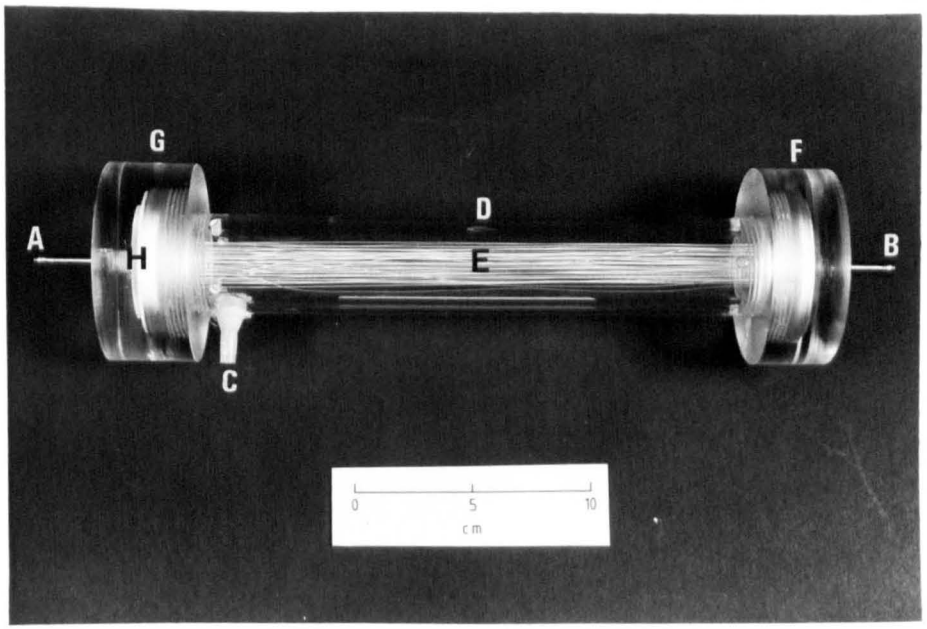

Figure 4.2 Hollow fibre test module.

legend:

A: Outlet blood port

B: Inlet blood port

C: Inlet gas port

D: Transparent cylindrical housing

E: Microporous hollow fibres

F: Inlet end cap

G: Outlet end cap

H: Outlet mixing chamber

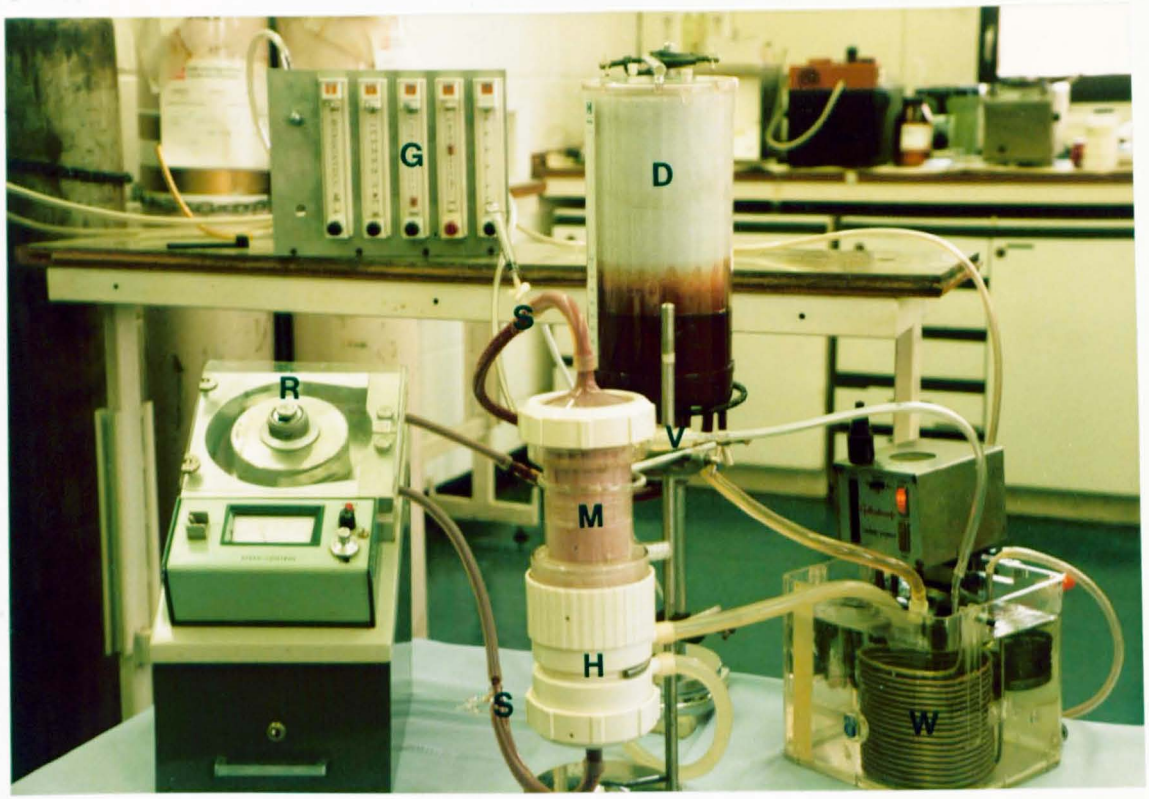

Figure 4.3 In vitro oxygenator-deoxygenator circuit.

legend:

D : Deoxygenator
G : Gas flow meters
H : Blood heat exchanger
M : Membrane oxygenator
R : Roller pump
S : Sampling ports
V : Ventilating gas line
W : Water bath at 37 °C and gas heat exchanger.

comparing experiment with theory. The ends of the fibres are embedded in silicone elastomer to form the bundle end plates. These plates are enclosed by a perspex cylindrical housing which is equipped with ports for gas distribution. Blood manifold end caps are screwed onto the housing to complete the assembly. The active fibre lengths varied slightly between different modules (23-24cm).

4.3 In Vitro Test Circuits and Procedures

4.3.1 TMO, modified TMO and CAPIOX II oxygenator tests

Bovine blood was used to evaluate carbon dioxide transfer in the above membrane lungs in a closed loop test circuit (Figure 4.3). Blood for any one set of tests were collected from a single cow, using EDTA (Ethylene diaminetetra-acetic acid) at a concentration of 1 g/ℓ as an anticoagulant. If the blood was not to be used immediately, it was stored at $4^{o}C$ and tests were performed within 24 hours of blood collection. To prevent bacterial growth about 0.1 mg/mℓ streptomycinsulfate (Boehringer Mannheim GmbH, W. Germany) was added to the blood. Before each transfer test, the blood was filtered and the circuit primed with isotonic saline solution (0.9% sodium chloride). About 2.5ℓ of blood was circulated in a closed loop containing a membrane lung in series with a calibrated roller pump and a bubble oxygenator operating in reverse mode i.e. as a deoxygenator. Since the flow resistance of the bubble oxygenator was small over the blood flow rate (Q_B) range tested (0.5 to 1.5 ℓ/min), single pump operation of the TMO unit was possible. The blood was maintained at $37^{o}C \pm 1^{o}C$ by means of a water bath from which water was circulated through the deoxygenator heat exchanger (and the CAPIOX II heat exchanger). Sample ports were located at

inlet and outlet of the membrane oxygenator. The haemoglobin content and base excess were adjusted to the desired levels by addition of isotonic saline and isotonic bicarbonate (84g $NaHCO_3$ in $1000cm^3$ of saline) respectively. Estimation of the amounts required is given in Appendix B. Blood inlet conditions to the membrane lung were obtained by adjustment of an O_2, CO_2 and N_2 gas mixture ventilating the bubble oxygenator. Each membrane lung was tested at least twice. In vitro performance was obtained at the reference inlet conditions specified in the proposed ISO Standards as given in Table 2.2. Blood samples were taken over a period of six hours. The first withdrawal filling the syringe with blood was flushed through the sample port before the actual sampling was taken for the blood measurements.

Haemoglobin and oxygen saturation (OSM-2 Hemoximeter, Radiometer), pO_2, pCO_2 and pH (BMS3 acid-base analyser, Radiometer) were determined on blood samples taken at inlet and outlet of the membrane lung. Calibration procedures and measurement techniques for the OSM-2 and BMS 3 analysers are given in Appendix C. The haematocrit of the blood in the bubble oxygenator reservoir was measured by the microhaematocrit method (Hawkesley microcentrifuge).

The CO_2 content of whole blood was determined by the Corning carbon dioxide analyser (Model 965, Corning Medical Ltd.). A special sampling technique was used for the CO_2 content determinations, namely, the syringe-to-syringe method of Rispens et al. (1980). Principle of operation and calibration of the Corning CO_2 analyser and details of the syringe-to-syringe method are given in Appendix C.

All membrane lungs were ventilated with dry air or air + O_2

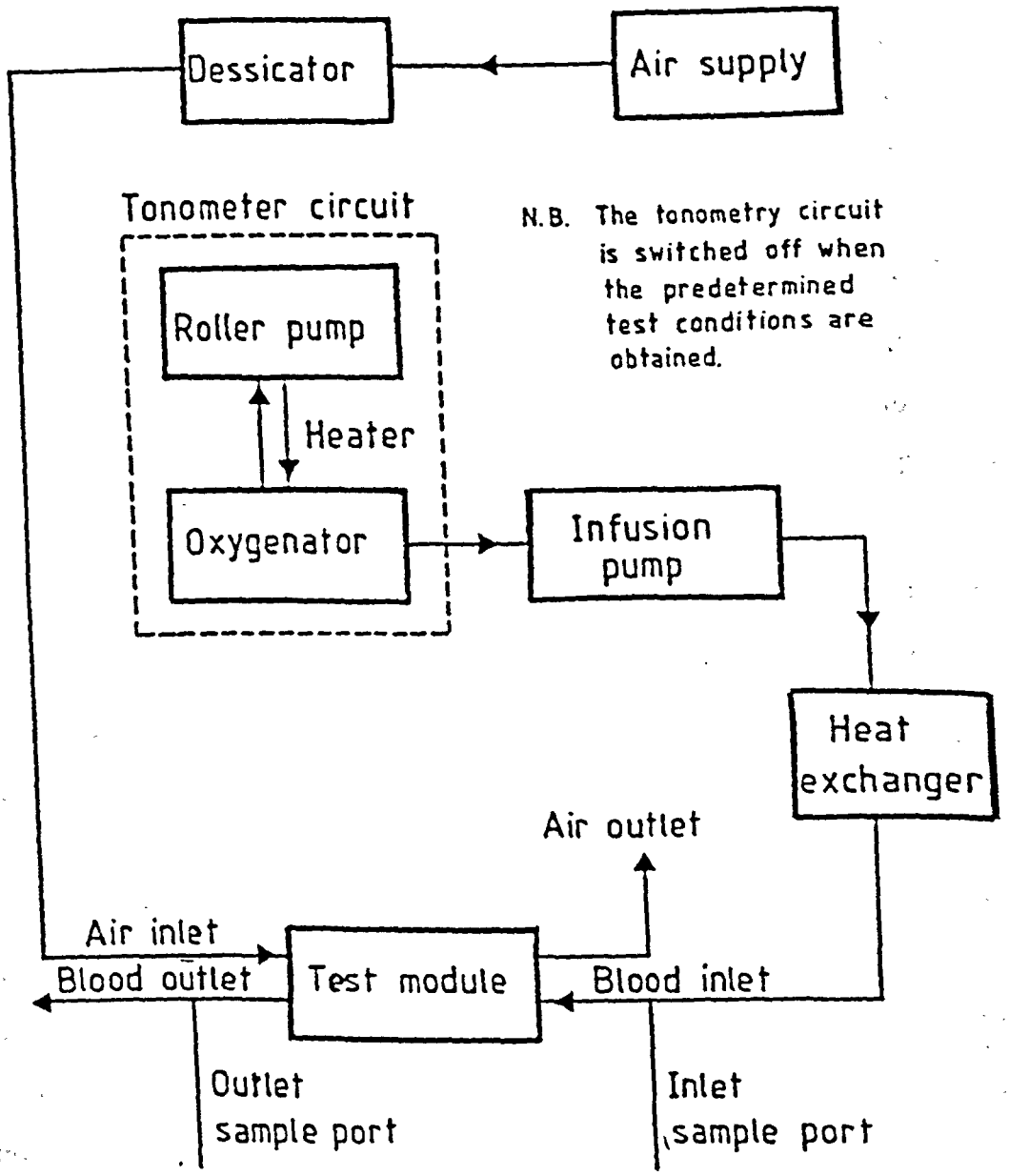

Figure 4.4 Experimental circuit for test modules.

heated to 37°C. To maximise CO_2 transfer, ventilation gas flow was countercurrent to blood flow in the Travenol TMO and Terumo CAPIOX II membrane lungs. Oxygenators should be operated at their maximum gas flow rates for efficient CO_2 transfer. For the Travenol TMO membrane oxygenator, the recommended maximum gas flow rate is 15 1/min (Travenol Laboratories, Inc. 1976) and this was used in the evaluations reported here. Recommended gas flow rates are not however specified for the Terumo CAPIOX II lungs. Terumo Corporation (1983) gives data on the CO_2 transfer rate as a function of gas flow rate for the CAPIOX II $1.6m^2$ and $3.3m^2$ units. Unfortunately, the data does not indicate the optimum gas flow rate operation for maximum CO_2 transfer. Therefore CO_2 transfer was evaluated for several gas flow rates which exceeded the manufacturer's range in order to determine the optimum ventilation. At the end of each blood test, the membrane lung was cleaned with saline and dried with air.

4.3.2 Hollow fibre module tests

Bovine blood, tonometered to the reference inlet conditions (Table 2.2), was delivered by a Harvard infusion pump via a heat exchanger through the test module (Figure 4.4). Inlet and outlet CO_2 contents were measured by the Corning carbon dioxide analyser. Ventilating gas flow was counter-current at 5 ℓ/min. Various blood flowrates through the test module were obtained and measured by volumetric timed collection in a pipette at the outlet. The blood flow rate through the test module is regulated by adjusting the pump speed and thus varying Z*. At each flowrate, three samples were taken at the outlet and one sample at the inlet. The total CO_2 content in each sample were measured from which $C_{Ti}-\bar{C}_{To}/C_{Ti} = \theta_c$ can be computed.

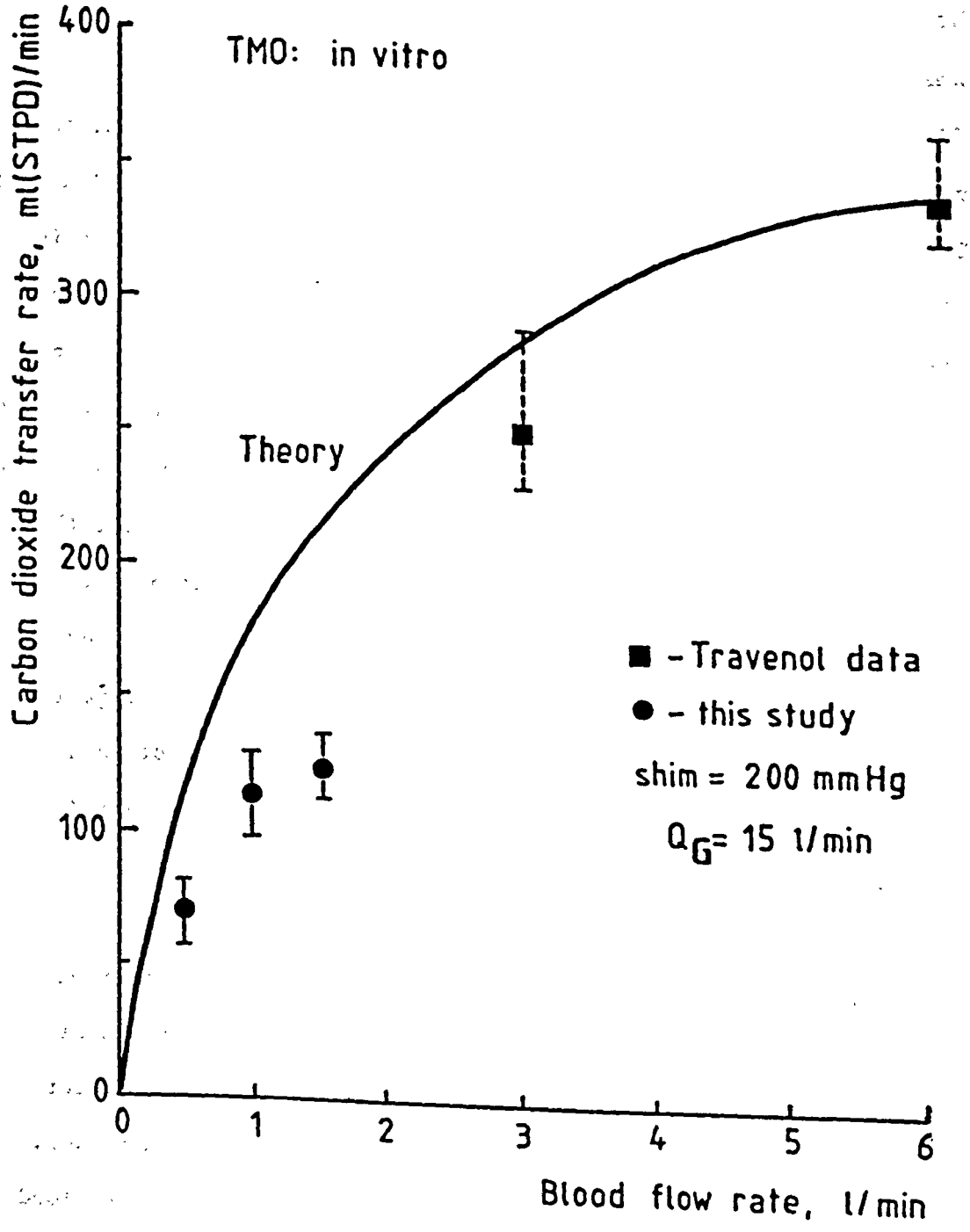

Figure 4.5 In vitro carbon dioxide transfer rate ($\dot{V}_{CO_2}$) as a function of blood flow rate (Q_B) and shim pressure as shown (● - mean ± 1 S.D., n=14 for each Q_B ; ■ - mean and range).

A small diameter steel rod was placed in the outlet blood manifold of the test module. A magnet was then used to rotate this steel rod when sampling to ensure a "good mix" and to prevent blood stagnation.

4.4 Results and Discussion

The results and discussion are presented for the Travenol TMO, the modified Travenol TMO, the Terumo CAPIOX II and the hollow fibre modules in sections 4.4.1, 4.4.2, 4.4.3, and 4.4.4 respectively. Experimental data are compiled in Appendices D and F.

4.4.1 Travenol TMO

The in vitro CO_2 transfer rates ($\dot{V}_{CO_2}$) obtained from four TMO lungs are shown in Figure 4.5 for blood flow rates (Q_B) of 0.5, 1.0 and 1.5 ℓ/min and a ventilation gas flow rate (Q_G) of 15 ℓ/min. The average $\dot{V}_{CO_2}$ are within 12 per cent of the empirical correlation (Equation 2.2) for $\dot{V}_{CO_2}$ as a function of Q_B as given by Karlson et al. (1974) for the earlier version of the TMO which used microporous PTFE membranes. The mean CO_2 transfer rate of 125 mℓ(STPD)/min at a blood flow rate of 1.5 ℓ/min for the adult Travenol TMO with 2.25m^2 membrane area is clearly inadequate for the $ECCO_2$ R-LFPPV application.

Also shown in Figure 4.5 are in vitro canine blood data given by the manufacturer (Travenol Inc., 1976) for Q_B values of 3.0 and 6.0 ℓ/min. These data were obtained for similar ventilation rate and blood input values as employed in the experiments carried out in this study. It would appear, from the trend in $\dot{V}_{CO_2}$ with Q_B, that the low flow results are not consistent with the manufacturer's high flow rate data. This statement is reinforced by comparison of the actual transfer rates with predicted values obtained by correlating the theory of Chapter 3 with the high flow rate data.

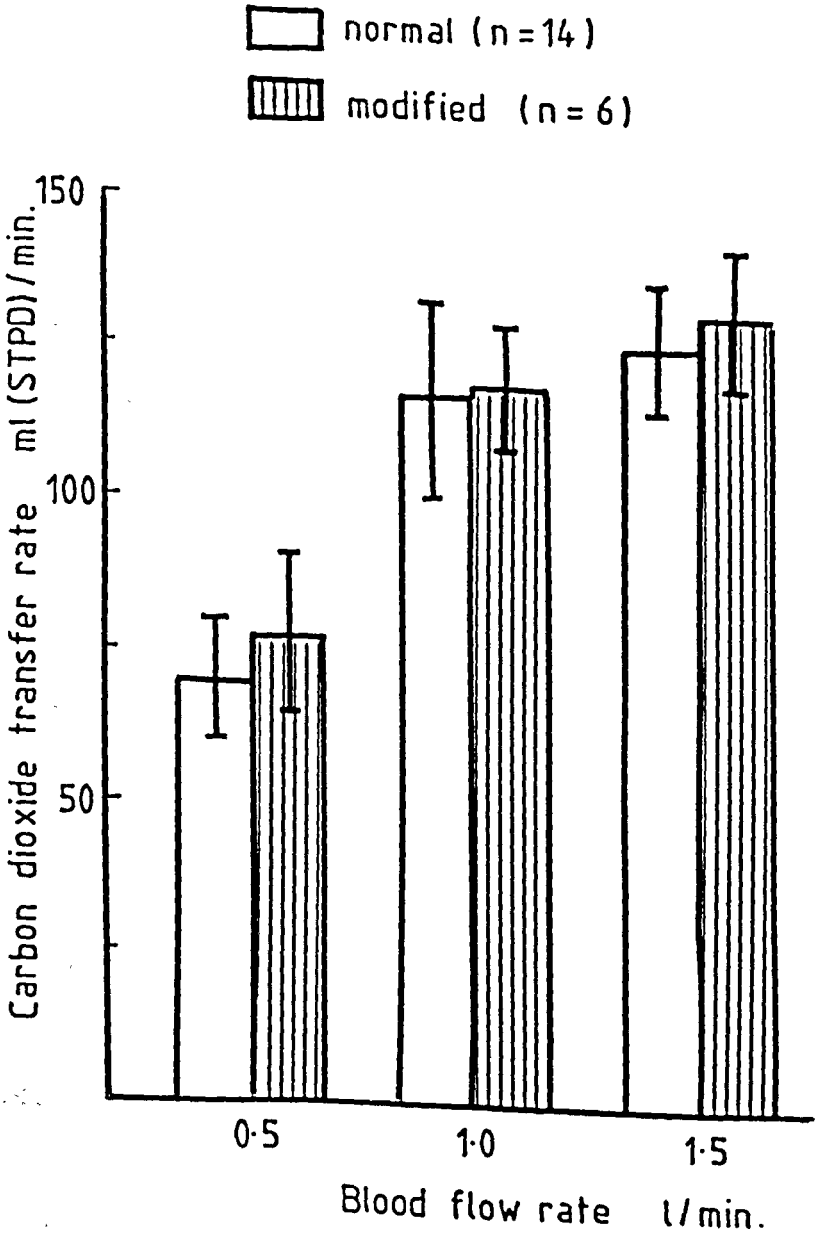

Figure 4.6 Carbon dioxide transfer in the Travenol TMO, normal and modified configuration.

For the correlation, the TMO lung was assumed to behave as a semi-infinite parallel plate geometry with a channel half-height as determined from priming volume and membrane area data. Allowance was made for finite pCO_2 in the gas phase. The wall resistance parameter, was adjusted until the predicted CO_2 removal equalled the quoted value at a blood flow rate of 6.0 ℓ/min. Details of the correlation procedure are given in Appendix E. The solid line in Figure 4.5 is that given by the theory for $\gamma = 0.01$ and $P_g = 8.5$ mmHg.

In the range $0.5 < Q_B < 1.5$ ℓ/min, the theory predicts far higher $\dot{V}_{CO_2}$ values than those actually measured in this study. For example at $Q_B = 1.5$ ℓ/min the predicted $\dot{V}_{CO_2}$ is 218.4 mℓ(STPD)/min compared with a measured rate of 125 mℓ(STPD)/min. Application of theory to the TMO lung analysis must be treated with caution because of the theoretical assumptions of uniform blood path thickness, rectilinear laminar flow and uniform blood and gas flow distribution in multiple channels. However, Bartlett et al. (1975) have observed areas of flow stagnation and maldistribution in individual flow channels of TMO lungs which had been operated at low blood flow rates. Such non-uniform flows might explain the observed decline in CO_2 removal. This hypothesis was tested with the TMO lungs modified as described in section 4.2.2.

4.4.2 Modified Travenol TMO

The modified TMO gave mean $\dot{V}_{CO_2}$ of 78.1, 118.6 and 131.7 mℓ(STPD)/min for Q_B of 0.5, 1.0 and 1.5 ℓ/min respectively, (2 data points for each Q_B, 3 membrane lungs tested). By comparison with the normal configuration (Figure 4.6) little improvement in performance was obtained with the modified TMO device. The inference is that flow maldistribution is not improved or is not a reason for the deviation between the theory and experiment.

The modified TMO lungs can be regarded for modelling purposes as a two-stage device of identical membrane channels connected in series. Each stage consists of 15 parallel-connected blood channels. If the blood is perfectly mixed before it enters the second stage then there should be an increase in transfer rate compared to the unmodified TMO lung. This is because the CO_2 concentration boundary layer is broken up in the mixing stage resulting in an increase in the pCO_2 driving force at entry to the second stage.

The magnitude of the expected increase in transfer of a 2-stage device was predicted from the parallel plate theory. The first stage was computed for ISO standard blood inlet conditions (Table 3.1) with the dimensionless wall resistance parameter $\gamma = 0.01$ and $P_g = 0.0$ mmHg. For zero P_g, the performance of the oxygenator will be at its maximum value. In the computation of the cup-mixed C_1 and C_2 at outlet of the first stage, these values must be corrected because of the non-linearity of the dissociation curve. In effect when reacted and dissolved CO_2 contents are mixed at outlet there will be an increase in C_2 and a corresponding decrease in C_1 if the values are to coincide on the dissociation curve. As the total cup-mixed CO_2 content at outlet, $\bar{C}_{To}$, is constant, the corrected cup-mixed C_1 and C_2 were found by an iterative procedure involving equation 3.17.

$$C_1 = \frac{C_2}{K'} 10^{C_2/\beta} \qquad (3.17)$$

The corrected cup-mixed C_1 at outlet of stage 1 together with $\bar{C}_{To}$ were used to compute the new set of input parameters for the second stage. The two-stage model can be represented as:

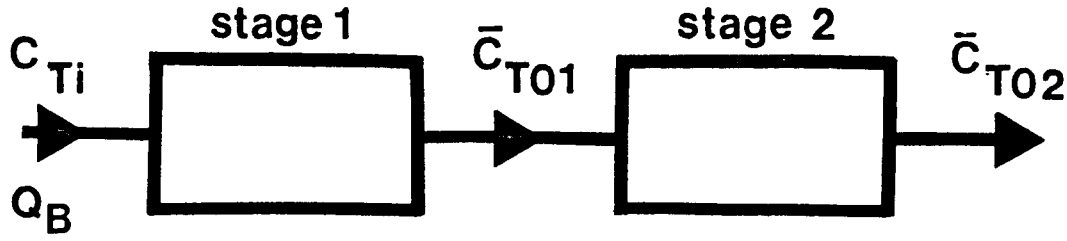

For stage 1 the fractional CO_2 removal, θ_1 is:

$$\theta_1 = \frac{C_{Ti} - \bar{C}_{To1}}{C_{Ti}} \tag{4.1}$$

For stage 2 the fractional CO_2 removal, θ_2 is:

$$\theta_2 = \frac{\bar{C}_{To1} - \bar{C}_{To2}}{\bar{C}_{To1}} \tag{4.2}$$

For the complete system the fractional CO_2 removal, θ_3 is:

$$\theta_3 = \frac{C_{Ti} - \bar{C}_{To2}}{C_{Ti}} \tag{4.3}$$

From equation 4.1 and 4.2

$$\bar{C}_{To2} = C_{Ti}\ (1-\theta_1)(1-\theta_2)$$

and substitution in equation 4.3 yields:

$$\theta_3 = \theta_1 + \theta_2 - \theta_1\theta_2 \tag{4.4}$$

The dimensionless length, z* for the unmodified TMO is

$$z^* = \frac{4WD_1NL}{3Q_B{}^a} \tag{4.5}$$

where the number of blood channels, N = 30.

Table 4.1 $\dot{V}_{CO_2}$ predictions of the two-stage TMO device and unmodified TMO.

MODIFIED TRAVENOL TMO

Stage 1

Q_B ℓ/min	1.5	1.0	0.5
z_1^*	0.26	0.39	0.78
$\bar{C}_1^\dagger$ mmol/ℓ	0.597	0.442	0.206
$\bar{C}_2^\dagger$ mmol/ℓ	16.451	14.509	10.096
θ_1	0.270	0.360	0.559

Stage 2

Q_B ℓ/min	1.5	1.0	0.5
z_2^*	0.26	0.39	0.78
$\bar{C}_1$ mmol/ℓ	0.597	0.442	0.206
$\bar{C}_2$ mmol/ℓ	16.451	14.509	10.096
θ_2	0.253	0.332	0.502
θ_3	0.455	0.573	0.783
$\dot{V}_{CO_2}$ mℓ(STPD)/min	354.7	297.7	203.5

UNMODIFIED TRAVENOL TMO

Q_B ℓ/min	1.5	1.0	0.5
z_1^*	0.52	0.78	1.56
$\bar{C}_1$ mmol/ℓ	0.335	0.206	0.067
$\bar{C}_2$ mmol/ℓ	12.829	10.096	5.148
θ_C	0.436	0.559	0.777
$\dot{V}_{CO_2}$ mℓ(STPD)/min	340.4	290.7	202.0

† $\bar{C}_1$ and $\bar{C}_2$ are corrected cup-mixed values

The dimensionless lengths, z_1^* and z_2^* for the first and second stages of the modified TMO are:

$$z_1^* \text{ (or } z_2^*) = \frac{4}{3} \frac{WD_1}{Q_B a} \frac{N}{2} L = \frac{z^*}{2} \tag{4.6}$$

The z_1^* and z_2^* values of 0.26, 0.39 and 0.78 correspond to Q_B of 1.5, 1.0 and 0.5 ℓ/min respectively for the modified TMO. $\dot{V}_{CO_2}$ is calculated from equation 3.28:

$$\dot{V}_{CO_2} = Q_B \theta_3 C_{Ti} \tag{3.28}$$

The results of the two-stage TMO device and unmodified TMO are shown in Table 4.1.

There is a small increase in the theoretical $\dot{V}_{CO_2}$ prediction for the modified TMO compared with the unmodified device. This improvement is greater for higher blood flow rates but amounts to only a 4% increase for Q_B = 1.5 ℓ/min. The corresponding increase found experimentally was 5% (131.8 mℓ(STPD)/min vs 124.8 mℓ(STPD)/min) although the absolute transfer rates are much lower because P_g is not zero in the experimental situation. The results therefore suggest that flow distribution is not altered with the modified TMO.

An alternative hypothesis to explain the reduced CO_2 performance at low Q_B is the reduction in eddy mixing as a result of lower blood velocities across the nylon screen mesh in the blood channels. The influence of eddy mixing is to enhance the diffusive transfer due to convection in a direction normal to the membrane surface. It is however difficult to predict the extent of eddy mixing given the complex flow regime that will exist in the blood channels of the TMO oxygenator.

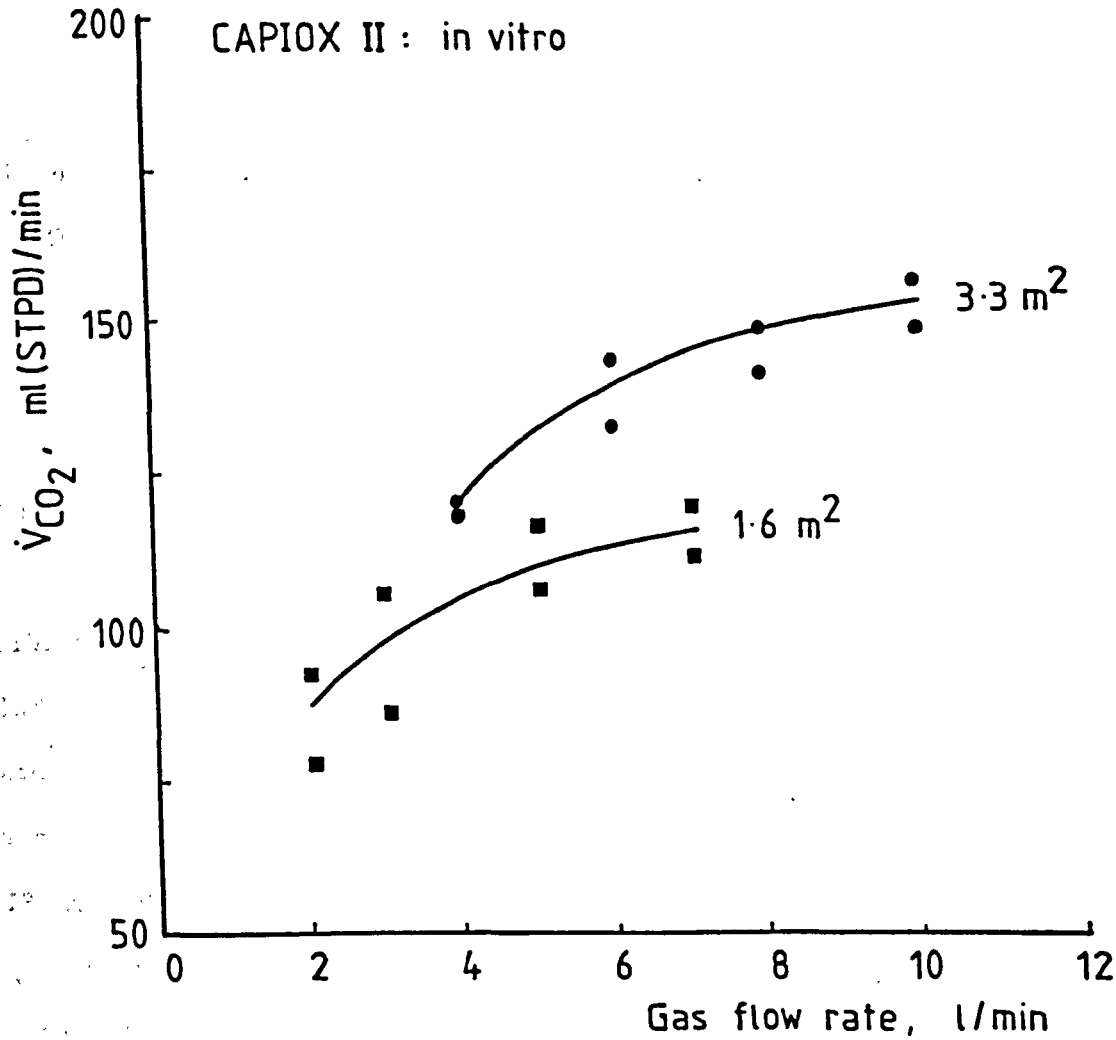

Figure 4.7 In vitro carbon dioxide transfer rate ($\dot{V}_{CO_2}$) as a function of gas flow rate for the Terumo CAPIOX II membrane lung (1·6 m^2 and 3·3 m^2) Blood flow rate, Q_B = 1·0 l/min.

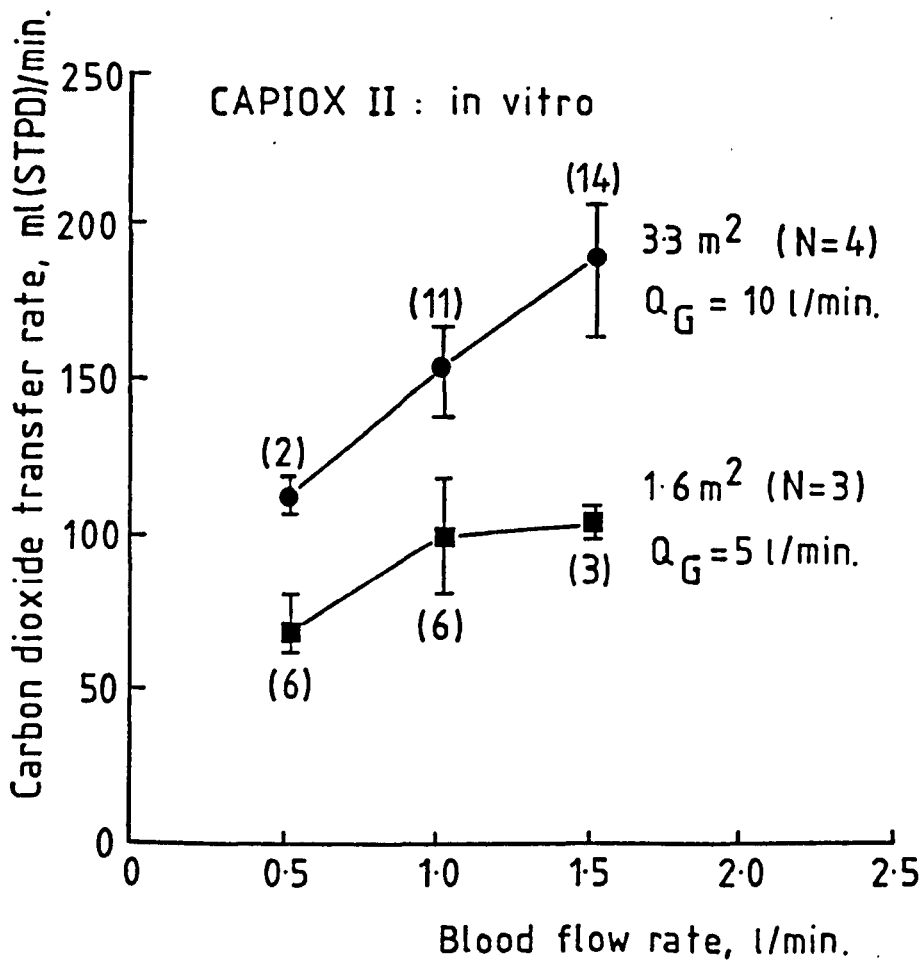

Figure 4.8 In vitro carbon dioxide transfer rate ($\dot{V}_{CO_2}$) as a function of blood flow rate (Q_B) for the Terumo CAPIOX II membrane lung. Gas flow rates (Q_G) were 10 l/min and 5 l/min for 3·3 m^2 and 1·6 m^2 units, respectively. Mean and range for each Q_B are given together with the number of data points in parentheses. N is number of membrane lungs tested.

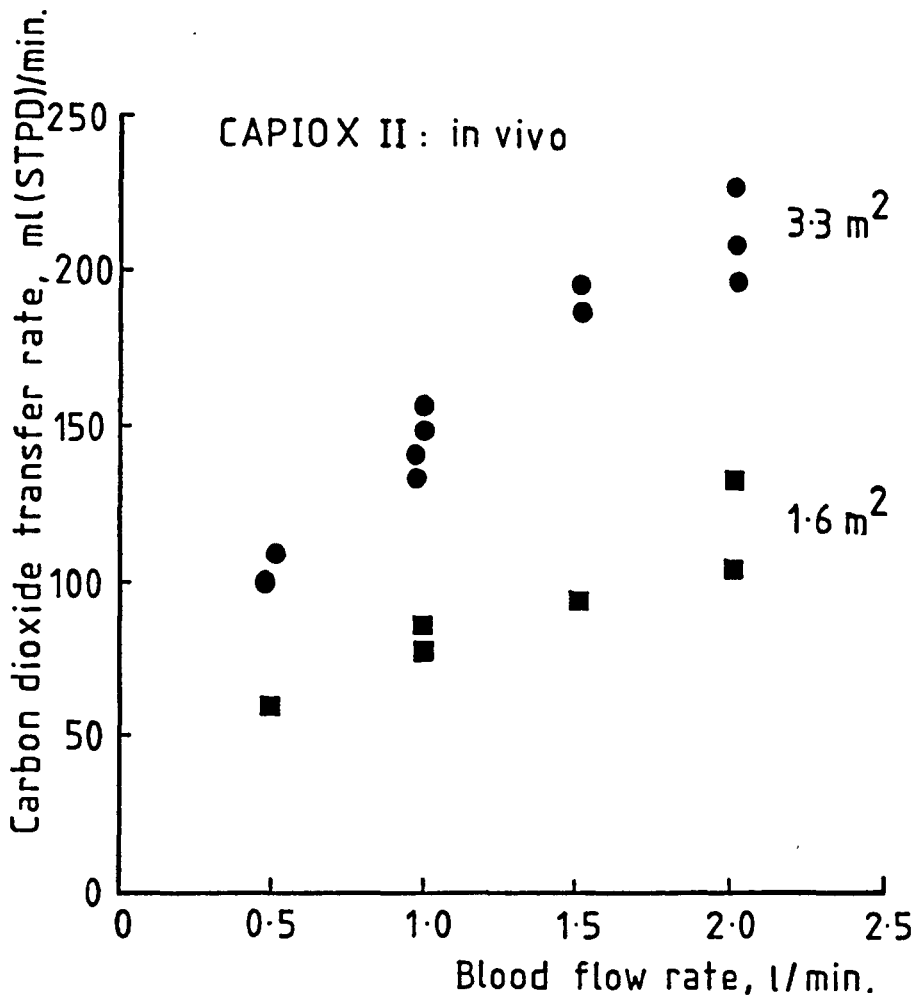

Figure 4.9 In vivo carbon dioxide transfer rate ($\dot{V}_{CO_2}$) as a function of blood flow rate (Q_B) for the Terumo CAPIOX II membrane lung. (after Mook et al. 1983).

$$z^* = \frac{D_1}{2Q_B} \times \frac{A}{2\pi R_i} \qquad (4.8)$$

Essentially z* is proportional to A/Q_B for constant R_i, wall resistance, γ and input conditions. Thus for similar A/Q_B ratios, θ_C should remain constant (Figure 3.3). Since $\dot{V}_{CO_2} = \theta_C C_{Ti} Q_B$ then it follows that $\dot{V}_{CO_2}/Q_B$ should be similar.

Table 4.2 shows the normalized ratios and relevant comparisons of the $1.6m^2$ and $3.3m^2$ units. For A/Q_B of 3.3 and 3.2 m^2.min/ℓ the $\dot{V}_{CO_2}/Q_B$ ratios are comparable allowing for the small difference between the A/Q_B ratios.

Table 4.2

A m^2	Q_B ℓ/min	$\dot{V}_{CO_2}$ mℓ(STPD)/min	A/Q_B m^2.min/ℓ	$\dot{V}_{CO_2}/Q_B$ mℓ(STPD)/ℓ
1.6	0.5	69	3.2	138.0
	1.0	96.5	1.6	96.5
	1.5	104.6	1.1	69.7
3.3	0.5	111.3	6.6	222.6
	1.0	152.0	3.3	152.0
	1.5	189.6	2.2	126.4

For the CAPIOX II $3.3m^2$ unit a gas phase outlet pCO_2 of about 12-14 mmHg is produced when operated at a Q_B of 1.5 ℓ/min and a ventilation flow rate of 10 ℓ/min. Higher ventilation flow rates may result in improvement in $\dot{V}_{CO_2}$ provided channelling of gas flow does not occur. It is however apparent from Figure 4.7 that for the $3.3m^2$ unit the increase in $\dot{V}_{CO_2}$ will not be substantial if

operated at gas flow rates 10 ℓ/min. Safe operation at higher ventilation rates is however possible for the Terumo CAPIOX II lungs as the gas phase flow resistance is very low. As the gas is vented to atmosphere after passage through the oxygenator the gas phase flow resistance is given by its input pressure, P_i. This was measured as a function of the gas flow rate Q_G and the results are presented in Figure 4.10 and 4.11 for the 3.3 and 1.6m^2 units respectively. At the maximum Q_G of 20 ℓ/min the input gas pressure for either unit does not exceed 3.0 cmH_2O (2.2 mmHg).

For safe operation of microporous membrane oxygenators the gas pressure should never exceed the blood pressure at any location along the exchange path otherwise gaseous microemboli will be introduced into the blood stream. In the $ECCO_2$ R-LFPPV application, assuming the oxygenator is operated in the partial veno-venous bypass mode, the gas input pressure would be opposed by the blood pressure in the return line to the patient. Since this pressure is the sum of the venous pressure (about 10mmHg in the femoral veins) plus the pressure drop across the venous cannula, introduction of microemboli will not occur even if the CAPIOX II devices were to be operated at Q_G of 20 ℓ/min.

4.4.4 Hollow fibre test modules

The experimental data is presented in Appendix F. Equation 3.16 and 3.21 were used to compute the fractional CO_2 removal, θ_C and dimensionless length z* respectively. The diffusion coefficient of CO_2 in blood was calculated in accordance with the relationship given in Appendix A. The results of separate tests on five modules are shown in Figure 4.12 together with theory predictions for various wall resistances, γ and input parameters corresponding to

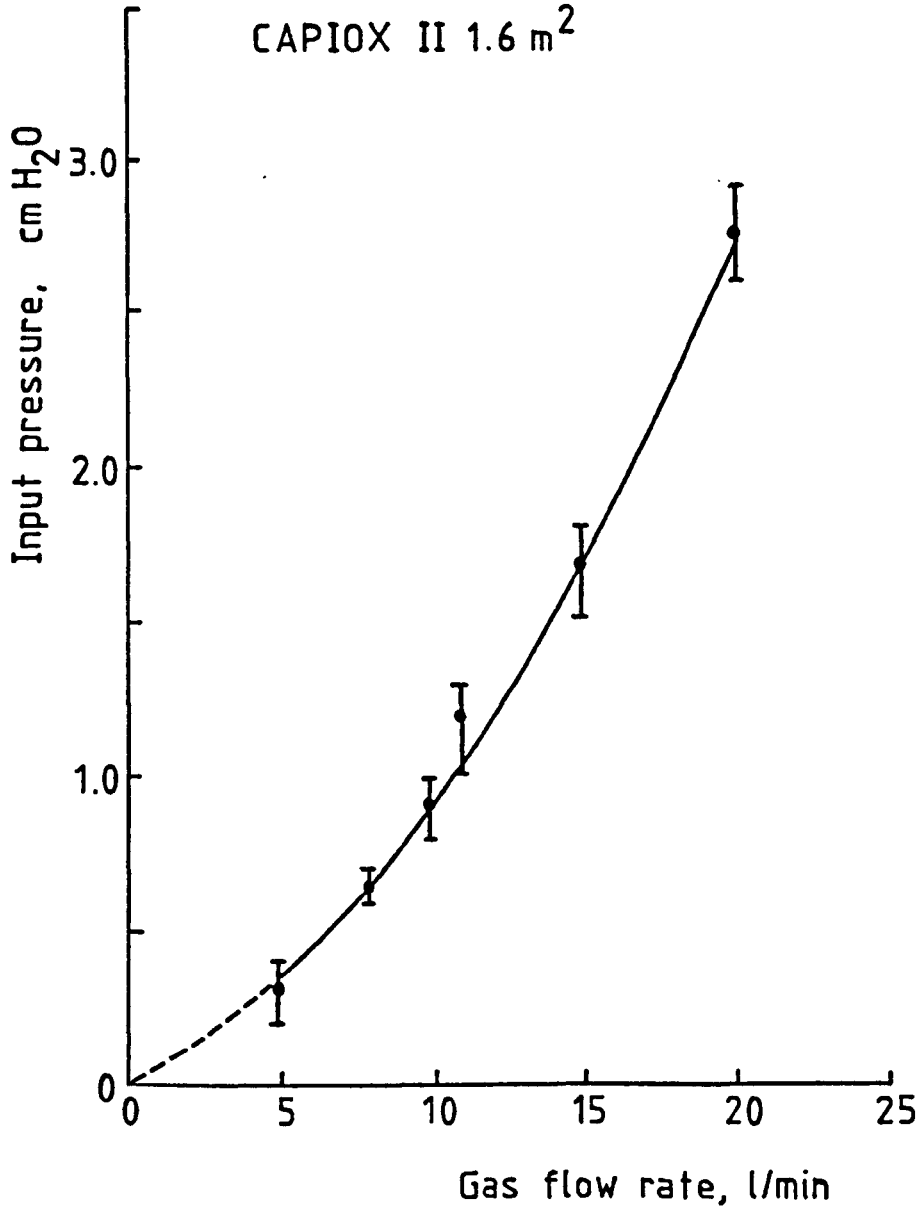

Figure 4.11 Gas phase input pressure (P_i) as a function of gas flow rate (Q_G).

n=3 for each Q_G, • - mean and range.

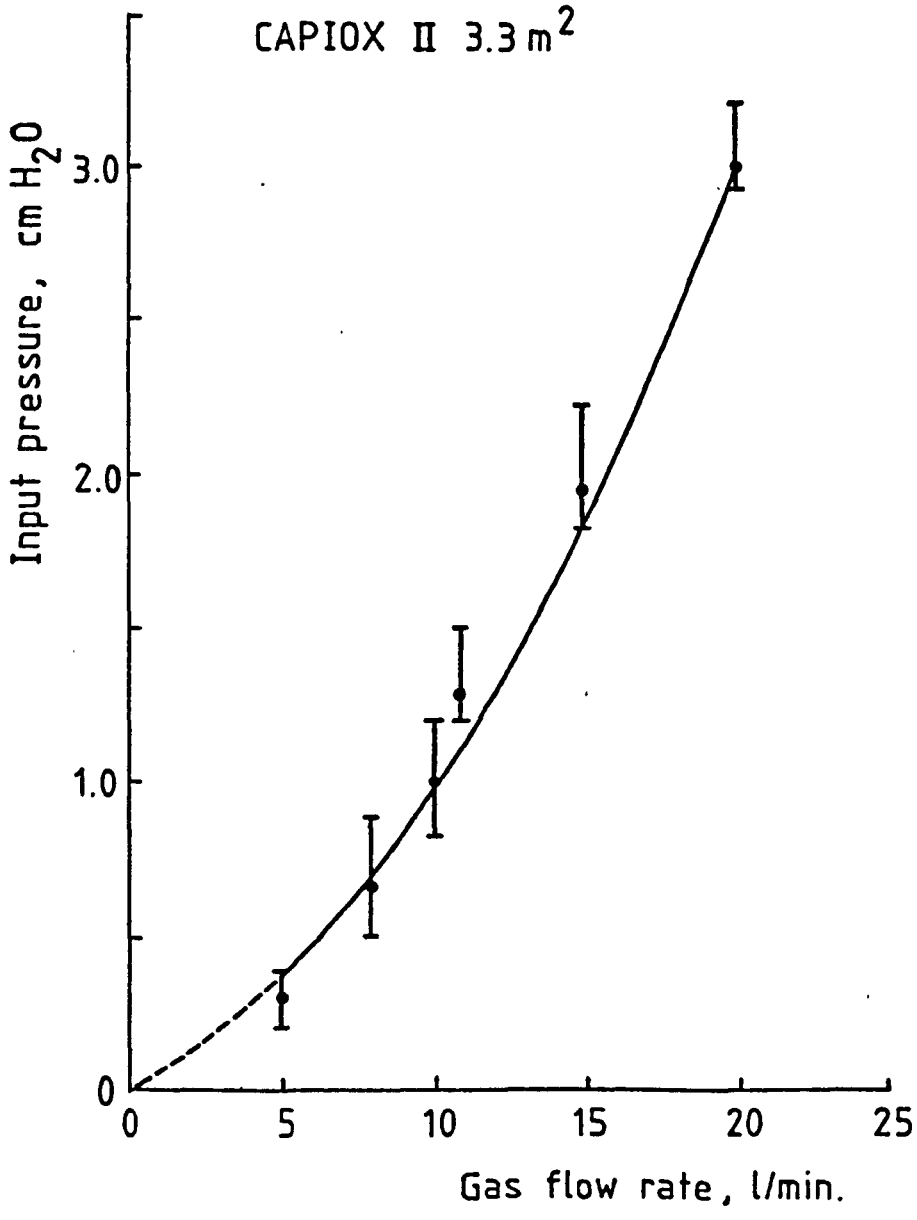

Figure 4.10 Gas phase input pressure(P_i) as a function of gas flow rate (Q_G).

n=4 for each Q_G, • - mean and range.

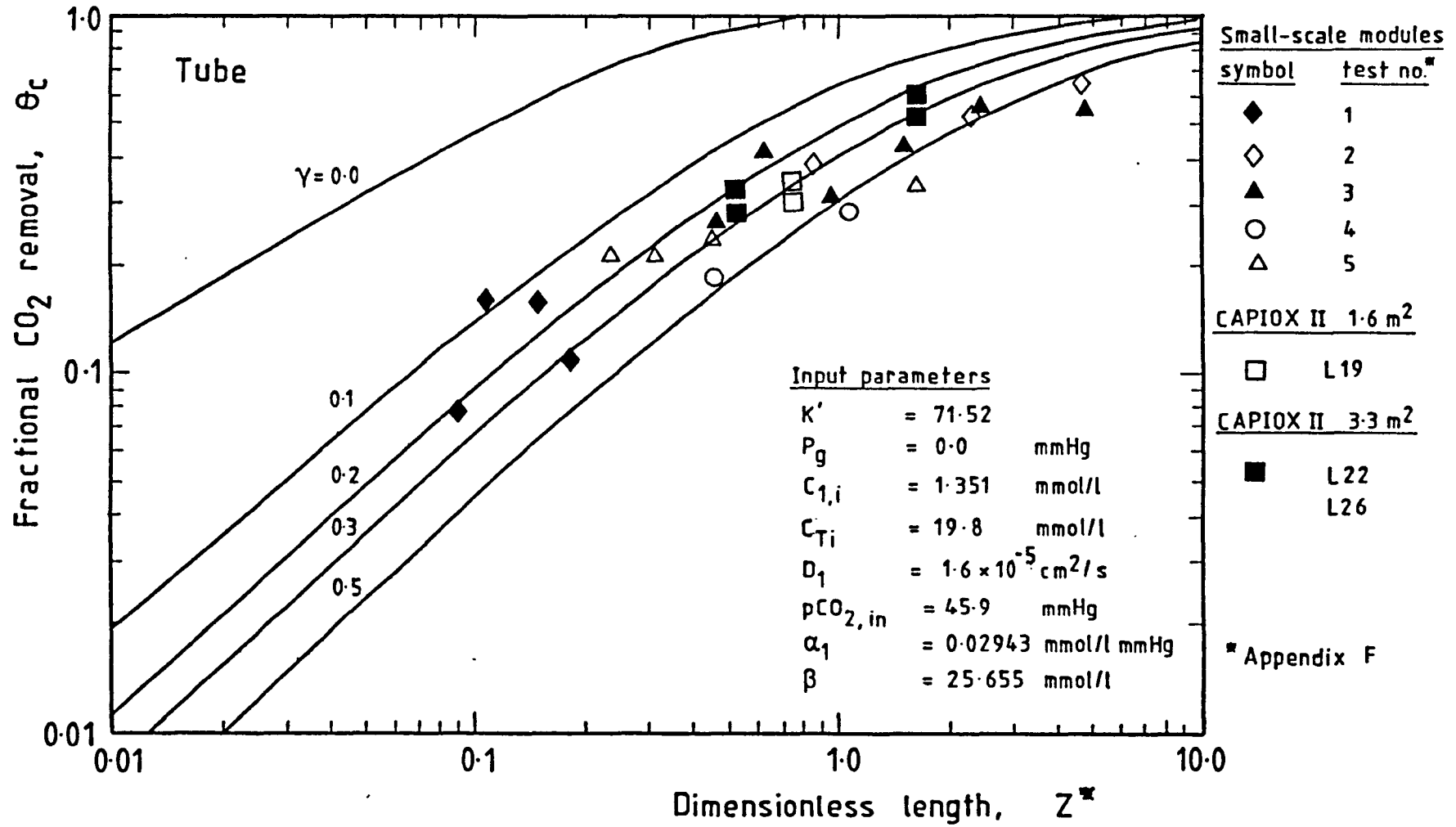

Figure 4.12 Comparison of CO_2 transfer with theory

the mean experimental values. The input blood conditions were: inlet pCO_2 of 45.9 $\pm$ 3.3 mmHg (n = 11), C_{Ti} of 19.8 $\pm$ 1.4 mmol/l (n = 38) and C_{Hb} of 12.1 $\pm$ 0.3 g% (n = 8), where n is the number of data points. The results show that the majority of the data points are clustered around a wall resistance, γ of 0.3. Also shown are selected data from the CAPIOX II membrane oxygenator evaluations at low Q_B (giving low outlet gas phase pCO_2) and inlet blood conditions within the experimental range of the hollow fibre module tests. The agreement between the two sets of data indicate that the fibres in the CAPIOX II membrane oxygenators are uniformly perfused and ventilated. The data show that a substantial wall resistance to CO_2 transfer in blood exists. The presence of a finite wall resistance for microporous hollow fibres is consistent with the study of Keller and Shultis (1979) on an analogous study on O_2 transfer through microporous membranes. They proposed a hypothesis that pore wetting due to liquid phase contact will give a considerable reduction in gas permeability or increase in wall resistance. The results of Katoh and Yoshida (1978) on CO_2 transfer in a similar membrane and those of Voorhees (1976) in a microporous tube support this hypothesis. As the theory prediction for zero membrane resistance (γ = 0) in Figure 4.12 shows, an improvement in CO_2 transfer may be achieved by reduction in membrane resistance. The design prediction for $ECCO_2R$-LFPPV presented in Chapter 3, Figure 3.5 and θ_C of 0.26, show that if γ were reduced by a factor of 6 i.e. to 0.05, then a 3.4 fold reduction in the number of tubes required for the same CO_2 removal would result.

During the tests, blood leakage in some of the modules occurred. This will affect the accuracy of the experiments. Further improvement in the design of the hollow fibre modules to eliminate leakage problems by trying different potting compounds (e.g. polyurethane)

is desirable.

Another feature of the present design was a small steel rod to mechanically mix the blood in the header volume at the module outlet. An improvement in the design would be to make the end header smaller, hence reducing the header volume and blood stagnation. At low blood flow rates, it is essential to avoid introducing foreign emboli into the test modules. If this occurs, uneven blood flow through the fibres or blockage may result. Filters incorporated in the circuit would reduce the event of fibre blockage or uneven flow.

MEMBRANE GAS TRANSMISSION RATE STUDIES UNDER GAS-MEMBRANE-LIQUID TEST CONDITIONS

5.1 Requirements for the Membrane Evaluation System

There is at present no standard method of evaluating carbon dioxide gas transmission through membranes for oxygenator applications. A suitable method would involve a gas-membrane-liquid test system, with negligible boundary layer resistances in gas and liquid phases and a satisfactory technique for measuring the permeant gas. In principle most permeation measurement techniques are of the same basic form. The permeant gas of interest passes from a source to a sink through the membrane which is the main resistance. The resistance is then measured by the rate of depletion in the source or by the rate of appearance of permeant in the sink. However, in a gas-membrane-liquid test system, the resistance of the fluid boundary layer cannot be neglected with respect to the total measured resistance. Keller and Shultis (1979) described a technique for determining oxygen gas transmission through homogeneous and microporous type membranes. They used a combination of high speed stirring and a chemical reaction in the liquid phase to reduce the fluid boundary layer resistance to a minimum level. Permeability was determined from a manometric system by observing the decrease in pressure in the gas phase at regular time intervals or by pO_2 electrodes in the liquid phase.

A similar approach to Keller and Shultis (1979) is adopted in this thesis to evaluate a test method for the determination of carbon dioxide gas transmission under liquid-contact conditions. The test system consists of using a dynamic test cell constructed in the Bioengineering Unit (Gaylor, 1970) based on the design by Babb et al. (1968) for measuring resistances of haemodialysis membranes, and is described in further detail in section 5.2. A rapid,

irreversible carbon dioxide scavenging reaction was carried out in the liquid phase. This allows the carbon dioxide crossing the membrane to be completely reacted in a region very close to the interface eliminating the need for the gas molecules to diffuse more than a few microns into the bulk of the liquid. Danckwerts (1981) has stated that liquid boundary layer resistances exist at gas-liquid interfaces, e.g. in bubble columns, and may be reduced by a suitable chemical reaction. The presence of a suitable scavenging reaction will maintain the partial pressure of dissolved carbon dioxide near to zero, hence the partial pressure of driving force across the membrane will be constant with time, i.e. steady state operation will exist.

The test system measures the carbon dioxide gas transmission from the gas phase (source) to the liquid phase (sink) via the membrane. Therefore, the process is that of absorption of carbon dioxide gas by a suitable reactive fluid which is subject to eddy turbulence generated by its flow through a porous membrane support. The absorption process occurring on the liquid side of the interface is influenced by two distinct sets of factors:

(a) Hydrodynamic factors:

geometry of the membrane support, and viscosity, density and flow rate of the liquid.

(b) Physico-chemical factors:

solubility and diffusivity of gas in the membrane and liquid, concentration of reagent; reaction velocity constant, and reaction-equilibrium constant.

In the evaluation of the test system, the above mentioned factors must be taken into account and are discussed in this

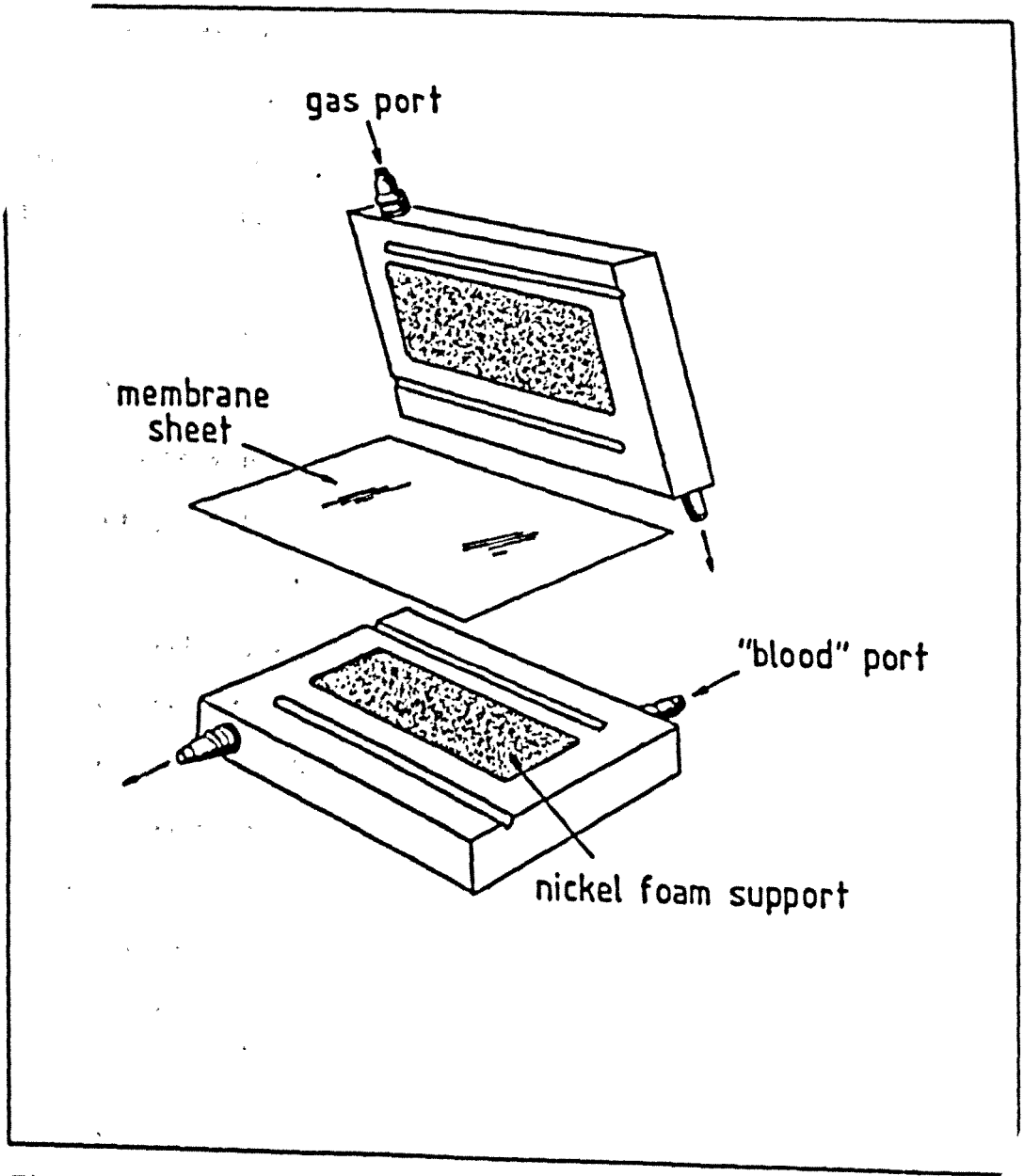

Figure 5.1 The dynamic test cell - Exploded view.

chapter with particular reference to the effect of varying concentration of the reactive solution and the fluid flow rate. The results obtained are compared with literature values.

5.2 Dynamic Test Cell

The dynamic test cell consists of two Perspex blocks (Figure 5.1) of dimensions 14.9cm. length; 12.4cm. width and 3.2cm. depth. Reticulated open-pore foam pads of nickel metal (10.8cm x 5.0cm x 0.36cm) are inserted into central recesses of the blocks and header chambers are located at the ends of the supports. The test membrane (14.9cm x 12.4cm) is sandwiched between the Perspex blocks which are held in place by a clamping assembly. Fluid stagnation areas in the foam support were avoided by impregnating a 1.0 x 5.0cm strip of the support at each end with silicone rubber (Silcoset, ICI Ltd.). A defined foam area was thus formed, 8.8cm x 50cm on each block giving a membrane area of 44.0cm^2. Since the nickel foam (Retimet, Dunlop Ltd.) had a void volume equal to 95% of the total volume (based on an apparent density of 0.39 g/cm^3), it was assumed that the percentage of membrane occluded by the support and therefore not available for gas transfer would be 5% of the total membrane area. The effective membrane transfer area was therefore 41.8cm^2.

The residence time of the reaction solution through the exchange region of the test cell can be calculated by the relationship:

$$\text{Residence time} = \text{Volume/flow rate} \qquad (5.1)$$

where the volume is the product of the effective area (41.8cm^2) and nickel foam thickness (0.36cm). Therefore the exposure of the reaction solution to the gas was between 0.23 to 0.90 s at flow rates of 1 to 4 l/min.

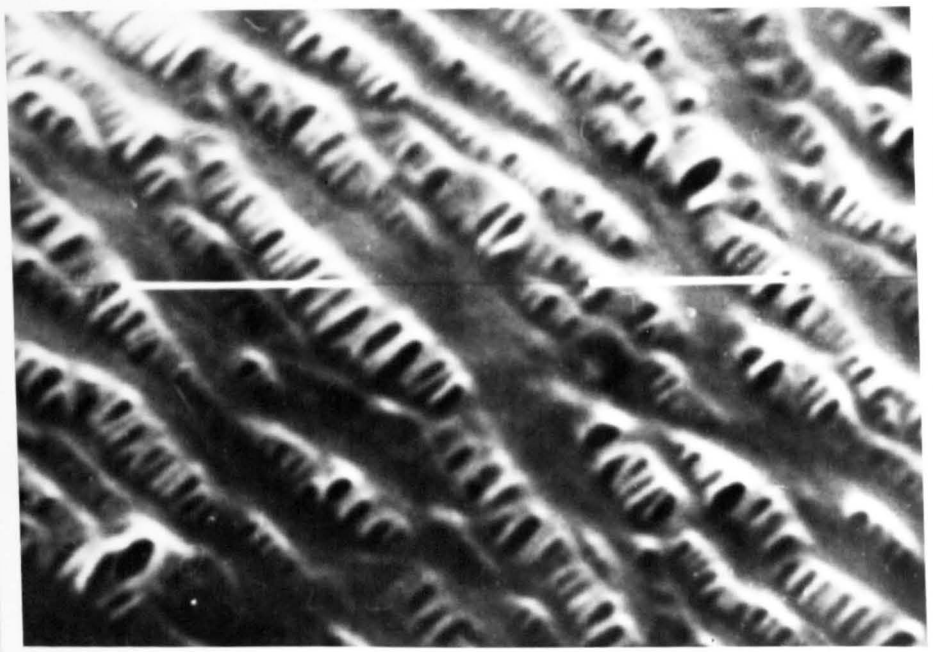

Figure 5.2 Scanning Electron Micrograph (SEM) of microporous polypropylene membrane.

5.2.1 Membrane description

Two types of membrane were investigated in this study namely, a microporous polypropylene material and a homogeneous silicone rubber material. Both types are currently used in membrane oxygenators.

The Celgard 2402 microporous membrane is a laminate of two sheets of polypropylene which possess discrete pores of 0.2μm x 0.02μm and a porosity of 45% (Figure 5.2). As the sheets are held together by static charges they may be readily separated and for the membrane evaluation, single sheets (25μm thick) were used. For most applications the membrane is hydrophobic in nature, a pressure of about 3.1×10^4 mmHg (4.14×10^6 N/m^2) being required to initiate water penetration (Gaylor et al. 1975).

5.3 Reaction Solution

Blood cannot be used in the dynamic test cell since haemolysis and blockage would result in the porous support. Also, as the gas transport relationships are non-linear, the interpretation of the carbon dioxide transmission rate of the membrane is more complex.

The reaction solution chosen in this evaluation is sodium hydroxide (NaOH). The choice of NaOH as a suitable alternative to blood for carbon dioxide transfer was prompted by the similarity in their reactions. Both the reaction processes result in the formation of the bicarbonate (HCO_3^-) and carbonate (CO_3^{2-}) species. If all the carbon dioxide gas crossing the membrane reacts chemically with NaOH to give the reacted species HCO_3^- and CO_3^{2-}, the total CO_2 content can be measured by the Corning carbon dioxide analyser.

5.3.1 Reaction kinetics of CO_2 absorption in NaOH solution

Sodium hydroxide has been investigated extensively as a carbon dioxide absorber in industrial applications. Consequently, much physico-chemical data of the CO_2-NaOH reaction is available (e.g. Danckwerts, 1981; Hikita et al. 1976; Astarita, 1967). When CO_2 is absorbed into aqueous alkaline solutions such as NaOH, the following two reactions take place:

$$CO_2 + OH^- \rightleftharpoons HCO_3^- \tag{5.2}$$

$$HCO_3^- + OH^- \rightleftharpoons CO_3^{2-} + H_2O \tag{5.3}$$

The values of the equilibrium constants K_1 and K_2 of reactions 5.2 and 5.3 respectively, are:

$$K_1 = \frac{[HCO_3^-]}{[CO_2][OH^-]} = 3.2 \times 10^7 \ \text{ℓ/mol} \tag{5.4}$$

$$K_2 = \frac{[CO_3^{2-}]}{[HCO_3^-][OH^-]} = 3.5 \times 10^3 \ \text{ℓ/mol} \tag{5.5}$$

at 30^oC and at infinite dilution. Reaction 5.2 is practically irreversible and is second order, i.e. first order with respect to both CO_2 and OH^- ions, the forward reaction rate constant k_1 being about 12.2×10^3 1/(mol.s) at 30^oC and infinite dilution. Reaction 5.3 is a proton transfer reaction and has a very much higher rate constant than reaction 5.2. Thus this reaction can be regarded as an instantaneous reversible reaction. When a substantial amount of free hydroxide is present, reaction 5.3 is completely displaced to the left.

The ratio of bicarbonate to carbonate is given by

$$\frac{[HCO_3^-]}{[CO_3^{2-}]} = \frac{1.7 \times 10^{-4}}{[OH^-]} \qquad (5.6)$$

and can be assumed to be zero whenever the OH^- concentration is larger than, say, 10^{-2} mol/l. The overall reaction which takes place during the absorption of carbon dioxide in hydroxide solutions may therefore be assumed to be the following:

$$CO_2 + 2OH^- = CO_3^{2-} + H_2O \qquad (5.7)$$

the kinetic constant at 25°C and at infinite dilution is about 6.0×10^3 l/(mol.s). Therefore the reactions which affect the absorption rate of CO_2 into aqueous NaOH solutions are the forward part of 5.2, which is irreversible and second order, and reaction 5.3 which proceeds instantaneously and reversibly.

Several assumptions are made in the CO_2-NaOH reaction system as applied to the dynamic test cell:

(1) The gas and liquid are at all times in equilibrium at the interface.

(2) Temperature effects at the surface of the liquid will be too small to affect the solubility or diffusivity of the gas, or the reaction-velocity constant.

(3) The physically dissolved carbon dioxide concentration on the liquid side is zero (assumes perfect mixing).

(4) Excess hydroxyl ions such that the reaction is tending towards the right of reaction 5.2.

Assumption (1) is reasonable once the gas crossing the membrane has reached steady-state conditions. Fast-reaction conditions are encountered at low CO_2 partial pressures and high hydroxide

concentrations. Astarita (1967) reported that the vapour pressure of CO_2 over solutions containing free hydroxide is negligible, hence indicating that the reaction of CO_2 with NaOH solutions is complete and CO_2 exists mainly in the reacted forms (i.e. HCO_3^- and CO_3^{2-}). Assumption (2) has been studied by Danckwerts (1981) in which he showed that the temperature rise associated with the absorption of CO_2 in NaOH solutions is negligible, and will not be great enough to affect the absorption rate of this reaction. The diffusivity of CO_2 (D_A) in NaOH solution is 1.8×10^{-5} cm^2/s and the ratio of D_A to the diffusivity of OH^- in NaOH solution, D_B is equal to 1.7 at 25°C (Danckwerts, 1981). Instantaneous reaction conditions (reaction 5.3) are never completely fulfilled because the hydroxyl ion concentration is never zero at the interface. In the equilibrium reaction 5.3, a finite concentration of the reaction product, CO_3^{2-} and a low concentration of OH^- ions will exist between the interface and the reaction plane, fulfilling assumptions (3) and (4).

A final requirement of the NaOH solution is that it whould not react with the polymer membranes so as to alter the permeability properties. Celgard 2402 membrane has shown no deterioration of the microporous structure when subject to highly caustic solutions (e.g. 40% potassium hydroxide) similar to NaOH (Bierenbaum et al. 1974). No information was obtained regarding the effects of NaOH on the silicone rubber membranes. However, both membranes exhibited time-independent gas transmission rates throughout the testing period. This would suggest that the membrane structure was not altered by the NaOH reaction solution.

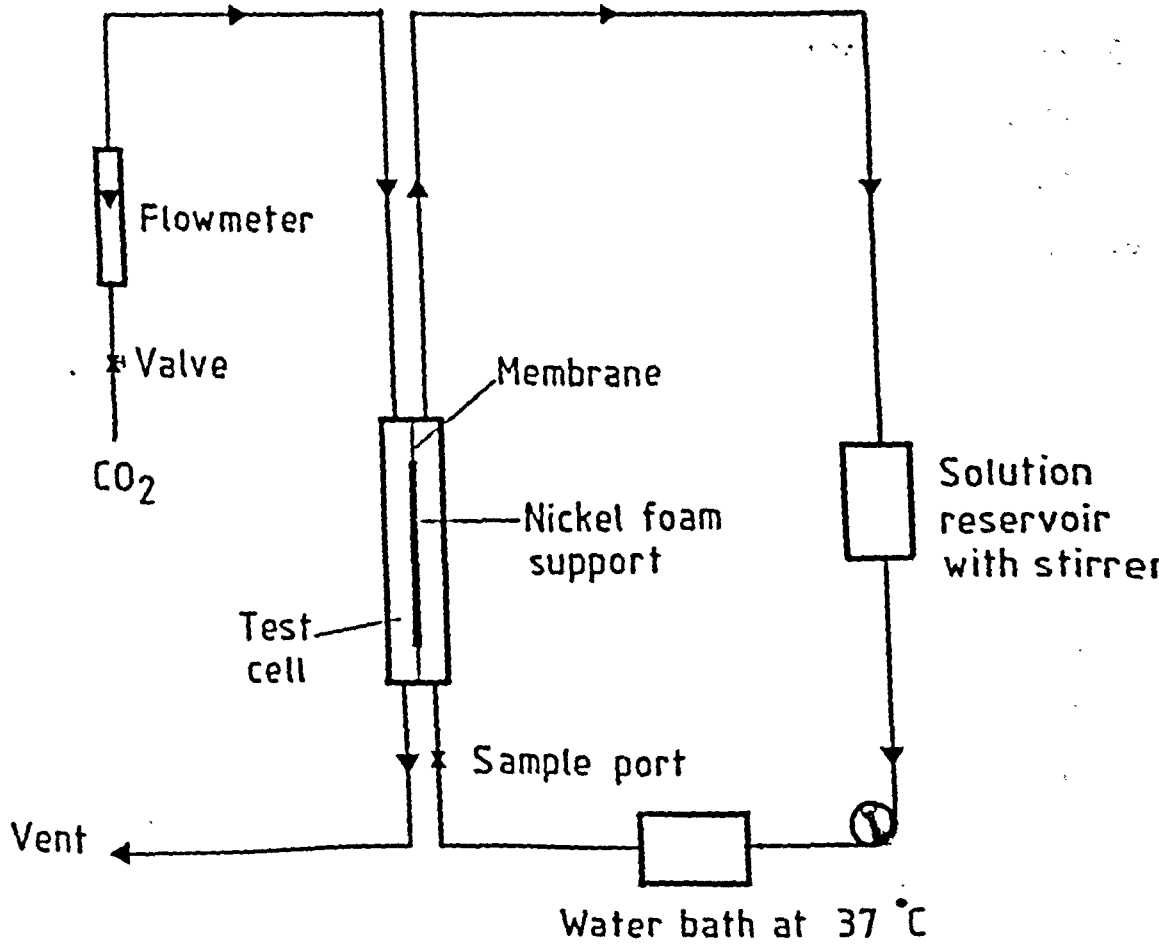

Figure Dynamic test cell flow circuit.

5.4 Experimental Circuit and Procedure

5.4.1 Test circuit

The closed-loop in vitro test circuit (Figure 5.3) consisted of a calibrated roller pump, connected in series to the dynamic test cell with the nickel foam pads in the vertical position. A reservoir containing 1.0 litre of the reaction solution was magnetically stirred and maintained at 37°C ± 0.05°C in a water bath (Grants Instruments, Cambridge Ltd). Solution was drawn from the reservoir and passed vertically upwards through the foam pads via the header chamber ports. The solution sampling port was located on the inlet side of the test cell. Carbon dioxide gas at a flow rate of 1.0 ℓ(STPD)/min measured by a rotameter (Platon Flowbits Ltd., England) was warmed to 37°C via a coiled heat exchanger in the water bath. The gas was passed countercurrent to the liquid flow in the dynamic test cell. The pressure drop at solution flow rates of 2.0 to 4.0 l/min ranged from 100 to 450 mmHg as shown in Figure 5.4. This pressure was 2 orders of magnitude smaller than that required to initiate water penetration in the Celgard 2402 microporous membrane as mentioned in section 5.2.1.

Preliminary tests showed that at high solution flow rates, small bubbles were generated in the test cell. This phenomenon has been observed in the dialysate of artificial kidney systems and is attributed to the release of dissolved gases when the liquid is heated and subsequently undergoes pressure changes (Chronic Uremia Program, 1977). The problem can be eliminated if the gases in the sodium hydroxide solution were removed under vacuum prior to circulation in the test cell.

After each test, the whole circuit was primed with slightly

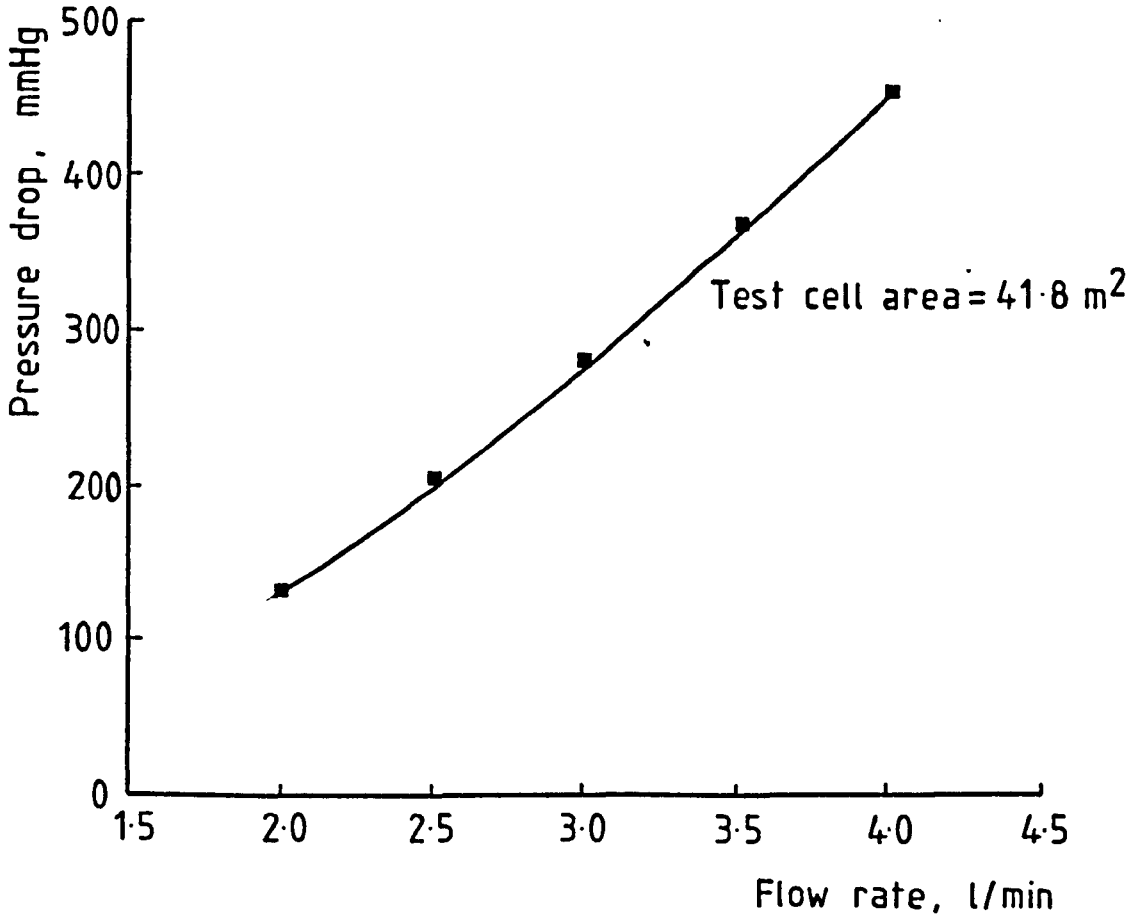

Figure 5.4 Pressure drop in the dynamic flow cell as a function of solution flow rate.

acidified (HCl) distilled water to remove residual carbon dioxide in the circuit and then rinsed with distilled water only. The dynamic test cell was dismantled after each experiment and air dried.

5.4.2 Test procedure

The rate of carbon dioxide uptake is obtained by sampling 100 µℓ of the reaction solution at regular time intervals after the carbon dioxide is introduced into the dynamic test cell. Measurements of the carbon dioxide content is performed by the Corning CO_2 analyser (Appendix C). The duration of the experiment is about 20 minutes. The procedure for each test can be summarised as follows:

(1) Prepare NaOH of known concentration in 1.0 litre of distilled water and vacuum.

(2) Assemble the in vitro circuit with the membrane positioned in the dynamic test cell.

(3) Circulate the reaction solution around the circuit for about 2 minutes (check for leakage).

(4) Measure the initial CO_2 content of the solution.

(5) Introduce the CO_2 gas supply (flow rate of about 1.0 ℓ(STPD)/min) and note starting time.

(6) Take the first sample at 30 seconds and measure the CO_2 content.

(7) Sample at 2 minute intervals for a duration of about 20 minutes.

5.5 Results

The unprocessed results are compiled in Appendix B together with the calculated CO_2 gas transmission rates, G_{CO_2}.

5.5.1 Calculation of gas transmission rate

If the assumptions of section 5.3.1 are satisfied then the rate of uptake by the reaction solution of CO_2 diffusing across the membrane will be constant with time. The measured CO_2 content should therefore be a linear function of time.

The gas transmission rate of the membrane is defined as:

G_{CO_2} = CO_2 transfer rate per unit area per unit pCO_2 driving force (5.8)

For the test system:

$$G_{CO_2} = \frac{(\text{slope of } CO_2 \text{ content vs time plot}) \times (\text{reservoir volume})}{(\text{effective membrane area}) \times (P_{ATM} - WVP) \times F_{CO_2}} \quad (5.9)$$

where P_{ATM} is the atmospheric pressure

WVP is the gas phase water vapour pressure

F_{CO_2} is the fraction of CO_2 in the gas.

In the calculation of the pCO_2 driving force the total pressure in the gas phase was taken to be that of atmospheric pressure CO_2, as the resistance to gas flow through the nickel foam was negligible. A sample calculation is given in Appendix B.

5.5.2 Effect of NaOH concentration

The effect of sodium hydroxide concentration [NaOH] on G_{CO_2} was investigated. Since the overall rate law and kinetics of the CO_2-NaOH reaction is highly dependent on the reaction concentration, CO_2 absorption into various concentrations of NaOH was studied. The NaOH solutions were prepared in concentrations of 4, 20, 40 and 60 g/l corresponding to molarities of 0.1, 0.5, 1.0 and 1.5 M. Figure 5.5 shows the CO_2 content as a function of time at different NaOH

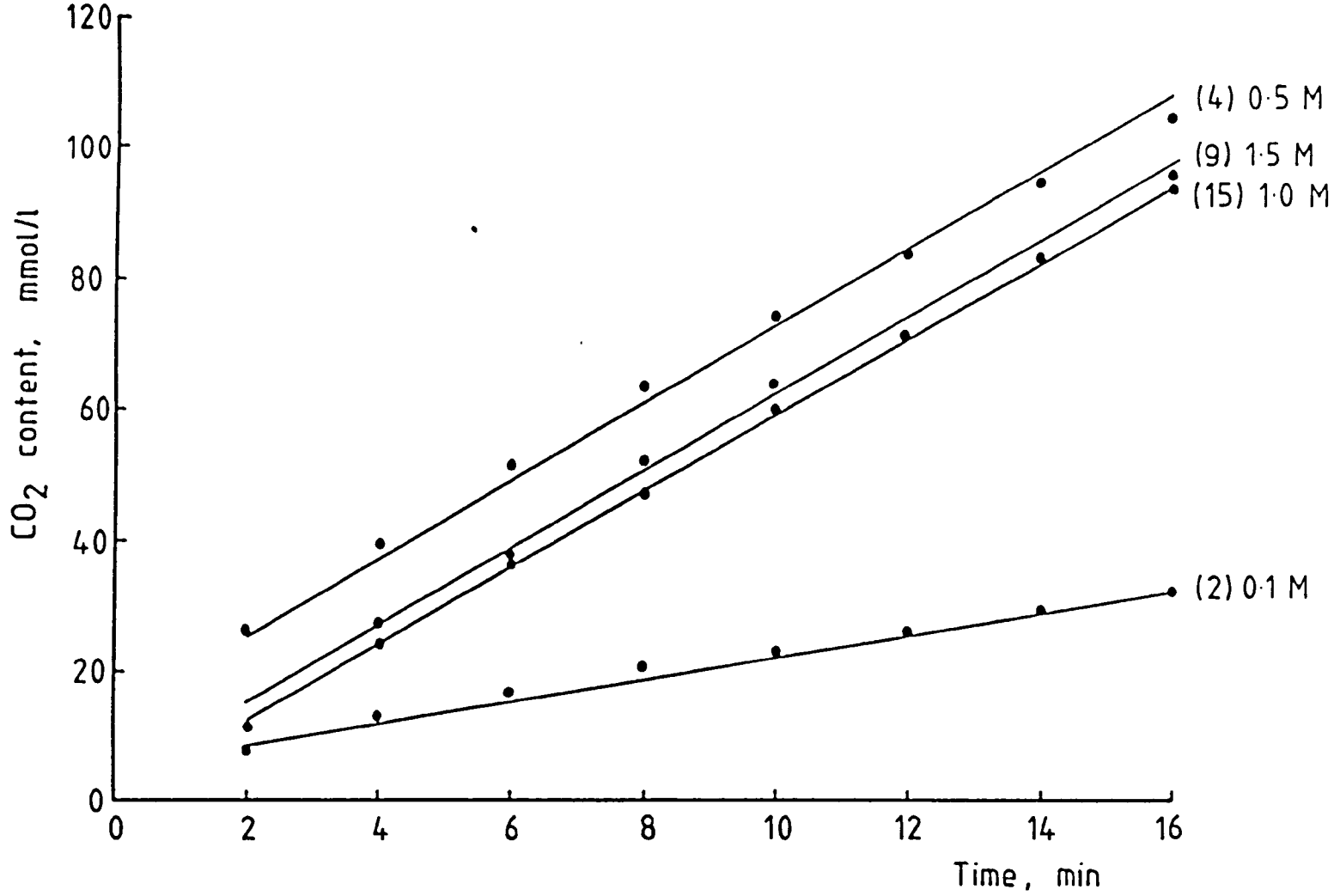

Figure 5.5 Carbon dioxide uptake as a function of time at different initial NaOH molar concentrations. ( ) - Test reference* for Celgard 2402 microporous polypropylene membrane.

*Appendix G

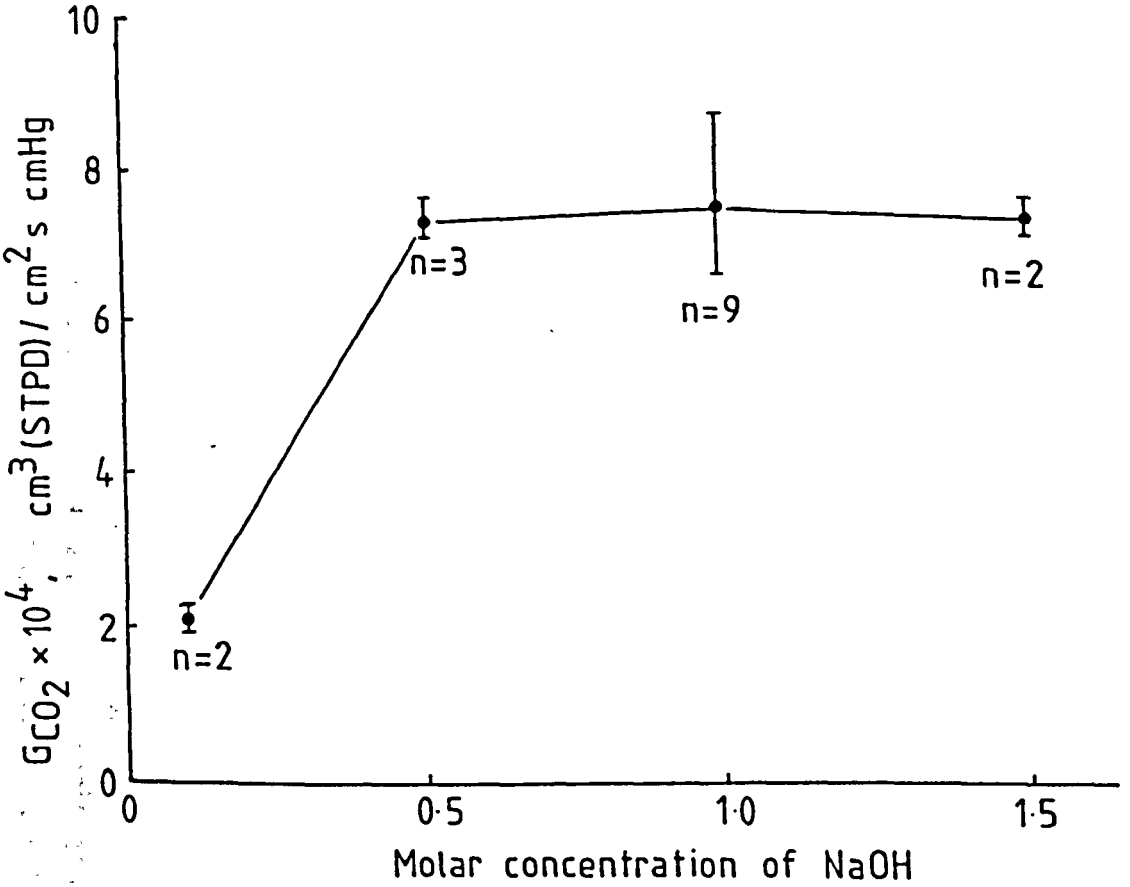

Figure 5.6 The effect of molar concentration of NaOH on CO_2 gas transmission at a flow rate of 0·5 l/min (n= no. of membranes tested).

molar concentrations. The slope of the line indicates the rate of CO_2 absorption. It may be seen that no change in the rate occurs for NaOH concentrations >0.5 M. Figure 5.6 shows the effect of [NaOH] on G_{CO_2} at a solution flow rate of 0.5 l/min. These results show that a NaOH molar concentration of 1.0 M may be used for the CO_2 absorption experiments in order to obtain the optimum G_{CO_2}. All the tests were carried out using this concentration.

5.5.3 Effect of solution flow rate

Tables 5.1 and 5.2 are the results for G_{CO_2} at different liquid flow rates for microporous polypropylene and silicone rubber membranes respectively. These results are presented graphically in Figure 5.7. Silicone rubber and microporous polypropylene membranes show a levelling off in G_{CO_2} in the flow rate range of 3 and 4 l/min respectively. At these flow rates one can assume that the liquid phase resistance is constant and has been reduced to the lowest level possible with the method of mixing in the test cell. The G_{CO_2} values obtained at the plateau regions (Figure 5.6) are 3.18×10^{-5} cm^3 (STPD)/(cm^2 s cmHg) and 12.11×10^{-4} cm^3(STPD)/(cm^2 s cmHg) for silicone rubber and microporous polypropylene respectively.

5.6 Discussion

The gas transmission rate for the reinforced silicone rubber membrane used in this study are compared with values obtained by previous workers as shown in Table 5.3, using liquid-membrane-gas systems. The values compare favourably allowing for variations in thickness, composition and test methods.

For the Celgard 2402 microporous polypropylene membrane a 5-fold reduction in G_{CO_2} is obtained with the liquid contact system used in this study compared with G_{CO_2} results from gas-membrane-gas tests (Gaylor et al. 1975). For the author's test system the

Table 5.1 Values of gas transmission rates (G_{CO_2}) as a function of flow rate (Q) for Celgard 2402 microporous polypropylene.

Q; l/min	0·5	2·0	2·5	3·0	3·5	4·0
$G_{CO_2} \times 10^4$, $cm^3(STPD)/cm^2 \, s \, cmHg$	7·75	10·94	11·46	12·38	10·85	11·73
	7·63	11·42	12·25	11·76	11·75	11·81
	8·78	12·03	13·38	12·50	11 96	13·20
	8·18	11·12	11·60	11·50	11·49	12·01
	6·69	10·34	10·88	11·04	11·06	12·08
	6·66	11·30	10·37	12·38	12·34	11·41
	7·66	10·74	11·75	11·45	10·90	12·19
	7·22				11·95	12·49
	6·87					
$\bar{x} \pm 1SD$	7·49± 0·71	11·13± 0·54	11·67± 0·97	11·86± 0·57	11·53± 0·55	12·11± 0·54

Unprocessed data is listed in Appendix G

Table 5.2 Values of gas transmission rates (G_{CO_2}) as a function of flow rate (Q) for Sci-Med silicone rubber.

Q, l/min	2·0	3·0	4·0
$G_{CO_2} \times 10^5$ $\frac{cm^3 (STPD)}{cm^2 . s . cmHg}$	2·41	3·41	2·74
	3·37	3·19	2·52
	3·40	3·40	2·61
	2·31	2·63	2·59
	2·54	3·71	3·55
		3·55	4·01
		2·39	2·37
$\bar{x} \pm 1$ SD.	2·81 ± 0·53	3·18 ± 0·49	2·91 ± 0·62

Unprocessed data is listed in Appendix G

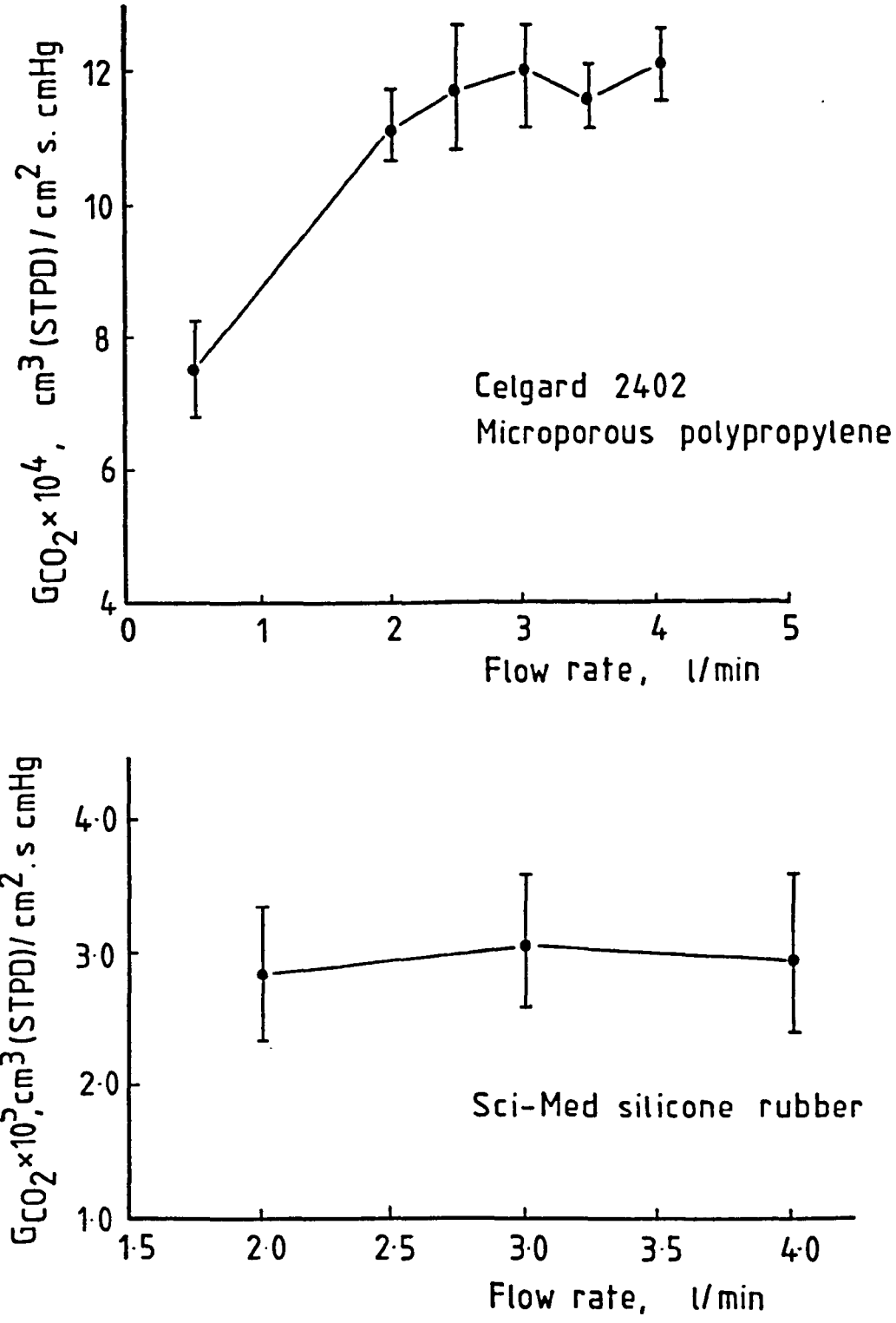

Figure 5.7 Carbon dioxide gas transmission rate as a function of solution flow rate.

Table 5.3 Carbon dioxide gas transmission rates for silicone rubber membranes under gas-membrane-liquid test conditions.

Membrane thickness μm	Manufacturer	G_{CO_2} $\frac{cm^3(STPD)}{cm^2 s\ cmHg}$	test system	reference
160	Dow Corning Silastic	3.0×10^{-5}	blood-to-gas	Ketteringham et al. (1975)
100	Fuji Systems Co.	3.4×10^{-5}	water-to-gas	Katoh and Yoshida (1978)
130	Sci-Med Inc.	3.18×10^{-5}	gas-to-NaOH	this study (1984)

G_{CO_2} value for the Celgard 2402 is 12.11 x 10^{-4} cm^3(STPD)/(cm^2 s cmHg). This value is about 3 times higher than the G_{CO_2} of 4.1 x 10^{-4} cm^3(STPD)/(cm^2 s cmHg) reported by Katoh and Yoshida (1978) for an unspecified Celgard membrane and about 8 times higher than the G_{CO_2} of 1.45 x 10^{-4} cm^3(STPD)/(cm^2 s cmHg) reported by Ketteringham et al. (1975) for an uncoated microporous polypropylene membrane at the highest reported blood flow rate as shown in Table 2.7. However, it was not certain from the paper by Ketteringham et al. (1975) the type of uncoated microporous membrane that was used, as an embossed microporous membrane was also one of the materials evaluated. Furthermore, it should be noted that the test system used did not reduce the liquid boundary layer resistance to its lowest level. Their G_{CO_2} results obtained at different blood flow rates indicated that further improvements in G_{CO_2} may be obtained at higher flow rates.

The higher G_{CO_2} value for microporous polypropylene obtained in this study appears to indicate that liquid boundary layer resistances may not have been reduced sufficiently in the test methods used by other workers. The G_{CO_2} value reported by Katoh and Yoshida (1978) was obtained in a mechanically stirred cell design with the rate of CO_2 desorption as a function of stirrer speed (n). Experimental results were analysed in a similar manner to the oxygen absorption experiments using Wilson plots as discussed in section 2.5.2. However, the main disadvantage of Wilson plot methods are the errors associated with the extrapolation technique. Due to the high permeability of the microporous membrane the intercept value will be small (Figure 2.13) and thus sensitive to the gradient of the extrapolated data fit. Another source of error may be attributed to the monitoring of CO_2

concentration which was carried out by a carbon dioxide electrode (Katoh and Yoshida, 1978). This type of electrode has a slow response time (typically 95% response in 3 minutes). At high stirrer speeds the rate of change of concentration actually measured is slower than that occurring (i.e. the actual membrane resistance is less than the measured resistance). Hence the true intercept will be smaller than the actual intercept on the Wilson plot. Finally it was not clear what type of Celgard microporous membrane Katoh and Yoshida used. Different Celgard membranes have different porosities. This would have to be known for a meaningful comparison with the data reported here.

The mechanism of gas permeation through microporous membranes under liquid contact conditions is a complex subject. A hypothesis has been proposed by Shultis (1980) that the main resistance to gas transfer is due to fluid residing in the pores. For the Celgard membranes, where the pore size is extremely small (0.02-0.2 μm), surface "roughness" may be an important consideration. The penetration of the fluid would be controlled by hysteresis, which implies a dynamic interaction rather than a simple equilibrium between the fluid and polymer. For example the fluid may be forced into the pore by a sudden fluctuation in pressure and be unable to return to the previous position arising from the "roughness" of the wall. The above discussion is just a hypothesis and further investigation into this phenomenon is required to verify it.

In the present work, the main resistance to gas transfer is due to liquid penetration in the pores as proposed by Shultis (1980), but a simple equilibrium model of diffusion is assumed in the pores. The reaction solution is NaOH of which a minute volume resides in the pore mouth. When CO_2 is absorbed by the

NaOH solution, sodium bicarbonate is formed. This reaction is completed in the pore mouth in a short time compared to the bulk reaction solution flowing in the channel of the test cell. Therefore, equilibrium is reached in the pores and the rate of gas permeation would then be determined by diffusion of bicarbonate ions and physically dissolved CO_2 through the reaction solution in the pore mouth before entering the bulk liquid phase. The initial homogeneous reaction to produce CO_3^{2-} is followed by depletion of OH^- at the surface leading in time to a diffusion-controlled reaction; superimposed on this is the secondary reaction leading to the formation of HCO_3^-. This occurs rapidly in the pores. This model of CO_2 permeation would approximate the condition for microporous membranes under gas-membrane-blood test systems if bicarbonate diffusion is considered to be an important diffusing species.

To verify the diffusion model, i.e. little reaction in the pore volume, a theoretical analysis similar to the approach reported by Shultis (1980) was used. The relationship used to test the applicability of the model is given by

$$\frac{J_i - J_o}{J_i} = \frac{\left[\frac{1}{3} k_1 D_A (\alpha p CO_2)^3\right]}{J_i^2} \qquad (5.10)$$

where J_i : observed flux of CO_2 into pore,
$G_{CO_2} \times P_{ATM}/\phi$ 22,260 mol/cm^{2}s

J_o : flux of CO_2 out of pore, mol/(cm^{2}s)

k_1 : second order reaction rate constant cm^3/mol.s

D_A : diffusivity of CO_2 in NaOH solution cm^2/s

α_{CO_2} : solubility of CO_2 in water at 37°C mol/cm^3 cmHg

pCO_2 : partial pressure of carbon dioxide cmHg

ϕ : porosity (0.45 for Celgard 2402).

If equation 5.10 approaches zero, most of the carbon dioxide passes through the pores unreacted, i.e. diffusion only.

Data is not readily available for the solubility and diffusivity of carbon dioxide in sodium hydroxide at 37°C. The solubility of CO_2 in sodium hydroxide is taken to be the same as in water, and at 37°C, α_{CO_2} is 0.547 $cm^3(STPD)/(cm^3 atm)$. Similarly, the diffusivity of CO_2 in sodium hydroxide at 37°C can be estimated from its value at 25°C (section 5.3.1) by analogy with the Stokes-Einstein relationship ($\frac{D\mu}{T}$ = constant) to give $D_{A,37^oC} = 2.41 \times 10^{-5}$ cm^2/s

Reaction rates usually increase with temperature. Given $k_1 = 12.2 \times 10^6$ $cm^3/mol\ s$ at 30°C (Hikita et al. 1976), the reaction rate constant can be determined at 37°C using the Arrhenius equation:

$$k_1 = A' \exp(-E/RT) \qquad (5.11)$$

where A' is a constant, known as the frequency factor

E is the activation energy, $= 5.545 \times 10^4$ $J\ mol^{-1}$

R is the gas constant, $= 8.314$ $JK^{-1}\ mol^{-1}$.

Using equation 5.11, the constant A was determined and k_1 at 37°C was calculated to be 19.9×10^6 $cm^3/mol\ s$.

Evaluation of equation 5.10, using G_{CO_2} of 12.11×10^{-4} obtained in this study gives a value of 0.028. Since the equation approaches zero, the theoretical analysis indicates that CO_2 transfer through the pore volume is predominantly that of diffusion with little reaction. However, further work would be required to verify this reaction mechanism of transfer.

CONCLUSIONS AND RECOMMENDATIONS

6.1 Conclusions

6.1.1 Oxygenator CO_2 performance

To satisfy CO_2 requirements for $ECCO_2R$-LFPPV therapy a carbon dioxide transfer rate to blood flow rate ratio ($\dot{V}_{CO_2}/Q_B$) of 120-140 mℓ CO_2 (STPD)/ℓ will be required in the treatment of an adult if Q_B is limited to 1.5 ℓ/min. Based on a literature review of current membrane oxygenators, a comparison of CO_2 performance data normalised for membrane area show that, for laminar flow devices, a Q_B/A ratio of $\leq$ 0.5 $\ell/min^{-1}m^{-2}$ would be required. At this Q_B/A ratio of membrane areas $\geq$ 3 m^2 would be required if the maximum Q_B is limited to 1.5 ℓ/min. Although secondary flow devices were not evaluated in this study the desired CO_2 removal is more readily achieved in these devices. For example, in the pulsed-vortex oxygenator a corresponding Q_B/A ratio of about 1.7 1 min^{-1} m^{-2} is obtained with a membrane area of 0.9 m^2.

The CO_2 transfer theory of Voorhees (1976) as described in chapter 3 has been used to study the effect of the wall resistance parameter on CO_2 transfer. An extension of Voorhees' transfer model was to include the effects of gas phase partial pressure. In membrane oxygenators, the influence of gas phase resistance is an important consideration since a small partial pressure driving force is available for CO_2 transfer. Any build up of the gas phase partial pressure would result in a reduction of CO_2 transfer and hence in the membrane oxygenator performance. The wall resistance and gas phase partial pressure effects are useful in providing guidelines for efficient oxygenator design for CO_2 removal and identifying areas where improvements can be made.

Based on the in vitro membrane oxygenator evaluations, only

the CAPIOX II 3.3 m^2 unit with a $\dot{V}_{CO_2}/Q_B$ ratio of 126 mℓ CO_2(STPD)/ℓ satisfies marginally the CO_2 removal criteria necessary for the treatment of an adult, as also predicted from the Q_B/A ratio. Although the 2.25 m^2 Travenol TMO membrane oxygenator is not adequate for the new application it is however, on a unit area basis, comparable with the CAPIOX II 3.3 m^2 device.

Correlation with theory for the CAPIOX II unit indicates a substantial membrane resistance to CO_2 transfer and further increase in $\dot{V}_{CO_2}$ may be expected at all blood flow rates if the membrane resistance were to be reduced. Further improvements in CO_2 removal may also be obtained by an increase in ventilation flow rate (>10 ℓ/min).

The influence of possible blood flow maldistribution has been investigated in the Travenol TMO device. The experimental unit was modified and a theoretical analysis performed. An increase in CO_2 transfer was predicted if a mixing stage was included. This effect was quantified with the theoretical model under optimal operating conditions assuming zero gas phase partial pressure (Pg = 0). The result of $\dot{V}_{CO_2}$ with the two stage model showed little improvement compared with the unstaged device. The implication is that staging would not be a practical proposition. Furthermore, blood flow maldistribution is not an explanation for the sharp decline in CO_2 performance at low blood flow rates compared with the theoretical predictions. Shim pressure effects have been reported to influence $\dot{V}_{CO_2}$ (Murphy et al. 1974), but were not investigated in this thesis. This may be an alternative explanation for the fall in CO_2 performance at low blood flow rates.

6.1.2 Membrane evaluation

In the present gas-membrane-liquid test method, the G_{CO_2} value of 3.18×10^{-5} cm^3(STPD)/(cm^2s cmHg) for a homogeneous silicone

membrane was consistent with reported literature values for membranes of similar thickness which were also tested under gas-membrane-liquid conditions.

A 5-fold reduction in G_{CO_2} for the single-ply Celgard 2402 microporous polypropylene membrane has been demonstrated under a gas-membrane-liquid test system compared to gas-membrane-gas test reported in the literature. However, the G_{CO_2} value of 12.11×10^{-4} $cm^3(STPD)/(cm^2 s\ cmHg)$ found here was much higher than values reported by other investigators using liquid contact systems. Previous systems used to determine CO_2 gas transmission for microporous membranes have not completely reduced the liquid boundary layer resistance. This is particularly important with high permeability microporous membranes.

6.2 Recommendations for future work

The following topics are suggested for future research in this area:

(1) Polymer-coated microporous membranes should be assessed for CO_2 gas transmission to validate the hypothesis proposed by Keller and Shultis (1979). They showed a higher G_{O_2} through polymer-coated microporous membranes than the uncoated material. This observation was attributed to liquid diffusional resistance due to wetting of the micropores.

(2) A range of hydrophobic Celgard microporous membranes of different porosities and pore sizes should be evaluated for G_{CO_2}. There has not been a systematic attempt to characterise their gas transmission properties in order to determine the best one for the oxygenator application. Where reported values have been given, it is not always specified as to which particular Celgard microporous membrane used. This is important if meaningful comparisons are to be made.

(3) Prolonged blood contact has been shown to affect membrane O_2 permeability (Keller and Shultis, 1979). This phenomenon may have a significant effect on CO_2 transfer for long-term oxygenator applications. Therefore exposing the membrane to blood for varying time periods would indicate the effect of blood on the gas permeability of the membrane.

(4) A diffusion-limited transfer in the pores has been proposed to explain the transfer mechanism in microporous polypropylene membranes under liquid contact conditions. This hypothesis may be investigated by altering the pCO_2 in the gas phase of the test system reported here. If the transfer is diffusion limited in the pores, then changing the pCO_2 in the gas phase should not affect the G_{CO_2} value obtained.

(5) Improvement in the CO_2 performance may be obtained if a system can be incorporated in the oxygenator to give recirculation of the ventilation gas at high flow rates. The gas from the outlet of the oxygenator could be passed through a soda lime column in the recirculation loop to reduce its pCO_2 level. The recirculated gas would be replenished by fresh ventilating gas (zero pCO_2) added at inlet to the oxygenator at an economical flow rate and a corresponding flow removal at exit from the column.

bibliography

BIBLIOGRAPHY

The following journals have been abbreviated:

The Transactions of the American Society for Artificial Internal Organs (Trans. ASAIO).

The Proceedings of the European Society for Artificial Organs (Proc. ESAO).

BIBLIOGRAPHY

ADAMS, A.P., HAHN, C.E.W. (1982).
Principles and practice of blood-gas analysis.
Churchill Livingstone, Edinburgh.

ASTARITA, G. (1967)
Mass transfer with chemical reaction.
Elsevier Publishing Company, Amsterdam.

BABB, A.L., MAURER, C.J., FRY, D.L., POPOVICH, R.P., RAMOS, C.P. (1968)
Methods for the in vivo determination of membrane permeabilities and solute diffusivities.
Trans. ASAIO, 14:25.

BARTHELEMY, R., GALLETTI, P.M., TRUDELL, A., MacANDREW, J., RICHARDSON, P.D., PUEL, P., ENJALBERT, A. (1982).
Total extracorporeal CO_2 removal in a pumpless artery-to-vein shunt.
Trans. ASAIO, 28:354.

BARTLETT, R.H., FONG, S.W., WOLDANANSKI, C., HUNG, E., STYLER, D., MacARTHUR, C. (1975).
Hematologic responses to prolonged extracorporeal circulation (ECC) with microporous membrane devices.
Trans. ASAIO, 21:250.

BARTLETT, R.H., GAZZANIGA, A.B. (1978).
Extracorporeal circulation for cardiopulmonary failure: In current problems in surgery, (ed. M.M. Ravitch), Vol. 15:1.
Year Book Medical Publishers, Inc., London.

BAURMEISTER, U., JAMES, D.F., ZINGG, W. (1977).
Blood oxygenation in coiled silicone-rubber tubes of complex geometry.
Med. & Biol. Eng. & Comput., 15:106-117.

BEALL, A.C. Jr., SOLIS, R.T., KAKVAN, M., MORRIS, G.C., NOON, G.P. DeBAKEY, M.E. (1976).
Clinical experience with the Teflo Disposable membrane oxygenator.
Ann. Thorac. Surg., 21:2, 144-150.

BELL, G.H., EMSLIE-SMITH, D., PATERSON, C.R. (1976).
Textbook of Physiology and Biochemistry.
9th edition, Churchill Livingstone, Edinburgh.

BELLHOUSE, B.J., BELLHOUSE, F.H. (1969).
Fluid mechanics of model normal and stenosed aortic valves.
Circ. Res., 25:639.

BELLHOUSE, B.J., BELLHOUSE, F.H., CURL, C.M., MacMILLAN, T.I., GUNNING, A.J., SPRATT, E.H., MacMURRAY, S.B., NELEMS, J.M. (1973).
A high efficiency membrane oxygenator and pulsatile pumping system, and its application to animal trials.
Trans. ASAIO, 19:72-79.

BENN, J.A. (1974).
Carbon dioxide transfer from weak acids and blood : the effects of carbonic anhydrase and oxygen uptake on carbon dioxide transfer in an oxygenator.
Ph.D. thesis, Massachusetts Institute of Technology.

BIERENBAUM, H.S., ISAACSON, R.B., DRUIN, M.L., PLOVAN, S.G. (1974).
Microporous polymeric films.
Ind. Eng. Chem. Prod. Res. Develop., 13:1.

BIRNBAUM, D., BUCHERL, E.S. (1974).
CO_2 Removal in membrane oxygenator.
Proc. ESAO, 1:45-46.

BISWAS, C.K., RAMOS, J.M., AGROYANNIS, B., KERR, D.N.S. (1982).
Blood gas analysis: effect of air bubbles in syringe and delay in estimation.
Br. Med. J., 284:923-926.

BOCK, A.V., FIELD, H.F., ADAIR, G.S. (1924).
The oxygen and carbon dioxide dissociation curves of human blood.
J. Biol. Chem., 59:371.

BRADLEY, C.G., PIKE, R.W. (1971).
The transport of oxygen and carbon dioxide in blood flowing in a permeable tube.
Med. Instrumentation, 5:230.

BROWN, C.H., LEMUTH, R.F., HELLUMS, J.D., LEVERETT, L.B., ALFREY, C.P. (1975).
Response of human platelets to shear stress.
Trans. ASAIO, 21:35.

CALKINS, J.M. (1971).
Non Equilibrium Transfer in Tubular Membrane Oxygenators.
PhD dissertation. College Park, Md: University of Maryland.

CHANG, B.S., GARELLA, S. (1982).
Complete removal of metabolic CO_2 production by alkali infusion and dialysis in: Life Support Systems (ed. J. Belenger).
Proceedings of the IX Annual Meeting ESAO, Brussels, Belgium, W.B. Saunders Company Ltd.

CHRONIC UREMIA PROGRAM (1977).
Report of a study group for the artificial kidney - Evaluation of haemodialysers and dialysis membranes. U.S. Department of Health, Education and Welfare Public Health Service, National Institute of Health, National Institute of Arthritis, Metabolism and Digestive diseases, Bethesda , Maryland 20014 DHEW Publication No. (NIH) 77-1294.

COLTON, C.K. (1976).
Fundamentals of Gas Transport in Blood in: Artificial Lungs for Acute Respiratory Failure, (eds. W.M. Zapol and J. Qvist) pp3-41.
Academic Press, New York.

COMROE, J.H. (1965).
Physiology of Respiration.
Year Book Medical Publishers, Chicago.

COONEY, D.O. (1976).
Biomedical engineering principles: An introduction to fluid, heat and mass transport processes.
Vol. 2. Marcell Dekker, Inc. New York.

DANCKWERTS, P.V. (1970).
Gas-Liquid Reactions.
McGraw-Hill, New York.

DAVIES, D.D. (1970).
A method of gas chromatography for quantitative analysis of blood-gases.
Brit. J. Anaesth., 42:39.

DE JONG, J.C.F., SMIT SIBINGA, C.Th., WILDEVUUR, Ch.R.H. (1977).
Platelet behaviour in extracorporeal circulation (ECC) in: Artificial Organs (eds. R.M. Kenedi, J.M. Courtney, J.D.S. Gaylor and T. Gilchrist).
Macmillan Press Ltd., London.

DENNIS, C., SPRENG, D.S., Jr., NELSON, G.E., KARLSON, K.E., NELSON, R.M., THOMAS, J.V., EDER, W.P., VARCO, R.L. (1951).
Development of a pump-oxygenator to replace the heart and lungs; an apparatus applicable to human patients, and application to one case.
Ann. Surg., 134:709-721.

DEW, P.M., WALSH, J.E. (1981).
A set of library routines for solving parabolic equations in one space variables.
ACM Trans math Software, 7:3, 295-314.

DOHI, T., HAMADA, E., TERAMOTO, S., KANBAYASHI, T., (1981).
Development and clinical application of a new membrane oxygenator using a microporous polysulfone membrane.
Proc. Int. J. Artif. Organs, 5:804-808.

DORSON, W.J., LARSEN, K.G., ELGAS, R.J., VOORHEES, M.E. (1971).
Oxygen transfer to blood: data and theory.
Trans. ASAIO, 17:309.

DORSON, W.J.Jr., VOORHEES, M.E. (1974).
Limiting models for the trnasfer of CO_2 and O_2 in the membrane oxygenators.
Trans. ASAIO, 20:219-225.

DRINKER, P.A., BARTLETT, R.H., BIALER, R.M., NOYES, B.S. (1969).
Augmentation of membrane gas transfer by induced secondary flows.
Surgery, 66: 775-781.

DRINKER, P.A., BARTLETT, R.H. (1976).
Practical application of secondary flows in membrane oxygenators.
In: Artificial Lungs for Acute Respiratory Failure,
(eds. W.M. Zapol and J. Qvist).
Academic Press Inc., New York.

EBERHART, R.C., DENGLE, S.K., CURTIS, R.M. (1978).
Mathematical and experimental methods for design and evaluation of membrane oxygenators.
Artif. Organs., 2:19-34.

ESMOND, W.G., DIBELIUS, N.R. (1965).
Permselective ultra-thin disposable silicone rubber membrane blood oxygenator: Preliminary report.
Trans. ASAIO, 11:325-329.

FEIJEN, J. (1977).
Thrombogenesis caused by blood-foreign surface interaction.
In: Artificial Organs (eds. R.M. Kenedi, J.M. Courtney, J.D.S. Gaylor and T. Gilchrist).
Macmillan Press Ltd., London.

FEIJEN, J., BEUGELING, T., BANTJES, A., SMIT SIBINGA, C.Th. (1979).
Biomaterials and interfacial phenomena.
Adv. Cardiovasc. Phys., 3:100, Karger, Basel.

FLEMING, J.S., BECKET, J., MARKEY, A.W., MELROSE, D.G. (1981a).
The dialyser as a carbon exchanger.
Proc. ESAO, 8:296.

FELMING, J.S., HOWELL, A.D., ADAMS, S.J., MARKEY, A.W., BENTALL, H.H., SAPSFORD, R.N., STANBRIDGE, R., MELROSE, D.G. (1981b).
Extracorporeal Interpulse membrane oxygenator in clinical use.
Artif. Organs, (Suppl.), 5:817-819.

FOLKOW, B., NEIL, E. (1971).
Circulation.
Oxford University Press, London.

FORSTER, R.E., OBAID, A.L., GRANDALL, E.D., ITADA, N. (1980).
Cl^- and HCO_3^- movements across the red blood cell membrane in:
Biophysics and Physiology of Carbon Dioxide,
(eds. H. Bartels, G. Gros and C. Bauer).
Springer-Verlag, Berlin.

GALLETTI, P.M., RICHARDSON, P.D., SNIDER, M.T., FRIEDMAN, L.I. (1972).
Standardized method for defining the overall gas transfer performance of artificial lungs.
Trans. ASAIO, 18:359.

GALLETTI, P.M. (1980).
Impact of the artificial lung on medical care.
Int. J. Artif. Organs, 3:157.

GATTINONI, L., KOLOBOW, T., TOMLINSON, T., IAPICHINO, G., SAMAJA, M., WHITE, D., PIERCE, J. (1978).
Low-frequency positive pressure ventilation with extracorporeal carbon dioxide removal (LFPPV-ECCO$_2$R): An experimental study.
Anesth. Analg., 57:470.

GATTINONI, L., PESENTI, A., ROSSI, G.P., VESCONI, S., FOX, U., KOLOBOW, T., AGOSTONI, A., PELIZZOLA, A., LANGER, M., UZIEL, L., LONGONI, F., DAMIA, G. (1980).
Treatment of acute respiratory failure with low-frequency positive-pressure ventilation and extracorporeal removal of CO_2.
The Lancet, 9:292.

GATTINONI, L., PESENTI, A., PELIZZOLA, A., CASPANI, M.L., IAPICHINO, G., AGOSTONI, A., DAMIA, G., KOLOBOW, T. (1981).
Reversal of terminal acute respiratory failure by low-frequency positive pressure ventilation with extracorporeal removal of CO_2 (LFPPV-ECCO$_2$R).
Trans. ASAIO, 27:289.

GATTINONI, L., SOLCA, M., PESENTI, A., MARCOLIN, R., RIBONI, A., GAVAZZENI, V., BASSI, F., GIUFFRIDA, A., PRATO, P. (1983).
Combined use of artificial lung and kidney in the treatment of terminal acute respiratory distress syndrome in: Life Support Systems. Proceedings X. Annual Meeting ESAO., Bologna, Italy.
W.B. Saunders Company Ltd. Vol. 1 (Suppl. 1), 365.

GAYLOR, J.D.S., MURPHY, J.F., CAPRINI, J.A., ZUCKERMAN, L., MOCKROS, L.F. (1973).
Gas transfer and thrombogenesis in an annular membrane oxygenator with active blood mixing.
Trans. ASAIO, 20:516-524.

GAYLOR, J.D.S. (1970).
Theoretical and Experimental Aspects of Haemodialyser operation.
Ph.D. thesis, University of Strathclyde, Glasgow.

GAYLOR, J.D.S., MOCKROS, L.F. (1975a).
Artificial lung design: sheet membrane units.
Med. Biol. Eng., 14:425-435.

GAYLOR, J.D.S., LINDSAY, R.M., GILROY, K. (1975b).
Plastics materials in a membrane oxygenator: Functional and biocompatible aspects in: Plastics in Medicine and Surgery, pp.19.1-19.12.
The Plastics and Rubber Institute, London.

GAYLOR, J.D.S. (1980).
Artificial Organs in: A Textbook of Biomedical Engineering (ed. R.M. Kenedi).
Blackie and Son Ltd., Glasgow.

GIBBON, J.H.Jr. (1937).
Artificial maintenance of circulation during experimental occlusion of pulmonary artery.
Arch. Surg., 34:1105.

GIBBON, J.H.Jr. (1954).
Application of a mechanical heart and lung apparatus to cardiac surgery.
Minn. Med., 37:171.

GRIMSRUD, L., BABB, A.L. (1966).
Velocity and concentration profiles for laminar flow of a Newtonian fluid in a dialyser.
Chem. Eng., Progr., Symp. Ser., 62:19.

GUYTON, A.C. (1966).
Textbook of Medical Physiology.
3rd Edition, W.B. Saunders, Philadelphia, p.584.

HARRIS, G.W., TOMPKINS, F.C., DeFILIPPI, R.P., PORTER, J.H. (1970).
Development of capillary membrane blood oxygenators in: Blood Oxygenation (ed. D. Hershey), pp.334-354.
Plenum Press, New York.

HIKITA, H., ASAI, S., TAKATSUKA, T. (1976).
Absorption of carbon dioxide into aqueous sodium hydroxide and sodium carbonate-bicarbonate solutions.
Chem. Eng. J., 11:131-141.

HILL, J.D., IATRIDIS, A., O'KEEFE, R., KITRILAKIS, S. (1974).
Technique for achieving high gas exchange rates in membrane oxygenation.
Trans. ASAIO, 20:249-252.

HILL, J.D., RODVIEN, R., SNIDER, M.T., BARTLETT, R.H. (1978).
State of Art Address: Clinical extracorporeal membrane oxygenation for acute respiratory insufficiency.
Trans. ASAIO, 24:753.

HOOKE, R. (1667).
An account of an experiment made by M.Hooke of preserving animals alive by blowing through their lungs with bellows.
Phil. Trans. Roy. Soc., London 28:539.

IONESCU, M.I. (1981).
Techniques in Extracorporeal Circulation.
Butterworths, London.

INTERNATIONAL STANDARDS ORGANISATION (1981).
Draft Proposal DP7199.

JAMIESON, S.W., REITZ, B.A., OYER, P.E., BILLINGHAM, M., MODRY, D., BALDWIN, J., STINSON, E.B., HUNT, S., THEODORE, J., BIEBER, C.P., SHUMWAY, N.E. (1983).
Combined heart and lung transplantation.
The Lancet, 1:8334, 1130.

KATOH, S., YOSHIDA, F. (1972).
Rates of absorption of oxygen into blood under turbulent conditions.
Chem. Eng. J., 3:277-285.

KATOH, S., YOSHIDA, F. (1978).
Carbon dioxide transfer in a membrane blood oxygenator.
Ann. Biomed. Eng., 6:48-59.

KARLSON, K.E., MURPHY, W.R., KAKVAN, M., ANTHONY, P., COOPER, G.N.Jr., RICHARDSON, P.D. GALLETTI, P.M. (1974).
Total cardiopulmonary bypass with a new microporous teflon membrane oxygenator.
Surgery, 76:6, 935-945.

KARLSON, K.E., MASSIMINO, R.J., COOPER, G.N., SINGH, A.K., VARGAS, L.L. (1977).
Respiratory characteristics of a microporous membrane oxygenator.
Ann. Surg. 185:4, 397-401.

KELLER, K.H., SHULTIS, K.L. (1979).
Oxygen permeability in ultrathin and microporous membranes during gas-liquid transfer.
Trans. ASAIO, 25:469.

KELMAN, G.R., NUNN, J.F. (1968).
Computer Produced Physiological Tables for Calculations Involving the Relationships between Blood Oxygen Tension and Content.
Appleton-Century-Croft, New York.

KETTERINGHAM, J., ZAPOL, W., BIRKETT, J., NELSEN, L., MASSUCCO, A., RAITH, C. (1975).
A high permeability nonporous, blood compatible membrane for membrane lungs: in vivo and in vitro performance.
Trans. ASAIO, 21:233.

KHOO, G.T. (1984).
Personal Communications.
Bioengineering Unit, University of Strathclyde, Glasgow.

KOLOBOW, T., BOWMAN, K.L. (1963).
Construction and evaluation of an alveolar membrane artificial heart-lung.
Trans. ASAIO, 9:238.

KOLOBOW, T., SPRAGG, R.G., PIERCE, J., ZAPOL, W. (1971).
Extended term (to 16 days) partial extracorporeal blood gas exchange with the spiral membrane lung in unanaesthetized lambs.
Trans. ASAIO, 19:350.

KOBOLOW, T., STOOL, E.W., SACKS, K.L., VUREK, C.G. (1975).
Acute respiratory failure survival following ten days' support with a membrane lung.
J. Thorac. Cardiovasc. Surg., 69:6, 947-953.

KOLOBOW, T., GATTINONI, L., TOMLINSON, T., PIERCE, J. (1977a).
Control of breathing using an extracorporeal membrane lung.
Anesthesiology, 46:138.

KOLOBOW, T., GATTINONI, L., TOMLINSON, T., WHITE, D., PIERCE, J., IAPICHINO, G. (1977b).
The carbon dioxide membrane lung (CDML): A new concept.
Trans. ASAIO, 23:17.

KOLOBOW, T., GATTINONI, L., TOMLINSON, T. (1978).
An alternative to breathing.
J. THorac. Cardiovasc. Surg., 75:261.

LAUTIER, A., LAURENT, D., GRANGER, A., SAUSSE, A. (1970).
A testing device for evaluation of gas transfer through synthetic membranes.
J. Biomed. Mat. Res., 4:189.

LEONG, Y.M. (1983).
CO_2 transfer in tubular microporous membrane oxygenators (artificial lung).
B.Sc. thesis, University of Strathclyde, Glasgow.

LEVERETT, L.B., HELLUMS, J.D., ALFREY, C.P., LYNCH, E.C. (1972).
Red blood cell damage by shear stress.
Biophysical J., 12:257.

LIDDICOAT, J.E., BEKASSY, S.M., BEALL, A.C.Jr., GLAESSER, D.H., DEBAKEY, M.E. (1975).
Membrane vs bubble oxygenator: Clinical comparison.
Ann. Surgery, 181:747.

LINDEN, R.J., LEDSOME, J.R., NORMAN, J. (1965).
Simple methods for the determination of the concentrations of carbon dioxide and oxygen in blood.
Brit. J. Anaesth., 37:77.

LINDSAY, R.M., MASON, R.G., KIM, S.W., ANDRADE, J.D., HAKIM, R.M. (1980).
Blood surface interactions.
Trans. ASAIO, 26:603-610.

LONGMORE, D.B. (1981).
Towards Safer Cardiac Surgery.
MTP Press Ltd., Lancaster.

MADSEN, N.K., SINCOVEC, R.F. (1974).
The numerical solution of nonlinear partial differential equations.
Texas Institute for Computational Mechanics, Austin, Texas.

MADSEN, N.K. (1975).
The method of lines for the numerical solution of partial differential equations.
ACM Signum Newsletter, 10:4.

MARTIN, A.M. (1983).
The influence of dialysis and assisted ventilation on survival in acute renal failure.
Biomat. in Artificial Organs, (abstract) 5th Seminar, University of Strathclyde.

MAZAREI, A.F., SANDALL, O.C. (1980).
Diffusion coefficients for helium, hydrogen and carbon dioxide in water at 25°C.
A.I.Ch.E. Journal 26:1, 154-156.

MELROSE, D.S. (1959).
Pumping and oxygenating systems.
Brit. J. Anaesth., 31:393.

MELROSE, D.G. (1976).
Operational conditions underlying the design of membrane oxygenators in: Physiological and Clinical Aspects of Oxygenator Design (eds. S.G. Dawids and H.C. Engell).
Elsevier/North-Holland Biomedical Press, Amsterdam.

MESERKO, J., SINKEWICH, M., VALDES, F., KAMBIC, H., MALCHESKY, P., GOLDING, L., NOSE, Y. (1981).
Ex vivo evaluation of a new hollow fibre membrane oxygenator.
Proc. Am. Acad. Cardiovasc. Perf., 2:88-92.

MILTON, R.F., WATERS, W.A. (1955).
Manometric Techniques of Micro-analysis in: Methods of Quantitative Micro-Analysis.
2nd Edition, Arnold, London.

MOCKROS, L.F., GAYLOR, J.D.S. (1975).
Artificial lung design: tubular membrane units.
Med. Biol. Eng., 13:2, 171-181.

MOOK, P.H., WONG, P., WILDEVUUR, Ch.R.H., MAYES, P.J.D., GAYLOR, J.D.S. (1
Comparative performance of microporous polypropylene membrane lungs for CO_2 removal at low blood flow rates.
Trans. ASAIO, 29:215-220.

MURPHY, W., TRUDELL, L.A., FRIEDMAN, L.I., KAKVAN, M., RICHARDSON, P.D., KARLSON, K., GALLETTI, P.M. (1974).
Laboratory and clinical experience with a microporous membrane oxygenator.
Trans. ASAIO., 20:278.

MURPHY, W.R.C., GALLETTI, P.M., RICHARDSON, P.D. (1979).
Performance characteristics of the spiral coil membrane lung.
ASAIO Journal, 2:92-100.

NATIONAL INSTITUTE OF HEALTH (NIH) REPORT (1979).
Extracorporeal support for respiratory insufficiency.
U.S. Department of Health, Education and Welfare.
National Institute of Health, Bethesda, Maryland.

NUNN, J.F. (1971).
Applied Respiratory Physiology. Butterworths, London.

OHTAKE, S., KAWASHIMA, Y., HIROSE, H., MATSUDA, H., NAKANO, S., KAKU, K., OKUDA, A. (1983).
Experimental evaluation of pumpless arterio-venous ECMO with polypropylene hollow fibre membrane oxygenator for partial respiratory support.
Trans. ASAIO, 29:237-241.

PASSMORE, R., ROBSON, J.S. (1968).
A Comparison to Medical Studies: Vol. 1.
Blackwell Scientific Publications, Edinburgh.

PEACOCK, J.A., BELLHOUSE, B.J., ABEL, K., BELLHOUSE, E.L., BELLHOUSE, F.H., JEFFREE, M.A., SYKES, M.K., GARDAZ, J.P. (1983).
Initial in vitro evaluation of a pediatric vortex-mixing membrane lung.
Artif. Organs, 7:227.

PERRY, J.H. (1963).
Chemical Engineers' Handbook.
McGraw-Hill Book Company, Inc., New York.

PESENTI, A., KOLOBOW, T., RIBONI, A., GATTINONI, L., DAMIA, G. (1982).
Single vein cannulation for extracorporeal respiratory support in: Life Support Systems (ed. J. Belenger),
Proceedings of the IX Annual Meeting ESAO., W.B. Saunders Ltd., Brussels, Belgium.

PILLING, M.J. (1975).
Reaction Kinetics.
Claredon Press, Oxford.

RAWITSCHER, R.E., DUTTON, R.C., EDMUNDS, L.H.Jr. (1973).
Evaluation of hollow fibre and spiral coil membrane oxygenators designed for cardiopulmonary bypass in infants.
Circulation, 48:105 (Suppl.III).

RILEY, J.B. (1982).
Prediction of Arterial Blood pCO_2 by measuring the ventilating gas exit pCO_2 in a bubble oxygenator.
JECT., 14:1, 26-33.

RILEY, J.B., YOUNG, M.R., RIGATTI, R.L., KAUFFMAN, J.N. (1983).
Clinical experience with the Terumo 4.3m^2 hollow fibre membrane oxygenator.
Personal Communications: J. Riley, CCT.
Perfusion Services E-312,
Emory University Hospital,
1364 Clifton Rd., N.E. Atlanta,
GA 30322.

RILEY, J.B. (1982).
Prediction of arterial blood pCO_2 by measuring the ventilating gas exit pCO_2 in a bubble oxygenator.
JECT., 14:1, 26;33.

RISPENS, P., VAN ASSENDELFT, O.W., BRUNSTING, J.R., ZIJLSTRA, W.G., VAN KAMPEN, E.J., (1966).
A direct method for the determination of the HCO_3^- concentration as total carbon dioxide in blood and plasma.
Clin. Chim. Acta., 14:760-766.

RISPENS, P., FONGERS, T.M.E., ZIJLSTRA, W.G. (1980).
Determination of total carbon dioxide: II. Comparison between the Corning 965 carbon dioxide analyser and the cediometer.
5th Meeting of the International Federation of Chemistry, Copenhagen, p.46.

RØBB, W.L. (1968).
Thin silicone membranes: their permeation properties and some applications.
Ann. N.Y. Acad. Sci., 146:119.

ROGERS, C.E. (1971).
Permselective membranes.
Marcel Dekker, New York.

SAUNDERS, K.B. (1977).
Clinical physiology of the lung.
Blackwell Scientific Publications, Edinburgh.

SCHULTE, H.D, FALKE, K.J., BREULMAN, M., LEHNSEN, U., PESENTI, A., THIES, W.R., (1983).
Clinical application of extracorporeal CO_2 removal in severe ARDS.
Artificial Organs, 4th Congress of the International Society of Artificial Organs, Kyoto, vol.7 (abstracts).

SCHULTIS, K.L. (1980).
Determination of the oxygen permeability of artificial membranes by gas to liquid transfer methods.
M.Sc. Thesis, University of Minnesota, Minnesota.

SELLARS, J.R., TRIBUS, M., KLEIN, J.S. (1956).
Heat transfer to laminar flow in a round tube or flat conduit - The Graetz problem extended.
Trans. Amer. Soc. Mech. Eng., 78:441.

SIGGAARD-ANDERSEN, O. (1963).
Blood acid-base alignment nomogram.
Scand. J. Clin. Lab. Invest., 15:211.

SINKEWICH, E.E., MESERKO, J.J., GOLDING, L.R., LOOP, F.D. (1982).
Clinical evaluation of the Terumo hollow fibre oxygenator.
Proc. Amer. Acad. Cardiovasc. Perf., 3:13-16.

SIRS, J.A. (1970).
The interaction of carbon dioxide with the rate of exchange of oxygen by red cells in: Blood Oxygenation.
(ed. D. Hershey).
Plenum Press, New York.

SPAETH, E.E. (1970).
The oxygenation of blood in artificial membrane devices in: Blood Oxygenation (ed. D. Hershey). pp.276-305.
Plenum Press, New York.

SPRATT, E.H., MELROSE, D., BELLHOUSE, B., BADOLATO, A., THOMPSON, R. (1981).
Evaluation of a membrane oxygenator for clinical cardiopulmonary bypass.
Trans. ASAIO, 27:285.

ST.DENIS, C.E., FELL, C.J.D. (1971).
Diffusivity of oxygen in water.
Can. J. Chem. Eng., 49, 885.

SUMA, K., TSUJI, T., TAKEUCHI, Y., INOUE, K., SHIROMA, K., YOSHIKAWA, T., NARUMI, J., (1981).
Clinical Performance of Microporous Polypropylene Hollow-fibre Oxygenators.
Ann. Thorac. Surg., 32:6, 558-562.

TANISHITA, K., RICHARDSON, P.D., GALLETTI, P.M. (1975).
Tightly wound coils of microporous tubing: Process with secondary-flow blood oxygenator design.
Trans. ASAIO, 21:216-222.

TERUMO CORPORATION (1983).
Document no. 09012 1,000S.S. CAPIOX II 16 and 33.
Document no. 01303 500S.S. CAPIOX II 43.

TOLCHIN, N., ROBERTS, J.L., LEWIS, E.J. (1978).
Respiratory gas exchange by high-efficiency haemodialysers.
Nephron, 21:137.

TSUJI, T., SUMA, K., TANISHITA, K., FUKAZAWA, H., KANNO, M., HASEGAWA, H., TAKAHASHI, A. (1981).
Development and clinical evaluation of a hollow fibre membrane oxygenator.
Trans. ASIAO, 27:280-284.

TRAVENOL LABORATORIES (1976).
5M1430
TMO Total bypass membrane oxygenator - Adult with polypropylene membrane.
Document no. 8-19-15-118AA.

UPDIKE, S.J., SCHULTS, M.C. (1973).
Excretion of carbon dioxide using an artificial kidney.
J. Appl. Physiol., 34:274.

VAN SLYKE, D.D. NEILL, J.M. (1924).
The determination of gases in blood and other solutions by vacuum extraction and manometric measurements.
J. Biol. Chem., 61:523.

VILLAROEL, F., LANHAM, C.E., BISCHOFF, K.B., REGAN, T.M., CALKINS, J.M. (1970).
A mathematical model for the prediction of oxygen, carbon dioxide and pH profiles with augmented diffusion in capillary blood oxygenators in: Blood Oxygenation (ed. D. Hershey). pp.321-333.
Plenum Press, New York.

VILLARROEL, F., LANHAM, C.E. (1973).
A design calculation method for capillary tube oxygenators.
Med. Biol. Eng., 11:732-742.

VON FREY, M., GRUBER, M. (1885).
Untersuchungen Uberden Stoffwechsel isolirter Organe I. Ein Respirationsapparat fur isolirte Organe.
Arch. Anat. Physiol., Lpz. Physiol. abt., 519.

VOORHEES, M.E. (1976).
Mutual transfer of carbon dioxide and oxygen to and from blood flowing in macrochannel devices.
Ph.D. thesis, Arizona State University, Tempe, Arizona.

WEISSMAN, M.H., MOCKROS, L.F. (1967).
Oxygen transfer to blood flowing in round tubes.
J. Eng. Mech. Div., A.S.C.E., 93:225-244.

WEISSMAN, M.H., MOCKROS, L.F. (1969).
Oxygen and carbon dioxide transfer in membrane oxygenator.
Med. Biol. Eng., 7:169-184.

WHEATON, R. (1978).
Short term cardiopulmonary bypass with the Sci-Med Kolobow membrane lung.
AmSECT. Proc., 10:3, 155-160.

WHITE, J.J., MAZURE, D., KOTAS, R.V., HALLER, J.E. (1969).
Excess lactate production due to hyperventilation and respiratory alkalosis.
Surgery, 66:250.

WHITEAR, A.L., CHANIN, C.C., PETERSON, J. (1980).
A new instrumental method for measuring the carbon dioxide content of carbonated beverages.
J. Inst. Brew., 86:224-225.

WILDEVUUR, Ch.R.H. (1981).
Towards safer cardiopulmonary bypass in: Towards Safer Cardiac Surgery (ed. D.B. Longmore), pp.293-312.
MTP Press Ltd., Lancaster.

WILKE, C.R., CHANG, P. (1965).
Correlation of diffusion co-efficients in dilute solutions.
A.I.Ch.E. Journal, 1:264.

YANG, W.J. (1979).
Blood-gas interactions and physiological implications.
Adv. Cardiovasc. Phys., Vol.3, pp.45-99, Karger, Basel.

YASUDA, H., LAMAZE, C.E. (1971).
Permselectivity of solutes in homogeneous water-swollen polymer membranes in: permselective membranes (ed. C.E. Rogers),
Marcel Dekker Inc., New York.

ZAPOL, W.M., QVIST, J., PONTOPPIDAN, N., LILAND, A., McENANY, T., LAVER, M.B. (1975).
Extracorporeal perfusion for acute respiratory failure: recent experience with the spiral coil membrane lung.
J. Thorac. Cardiovasc. Surg., 69:439.

ZAPOL, W.M., QVIST, J. (1976).
Artificial lungs for acute respiratory failure.
Academic Pres, Inc., New York.

appendices

APPENDIX A

FORMULAE FOR CALCULATING SOLUBILITY AND DIFFUSIVITY OF CO_2 IN BLOOD

A.1 Solubility (Dorson and Voorhees, 1974)

At 37°C

$$\alpha_1 = 0.440H + 0.531\ (1-H)\ \frac{cm^3(STPD)}{cm^3.atm}$$

A.2 Diffusivity (modified from Dorson et al. 1971)

At 37°C

$$D_1 = 0.8312\ D_{O_2,plasma}\left[\frac{1-0.49H}{1+0.41H}\right]\ cm^2/s$$

where $D_{O_2,plasma} = 2.667 \times 10^{-5}\ cm^2/s$

H = haematocrit (expressed as a fraction).

A.3 Calculation of physical input parameters for the CO_2 theoretical model

Input conditions according to median values in ISO standards (Table 3.1).

(a) To calculate the haematocrit, H (as a fraction) from the haemoglobin content (Voorhees, 1976)

$$C_{Hb} = \frac{100H}{3}\ g\%$$

Therefore $$H = \frac{3C_{Hb}}{100} = \frac{3}{100} \times 12 = \underline{0.36}$$

(b) The buffer power, β is calculated from the relationship: (Voorhees, 1976)

$$\frac{1}{\beta} = 0.001074 + \frac{0.45864}{C_{Hb}} \quad \ell/\text{mmol}$$

$$= 3.9294 \times 10^{-2}$$

$$\beta = \underline{25.449} \text{ mmol}/\ell$$

(c) The solubility of CO_2 in blood at 37°C is given by the relationship:

$$\alpha_1 = 0.440H + 0.531(1-H) \frac{\text{cm}^3\text{(STPD)}}{\text{cm}^3\text{.atm}}$$

$$\alpha_1 = 0.49824 \frac{\text{cm}^3\text{(STPD)}}{\text{cm}^3\text{.atm}}$$

to convert α_1 to units of $\frac{\text{mmol}}{\ell\text{.mmHg}}$

$$\alpha_1 = \frac{0.49824}{22.26\times10^3\times\text{cm}^3\text{(STPD)/mol}} \times \frac{1}{760\text{mmHg}} \times 10^3 \times 10^3$$

$$\alpha_1 = \underline{2.945 \times 10^{-2}} \quad \frac{\text{mmol}}{\ell\text{.mmHg}}$$

(d) Dissolved CO_2 in blood at inlet is calculated by:

$$C_{1,i} = \alpha_1 pCO_{2,in} \quad \text{mmol}/\ell$$

$$C_{1,i} = \underline{1.3253} \quad \text{mmol}/\ell$$

(e) Total CO_2 concentration in blood at inlet is calculated from the relationship:

$$C_{Ti} = C_{1,i} + C_{2,i}$$

hence

$$C_{2,i} = 23.36 - 1.3253$$

$$C_{2,i} = \underline{22.0348} \quad \text{mmol}/\ell$$

(f) The constant K' in the dissociation curve can be calculated from the relationship:

$$C_{1,i} = \frac{C_{2,i}}{K'} 10^{C_{2,i}/\beta}$$

$$K' = \frac{C_{2,i}}{C_{1,i}} 10^{C_{2,i}/\beta}$$

$$K' = \underline{122.07}$$

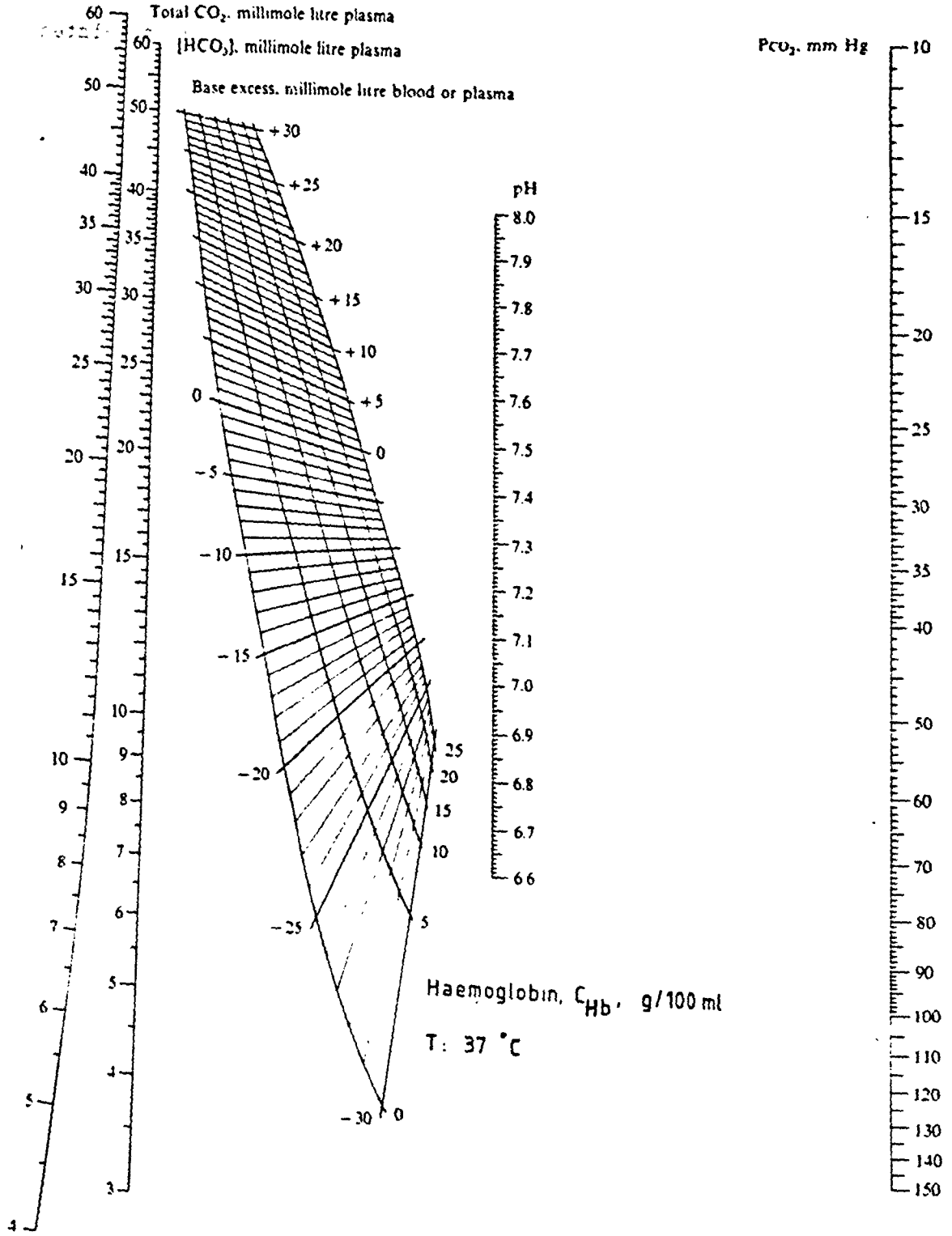

Figure B.1 Siggaard-Andersen alignment nomogram (after Siggaard-Andersen, 1963)

APPENDIX B

CORRECTION FOR ABNORMAL BASE EXCESS

Normal values = 0 $\pm$ 2 mEq/ℓ

PROCEDURE

1. Obtain the base excess (BE) in mEq/ℓ using the Radiometer Blood Gas Calculator, type BGC1 or the Siggaard-Andersen Alignment Nomogram shown in Figure B.1 with pCO_2, C_{Hb} and pH of blood sample as input.
2. Estimate the volume of blood circulating in the circuit.
3. Multiply the BE by the blood volume to give number of mEq of $NaHCO_3$ required for infusion

   1 mEq of $NaHCO_3$ = 1 mℓ of 1 Eq solution

   1 Eq solution of $NaHCO_3$ = 84g $NaHCO_3$ per litre

Note: in clinical practice it is usual to infuse half the required mEq of $NaHCO_3$ in order to prevent overcorrection.

APPENDIX C

BLOOD GAS AND ACID-BASE MEASUREMENTS

C.1 Total CO_2 content

There is no simple and accurate method available to measure the total concentration of CO_2 in whole blood. Most of the established methods rely on the initial release of CO_2 gas through reaction with an acid and various techniques have been used to measure the released CO_2. For example the Van Slyke manometric or volumetric methods (Van Slyke and Neill, 1924), Corning CO_2 analyser based on a thermal conductivity principle (Corning Medical Ltd) or gas chromatography (Davies, 1970). Indirect methods such as pH and pCO_2 electrodes and the use of nomograms to estimate total CO_2 in whole blood are quick and easy, but these methods lack accuracy and are often unreliable.

Gas chromatography is a rather complicated technique for measuring the released CO_2 from whole blood. The technique involves four main stages: the extraction of the gases from the blood and subsequent injection on to the chromatographic columns; separation in the columns of the gas mixture into its individual components using selective adsorption on solid adsorption media; detection of the indivudal gases; and finally recording the results from the detector. Gas chromatography is a relatively slow (about 4 minutes per analysis) method and with the procedure it is difficult to achieve reproducible results (Davies, 1970).

The Van Slyke manometric method was used initially for the total blood CO_2 content measurements. Although the method is highly accurate once the operating skills have been mastered, each

blood sample analysis takes approximately 15 minutes to perform. This is the main disadvantage of the technique where triplicate analyses of each inlet and outlet blood samples are required within a short time after blood sample collection. Test L1 to L4 (Appendix C) were carried out with the Van Slyke manometric method, and was later abandoned in preference for the recently introduced Corning analyser. This instrument has the advantage of ease and rapidity of operation. Each analysis takes about 36 seconds to complete. Hence, the Corning analyser was used for the CO_2 oxygenator and gas transmission evaluations.

C.2 Corning 965 Carbon dioxide analyser

The Corning model 965 analyser has been introduced in recent years for measuring carbon dioxide content of biological fluids (Whitear et al. 1980) and whole blood (Rispens et al. 1980). The 965 uses the release of carbon dioxide by reaction with a reagent containing lactic acid (CO_2 reagent) and measures the released carbon dioxide concentration by means of a thermal conductivity detector. A fixed volume (100 µl) of blood sample is delivered into a sealed reaction chamber. The sample and CO_2 reagent are mixed by means of the stirrer in the reaction chamber, with the result that all CO_2 present (HCO_3^-, CO_3^{2-}, $RNCOO^-$, H_2CO_3 and dissolved CO_2) is released. The gas mixture containing the released CO_2 is then transferred to the thermal conductivity detector. The change in thermal conductivity, which is proportional to the CO_2 content of the gas mixture, is measured by a bridge circuit containing a closed loop reference cell filled with ambient air.

After each analysis, the 965 is adjusted to zero point using the CO_2 reagent only. Calibration is carried out with the aid of

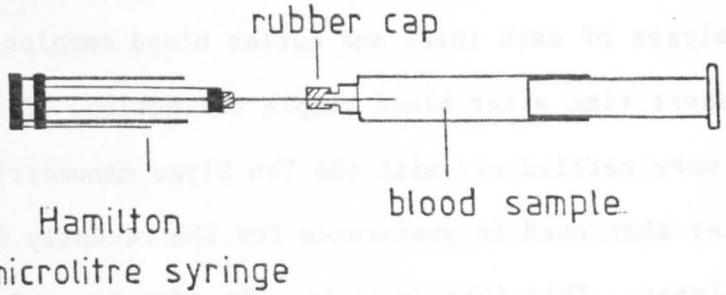

(a) The syringe-to-syringe sampling technique for anaerobic transfer of blood.

(b) Hamilton gas-tight syringe (model 81034, 1710RNCH).

Figure C.1

Standard Na_2CO_3 solutions of 15, 30 and 45 mmol/l. The linearity of the instrument is given over the range of CO_2 concentration from 0 to 60 mmol/l to be within $\pm$ 1 mmol/l. (Corning Medical Ltd., England).

A special syringe-to-syringe sampling technique is employed to measure an accurate volume (100 µl) of the blood sample for the CO_2 determinations using the Corning analyser.

C.3 Syringe-to-Syringe Sampling Technique

Glass sampling syringes were used to collect about 5 ml of blood from the test circuit. The glass syringe should be capped immediately the sample has been taken. Trapping air bubbles under the cap is minimized by ejecting a little blood from the syringe just as the capping is carried out. Since metabolic processes continue in blood after sampling even if the syringe containing the sample is sealed, blood samples should be stored for as short a time as possible. Metabolism in the blood leads to a fall of pO_2 and pH, and an increase in pCO_2. However, the metabolic processes can be reduced to a minimum by immersing the glass sample syringe in a mixture of ice and water at a temperature of $0^{o}C$. This procedure is carried out if the blood sample is awaiting CO_2 determination by a syringe-to-syringe sampling technique in order to transfer 100 µl blood sample for the Corning analyser. The syringe-to-syringe technique as shown in Figure C1 enables anaerobic transfer without blood loss. Each blood sample was determined in triplicate for CO_2 content.

Adams and Hahn (1982) and Biswas et al. (1982) have carried out studies on blood-gas measurement errors arising from blood sampling. Accurate blood-gas analysis can be obtained if air bubbles are eliminated from the syringes and determinations

performed within 10 minutes of blood collection if not stored at a temperature of 0°C. At room temperature the rise in pCO_2 is about 2.5 mmHg/hour but is only 0.6 mmHg/hour at 0-4°C.

C.4 Radiometer OSM2

The OSM2 Hemoximeter measures the oxygen saturation and haemoglobin content of blood using an absorption spectroscopic principle at two selected wavelengths of 506.5 and 600.0 nm. An integral computer solves the absorbance equations yielding the oxygen saturation and total haemoglobin content. The sample volume is about 20 µℓ, and the time taken for complete analysis including the rinsing cycle is about 57 seconds. Calibration was performed by instrument zero with distilled water and with blood samples of zero and 100% oxygen saturation. The total haemoglobin content calibration was performed by using Drabkin's solution - blood mixtures. The calibration is based upon the formation of cyanmethaemoglobin, HiCN.

C.5 Radiometer BMS3

The BMS3 measures blood pH, pO_2 and pCO_2 via electrodes maintained at 37°C or ambient temperature by a water bath. The pH electrode is a standard glass capillary type with a reference calomel electrode. The pO_2 electrode consists of a combined platinum cathode and a silver/silver chloride anode in contact with a phosphate buffer/KCl solution as an electrolyte. The cathode, anode and electrolyte is separated from the blood sample by a polypropylene membrane which, although freely permeable to oxygen, is impermeable to water, proteins, blood cells and ions.

The pCO_2 electrode is a combined glass and silver/silver chloride electrode in contact with a bicarbonate solution. The

bicarbonate solution is separated from the blood sample by a silicone rubber membrane.

The output signals from the electrodes are amplified and digitally displayed in a Digital Acid-Base Analyser (PHM 726, Radiometer) incorporating pO_2 and pCO_2 modules (PHA932 and PHA 933). A two point pH calibration was employed with precision buffer solutions of 7.382 $\pm$ 0.005 and 6.838 $\pm$ 0.005 pH units at 37°C (Corning Ltd., Essex). The pO_2 electrode was calibrated with an oxygen free solution (approximately 20 mg sodium dithionite in 2 mℓ 0.01 M Borax solution) and with water equilibrated with oxygen from atmospheric air. The pCO_2 electrode was calibrated by using humidified gases at 37°C containing 3.59% CO_2 in air and 7.21% CO_2 in air supplied by a Gas Mixing Apparatus (GMA1, Radiometer). A 'low' and a 'high' calibration point are calculated and the machine is set to give these readings. These calibration points are calculated with reference to the barometric pressure, the saturated water vapour pressure and the percentage carbon dioxide from the Gas Mixing Apparatus. A linear relationship between these two calibration points is assumed.

The readout for pCO_2 and pO_2 is in mmHg and is generally held to be accurate to one decimal place. Problems were encountered with this machine, regarding when to take the reading. It does not give an instantaneous readout but rather rises (or falls) in an almost exponential fashion. Generally, the readout will give a stable value after about two minutes, and this is then recorded. During the tests, the BMS3 was prone to drifting hence re-calibration is required after a set of sample measurements.

APPENDIX D

EXPERIMENTAL DATA FOR TMO AND CAPIOX TESTS

The CO_2 transfer rates ($\dot{V}_{CO_2}$) were calculated as follows:

Van Slyke Manometric Method

$$\dot{V}_{CO_2} = (V_{0,760,in} - V_{0,760,out})\ \text{ml/100ml} \times Q_B\ \text{ml/min} \qquad (D.1)$$

where $V_{0,760,in}$, $V_{0,760,out}$ - volume of CO_2 gas at blood inlet and outlet respectively at STPD.

Corning CO_2 analyser

$$\dot{V}_{CO_2} = (\bar{C}_{Ti} - \bar{C}_{To})\text{mmol/}\ell \times Q_B\ \text{l/min} \times 22.26\ \text{ml/mmol} \qquad (D.2)$$

Oxygenator specification

* - indicate no. of use.

Test no: L1 Date: 24.7.81 Barometric pressure: 758 mmHg Oxygenator specification: Travenol TMO*

INLET							OUTLET						
Q_B ℓ/min	pH	pCO_2	P_1	P_2	$P_{(CO_2)}$	$V_{O,760}$	pH	pCO_2	P_1	P_2	$P_{(CO_2)}$	$V_{O,760}$	$\dot{V}_{CO_2}$ ml(STPD)/min
0.5	7.40	44.2	369.0	157.0	209.0	54.2	7.71	21.5	326.0	172.0	151.0	44.6	48.0
0.5	7.40	43.8	375.0	160.0	212.0	54.9	7.63	23.5	339.5	174.5	162.0	42.0	64.5
1.0	7.44	45.6	366.0	160.0	203.0	52.9	7.66	25.0	330.0	168.5	161.5	41.3	116.0
1.0	7.46	44.6	372.0	162.0	207.0	53.7	7.64	27.3	345.0	172.5	169.5	43.9	98.0
1.5	7.38	48.7	380.5	165.0	212.5	54.8	7.50	36.4	358.0	174.0	181.0	46.7	121.5
1.5	7.43	43.4	373.0	163.5	206.5	53.3	7.51	31.9	353.0	175.0	175.0	45.2	121.5

Deoxygenator specification: Bentley Temptrol Q200A

Q_B ℓ/min	N_2 ℓ/min	CO_2 ℓ/min
0.5	2.5	0.18
1.0	5.0	0.38
1.5	7.8	0.71

	INLET	OUTLET
pO_2	41.9 ± 3.4	261.8 - 504.8
O_2sat	66.7 ± 2.9	98.5 - 100.4
Hb	12.1 ± 0.4	11.3 - 12.2

Values represent the mean ± 1 S.D. (n = 6)

Values represent the range

Haematocrit = not measured

Water Jacket Temperature = 25°C

$C = P_1 - P_2 = 149.0-146.0 = 3.0$

DATA	UNITS
pCO_2 or pO_2	mmHg
O_2 sat	%
Hb	g%
C_{Ti} or C_{To}	mmol/ℓ

Test no: L2 Date: 3.9.81 Barometric pressure: 770 mmHg Oxygenator specification: Travenol TMO*

INLET							OUTLET						
Q_B ℓ/min	pH	pCO_2	P_1	P_2	$P_{(CO_2)}$	$V_{O,760}$	pH	pCO_2	P_1	P_2	$P_{(CO_2)}$	$V_{O,760}$	$\dot{V}_{CO_2}$ ml(STPD)/min
0.5	7.34	48.0	376.0	168.0	207.0	53.4	7.63	15.9	337.0	177.0	159.0	41.0	62.0
0.5	7.36	45.1	372.0	169.0	202.0	52.1	7.64	15.7	314.0	182.0	131.0	33.8	error
1.0	7.30	47.0	368.0	172.0	195.0	50.3	7.51	-	338.0	186.0	151.0	38.9	114.0
1.0	7.36	44.3	373.0	172.0	200.0	51.6	7.48	32.6	335.0	187.0	147.0	37.9	137.0
1.5	7.34	47.4	362.0	171.0	190.0	49.0	7.51	27.6	350.0	198.0	151.0	38.9	151.0
1.5	7.36	44.8	367.0	176.0	190.0	49.0	7.52	26.4	340.0	184.0	155.0	40.0	135.0

Deoxygenator specification:

Q_B ℓ/min	N_2 ℓ/min	CO_2 ℓ/min
0.5	1.75	0.16
1.0	0.61	0.61
1.5	1.16	1.13

	INLET	OUTLET
pO_2	38.9 ± 3.5	296.0 - 500.9
O_2sat	65.8 ± 0.9	97.9 - 98.4
Hb	11.9 ± 0.2	11.3 - 11.8

Values represent the mean ± 1 S.D. (n = 6)

Values represent the range

Haematocrit = not measured

Water Jacket Temperature = 26°C

$C = P_1 - P_2 = 155.0-154.0 = 1.0$

DATA	UNITS
pCO_2 or pO_2	mmHg
O_2 sat	%
Hb	g%
C_{Ti} or C_{To}	mmol/ℓ

Test no: L3 Date: 4.11.81 Barometric pressure: 756 mmHg Oxygenator specification: Travenol TMO**

INLET							OUTLET						
Q_B ℓ/min	pH	pCO_2	P_1	P_2	$P_{(CO_2)}$	$V_{0,760}$	pH	pCO_2	P_1	P_2	$P_{(CO_2)}$	$V_{0,760}$	$\dot{V}_{CO_2}$ mℓ(STPD)/min
0.5	7.51	38.0	417.0	163.0	247.0	65.4	7.84	14.6	360.0	171.0	182.0	48.2	86.0

Deoxygenator specification:

Q_B ℓ/min	N_2 ℓ/min	CO_2 ℓ/min
0.5	3.0	0.25

	INLET	OUTLET	DATA	UNITS
pO_2	28.9	284.0	pCO_2 or pO_2	mmHg
O_2sat	67.7	100.1	O_2 sat	%
Hb	11.6	11.3	Hb	g%
			C_{Ti} or C_{To}	mmol/ℓ

Values represent the mean ± 1 S.D. (n = 1)

Values represent the range

Haematocrit = not measured

Water Jacket Temperature = 22°C

$C = P_1 - P_2 = 148.0-141.0 = 7.0$

Test no: L4 Date: 13.11.81 Barometric pressure: 758 mmHg Oxygenator specification: Travenol TMO***

INLET							OUTLET						
Q_B ℓ/min	pH	pCO_2	P_1	P_2	$P_{(CO_2)}$	$V_{0,760}$	pH	pCO_2	P_1	P_2	$P_{(CO_2)}$	$V_{0,760}$	$\dot{V}_{CO_2}$ mℓ(STPD)/min
0.5	7.33	32.2	356.0	167.0	187.0	48.5	7.56	21.7	324.0	183.0	139.0	36.0	62.5
0.5	7.36	32.1	361.0	169.0	190.0	49.3	7.56	30.4	325.0	183.0	140.0	36.3	65.0
0.5	7.40	48.9	379.0	167.0	210.0	54.5	7.65	22.8	333.0	181.0	150.0	38.9	78.0
0.5	7.41	46.8	373.0	170.0	201.0	52.1	7.64	22.9	337.0	184.0	151.0	39.2	64.5
1.0	7.32	49.0	379.0	172.0	205.0	53.2	7.51	30.0	346.0	181.0	163.0	42.3	109.0
1.0	7.39	44.3	367.0	170.0	195.0	50.6	7.55	28.0	345.0	182.0	161.0	41.8	88.0
1.5	7.37	48.3	380.0	176.0	202.0	52.4	7.50	34.3	359.0	183.0	174.0	45.1	109.5
1.5	7.39	49.5	380.0	177.0	201.0	52.1	7.51	32.7	353.0	181.0	170.0	44.1	120.0

Deoxygenator specification:

Q_B ℓ/min	N_2 ℓ/min	CO_2 ℓ/min
0.5	4.0	0.3
1.0	5.0	0.4
1.5	3.5	0.3

	INLET	OUTLET	DATA	UNITS
pO_2	55.0 ± 11.6	261.0 - 498.0	pCO_2 or pO_2	mmHg
O_2sat	72.1 ± 9.3	100.0 - 100.6	O_2 sat	%
Hb	12.2	11.8 - 11.9	Hb	g%
			C_{Ti} or C_{To}	mmol/ℓ

Values represent the mean ± 1 S.D. (n = 8)

Values represent the range

Haematocrit = not measured

Water Jacket Temperature = 25°C

$C = P_1 - P_2 = 151.0-149.0 = 2.0$

Test no: L5 Date: 18.11.81 Barometric pressure: 740 mmHg Oxygenator specification: Travenol TMO**

INLET							OUTLET						
Q_B ℓ/min	pH	pCO_2	(1)C_{Ti}	(2)C_{Ti}	(3)C_{Ti}	$\bar{C}_{Ti}$	pH	pCO_2	(1)C_{To}	(2)C_{To}	(3)C_{To}	$\bar{C}_{To}$	$\dot{V}_{CO_2}$ ml(STPD)/min
0.5	7.33	43.1	22.0	22.2	23.5	22.6	7.54	23.5	17.1	17.7	17.5	17.4	57.9
0.5	7.35	41.0	22.1	22.2	22.3	22.2	7.55	22.2	16.1	16.1	16.4	16.2	66.8
1.0	7.29	45.9	21.5	20.9	20.4	20.9	7.45	30.2	18.3	18.3	17.9	18.2	60.1
1.0	7.33	42.3	21.6	21.5	21.1	21.4	7.44	30.3	17.6	17.3	17.4	17.4	89.0
1.5	7.32	42.5	19.5	20.2	20.0	19.9	7.42	33.2	18.1	17.9	18.3	18.1	60.1
1.5	7.32	44.9	19.8	20.3	20.5	20.2	7.40	34.4	17.7	17.8	17.2	17.6	86.8

Deoxygenator specification: Harvey H200

Q_B ℓ/min	N_2 ℓ/min	CO_2 ℓ/min
0.5	2.0	0.19
1.0	4.8	0.45
1.5	9.0	0.95

INLET		OUTLET	DATA	UNITS
pO_2	43.2 ± 1.4	101 - 370	pCO_2 or pO_2	mmHg
O_2sat	64.0 ± 1.6	92.7 - 95.4	O_2 sat	%
Hb	11.6	11.1 - 11.4	Hb	g%
			C_{Ti} or C_{To}	mmol/ℓ

Values represent the mean ± 1 S.D. (n = 4)

Values represent the range

Haematocrit = not measured

Test no: L6 Date: 25.11.81 Barometric pressure: 756 mmHg Oxygenator specification: Travenol TMO***

INLET							OUTLET						
Q_B ℓ/min	pH	pCO_2	(1)C_{Ti}	(2)C_{Ti}	(3)C_{Ti}	$\bar{C}_{Ti}$	pH	pCO_2	(1)C_{To}	(2)C_{To}	(3)C_{To}	$\bar{C}_{To}$	$\dot{V}_{CO_2}$ ml(STPD)/min
0.5	7.43	47.5	28.5	29.2	30.0	29.2	7.69	25.8	22.3	22.4	22.1	22.3	76.8
0.5	7.44	47.7	28.7	28.8	29.1	28.9	7.67	26.5	22.5	23.1	22.8	22.8	67.9
1.0	7.42	47.4	27.7	28.0	28.1	27.9	7.58	30.2	23.1	22.8	23.1	23.0	109.1
1.0	7.45	45.3	27.3	26.9	26.5	26.9	7.59	31.1	23.1	23.3	23.1	23.2	82.4
1.5	7.45	45.4	27.5	27.5	27.3	27.4	7.56	33.9	23.8	23.8	23.7	23.8	120.2
1.5	7.47	43.7	26.8	26.4	27.3	26.8	7.56	35.1	23.2	23.6	23.8	23.5	110.2

Deoxygenator specification: Harvey H200

Q_B ℓ/min	N_2 ℓ/min	CO_2 ℓ/min
0.5	4.0	0.35
1.0	9.0	0.85
1.5	7.0	0.65

INLET		OUTLET	DATA	UNITS
pO_2	40.0 ± 2.6	41.2 - 480	pCO_2 or pO_2	mmHg
O_2sat	64.9 ± 2.5	81.9 - 99.7	O_2 sat	%
Hb	11.2 ± 0.2	10.7 - 11.2	Hb	g%
			C_{Ti} or C_{To}	mmol/ℓ

Values represent the mean ± 1 S.D. (n = 6)

Values represent the range

Haematocrit = not measured

Test no: L7 Date: 3.12.81 Barometric pressure: 762 mmHg Oxygenator specification: Travenol TMO*

INLET							OUTLET						
Q_B ℓ/min	pH	pCO_2	(1)C_{Ti}	(2)C_{Ti}	(3)C_{Ti}	$\bar{C}_{Ti}$	pH	pCO_2	(1)C_{To}	(2)C_{To}	(3)C_{To}	$\bar{C}_{To}$	$\dot{V}_{CO_2}$ ml(STPD)/min
0.5	7.52	43.8	28.8	28.3	28.9	28.7	7.85	17.0	21.3	21.2	20.9	21.1	84.6†
0.5	7.51	43.4	28.4	28.9	29.2	28.8	7.85	19.8	22.2	22.2	21.8	22.1	74.6†
0.5	7.47	44.6	27.7	27.7	27.6	27.7	7.80	17.6	20.4	20.0	20.3	20.2	83.5
0.5	7.47	44.2	28.4	28.4	28.0	28.3	7.80	20.2	20.1	20.4	20.7	20.4	87.9

Deoxygenator specification: Harvey H200

Q_B ℓ/min	N_2 ℓ/min	CO_2 ℓ/min
0.5	4.0	0.36

	INLET	OUTLET
pO_2	40.1 ± 2.9	470 - 520
O_2sat	64.1 ± 2.1	100.3
Hb	11.3	10.9 - 11.0

Values represent the mean ± 1 S.D. (n = 4)

Values represent the range

Haematocrit = 35%

†Modified Travenol TMO

DATA	UNITS
pCO_2 or pO_2	mmHg
O_2 sat	%
Hb	g%
C_{Ti} or C_{To}	mmol/ℓ

Test no: L8 Date: 9.12.81 Barometric pressure: 734 mmHg Oxygenator specification: Travenol TMO**

INLET							OUTLET						
Q_B ℓ/min	pH	pCO_2	(1)C_{Ti}	(2)C_{Ti}	(3)C_{Ti}	$\bar{C}_{Ti}$	pH	pCO_2	(1)C_{To}	(2)C_{To}	(3)C_{To}	$\bar{C}_{To}$	$\dot{V}_{CO_2}$ ml(STPD)/min
1.0	7.46	43.5	21.1	21.4	21.2	21.2	7.63	24.5	15.9	16.0	15.9	15.9	117.9
1.0	7.39	43.9	21.6	22.2	22.1	21.9	7.63	26.2	16.2	16.3	16.0	16.3	124.7
1.0	7.34	44.4	21.5	20.9	21.2	21.2	7.57	26.0	16.2	16.0	15.9	16.0	115.7†
1.0	7.36	45.1	21.0	20.8	20.7	20.8	7.57	27.7	14.7	14.8	14.6	14.7	135.8†
1.5	7.29	44.6	20.8	20.8	20.6	20.7	7.49	28.5	15.4	15.5	15.6	15.5	173.6†

Deoxygenator specification: Harvey H200

Q_B ℓ/min	N_2 ℓ/min	CO_2 ℓ/min
1.0	3.6	0.43
1.5	5.0	0.6

	INLET	OUTLET
pO_2	41.2 ± 2.9	42 - 50
O_2sat	60.0 ± 1.3	81.3 - 86.3
Hb	11.4 ± 0.1	11.0 - 11.3

Values represent the mean ± 1 S.D. (n = 6)

Values represent the range

Haematocrit = not measured

†Modified Travenol TMO

DATA	UNITS
pCO_2 or pO_2	mmHg
O_2 sat	%
Hb	g%
C_{Ti} or C_{To}	mmol/ℓ

Test no: L9 Date: 17.12.81 Barometric pressure: 748 mmHg Oxygenator specification: Travenol TMO***

INLET							OUTLET						
Q_B ℓ/min	pH	pCO_2	(1)C_{Ti}	(2)C_{Ti}	(3)C_{Ti}	$\bar{C}_{Ti}$	pH	pCO_2	(1)C_{To}	(2)C_{To}	(3)C_{To}	$\bar{C}_{To}$	$\dot{V}_{CO_2}$ ml(STPD)/min
0.5	7.33	45.3	22.7	22.4	22.8	22.6	7.66	20.1	15.6	15.4	15.3	15.4	80.1
0.5	7.36	48.7	22.8	22.6	22.2	22.5	7.63	22.0	15.6	15.4	15.2	15.4	79.0
0.5	7.32	48.9	22.7	23.2	23.1	23.0	7.65	18.9	14.0	13.8	14.3	14.0	100.2†
0.5	7.36	44.7	21.4	21.3	21.6	21.4	7.67	18.2	14.0	14.3	13.7	14.0	82.4†
1.0	7.33	43.6	20.5	20.8	21.4	20.9	7.54	24.9	15.7	15.4	15.2	15.4	122.4†
1.0	7.35	43.3	21.3	21.3	21.0	21.2	7.54	25.4	16.1	15.7	15.7	15.8	120.2†
1.0	7.32	46.9	21.4	21.5	21.3	21.4	7.55	25.1	16.1	16.8	16.6	16.5	109.1
1.0	7.35	48.2	22.1	22.3	22.2	22.2	7.54	26.2	17.1	16.9	17.1	17.0	115.8
1.5	7.32	45.1	21.6	21.7	21.6	21.6	7.48	32.7	17.9	18.1	18.0	18.0	120.2
1.5	7.35	46.1	21.4	21.2	21.9	21.5	7.48	32.8	18.4	17.9	17.8	18.0	116.9

Deoxygenator specification: Harvey H200

Q_B ℓ/min	N_2 ℓ/min	CO_2 ℓ/min
0.5	2.0	0.24
1.0	4.0	0.49
1.5	4.9	0.63
0.5†	3.0	0.36
1.0†	4.1	0.49

	INLET	OUTLET
pO_2	42.6 ± 2.2	43.6 - 100.5
O_2sat	64.8 ± 2.5	80.5 - 97.4
Hb	12.7 ± 0.1	12.1 - 12.7

Values represent the mean ± 1 S.D. (n =)

Values represent the range

Haematocrit = 35.5%

†Modified Travenol TMO

DATA	UNITS
pCO_2 or pO_2	mmHg
O_2 sat	%
Hb	g%
C_{Ti} or C_{To}	mmol/ℓ

Test no: L9 Date: 17.12.81 Barometric pressure: 748 mmHg Oxygenator specification: Travenol TMO***

INLET							OUTLET						
Q_B ℓ/min	pH	pCO_2	(1)C_{Ti}	(2)C_{Ti}	(3)C_{Ti}	$\bar{C}_{Ti}$	pH	pCO_2	(1)C_{To}	(2)C_{To}	(3)C_{To}	$\bar{C}_{To}$	$\dot{V}_{CO_2}$ ml(STPD)/min
1.5	7.29	48.2	22.0	21.5	21.8	21.8	7.48	32.5	17.7	17.6	17.4	17.6	140.2†
1.5	7.34	48.8	22.2	21.6	22.1	22.0	7.48	32.9	17.6	17.6	17.5	17.6	146.9†

Deoxygenator specification: Harvey H200

Q_B ℓ/min	N_2 ℓ/min	CO_2 ℓ/min
0.5	2.0	0.24
1.0	4.0	0.49
1.5	4.9	0.63
0.5†	3.0	0.36
1.0†	4.1	0.49

	INLET	OUTLET
pO_2	42.6 ± 2.2	43.6 - 100.5
O_2sat	64.8 ± 2.5	80.5 - 97.4
Hb	12.7 ± 0.1	12.1 - 12.7

Values represent the mean ± 1 S.D. (n = 12)

Values represent the range

Haematocrit = 35.5%

†Modified Travenol TMO

DATA	UNITS
pCO_2 or pO_2	mmHg
O_2 sat	%
Hb	g%
C_{Ti} or C_{To}	mmol/ℓ

Test no: L10 Date: 21.12.81 Barometric pressure: 737 mmHg Oxygenator specification: Travenol TMO*

INLET							OUTLET						
Q_B ℓ/min	pH	pCO_2	(1)C_{Ti}	(2)C_{Ti}	(3)C_{Ti}	$\bar{C}_{Ti}$	pH	pCO_2	(1)C_{To}	(2)C_{To}	(3)C_{To}	$\bar{C}_{To}$	$\dot{V}_{CO_2}$ mℓ(STPD)/min
0.5	7.37	43.4	21.5	21.5	21.4	21.5	7.75	15.1	11.6	11.7	11.9	11.7	109.1
0.5	7.36	43.7	21.3	20.8	20.9	21.0	7.77	14.6	11.8	11.5	11.3	11.5	105.7
0.5	7.32	42.0	20.2	20.7	20.6	20.5	7.57	22.3	14.8	14.4	14.4	14.5	66.8†
0.5	7.33	41.7	20.0	19.9	20.5	20.1	7.56	24.7	14.9	14.3	14.9	14.7	60.1†
1.0	7.30	42.0	19.7	19.1	19.1	19.3	7.53	24.3	14.5	14.7	14.2	14.5	106.8†
1.0	7.33	41.7	19.4	19.6	19.3	19.4	7.50	25.3	14.4	14.4	14.5	14.4	111.3†
1.0	7.30	42.1	19.0	19.3	19.1	19.1	7.56	20.8	12.7	12.9	12.9	12.8	140.2
1.0	7.32	42.6	18.8	19.0	18.8	18.9	7.53	23.2	13.2	21.9	13.0	13.0	131.3

Deoxygenator specification: Harvey H200

Q_B ℓ/min	N_2 ℓ/min	CO_2 ℓ/min
0.5	1.7	0.24
1.0†	0.5	0.13
1.0	2.0	0.26

	INLET	OUTLET	DATA	UNITS
pO_2	46.8 ± 2.7	45.0 - 60.0	pCO_2 or pO_2	mmHg
O_2sat	64.3 ± 2.4	77.7 - 88.3	O_2 sat	%
Hb	12.5 ± 0.1	12.0 - 12.5	Hb	g%
			C_{Ti} or C_{To}	mmol/ℓ

Values represent the mean ± 1 S.D. (n = 8)

Values represent the range

Haematocrit = 35%

†Modified Travenol TMO

Test no: L11 Date: 7.5.82 Barometric pressure: 750 mmHg Oxygenator specification: Travenol TMO****

INLET							OUTLET						
Q_B ℓ/min	pH	pCO_2	(1)C_{Ti}	(2)C_{Ti}	(3)C_{Ti}	$\bar{C}_{Ti}$	pH	pCO_2	(1)C_{To}	(2)C_{To}	(3)C_{To}	$\bar{C}_{To}$	$\dot{V}_{CO_2}$ mℓ(STPD)/min
0.5	7.31	46.5	20.7	20.5	20.6	20.6	7.66	23.0	13.9	14.5	14.7	14.4	69.0
0.5	7.36	45.4	19.4	19.4	20.0	19.6	7.62	22.1	13.2	14.8	14.3	14.4	57.9
1.0	7.35	45.4	20.5	21.2	19.8	20.5	7.51	29.4	17.0	17.0	17.1	17.0	77.9
1.0	7.36	45.2	19.4	19.4	19.3	19.4	7.51	29.8	16.2	16.2	15.2	16.2	71.2
1.5	7.32	45.2	18.1	17.8	18.4	18.1	7.46	36.3	15.5	15.7	15.8	15.7	80.1
1.5	7.37	46.4	19.2	18.7	18.9	18.9	-	35.9	16.4	16.7	16.4	16.5	80.1

Deoxygenator specification: Harvey H200

Q_B ℓ/min	N_2 ℓ/min	CO_2 ℓ/min
0.5	3.3	0.37
1.0	5.5	0.6
1.5	5.5	0.6

	INLET	OUTLET	DATA	UNITS
pO_2	37.7 ± 0.8	38.8 - 51.8	pCO_2 or pO_2	mmHg
O_2sat	58.3 ± 1.6	68.9 - 91.2	O_2 sat	%
Hb	12.0 ± 0.1	11.5 - 12.0	Hb	g%
			C_{Ti} or C_{To}	mmol/ℓ

Values represent the mean ± 1 S.D. (n = 6)

Values represent the range

Haematocrit = 35%

Test no: L12 Date: 3.6.82 Barometric pressure: 755 mmHg Oxygenator specification: Travenol TMO***

INLET							OUTLET						
Q_B ℓ/min	pH	pCO_2	(1)C_{Ti}	(2)C_{Ti}	(3)C_{Ti}	$\bar{C}_{Ti}$	pH	pCO_2	(1)C_{To}	(2)C_{To}	(3)C_{To}	$\bar{C}_{To}$	$\dot{V}_{CO_2}$ mℓ(STPD)/min
0.5	7.44	49.8	17.6	17.5	17.6	17.6	7.70	25.1	12.7	12.5	12.7	12.6	55.7
0.5	7.47	45.0	17.3	16.9	16.8	17.0	7.71	22.6	12.8	12.4	12.1	12.4	51.2
1.0	7.37	43.1	16.9	17.4	17.2	17.2	7.56	31.9	13.5	13.7	13.3	13.5	82.4
1.0	7.41	42.4	16.2	16.2	16.4	16.3	7.57	32.2	13.8	13.5	13.6	13.6	60.1
1.5	7.32	43.9	16.4	16.5	16.4	16.4	7.50	34.9	14.8	14.2	14.2	14.4	66.8
1.5	7.40	43.3	16.6	16.5	16.2	16.4	7.51	34.5	14.0	13.8	13.9	13.9	83.5
0.5	7.31	45.1	16.7	16.2	16.7	16.5	7.57	31.4	12.5	12.6	12.6	12.6	43.4†
0.5	7.42	45.6	16.2	16.3	16.0	16.2	7.58	30.7	12.9	12.6	12.6	12.7	39.0†
1.0	7.32	41.9	15.8	16.2	16.0	16.0	7.53	32.4	13.3	13.0	12.9	13.1	64.5†
1.0	7.41	44.3	15.6	15.1	15.2	15.3	7.53	33.5	13.0	12.5	13.1	12.9	53.4†

Deoxygenator specification: Harvey H200

Q_B ℓ/min	N_2 ℓ/min	CO_2 ℓ/min
0.5	3.5	0.3
1.0	3.5	0.27
1.5	7.0	0.6
0.5†	2.2	0.2
1.0†	4.6	0.46
1.5†	7.0	0.7

	INLET	OUTLET
pO_2	39.5 ± 1.5	40.3 - 60.0
O_2sat	61.6 ± 1.7	75.1 - 93.6
Hb	10.7 ± 0.1	10.3 - 10.8

Values represent the mean ± 1 S.D. (n = 12)

Values represent the range

Haematocrit = 32%

†Modified Travenol TMO

DATA	UNITS
pCO_2 or pO_2	mmHg
O_2 sat	%
Hb	g%
C_{Ti} or C_{To}	mmol/ℓ

Test no: L12 Date: 3.6.82 Barometric pressure: 755 mmHg Oxygenator specification: Travenol TMO***

INLET							OUTLET						
Q_B ℓ/min	pH	pCO_2	(1)C_{Ti}	(2)C_{Ti}	(3)C_{Ti}	$\bar{C}_{Ti}$	pH	pCO_2	(1)C_{To}	(2)C_{To}	(3)C_{To}	$\bar{C}_{To}$	$\dot{V}_{CO_2}$ mℓ(STPD)/min
1.5	7.43	43.7	15.2	15.4	15.2	15.3	7.54	36.0	13.1	13.2	13.3	13.2	70.1†
1.5	7.43	44.8	15.4	15.4	15.4	15.4	7.52	36.8	13.7	13.4	13.4	13.5	63.4†

Deoxygenator specification: Harvey H200

Q_B ℓ/min	N_2 ℓ/min	CO_2 ℓ/min
0.5	3.5	0.3
1.0	3.5	0.27
1.5	7.0	0.6
0.5†	2.2	0.2
1.0†	4.6	0.45
1.5†	7.0	0.7

	INLET	OUTLET
pO_2	39.5 ± 1.5	40.3 - 60.0
O_2sat	61.6 ± 1.7	75.1 - 93.6
Hb	10.7 ± 0.1	10.3 - 10.8

Values represent the mean ± 1 S.D. (n = 12)

Values represent the range

Haematocrit = 32%

†Modified Travenol TMO

DATA	UNITS
pCO_2 or pO_2	mmHg
O_2 sat	%
Hb	g%
C_{Ti} or C_{To}	mmol/ℓ

Test no: L13 — Date: 23.6.82 Barometric pressure: 746 mmHg Oxygenator specification: Travenol TMO*

INLET							OUTLET						
Q_B ℓ/min	pH	pCO_2	(1)C_{Ti}	(2)C_{Ti}	(3)C_{Ti}	$\bar{C}_{Ti}$	pH	pCO_2	(1)C_{To}	(2)C_{To}	(3)C_{To}	$\bar{C}_{To}$	$\dot{V}_{CO_2}$ mℓ(STPD)/min
1.0	7.34	44.7	18.5	19.0	19.0	18.8	7.56	22.5	13.5	13.1	13.2	13.3	122.4
1.0	7.33	45.1	19.2	19.6	19.7	19.5	7.57	22.0	13.5	13.1	13.3	13.3	138.0
1.5	7.31	43.9	17.9	18.3	18.1	18.1	7.49	26.6	14.0	13.8	14.1	14.0	136.9
1.5	7.34	44.5	17.7	18.0	18.1	17.9	7.49	27.1	14.1	14.0	13.9	14.0	130.2
3.0	7.36	41.6	17.8	18.1	17.9	17.9	7.36	30.3	14.4	14.2	14.4	14.3	240.4
3.0	7.37	41.1	17.2	17.6	17.6	17.5	7.37	30.5	14.8	14.9	15.0	14.9	173.6
1.5	7.31	44.3	18.0	18.0	17.6	17.9	7.47	28.0	14.2	13.8	14.7	14.2	123.5†
1.5	7.32	44.6	18.5	18.2	18.6	18.4	7.47	28.3	14.7	14.2	13.9	14.3	136.9†
3.0	7.31	41.3	20.6	20.8	20.7	20.7	7.49	31.5	17.2	17.2	17.3	17.2	233.7†
3.0	7.39	41.3	19.7	19.6	19.6	19.6	7.48	32.0	15.8	16.2	16.5	16.2	227.1†

Deoxygenator specification: Harvey H200

Q_B ℓ/min	N_2 ℓ/min	CO_2 ℓ/min
1.0	6.0	0.8
1.5	8.0	1.1
3.0	8.0	1.1

	INLET	OUTLET
pO_2	43.2 ± 0.9	47.4 - 54.0
O_2sat	65.5 ± 2.2	80.5 - 89.5
Hb	12.1 ± 0.1	11.7 - 12.2

Values represent the mean ± 1 S.D. (n = 10)

Values represent the range

Haematocrit = 36%

†Modified Travenol TMO

DATA	UNITS
pCO_2 or pO_2	mmHg
O_2 sat	%
Hb	g%
C_{Ti} or C_{To}	mmol/ℓ

Test no: L14 Date: 19.10.82 Barometric pressure: 743 mmHg Oxygenator specification: Travenol TMO**

INLET							OUTLET						
Q_B ℓ/min	pH	pCO_2	(1)C_{Ti}	(2)C_{Ti}	(3)C_{Ti}	$\bar{C}_{Ti}$	pH	pCO_2	(1)C_{To}	(2)C_{To}	(3)C_{To}	$\bar{C}_{To}$	$\dot{V}_{CO_2}$ mℓ(STPD)/min
1.0	7.44	44.0	17.3	17.0	17.3	17.2	7.55	21.4	11.9	11.9	11.5	11.8	120.2
1.0	7.38	44.7	16.8	17.0	17.0	17.0	7.59	26.3	11.8	11.8	11.7	11.8	113.5
1.5	7.36	46.3	16.8	17.1	17.2	17.0	7.51	26.3	13.4	13.4	13.4	13.4	120.2
1.5	7.35	47.1	17.1	17.9	17.4	17.5	7.54	26.0	13.7	13.6	13.3	13.5	133.6
3.0	7.32	47.0	17.6	18.0	18.0	17.9	7.41	33.4	15.0	15.2	14.8	15.0	193.7
3.0	7.33	41.4	16.7	17.1	16.8	16.9	7.44	30.0	14.1	14.2	14.2	14.1	187.0
1.0	7.30	44.5	16.8	17.0	16.7	16.8	7.54	21.4	12.0	11.8	11.9	11.9	109.1†
1.0	7.31	44.2	17.0	16.8	16.8	16.9	7.55	21.6	12.2	12.2	12.2	12.2	104.6†
1.5	7.25	46.1	16.7	16.7	17.0	16.8	7.49	30.1	13.3	13.4	13.0	13.2	120.2†
1.5	7.33	46.1	16.8	16.7	17.0	16.8	7.51	30.0	13.0	13.2	13.2	13.1	123.5†

Deoxygenator specification: Harvey H200

Q_B ℓ/min	N_2 ℓ/min	CO_2 ℓ/min
1.0	6.4	0.75
1.5	8.0	1.1
3.0	8.0	1.1
1.0†	7.5	0.8
1.5†	8.0	1.1

	INLET	OUTLET
pO_2	44.8 ± 3.9	42.3 - 59.0
O_2sat	67.0 ± 1.6	80.2 - 90.8
Hb	11.6 ± 0.2	11.1 - 11.7

Values represent the mean ± 1 S.D. (n = 10)

Values represent the range

Haematocrit = 34%

†Modified Travenol TMO

DATA	UNITS
pCO_2 or pO_2	mmHg
O_2 sat	%
Hb	g%
C_{Ti} or C_{To}	mmol/ℓ

Test no: L15 Date: 21.10.82 Barometric pressure: 745 mmHg Oxygenator specification: Terumo CAPIOX II 1.6 m^2 *

INLET							OUTLET						
Q_B ℓ/min	pH	pCO_2	(1)C_{Ti}	(2)C_{Ti}	(3)C_{Ti}	$\bar{C}_{Ti}$	pH	pCO_2	(1)C_{To}	(2)C_{To}	(3)C_{To}	$\bar{C}_{To}$	$\dot{V}_{CO_2}$ mℓ(STPD)/min
2.0	7,42	43.4	21.8	21.2	22.2	21.7	7.54	28.0	18.1	18.2	18.3	18.2	77.9
2.0	7.41	44.1	21.9	22.3	22.1	22.1	7.53	29.9	18.0	18.1	17.7	17.9	93.5
3.0	7.36	47.0	21.1	21.1	21.6	21.3	7.55	29.5	17.1	17.5	17.5	17.4	86.8
3.0	7.42	45.9	21.6	21.0	21.8	21.5	7.56	28.8	16.6	16.7	16.9	16.7	106.8
5.0	7.33	44.7	20.1	20.5	20.7	20.4	7.58	21.8	15.6	15.8	15.5	15.6	106.8
5.0	7.40	44.1	20.0	20.3	20.3	20.2	7.58	26.1	15.0	14.8	15.0	14.9	118.0
2.0	7.33	50.8	19.9	20.1	20.5	20.2	7.49	36.6	16.8	16.6	16.5	16.6	80.1
2.0	7.40	46.0	19.3	19.4	19.9	19.5	7.51	33.3	15.9	15.8	15.9	15.9	80.1
7.0	7.43	42.1	19.5	19.5	19.6	19.5	7.61	21.1	14.8	14.3	14.1	14.4	113.5
7.0	7.41	43.7	19.5	19.9	19.7	19.7	7.59	25.3	14.0	14.3	14.6	14.3	120.2

Deoxygenator specification: Harvey H200

Q_B ℓ/min	N_2 ℓ/min	CO_2 ℓ/min
2.0	6.5	0.6
3.0	6.4	0.62
5.0	4.2	0.4
7.0	4.8	0.45

	INLET	OUTLET
pO_2	40.7 ± 1.6	111.8 - 233.8
O_2sat	63.5 ± 1.7	97.1 - 97.5
Hb	11.9 ± 0.2	11.4 - 11.8

Values represent the mean ± 1 S.D. (n = 10)

Values represent the range

Haematocrit = 33%

Q_B = 1.0 ℓ/min

DATA	UNITS
pCO_2 or pO_2	mmHg
O_2 sat	%
Hb	g%
C_{Ti} or C_{To}	mmol/ℓ

Test no: L16 Date: 27.10.82 Barometric pressure: 752 mmHg Oxygenator specification: Terumo CAPIOX II 1.6 m^2 **

INLET							OUTLET						
Q_B ℓ/min	pH	pCO_2	(1)C_{Ti}	(2)C_{Ti}	(3)C_{Ti}	$\bar{C}_{Ti}$	pH	pCO_2	(1)C_{To}	(2)C_{To}	(3)C_{To}	$\bar{C}_{To}$	$\dot{V}_{CO_2}$ mℓ(STPD)/min
7.0	7,38	43.6	19.1	19.2	19.5	19.3	7.55	26.8	14.4	14.3	14.5	14.4	109.1
7.0	7.38	44.0	18.9	19.2	18.9	19.0	7.54	28.2	14.3	14.4	14.6	14.4	102.4
7.0	7.38	44.8	18.5	18.6	18.5	18.5	7.54	28.3	14.7	14.8	14.7	14.7	84.6
5.0	7.35	45.2	18.9	19.1	19.2	19.1	7.45	27.6	14.6	14.4	14.7	14.6	100.2
5.0	7.32	45.9	18.7	19.2	19.1	19.0	7.47	27.8	14.6	14.8	14.6	14.7	95.7
5.0	7.32	45.9	18.4	18.7	19.0	18.7	7.47	26.6	14.3	14.6	14.3	14.4	95.7
2.0	7.39	45.3	22.3	21.7	22.5	22.2	7.53	31.2	18.8	19.1	19.1	19.0	71.2
2.0	7.38	45.1	23.1	23.3	22.8	23.1	7.52	28.9	19.3	18.8	19.4	19.2	86.8
9.0	7.48	41.0	21.8	22.0	21.7	21.8	7.48	21.4	16.8	17.1	17.2	17.0	106.8
9.0	7.39	46.1	23.0	23.2	23.2	23.1	7.60	24.9	17.4	17.4	17.7	17.5	124.7

Deoxygenator specification: Harvey H200

Q_B ℓ/min	N_2 ℓ/min	CO_2 ℓ/min
7.0	8.2	0.82
5.0	7.5	0.77
2.0	5.0	0.51
9.0	5.0	0.46

	INLET	OUTLET
pO_2	40.7 ± 1.6	111.8 - 233.8
O_2sat	64.4 ± 2.3	99.6 - 101.1
Hb	12.2 ± 0.1	11.7 - 12.0

Values represent the mean ± 1 S.D. (n = 10)

Values represent the range

Haematocrit = not measured

DATA	UNITS
pCO_2 or pO_2	mmHg
O_2 sat	%
Hb	g%
C_{Ti} or C_{To}	mmol/ℓ

Test no: L17 Date: 1.11.82 Barometric pressure: 757 mmHg Oxygenator specification: Terumo CAPIOX II 1.6 m^2 *

INLET							OUTLET						
Q_B ℓ/min	pH	pCO_2	(1)C_{Ti}	(2)C_{Ti}	(3)C_{Ti}	$\bar{C}_{Ti}$	pH	pCO_2	(1)C_{To}	(2)C_{To}	(3)C_{To}	$\bar{C}_{To}$	$\dot{V}_{CO_2}$ mℓ(STPD)/min
0.5	7.31	49.2	17.6	17.9	17.9	17.8	7.60	19.6	11.7	11.9	12.0	11.9	65.7
0.5	7.35	44.4	17.0	17.2	17.3	17.2	7.64	15.9	11.3	11.3	11.5	11.4	64.6
1.0	7.31	45.2	17.4	17.1	17.3	17.3	7.42	28.1	13.2	13.5	13.4	13.4	86.8
1.0	7.33	43.1	17.0	16.9	16.8	16.9	7.44	26.0	13.4	13.7	13.3	13.5	75.7
1.5	7.29	44.0	17.6	17.8	17.8	17.7	7.43	33.4	14.9	14.3	14.4	14.5	106.8
1.5	7.34	46.5	17.2	17.3	17.6	17.4	7.42	31.8	14.3	14.4	14.2	14.3	103.5

Deoxygenator specification: Harvey H200

Q_B ℓ/min	N_2 ℓ/min	CO_2 ℓ/min
0.5	5.0	0.5
1.0	9.0	0.85
1.5	8.5	0.85

	INLET	OUTLET
pO_2	37.2 ± 2.7	44.3 - 562.4
O_2sat	64.2 ± 1.8	85.7 - 102.4
Hb	11.6 ± 0.2	11.0 - 11.6

Values represent the mean ± 1 S.D. (n = 6)

Values represent the range

Haematocrit = 32%

DATA	UNITS
pCO_2 or pO_2	mmHg
O_2 sat	%
Hb	g%
C_{Ti} or C_{To}	mmol/ℓ

Test no: L18 Date: 9.11.82 Barometric pressure: 727 mmHg Oxygenator specification: Terumo CAPIOX II 1.6 m^2 **

INLET							OUTLET						
Q_B ℓ/min	pH	pCO_2	(1)C_{Ti}	(2)C_{Ti}	(3)C_{Ti}	$\bar{C}_{Ti}$	pH	pCO_2	(1)C_{To}	(2)C_{To}	(3)C_{To}	$\bar{C}_{To}$	$\dot{V}_{CO_2}$ mℓ(STPD)/min
0.5	7.34	47.4	20.2	20.5	20.3	20.3	7.67	21.3	14.1	14.3	14.2	14.2	67.9
0.5	7.36	43.9	20.0	20.0	19.8	19.9	7.70	18.4	14.3	14.1	13.9	14.1	64.6
1.0	7.34	43.8	19.7	20.1	19.6	19.8	7.55	27.0	15.3	15.6	15.1	15.3	100.2
1.0	7.36	43.9	19.6	19.9	19.7	19.7	7.56	26.2	15.5	15.8	15.5	15.6	91.3

Deoxygenator specification: Harvey H200

Q_B ℓ/min	N_2 ℓ/min	CO_2 ℓ/min
0.5	2.5	0.25
1.0	6.0	0.58

	INLET	OUTLET
pO_2	43.1 ± 1.3	432.3 - 606.0
O_2sat	67.9 ± 1.8	100.1 - 100.3
Hb	10.8	10.4 - 10.5

Values represent the mean ± 1 S.D. (n = 4)

Values represent the range

Haematocrit = 28%

DATA	UNITS
pCO_2 or pO_2	mmHg
O_2 sat	%
Hb	g%
C_{Ti} or C_{To}	mmol/ℓ

Test no: L19 Date: 18.11.82 Barometric pressure: 734 mmHg Oxygenator specification: Terumo CAPIOX II 1.6 m^2 *

	INLET						OUTLET						
Q_B ℓ/min	pH	pCO_2	(1)C_{Ti}	(2)C_{Ti}	(3)C_{Ti}	$\bar{C}_{Ti}$	pH	pCO_2	(1)C_{To}	(2)C_{To}	(3)C_{To}	$\bar{C}_{To}$	$\dot{V}_{CO_2}$ mℓ(STPD)/min
0.5	7.37	46.5	19.8	20.0	20.1	20.0	7.75	14.2	12.8	12.6	12.7	12.7	81.2
0.5	7.41	40.0	19.1	19.0	18.9	19.0	7.69	13.8	12.8	12.5	12.8	12.7	70.1
1.0	7.39	33.4	17.8	17.3	17.6	17.6	7.61	18.9	13.2	13.3	13.1	13.2	97.9
1.0	7.39	33.0	16.7	16.7	17.1	16.8	7.58	17.5	13.1	12.9	12.9	13.0	84.6
1.5	7.42	31.7	16.3	16.6	16.6	16.5	7.56	19.3	13.0	12.9	12.9	12.9	120.2
1.5	7.38	36.0	19.7	19.6	19.5	19.6	7.46	28.0	15.6	15.1	15.6	15.4	140.2
1.5	7.38	37.6	17.6	17.5	17.5	17.5	7.53	24.1	14.3	14.5	14.4	14.4	103.5

Deoxygenator specification: Harvey H200

Q_B ℓ/min	N_2 ℓ/min	CO_2 ℓ/min
0.5	3.0	0.25
1.0	2.5	0.25
1.5	3.0	0.25

	INLET	OUTLET
pO_2	38.2 ± 2.0	37.0 - 556.0
O_2sat	67.9 ± 2.7	72.8 - 100.5
Hb	12.3 ± 0.1	11.8 - 12.4

Values represent the mean ± 1 S.D. (n = 6)

Values represent the range

Haematocrit = 39%

DATA	UNITS
pCO_2 or pO_2	mmHg
O_2 sat	%
Hb	g%
C_{Ti} or C_{To}	mmol/ℓ

Test no: L20 Date: 25.11.82 Barometric pressure: 732 mmHg Oxygenator specification: Terumo CAPIOX II 1.6 m^2 **

	INLET						OUTLET						
Q_B ℓ/min	pH	pCO_2	(1)C_{Ti}	(2)C_{Ti}	(3)C_{Ti}	$\bar{C}_{Ti}$	pH	pCO_2	(1)C_{To}	(2)C_{To}	(3)C_{To}	$\bar{C}_{To}$	$\dot{V}_{CO_2}$ mℓ(STPD)/min
0.5	7.42	38.2	19.8	19.6	19.5	19.6	7.70	15.3	14.5	14.6	14.7	14.6	55.7
0.5	7.49	30.5	18.1	17.8	18.5	18.1	7.75	12.3	12.9	12.7	13.2	12.9	57.9
1.0	7.40	37.0	18.2	18.5	18.8	18.5	7.57	21.6	14.5	14.6	14.4	14.5	89.0
1.0	7.42	35.6	17.8	17.9	17.9	17.9	7.56	21.1	14.4	14.6	14.5	14.5	75.7
1.5	7.45	34.6	18.2	18.1	18.3	18.2	7.56	24.0	15.2	15.1	15.1	15.1	103.5
1.5	7.45	35.0	17.4	17.5	17.6	17.5	7.55	21.2	15.1	15.3	15.1	15.2	76.8

Deoxygenator specification: Harvey H200

Q_B ℓ/min	N_2 ℓ/min	CO_2 ℓ/min
0.5	3.5	0.25
1.0	7.0	0.70
1.5	9.0	0.90

	INLET	OUTLET
pO_2	37.8 ± 0.9	43.2 - 548.8
O_2sat	64.3 ± 1.4	85.0 - 102.3
Hb	12.4 ± 0.1	11.8 - 12.2

Values represent the mean ± 1 S.D. (n = 6)

Values represent the range

Haematocrit = 34%

DATA	UNITS
pCO_2 or pO_2	mmHg
O_2 sat	%
Hb	g%
C_{Ti} or C_{To}	mmol/ℓ

Test no: L21 Date: 30.11.82 Barometric pressure: 760 mmHg Oxygenator specification: Terumo CAPIOX II 3.3 m^2 *

INLET							OUTLET						
Q_B ℓ/min	pH	pCO_2	(1)C_{Ti}	(2)C_{Ti}	(3)C_{Ti}	$\bar{C}_{Ti}$	pH	pCO_2	(1)C_{To}	(2)C_{To}	(3)C_{To}	$\bar{C}_{To}$	$\dot{V}_{CO_2}$ mℓ(STPD)/min
4.0	7.34	43.5	16.7	16.4	16.8	16.6	7.55	18.8	11.4	11.2	11.2	11.3	118.0
4.0	7.38	42.5	16.4	16.2	16.4	16.3	7.57	17.3	11.2	10.8	10.9	11.0	118.0
6.0	7.36	39.6	16.0	16.3	16.4	16.2	7.64	15.7	9.7	9.7	9.7	9.7	144.7
6.0	7.35	41.1	15.7	16.1	15.7	15.8	7.63	16.3	9.7	9.7	9.8	9.8	133.6
8.0	7.27	41.7	15.9	15.3	15.7	15.6	7.59	14.6	9.2	9.3	9.3	9.3	140.2
8.0	7.29	39.5	15.9	15.7	16.0	15.9	7.56	14.8	9.4	9.1	9.1	9.2	149.1
10.0	7.30	35.7	15.4	15.9	15.8	15.7	7.66	9.6	9.1	9.0	8.9	9.0	149.1
10.0	7.34	35.6	15.9	15.8	16.0	15.9	7.65	9.7	9.3	9.1	9.1	9.2	149.1

Deoxygenator specification: Harvey H200

Q_B ℓ/min	N_2 ℓ/min	CO_2 ℓ/min
4.0	8.0	0.8
6.0	8.0	0.8
8.0	8.0	0.8
10.0	8.0	0.8

	INLET	OUTLET
pO_2	42.0 ± 1.5	182.9 - 430.1
O_2sat	64.5 ± 0.6	99.6 - 100.2
Hb	11.8 ± 0.1	11.3 - 11.6

Values represent the mean ± 1 S.D. (n = 8)

Values represent the range

Haematocrit = 34%

Q_B = 1.0 ℓ/min

DATA	UNITS
pCO_2 or pO_2	mmHg
O_2 sat	%
Hb	g%
C_{Ti} or C_{To}	mmol/ℓ

Test no: L22 Date: 16.12.82 Barometric pressure: 729 mmHg Oxygenator specification: Terumo CAPIOX II 3.3 m^2 **

INLET							OUTLET						
Q_B ℓ/min	pH	pCO_2	(1)C_{Ti}	(2)C_{Ti}	(3)C_{Ti}	$\bar{C}_{Ti}$	pH	pCO_2	(1)C_{To}	(2)C_{To}	(3)C_{To}	$\bar{C}_{To}$	$\dot{V}_{CO_2}$ mℓ(STPD)/min
1.5	7.27	45.4	16.5	16.7	16.5	16.6	7.57	19.0	11.5	11.4	11.2	11.4	173.6
1.5	7.31	44.4	16.3	16.7	16.7	16.6	7.56	20.9	11.5	11.4	11.4	11.4	173.6
1.0	7.34	45.2	18.4	18.2	18.1	18.2	7.63	16.8	10.9	11.2	11.1	11.1	158.0
1.0	7.37	45.4	17.7	17.8	17.5	17.7	7.67	15.1	11.1	10.9	10.9	11.0	149.1
0.5	7.31	44.8	17.6	17.9	17.9	17.8	7.75	7.0	8.4	8.3	8.2	8.3	105.7
0.5	7.36	53.7	17.9	17.9	18.2	18.0	7.82	7.8	7.7	7.3	7.4	7.5	116.9

Deoxygenator specification: Harvey H200

Q_B ℓ/min	N_2 ℓ/min	CO_2 ℓ/min
1.5	8.0	1.08
1.0	6.0	0.75
0.5	2.5	0.35

	INLET	OUTLET
pO_2	40.0 ± 0.9	60.0 - 204.1
O_2sat	64.7 ± 2.3	92.8 - 99.6
Hb	12.6 ± 0.3	11.8 - 12.5

Values represent the mean ± 1 S.D. (n = 4)

Values represent the range

Haematocrit = 43%

DATA	UNITS
pCO_2 or pO_2	mmHg
O_2 sat	%
Hb	g%
C_{Ti} or C_{To}	mmol/ℓ

Test no: L23 Date: 22.12.82 Barometric pressure: 742 mmHg Oxygenator specification: Terumo CAPIOX II 3.3 m^2 *

INLET							OUTLET						
Q_B ℓ/min	pH	pCO_2	(1)C_{Ti}	(2)C_{Ti}	(3)C_{Ti}	$\bar{C}_{Ti}$	pH	pCO_2	(1)C_{To}	(2)C_{To}	(3)C_{To}	$\bar{C}_{To}$	$\dot{V}_{CO_2}$ mℓ(STPD)/min
1.5	7.31	54.5	18.2	18.6	19.0	18.6	7.54	27.5	13.0	12.6	12.6	12.7	197.0
1.5	7.33	53.1	18.3	18.3	18.4	18.3	7.60	24.3	12.6	12.8	12.7	12.7	187.0
1.5	7.30	45.5	18.0	17.9	17.8	17.9	7.61	20.5	11.7	11.5	11.8	11.7	207.0
1.5	7.38	44.0	17.3	17.0	16.8	17.0	7.62	19.0	11.8	11.4	11.3	11.5	183.6
1.0	7.34	45.2	17.1	16.6	16.3	16.7	7.76	13.1	10.3	9.8	9.9	10.0	149.1
1.0	7.45	37.9	15.1	15.9	15.5	15.5	7.72	13.9	9.3	9.6	9.1	9.3	138.0
1.0	7.41	40.8	15.6	15.7	15.5	15.6	7.72	13.9	9.7	9.4	9.4	9.5	135.8
1.0	7.37	45.3	16.9	16.8	16.5	16.7	7.70	13.1	9.8	9.8	9.8	9.8	153.6
1.0	7.26	52.2	17.2	17.4	17.2	17.3	7.67	15.9	9.9	9.4	9.5	9.6	171.4
1.0	7.26	59.7	18.6	18.5	18.1	18.4	7.64	18.6	9.9	10.1	10.4	10.1	184.8

Deoxygenator specification: Harvey H200

Q_B ℓ/min	N_2 ℓ/min	CO_2 ℓ/min
1.5	7.6	1.20
1.0	3.6	0.40

	INLET	OUTLET
pO_2	38.8 ± 2.8	48.5 - 94.4
O_2sat	62.5 ± 1.2	94.1 - 99.7
Hb	11.2 ± 0.2	10.5 - 11.1

Values represent the mean ± 1 S.D. (n = 10)

Values represent the range

Haematocrit = 31%

DATA	UNITS
pCO_2 or pO_2	mmHg
O_2 sat	%
Hb	g%
C_{Ti} or C_{To}	mmol/ℓ

Test no: L24 Date: 11.1.83 Barometric pressure: 751 mmHg Oxygenator specification: Terumo CAPIOX II 3.3 m^2*

INLET							OUTLET						
Q_B ℓ/min	pH	pCO_2	(1)C_{Ti}	(2)C_{Ti}	(3)C_{Ti}	$\bar{C}_{Ti}$	pH	pCO_2	(1)C_{To}	(2)C_{To}	(3)C_{To}	$\bar{C}_{To}$	$\dot{V}_{CO_2}$ mℓ(STPD)/min
1.5	7.35	49.7	17.7	17.9	17.8	17.8	7.58	24.9	12.4	12.5	12.8	12.6	173.6
1.5	7.31	56.2	18.5	18.9	18.6	18.7	7.57	24.3	13.1	13.1	13.3	13.2	183.6
1.5	7.31	57.4	18.8	18.3	18.6	18.6	7.57	23.1	13.2	13.0	12.9	13.0	187.0

Deoxygenator specification: Harvey H200

Q_B ℓ/min	N_2 ℓ/min	CO_2 ℓ/min
1.5	7.6	1.1

	INLET	OUTLET
pO_2	41.9	62.5 - 70.9
O_2sat	68.3	96.4 - 97.8
Hb	11.0	10.7 - 10.8

Values represent the mean ± 1 S.D. (n =)

Values represent the range

Haematocrit = 32%

DATA	UNITS
pCO_2 or pO_2	mmHg
O_2 sat	%
Hb	g%
C_{Ti} or C_{To}	mmol/ℓ

Test no: L25 Date: 18.1.83 Barometric pressure: 746 mmHg Oxygenator specification: Terumo CAPIOX II 3.3 m^{2**}

INLET							OUTLET						
Q_B ℓ/min	pH	pCO_2	(1)C_{Ti}	(2)C_{Ti}	(3)C_{Ti}	$\bar{C}_{Ti}$	pH	pCO_2	(1)C_{To}	(2)C_{To}	(3)C_{To}	$\bar{C}_{To}$	$\dot{V}_{CO_2}$ mℓ(STPD)/min
1.5	7.37	53.4	18.8	18.2	18.8	18.6	7.64	21.0	12.6	12.7	12.6	12.6	200.3
1.5	7.36	53.3	18.3	18.3	18.4	18.3	7.64	22.3	12.7	12.5	12.5	12.5	193.7
1.5	7.42	44.8	17.7	17.6	17.6	17.6	7.64	19.2	11.5	11.5	11.3	11.4	207.0
1.5	7.43	43.5	16.9	16.9	16.8	16.9	7.65	18.6	12.3	11.9	11.9	12.0	163.6
1.0	7.28	58.4	18.5	18.1	18.1	18.2	7.64	17.7	11.0	10.8	10.5	10.8	164.7
1.0	7.33	51.4	17.3	17.8	17.6	17.6	7.65	17.6	10.2	10.2	9.7	10.0	169.2
1.0	7.32	52.8	17.7	17.6	16.9	17.4	7.64	20.2	10.4	10.1	10.2	10.2	160.3
1.0	7.32	43.4	16.8	16.6	16.8	16.7	7.69	17.7	10.3	10.5	10.3	10.4	140.2
1.0	7.38	43.4	16.6	17.0	16.9	16.8	7.69	17.6	10.5	10.3	10.3	10.4	142.5

Deoxygenator specification: Harvey H200

Q_B ℓ/min	N_2 ℓ/min	CO_2 ℓ/min
1.5	8.0	1.1
1.0	3.3	0.55

INLET		OUTLET	DATA	UNITS
pO_2	46.4 ± 2.8	67.3 - 136.9	pCO_2 or pO_2	mmHg
O_2sat	64.8 ± 1.7	94.4 - 100.5	O_2 sat	%
Hb	10.0 ± 0.2	9.5 - 9.9	Hb	g%
			C_{Ti} or C_{To}	mmol/ℓ

Values represent the mean ± 1 S.D. (n = 9)

Values represent the range

Haematocrit = 28%

Test no: L26 Date: 20.1.83 Barometric pressure: 762 mmHg Oxygenator specification: Terumo CAPIOX II 3.3 m^{2} *

INLET							OUTLET						
Q_B ℓ/min	pH	pCO_2	(1)C_{Ti}	(2)C_{Ti}	(3)C_{Ti}	$\bar{C}_{Ti}$	pH	pCO_2	(1)C_{To}	(2)C_{To}	(3)C_{To}	$\bar{C}_{To}$	$\dot{V}_{CO_2}$ mℓ(STPD)/min
1.5	7.33	53.8	21.2	20.8	20.7	20.9	7.58	24.3	14.9	14.7	14.7	14.8	203.7
1.5	7.34	54.0	20.2	20.5	20.8	20.5	7.58	24.0	14.4	14.2	14.3	14.3	207.0
1.5	7.38	46.2	20.0	19.6	20.0	19.9	7.61	22.1	13.9	13.7	13.9	13.8	203.7
1.5	7.41	45.2	20.4	20.2	19.8	20.1	7.62	22.0	14.2	14.2	14.0	14.1	200.3
1.0	7.32	55.4	21.8	21.5	21.5	21.6	7.66	18.8	13.2	12.7	12.8	12.9	193.7
1.0	7.34	55.0	21.4	20.8	21.0	21.1	7.67	19.3	12.8	12.8	12.8	12.9	182.5
1.0	7.35	46.3	19.6	19.8	19.7	19.7	7.66	18.2	12.5	12.6	12.5	12.5	160.3
1.0	7.40	44.4	19.2	19.8	19.7	19.6	7.68	17.4	11.9	12.2	12.1	12.1	167.0

Deoxygenator specification: Harvey H200

Q_B ℓ/min	N_2 ℓ/min	CO_2 ℓ/min
1.5	8.0	1.16
1.0	3.3	0.57

INLET		OUTLET	DATA	UNITS
pO_2	41.3 ± 2.5	53.9 - 76.8	pCO_2 or pO_2	mmHg
O_2sat	63.7 ± 0.7	94.4 - 99.1	O_2 sat	%
Hb	12.1 ± 0.2	11.6 - 11.9	Hb	g%
			C_{Ti} or C_{To}	mmol/ℓ

Values represent the mean ± 1 S.D. (n = 8)

Values represent the range

Haematocrit = 34%

Test no: L27 Date: 25.1.83 Barometric pressure: 750 mmHg Oxygenator specification: Terumo CAPIOX II 3.3 m^2 **

INLET							OUTLET						
Q_B ℓ/min	pH	pCO_2	(1)C_{Ti}	(2)C_{Ti}	(3)C_{Ti}	$\bar{C}_{Ti}$	pH	pCO_2	(1)C_{To}	(2)C_{To}	(3)C_{To}	$\bar{C}_{To}$	$\dot{V}_{CO_2}$ mℓ(STPD)/min
1.5	7.32	55.2	20.0	20.0	20.4	20.1	7.62	23.2	13.7	13.9	13.7	13.8	210.4
1.5	7.33	55.4	21.4	20.9	21.2	21.2	7.62	23.5	14.2	14.0	14.0	14.1	237.1
1.5	7.38	46.9	19.0	18.9	19.3	19.1	7.64	20.7	13.2	12.7	12.7	12.9	207.0
1.5	7.39	46.0	18.7	19.3	19.3	19.1	7.64	22.2	13.5	13.1	13.2	13.3	193.6
1.0	7.28	54.3	19.8	20.0	19.6	19.8	7.70	19.0	11.8	11.7	11.6	11.7	180.3
1.0	7.33	54.8	20.0	20.2	20.1	20.1	7.70	16.8	11.9	11.7	11.9	11.8	184.8
1.0	7.45	44.6	18.3	18.5	18.2	18.3	7.76	15.6	11.4	11.1	10.9	11.1	160.3
1.0	7.40	45.2	18.6	18.5	18.5	18.5	7.74	16.3	11.6	11.4	11.4	11.5	155.8

Deoxygenator specification: Harvey H200

Q_B ℓ/min	N_2 ℓ/min	CO_2 ℓ/min
1.5	7.5	1.19
1.0	3.3	0.6

	INLET	OUTLET
pO_2	42.0 ± 2.0	52.6 - 93.8
O_2sat	63.1 ± 1.7	93.5 - 99.6
Hb	11.5 ± 0.1	11.0 - 11.2

Values represent the mean ± 1 S.D. (n = 8)

Values represent the range

Haematocrit = 30%

DATA	UNITS
pCO_2 or pO_2	mmHg
O_2 sat	%
Hb	g%
C_{Ti} or C_{To}	mmol/ℓ

Test no: L28 Date: 24.3.83 Barometric pressure: 743 mmHg Oxygenator specification: Terumo CAPIOX II 3.3 m^2 *

INLET							OUTLET						
Q_G ℓ/min	pH	pCO_2	(1)C_{Ti}	(2)C_{Ti}	(3)C_{Ti}	$\bar{C}_{Ti}$	pH	pCO_2	(1)C_{To}	(2)C_{To}	(3)C_{To}	$\bar{C}_{To}$	$\dot{V}_{CO_2}$ mℓ(STPD)/min
8.0	7.35	46.4	20.0	19.6	20.3	20.0	7.56	23.7	14.4	14.5	14.1	14.3	190.3
8.0	7.37	44.2	19.4	19.4	19.3	19.4	7.58	22.9	14.0	14.3	14.2	14.2	173.6
8.0	7.37	44.7	19.3	19.6	19.2	19.4	7.55	23.3	13.7	13.9	14.1	13.9	183.6
10.0	7.38	44.3	20.5	20.7	20.7	20.6	7.58	22.6	14.9	14.5	14.9	14.8	193.7
10.0	7.37	44.6	20.3	21.0	20.7	20.7	7.59	22.1	14.8	14.7	15.0	14.8	197.0
10.0	7.37	45.2	20.2	20.5	20.3	20.3	7.58	22.9	15.1	15.0	14.9	15.0	177.0
12.0	7.35	44.0	21.3	21.2	21.3	21.3	7.58	21.2	14.6	14.2	14.4	14.4	230.4
12.0	7.36	45.7	21.5	21.4	21.5	21.5	7.58	21.5	14.2	14.2	14.4	14.3	240.4
12.0	7.36	44.5	20.7	20.6	20.6	20.6	7.58	21.2	14.6	16.5	14.3	14.4	207.0

Deoxygenator specification: Harvey H200

Q_G ℓ/min	N_2 ℓ/min	CO_2 ℓ/min
8.0	5.0	0.65
10.0	5.0	0.65
12.0	4.2	0.63
15.0	4.2	0.63

	INLET	OUTLET
pO_2	not measured	
O_2sat	63.6 ± 2.1	81.2 - 88.9
Hb	12.5 ± 0.1	12.2 - 12.5

Values represent the mean ± 1 S.D. (n = 15)

Values represent the range

Haematocrit = 35%

Q_B = 1.5 ℓ/min

DATA	UNITS
pCO_2 or pO_2	mmHg
O_2 sat	%
Hb	g%
C_{Ti} or C_{To}	mmol/ℓ

Test no: L28 Date: 24.3.83 Barometric pressure: 743 mmHg Oxygenator specification: Terumo CAPIOX II 3.3 m^2 *

	INLET						OUTLET						
Q_G ℓ/min	pH	pCO_2	(1)C_{Ti}	(2)C_{Ti}	(3)C_{Ti}	$\bar{C}_{Ti}$	pH	pCO_2	(1)C_{To}	(2)C_{To}	(3)C_{To}	$\bar{C}_{To}$	V_{CO_2} mℓ(STPD)/min
15.0+	7,33	43.0	20.5	20.8	20.7	20.7	7.58	19.5	13.8	13.5	13.3	13.5	240.4
15.0+	7.35	43.5	20.5	21.0	21.1	20.9	7.58	20.4	13.3	13.8	13.8	13.6	243.7
15.0+	7.36	43.3	20.1	20.6	20.7	20.5	7.58	20.8	13.2	13.3	13.3	13.3	240.1
15.0++	7.34	43.5	20.3	20.5	20.1	20.3	7.64	16.7	12.0	12.0	12.0	12.0	184.8
15.0++	7.35	44.1	19.7	20.2	20.0	20.0	7.65	16.3	12.7	12.5	12.7	12.6	164.7
15.0++	7.36	48.3	20.2	20.6	20.7	20.5	7.63	16.2	12.1	12.2	12.2	12.2	184.8

Deoxygenator specification: Harvey H200

Q_G ℓ/min	N_2 ℓ/min	CO_2 ℓ/min
8.0	5.0	0.65
10.0	5.0	0.65
12.0	4.2	0.63
15.0	4.2	0.63

	INLET	OUTLET
pO_2	not measured	
O_2sat	63.6 ± 2.1	81.2 - 88.9
Hb	12.5 ± 0.1	12.2 - 12.5

Values represent the mean ± 1 S.D. (n = 15)

Values represent the range

Haematocrit = 35%

$^{+}Q_B$ = 1.5 ℓ/min $^{++}Q_B$ = 1.0 ℓ/min

DATA	UNITS
pCO_2 or pO_2	mmHg
O_2 sat	%
Hb	g%
C_{Ti} or C_{To}	mmol/ℓ

Lung	Q_B l/min	Test no.	$\dot{V}_{CO_2}$ ml/min		$\bar{\dot{V}}_{CO_2}$ ml/min
Travenol TMO	0·5	L1	48·0	64·5	70·1 ± 11·3
		L4	78·0	64·5	
		L5	57·9	66·8	
		L6	76·8	67·9	
		L7	83·5	87·9	
		L9	80·1	79·0	
		L11	69·0	57·9	
	1·0	L2	114·0	137·0	117·1 ± 17·3
		L4	109·0	88·0	
		L6	109·1	82·4	
		L8	117·9	124·7	
		L9	109·1	115·8	
		L10	140·2	131·3	
		L13	122·4	138·0	
	1·5	L1	121·5	121·5	124·8 ± 11·3
		L2	151·0	135·0	
		L4	109·5	120·0	
		L6	120·2	110·2	
		L9	120·2	116·9	
		L13	136·9	130·2	
		L14	120·2	133·6	

Lung	Q_B l/min	Test no.	$\dot{V}_{CO_2}$ ml/min		$\bar{\dot{V}}_{CO_2}$ ml/min
Travenol TMO-modified	0·5	L7	84·6	74·6	
		L9	100·2	82·4	78·1 ± 14·2
		L10	66·8	60·1	
	1·0	L8	115·7	135·8	
		L9	122·4	120·2	118·7 ± 10·1
		L10	106·8	111·3	
	1·5	L9	140·2	146·9	
		L13	123·5	136·9	131·8 ± 10·9
		L14	120·2	123·5	
Terumo CAPIOX II 1·6 m^2	0·5	L17	65·7	64·6	
		L18	67·9	64·6	69·0
		L19	81·2	70·1	
	1·0	L15	106·8	118·0	
		L17	86·8	75·7	96·5
		L18	100·2	91·3	
	1·5	L17	106·8	103·5	104·6
		L19	103·5		

Lung	Q_B l/min	Test no.	$\dot{V}_{CO_2}$ ml/min		$\bar{\dot{V}}_{CO_2}$ ml/min
Terumo CAPIOX II 3·3 m^2	0·5	L22	105·7	116·9	111·3
	1·0	L22	158·0	149·1	
		L23	149·1	135·8	
		L23	153·6		
		L25	140·2	142·5	152·0
		L26	160·3	167·0	
		L27	160·3	155·8	
	1·5	L22	173·6	173·6	
		L23	207·0	183·6	
		L24	173·6		
		L25	207·0	163·6	189·6
		L26	200·3	203·7	
		L27	207·0	193·6	
		L28	193·7	197·0	
		L28	177·0		

APPENDIX E

CORRELATION FOR TRAVENOL TMO

E.1 Calculation of the half-channel height, a.

Area, $A = 2.25\ m^2$

Priming Volume, PV = 420 ml at shim pressure of 200 mmHg

$$PV = NWL.2a$$

$$A = NWL.2$$

$$a = \frac{PV}{A} = \frac{420}{2.25 \times 10^4} = \underline{1.866 \times 10^{-2}}\ cm$$

E.2 To calculate θ_c

From manufacturers' data sheet:

$$Q_B = 6000\ ml/min$$

$$\dot{V}_{CO_2} = 338\ ml(STPD)/min \quad at \quad Q_{gi} = 15.0\ l/min$$

Assume $C_{Ti} = 52\ \frac{ml.CO_2}{100ml}$

$$\dot{V}_{CO_2} = Q_B\ \theta_c\ C_{Ti} \qquad (3.28)$$

$$\theta_c = \frac{\dot{V}_{CO_2}}{Q_B C_{Ti}}$$

$$\theta_c = \frac{338}{6000 \times 0.52} = \underline{0.108}$$

E.3 Gas phase calculations

$Q_B = 6000$ ml/min

$\dot{V}_{CO_2} = 338$ ml(STPD)/min

$\dot{V}_{O_2} = 350$ ml(STPD)/min

$Q_{gi} = 15$ ℓ/min

} from manufacturers' data sheet

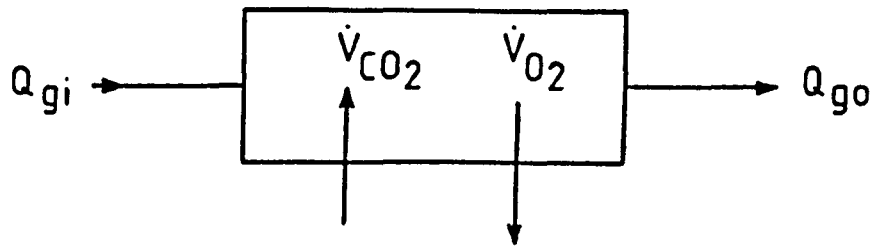

Outlet gas flow rate, Q_{go} is given by an overall volumetric balance:

$$Q_{go} = Q_{gi} + \dot{V}_{CO_2} - \dot{V}_{O_2}$$

and the gas phase partial pressure at outlet, P_{go} is:

$$P_{go} = \frac{\dot{V}_{CO_2}}{Q_{go}} \times P_{ATM}$$

$$P_{go} = \frac{338}{15000 + 338 - 350} \times 760 \quad \text{mmHg}$$

$$P_{go} = 17.14 \text{ mmHg}$$

Assume mean gas phase partial pressure $\bar{P}_g$ in the gas path to be given by the arithmetic mean of inlet and outlet values, thus:

$$\bar{P}_g \simeq 8.5 \text{ mmHg}$$

E.4 To calculate z*

At Q_B = 6 ℓ/min

Given $$z^* = \frac{4\ WD_1NL}{3\ Q_B a} = \frac{2\ D_1\ A}{3\ Q_B\ a} \quad .$$

Therefore

$$z^* = \frac{2 \times 1.6 \times 10^{-5} \times 2.25 \times 10^{-4} \times 60}{3 \times 6000 \times 1.866 \times 10^{-2}}$$

$$\underline{z^* = 0.129}$$

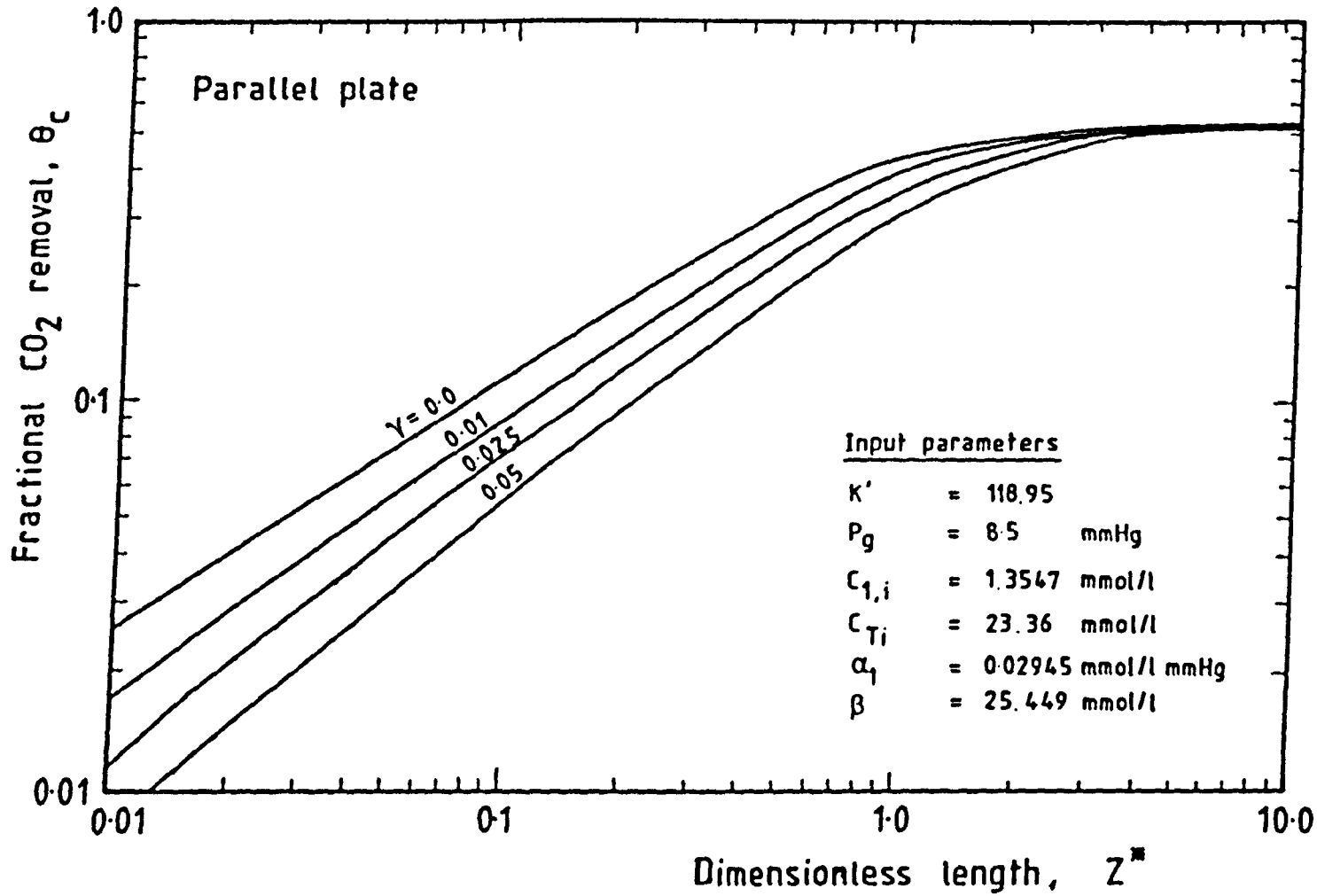
Parallel plate
Fractional CO_2 removal, θ_c
1·0
0·1
0·01
0·01
0·1
1·0
10·0
Dimensionless length, Z^*
Y= 0·0
0·01
0·025
0·05
Input parameters
K' = 118.95
P_g = 8·5 mmHg
$C_{1,i}$ = 1.3547 mmol/l
C_{Ti} = 23.36 mmol/l
α_1 = 0·02945 mmol/l mmHg
β = 25.449 mmol/l

Figure E.1

E.5 Input parameters for TMO theory

Specified		Derived	
C_{Ti}	: 23.36 mmol/ℓ	H	: 36%
$pCO_{2,in}$	: 46.0 mmHg	β	: 25.449 mmol/ℓ(T=37°C)
C_{Hb}	: 12.0 g%	K'	: 118.95
D_2/D_1	: 0.6	α_l	: 0.02945 mmol/ℓ.mmHg
γ	: 0.0, 0.005, 0.01, 0.025, 0.05	$C_{l,i}$	: 1.3547 mmol/ℓ
P_g	: 8.5 mmHg		

Figure E.1 shows the graphical output of θ_c as a function of z^* at various γ values.

At Q_B = 6 l/min the corresponding θ_c and z^* is respectively 0.108 and 0.13. This coincides with a dimensionless wall resistance, γ of 0.01.

E.6 Theory prediction

Assuming γ = 0.01 and P_g = 8.5 mmHg and equation 3.28

$$\dot{V}_{CO_2} = Q_B \, \theta_c \, C_{Ti} \qquad (3.28)$$

For specified Q_B and hence z^*, θ_c may be obtained and hence $\dot{V}_{CO_2}$ for specified C_{Ti}.

Note: 1 mole of CO_2 at STPD occupies 22.26 litres

sample calculation

At Q_B = 3.0 ℓ/min, z^* = 0.26 and θ_c = 0.19

C_{Ti} = 23.36 mmol/ℓ (= 52 ml(STPD)/100 ml).

$$\dot{V}_{CO_2} = 0.19 \times (23.36 \times 22.26) \times 3.0$$

$$= 288.6 \text{ ml(STPD)/min.}$$

Table E.1 - The $\dot{V}_{CO_2}$ theory predictions at different Q_B.

Q_B ℓ/min	z^*	θ_c	$\dot{V}_{CO_2}$ ml(STPD)/min
0.25	3.12	0.50	65.0
0.50	1.56	0.45	117.0
1.0	0.78	0.36	187.2
1.5	0.52	0.28	218.4
3.0	0.26	0.19	288.6
6.0	0.13	0.11	338.0

APPENDIX F

EXPERIMENTAL DATA FOR HOLLOW FIBRE MODULES

Test no.1

Sample	Q_B cm^3/s	C_{Ti} mmol/ℓ (1)	(2)	(3)	C_{To} mmol/ℓ (1)	(2)	(3)	$\bar{C}_{To}$ mmol/ℓ	θ_c	Z*
Start										
1	0.222	23.4			20.0	19.4	19.7	19.7	0.079	0.090
2	0.179	21.1			18.3	18.0	17.7	18.0	0.159	0.111
3	0.130	20.5			17.5	18.4	18.3	18.1	0.154	0.153
4	0.103	20.7			19.1	19.2	19.1	19.1	0.107	0.193
End										

$\bar{C}_{Ti}$ = 21.4

Barometric pressure : 756 mmHg
No. of tubes, N : 33
Tube length, L : 24 cm
Inlet pCO_2 : 45.8 mmHg
Hb content : 12.4 g%
O_2 saturation : 64.3 %
Hct : 36.5 %

Test no.2

Sample	Q_B cm^3/s	C_{Ti} mmol/ℓ (1)	(2)	(3)	C_{To} mmol/ℓ (1)	(2)	(3)	mmol/ℓ	θ_c	Z*
Start		19.7	19.6	19.8						
1	0.0462				13.0	12.5	11.9	12.5	0.387	0.888
2	0.0174				10.1	10.1	10.0	10.1	0.505	2.356
3	0.0086				7.8	7.7	7.9	7.8	0.618	4.767
End		21.1	21.0	21.2						

$\bar{C}_{Ti}$ = 20.4

Barometric pressure : 737 mmHg
No. of tubes, N : 68
Tube length, L : 24 cm
Inlet pCO_2 : 48.0 mmHg
Hb content : 12.2 g%
O_2 saturation : 58.7 %
Hct : 34.7 %

Test no.3

Sample	Q_B cm^3/s	C_{Ti} mmol/ℓ (1)	(2)	(3)	C_{To} mmol/ℓ (1)	(2)	(3)	$\bar{C}_{To}$ mmol/ℓ	θ_c	Z*
Start		21.1	21.3	21.4						
1	0.0449				14.6	14.8	14.7	14.7	0.307	0.940
2	0.0172				9.5	9.8	9.7	9.7	0.542	2.455
3	0.0930				15.2	15.7	15.7	15.5	0.269	0.454
End		21.2	21.2	20.9						

$\bar{C}_{Ti}$ = 21.2

Barometric pressure : 735 mmHg
No. of tubes, N : 70
Tube length, L : 24 cm

Inlet pCO_2 : 45.0 mmHg
Hb content : 11.7 g%
O_2 saturation : 66.2 %
Hct : 33 %

Test no.3 continued

Sample	Q_B cm^3/s	C_{Ti} mmol/ℓ (1)	(2)	(3)	C_{To} mmol/ℓ (1)	(2)	(3)	$\bar{C}_{To}$ mmol/ℓ	θ_c	Z*
Start		18.1	17.8	17.9						
1	0.0268				10.6	10.6	10.4	10.5	0.413	1.575
2	0.0086				8.2	8.2	8.1	8.2	0.542	4.910
3	0.0678				10.6	10.9	10.2	10.6	0.408	0.623
End		17.5	18.0	18.0						

$\bar{C}_{Ti}$ = 17.9

Barometric pressure : 735 mmHg
No. of tubes, N : 70
Tube length, L : 24 cm

Inlet pCO_2 : 45.0 mmHg
Hb content : 11.7 g%
O_2 saturation : 66.2 %
Hct : 33 %

Test no.4

Sample	Q_B cm^3/s	C_{Ti} mmol/ℓ (1)	(2)	(3)	C_{To} mmol/ℓ (1)	(2)	(3)	$\bar{C}_{To}$ mmol/ℓ	θ_c	Z*
Start		19.5	19.3	19.0						
1	0.0459				15.6	15.5	15.5	15.5	0.180	0.460
2	0.0182				14.0	14.3	14.4	14.2	0.249	-
3	0.0089				13.9	13.7	13.3	13.6	0.280	1.084†
End		18.6	18.4	18.6						

$\bar{C}_{Ti}$ = 18.9

Barometric pressure : 734 mmHg
No. of tubes, N : 35
Tube length, L : 24 cm

Inlet pCO_2 : 43.0 mmHg
Hb content : 11.8 g%
O_2 saturation : 68.8 %
Hct : 35 %

†N = 16 (19 tubes were blocked at the end of the experiment).

Test no.5

Sample	Q_B cm^3/s	C_{Ti} mmol/ℓ (1)	(2)	(3)	C_{To} mmol/ℓ (1)	(2)	(3)	$\bar{C}_{To}$ mmol/ℓ	θ_c	Z*
Start										
1	0.137	21.2			16.9	16.9	15.9	16.6	0.206	0.308
2	0.087	19.6			16.0	15.5	15.8	15.8	0.244	0.485
3	0.024	21.5			14.8	14.1	13.9	14.3	0.316	1.760
4	0.180	21.1			16.1	16.8	16.8	16.6	0.206	0.234
End										

$\bar{C}_{Ti}$ = 20.9

Barometric pressure : 755 mmHg
No. of tubes, N : 70
Tube length, L : 24 cm

Inlet pCO_2 : 46.4 mmHg
Hb content : 11.9 g%
O_2 saturation : 61.5 %
Hct : 35 %

CAPIOX II Model	Q_B cm^3/s	inlet pCO_2 mmHg	$\bar{C}_{Ti}$ mmol/l	$\bar{C}_{To}$ mmol/l	N	L cm	θ_c	Z*	Reference [+]
1.6 m^2	8.3	46.5	20.0	12.7	2×10^4	13	0.365	0.787	Test L19
	8.3	40.0	19.0	12.7	2×10^4	13	0.326	0.787	Test L19
3.3 m^2	8.3	44.8	17.8	8.3	3.8×10^4	14	0.534	1.611	Test L22
	8.3	53.7	18.0	7.5	3.8×10^4	14	0.583	1.611	Test L22
	25.0	46.2	19.9	13.8	3.8×10^4	14	0.307	0.535	Test L26
	25.0	45.2	20.1	14.1	2.8×10^4	14	0.299	0.535	Test L26

[+]Appendix D - Corresponding to hollow fibre modules input conditions.

APPENDIX G

EXPERIMENTAL DATA FOR MEMBRANE EVALUATION

A least squares program using the BBC microcomputer model B was obtained to analyse the experimental data from the membrane evaluations described in chapter 5. The program computes the best straight line fit for the CO_2 content versus time plot. The gradient of the line is used to calculate G_{CO_2} from equation 5.8 (Chapter 5):

$$G_{CO_2} = \text{gradient } \frac{\text{mmol}/\ell}{\text{min}} \times \frac{22.26 \text{ cm}^3 \text{ (STPD)/mmol} \times 1.0\ell}{60 \text{ s/min} \times 41.8 \text{ cm}^2 \times P_{ATM}\text{cmHg}}$$

$$= \frac{\text{cm}^3\text{(STPD)}}{\text{cm}^2 \text{ s cmHg}}$$

The computer program and the results of the membrane evaluations are shown.

```
 LIST
 10 REM linear regressions
 20 ON ERROR @%=&A0A:PRINT:REPORT:PRINT" in line ";ERL:VDU3:END
 30 MODE 3:REM INPUT''"Decimal places", dp
 40 @%=&A0A
 50 MODE 3:PRINT''"1: PRINTER ON"'"2: PRINTER OFF"
 60 REPEAT:INPUT prin:UNTIL prin=1 OR prin=2
 70 IF prin=2 THEN GOTO 180
 80 PRINT''"1. DIABLO"'"2. EPSON"
 90 REPEAT:INPUT prin:UNTIL prin=1 OR prin=2
100 VDU2
110 IF prin=1 GOTO 150
120 *FX5,0
130 *FX6,10
140 GOTO 180
150 *FX 5,2
160 *FX8,3
170 *FX6,0
180 READ NUM%
190 DIM X(NUM%),Y(NUM%)
200 PRINT''SPC16"#"SPC15"X"SPC16"Y"
210 PRINT
220 FOR I%=1 TO NUM%
230 READ X(I%)
240 NEXT
250 FOR I%=1 TO NUM%
260 READ Y(I%)
270 @%=&A11:PRINT I%;:@%=&20111:PRINT X(I%),Y(I%)
280 NEXT
290 REM @%=&20011+dp"&100
300 PROC_LINREG(NUM%)
310 VDU3
320 END
330
340 DEF PROC_LINREG(NUM%)
350 REM linear regression of X() on Y()
360 SUMX=0:SUMXSQ=0:SUMY=0:SUMYSQ=0:SUMCROSS=0
370 LOCAL I%
380 FOR I%=1 TO NUM%
390 SUMX=SUMX+X(I%)
400 SUMXSQ=SUMXSQ+X(I%)*X(I%)
410 SUMY=SUMY+Y(I%)
420 SUMYSQ=SUMYSQ+Y(I%)*Y(I%)
430 SUMCROSS=SUMCROSS+X(I%)*Y(I%)
440 NEXT
450 SX=SUMXSQ-SUMX*SUMX/NUM%
460 SY=SUMYSQ-SUMY*SUMY/NUM%
470 SC=SUMCROSS-SUMX*SUMY/NUM%
480 GRADIENT=SC/SX
490 INCEPT=SUMY/NUM%-GRADIENT*SUMX/NUM%
500 CORR=SC/SQR(SX*SY)
510 YINTER=-INCEPT/GRADIENT
520 PRINT''SPC10"gradient"SPC8"X-intercept"SPC6"Y-intercept"SPC5"correlation"
530 @%=&20311:PRINT GRADIENT,INCEPT,YINTER;:@%=&20411:PRINT CORR''
540 INPUT TAB(26)"TEST NO.  = "T
550 INPUT TAB(26)"FLOW RATE = "F
550 INPUT TAB(26)"FLOW RATE = "F
560 INPUT TAB(26)"NaOH CONC = "C
570 INPUT TAB(26)"PRESSURE  = "P
580 G = GRADIENT*1.0*22.26/(60.0*41.8*P)
590 @%=&10411:PRINT TAB(18);"GAS TRANSMISSION  = "; G
600 @%=&A0A
610 ENDPROC
620 REM DATA NUM%,X()'s,Y()'s
630 DATA 12,0,0.5,2,4,6,8,10,12,14,16,18,20
640 DATA 1.2,5,17.8,35.3,51.1,67.5,84.8,99.8,115.5,130.9,145.4,159.2
>
```

TEST NO. 1 - 75 CELGARD 2402

#	X	Y
1	0.0	0.2
2	2.0	8.4
3	4.0	12.8
4	6.0	16.8
5	8.0	21.1
6	10.0	24.6
7	12.0	28.2
8	14.0	31.5
9	16.0	33.4
10	18.0	36.6
11	20.0	39.6

gradient	X-intercept	Y-intercept	correlation
1.855	4.468	-2.409	0.9885

TEST NO. = 1
FLOW RATE = 0.5
NaOH CONC = 0.1
PRESSURE = 71.0
GAS TRANSMISSION = 2.319E-4

#	X	Y
1	0.0	0.6
2	2.0	8.7
3	4.0	13.3
4	6.0	17.1
5	8.0	20.2
6	10.0	23.5
7	12.0	26.5
8	14.0	29.2
9	16.0	32.0
10	18.0	34.2
11	20.0	37.1

gradient	X-intercept	Y-intercept	correlation
1.687	5.168	-3.068	0.9855

TEST NO. = 2
FLOW RATE = 0.5
NaOH CONC = 0.1
PRESSURE = 71.0
GAS TRANSMISSION = 2.109E-4

#	X	Y
1	0.0	3.2
2	2.0	23.4
3	4.0	34.1
4	8.0	55.0
5	10.0	65.8

gradient	X-intercept	Y-intercept	correlation
5.959	7.695	-1.291	0.9912

TEST NO. = 3
FLOW RATE = 0.5
NaOH CONC = 0.5
PRESSURE = 71.0
GAS TRANSMISSION = 7.450E-4

#	X	Y
1	0.0	2.0
2	2.0	26.2
3	4.0	39.3
4	6.0	52.0
5	8.0	63.8
6	10.0	74.8
7	12.0	84.2
8	14.0	95.1
9	16.0	104.4

gradient	X-intercept	Y-intercept	correlation
6.074	11.607	-1.911	0.9907

TEST NO. = 4
FLOW RATE = 0.5
NaOH CONC = 0.5
PRESSURE = 71.0
GAS TRANSMISSION = 7.593E-4

#	X	Y
1	0.0	2.0
2	2.0	21.1
3	4.0	32.9
4	6.0	45.0
5	8.0	56.2
6	10.0	67.3
7	12.0	76.1
8	14.0	86.5
9	16.0	96.8

gradient	X-intercept	Y-intercept	correlation
5.701	8.160	-1.431	0.9955

TEST NO. = 5
FLOW RATE = 0.5
NaOH CONC = 0.5
PRESSURE = 71.0
GAS TRANSMISSION = 7.127E-4

#	X	Y
1	0.0	4.2
2	2.0	23.1
3	4.0	35.3
4	6.0	47.7
5	8.0	60.2
6	10.0	70.4
7	12.0	82.8
8	14.0	93.5
9	16.0	105.1

gradient	X-intercept	Y-intercept	correlation
6.104	9.200	-1.507	0.9976

TEST NO. = 7
FLOW RATE = 0.5
NaOH CONC = 1.0
PRESSURE = 71.0
GAS TRANSMISSION = 7.631E-4

#	X	Y
1	0.0	7.2
2	2.0	29.1
3	4.0	41.2
4	6.0	53.3
5	8.0	65.4
6	10.0	76.4
7	12.0	87.6
8	14.0	99.1
9	16.0	111.7

gradient	X-intercept	Y-intercept	correlation
6.199	13.851	-2.234	0.9961

TEST NO. = 6
FLOW RATE = 0.5
NaOH CONC = 1.0
PRESSURE = 71.0
GAS TRANSMISSION = 7.749E-4

#	X	Y
1	0.0	1.6
2	4.0	22.5
3	6.0	35.8
4	8.0	52.4
5	10.0	62.2
6	14.0	76.9

gradient	X-intercept	Y-intercept	correlation
5.617	2.581	-0.460	0.9918

TEST NO. = 8
FLOW RATE = 0.5
NaOH CONC = 1.5
PRESSURE = 70.8
GAS TRANSMISSION = 7.041E-4

#	X	Y
1	0.0	2.0
2	4.0	27.0
3	6.0	37.1
4	8.0	52.4
5	10.0	64.0
6	16.0	95.2
7	18.0	112.7

gradient	X-intercept	Y-intercept	correlation
6.011	2.534	-0.422	0.9987

TEST NO. = 9
FLOW RATE = 0.5
NaOH CONC = 1.5
PRESSURE = 70.5
GAS TRANSMISSION = 7.567E-4

#	X	Y
1	0.0	0.9
2	0.5	3.1
3	2.0	14.7
4	4.0	29.7
5	6.0	45.3
6	8.0	59.5
7	10.0	74.6
8	12.0	86.8
9	14.0	101.2
10	16.0	113.3
11	18.0	126.1
12	20.0	138.4

gradient	X-intercept	Y-intercept	correlation
6.973	1.927	-0.276	0.9993

TEST NO. = 10
FLOW RATE = 0.5
NaOH CONC = 1.0
PRESSURE = 70.5
GAS TRANSMISSION = 8.778E-4

#	X	Y
1	0.0	1.8
2	0.5	3.9
3	2.0	13.8
4	4.0	27.6
5	6.0	41.3
6	8.0	54.1
7	10.0	67.7
8	12.0	80.0
9	14.0	92.2
10	16.0	104.4

gradient	X-intercept	Y-intercept	correlation
6.501	1.545	-0.238	0.9998

TEST NO. = 11
FLOW RATE = 0.5
NaOH CONC = 1.0
PRESSURE = 70.5
GAS TRANSMISSION = 8.185E-4

#	X	Y
1	0.0	4.1
2	0.5	4.9
3	2.0	13.0
4	4.0	24.4
5	6.0	35.1
6	8.0	46.1
7	10.0	56.7
8	12.0	67.3
9	14.0	78.0
10	16.0	87.9
11	18.0	99.5
12	20.0	109.7

gradient	X-intercept	Y-intercept	correlation
5.342	3.031	-0.567	0.9999

TEST NO. = 12
FLOW RATE = 0.5
NaOH CONC = 1.0
PRESSURE = 70.9
GAS TRANSMISSION = 6.688E-4

#	X	Y
1	0.0	2.2
2	0.5	3.3
3	2.0	11.2
4	4.0	23.0
5	6.0	33.8
6	8.0	44.1
7	10.0	55.4
8	12.0	65.9
9	14.0	76.5
10	16.0	86.4
11	18.0	97.1
12	20.0	107.3

gradient	X-intercept	Y-intercept	correlation
5.321	1.517	-0.285	0.9999

TEST NO. = 13
FLOW RATE = 0.5
NaOH CONC = 1.0
PRESSURE = 70.9
GAS TRANSMISSION = 6.661E-4

#	X	Y
1	0.0	1.4
2	0.5	1.1
3	2.0	1.4
4	4.0	1.5
5	6.0	1.4
6	8.0	1.4
7	10.0	1.3

gradient	X-intercept	Y-intercept	correlation
0.006	1.329	-208.436	0.1913

TEST NO. = 14 - CONTROL
FLOW RATE = 0.5
NaOH CONC = 1.0
PRESSURE = 68.9
GAS TRANSMISSION = 8.216E-7

#	X	Y
1	0.0	1.6
2	0.5	2.6
3	2.0	10.3
4	4.0	23.9
5	6.0	36.2
6	8.0	47.4
7	10.0	60.3
8	12.0	72.0
9	14.0	84.0
10	16.0	94.5
11	18.0	106.2
12	20.0	119.6

gradient	X-intercept	Y-intercept	correlation
5.946	0.135	-0.023	0.9998

TEST NO. = 15
FLOW RATE = 0.5
NaOH CONC = 1.0
PRESSURE = 68.9
GAS TRANSMISSION = 7.659E-4

#	X	Y
1	0.0	2.0
2	0.5	3.5
3	2.0	12.1
4	4.0	23.6
5	6.0	35.2
6	8.0	46.5
7	10.0	57.9
8	12.0	68.5
9	14.0	79.9
10	16.0	89.9
11	18.0	99.7
12	20.0	109.9

gradient	X-intercept	Y-intercept	correlation
5.481	1.924	-0.351	0.9997

TEST NO. = 16
FLOW RATE = 0.5
NaOH CONC = 1.0
PRESSURE = 67.4
GAS TRANSMISSION = 7.217E-4

#	X	Y
1	0.0	1.6
2	0.5	3.1
3	2.0	11.4
4	4.0	22.6
5	6.0	33.1
6	8.0	44.4
7	10.0	54.8
8	12.0	65.3
9	14.0	76.5
10	16.0	85.6
11	18.0	96.3
12	20.0	102.7

gradient	X-intercept	Y-intercept	correlation
5.217	1.743	-0.334	0.9993

TEST NO. = 17
FLOW RATE = 0.5
NaOH CONC = 1.0
PRESSURE = 67.4
GAS TRANSMISSION = 6.870E-4

#	X	Y
1	0.0	2.3
2	0.5	5.0
3	2.0	15.2
4	4.0	28.3
5	6.0	41.8
6	8.0	54.6
7	10.0	68.1
8	12.0	79.3
9	14.0	93.3
10	16.0	106.7
11	18.0	117.6
12	20.0	130.7

gradient	X-intercept	Y-intercept	correlation
6.446	2.549	-0.395	0.9999

TEST NO. = 18
FLOW RATE = 1.0
NaOH CONC = 1.0
PRESSURE = 67.4
GAS TRANSMISSION = 8.489E-4

#	X	Y
1	0.0	1.8
2	0.5	5.0
3	2.0	16.7
4	4.0	32.0
5	6.0	47.3
6	8.0	62.5
7	10.0	78.1
8	12.0	92.0
9	14.0	107.4
10	16.0	122.7
11	18.0	135.7
12	20.0	148.1

gradient	X-intercept	Y-intercept	correlation
7.429	2.364	-0.318	0.9997

TEST NO. = 19
FLOW RATE = 1.5
NaOH CONC = 1.0
PRESSURE = 67.4
GAS TRANSMISSION = 9.783E-4

#	X	Y
1	0.0	2.3
2	0.5	5.3
3	2.0	17.5
4	4.0	33.7
5	6.0	49.6
6	8.0	65.0
7	10.0	82.3
8	12.0	97.5
9	14.0	112.4
10	16.0	126.7
11	18.0	142.6
12	20.0	159.2

gradient	X-intercept	Y-intercept	correlation
7.846	2.257	-0.288	0.9999

TEST NO. = 20
FLOW RATE = 2.0
NaOH CONC = 1.0
PRESSURE = 69.8
GAS TRANSMISSION = 9.977E-4

#	X	Y
1	0.0	1.4
2	0.5	5.5
3	2.0	17.0
4	4.0	34.0
5	6.0	50.4
6	8.0	67.3
7	10.0	84.5
8	12.0	98.6
9	14.0	116.3
10	16.0	127.7
11	18.0	141.7
12	20.0	154.2

gradient	X-intercept	Y-intercept	correlation
7.792	3.131	-0.402	0.9989

TEST NO. = 21
FLOW RATE = 3.0
NaOH CONC = 1.0
PRESSURE = 70.8
GAS TRANSMISSION = 9.768E-4

#	X	Y
1	0.0	0.6
2	0.5	4.2
3	2.0	17.1
4	4.0	34.5
5	6.0	50.7
6	8.0	68.2
7	10.0	84.3
8	12.0	102.0
9	14.0	118.1
10	16.0	130.5
11	18.0	144.5
12	20.0	158.5

gradient	X-intercept	Y-intercept	correlation
8.024	2.211	-0.276	0.9991

TEST NO. = 23
FLOW RATE = 2.5
NaOH CONC = 1.0
PRESSURE = 71.3
GAS TRANSMISSION = 9.989E-4

#	X	Y
1	0.0	1.3
2	0.5	4.4
3	2.0	17.2
4	4.0	33.9
5	8.0	66.6
6	10.0	85.6
7	12.0	102.2
8	14.0	117.8
9	16.0	132.0
10	18.0	148.1

gradient	X-intercept	Y-intercept	correlation
8.258	1.129	-0.137	0.9997

TEST NO. = 22
FLOW RATE = 2.5
NaOH CONC = 1.0
PRESSURE = 70.8
GAS TRANSMISSION = 1.035E-3

#	X	Y
1	0.0	1.7
2	0.5	5.0
3	2.0	17.6
4	4.0	35.1
5	6.0	52.3
6	8.0	68.8
7	10.0	85.6
8	12.0	100.3
9	14.0	117.9
10	16.0	132.9
11	18.0	147.9
12	20.0	159.7

gradient	X-intercept	Y-intercept	correlation
8.072	2.741	-0.340	0.9994

TEST NO. = 24
FLOW RATE = 3.0
NaOH CONC = 1.0
PRESSURE = 71.3
GAS TRANSMISSION = 1.005E-3

#	X	Y
1	0.0	2.3
2	2.0	19.4
3	4.0	37.7
4	6.0	56.4
5	8.0	74.7
6	10.0	93.7
7	12.0	111.0
8	14.0	127.4
9	16.0	144.0
10	18.0	161.8

gradient	X-intercept	Y-intercept	correlation
8.906	2.685	-0.302	0.9998

TEST NO. = 25
FLOW RATE = 3.5
NaOH CONC = 1.0
PRESSURE = 71.3
GAS TRANSMISSION = 1.109E-3

#	X	Y
1	0.0	2.4
2	0.5	6.2
3	2.0	21.0
4	4.0	40.6
5	6.0	61.1
6	10.0	100.9
7	12.0	119.5
8	14.0	139.4
9	16.0	156.6

gradient	X-intercept	Y-intercept	correlation
9.767	1.969	-0.202	0.9999

TEST NO. = 26
FLOW RATE = 4.0
NaOH CONC = 1.0
PRESSURE = 71.3
GAS TRANSMISSION = 1.216E-3

#	X	Y
1	0.0	1.8
2	0.5	4.8
3	2.0	18.0
4	4.0	35.1
5	6.0	51.9
6	8.0	69.5
7	10.0	85.3
8	12.0	103.0
9	14.0	118.3
10	16.0	133.7
11	18.0	151.9

gradient	X-intercept	Y-intercept	correlation
8.347	1.629	-0.195	0.9999

TEST NO. = 27
FLOW RATE = 3.5
NaOH CONC = 1.0
PRESSURE = 71.1
GAS TRANSMISSION = 1.042E-3

#	X	Y
1	0.0	1.3
2	0.5	7.3
3	2.0	20.8
4	4.0	40.4
5	6.0	60.2
6	8.0	77.0
7	10.0	97.7
8	12.0	115.6
9	14.0	135.8
10	18.0	165.6

gradient	X-intercept	Y-intercept	correlation
9.275	3.071	-0.331	0.9993

TEST NO. = 28
FLOW RATE = 4.0
NaOH CONC = 1.0
PRESSURE = 71.1
GAS TRANSMISSION = 1.158E-3

#	X	Y
1	0.0	1.0
2	0.5	1.7
3	2.0	4.8
4	4.0	9.0
5	6.0	13.5
6	8.0	17.9
7	10.0	22.0
8	12.0	26.7
9	14.0	31.3
10	16.0	35.6
11	18.0	40.2
12	20.0	43.2

gradient	X-intercept	Y-intercept	correlation
2.167	0.618	-0.285	0.9997

TEST NO. = 29
FLOW RATE = 3.5
NaOH CONC = 1.0
PRESSURE = 67.6
GAS TRANSMISSION = 8.243E-4

#	X	Y
1	0.0	1.2
2	0.5	2.2
3	2.0	5.4
4	4.0	9.8
5	6.0	14.0
6	8.0	18.2
7	10.0	22.9
8	12.0	26.7
9	14.0	31.1
10	16.0	35.5
11	18.0	39.7
12	20.0	43.8

gradient	X-intercept	Y-intercept	correlation
2.138	1.191	-0.557	1.0000

TEST NO. = 30
FLOW RATE = 3.5
NaOH CONC = 1.0
PRESSURE = 67.6
GAS TRANSMISSION = 8.130E-4

#	X	Y
1	0.0	1.1
2	0.5	2.2
3	2.0	5.6
4	4.0	10.3
5	6.0	15.7
6	8.0	20.9
7	10.0	25.1
8	12.0	30.2
9	14.0	34.6
10	16.0	40.0
11	18.0	44.3

gradient	X-intercept	Y-intercept	correlation
2.421	0.993	-0.410	0.9998

TEST NO. = 31
FLOW RATE = 4.0
NaOH CONC = 1.0
PRESSURE = 67.6
GAS TRANSMISSION = 9.207E-4

#	X	Y
1	0.0	1.6
2	0.5	2.2
3	2.0	5.8
4	4.0	11.3
5	6.0	16.3
6	8.0	22.2
7	10.0	27.8
8	12.0	32.4
9	14.0	37.9
10	16.0	42.7
11	18.0	49.7
12	20.0	53.8

gradient	X-intercept	Y-intercept	correlation
2.655	0.859	-0.323	0.9996

TEST NO. = 32
FLOW RATE = 4.0
NaOH CONC = 1.0
PRESSURE = 68.6
GAS TRANSMISSION = 9.951E-4

#	X	Y
1	0.0	0.6
2	0.5	2.3
3	2.0	7.0
4	4.0	12.9
5	6.0	18.8
6	8.0	24.6
7	10.0	31.2
8	12.0	37.7
9	14.0	43.3
10	16.0	48.4
11	18.0	55.1
12	20.0	60.9

gradient	X-intercept	Y-intercept	correlation
3.012	0.830	-0.276	0.9999

TEST NO. = 33
FLOW RATE = 3.0
NaOH CONC = 1.0
PRESSURE = 70.1
GAS TRANSMISSION = 1.105E-3

#	X	Y
1	0.0	0.9
2	0.5	2.8
3	2.0	6.8
4	4.0	13.0
5	6.0	19.3
6	8.0	25.2
7	10.0	31.5
8	12.0	37.3
9	14.0	43.9
10	16.0	49.9
11	18.0	55.1
12	20.0	62.4

gradient	X-intercept	Y-intercept	correlation
3.050	0.922	-0.302	0.9999

TEST NO. = 35
FLOW RATE = 3.5
NaOH CONC = 1.0
PRESSURE = 70.1
GAS TRANSMISSION = 1.119E-3

#	X	Y
1	0.0	1.4
2	0.5	2.3
3	2.0	6.3
4	4.0	11.7
5	6.0	17.6
6	8.0	22.7
7	10.0	29.0
8	12.0	33.6
9	14.0	40.6
10	16.0	44.7
11	18.0	51.4
12	20.0	56.7

gradient	X-intercept	Y-intercept	correlation
2.784	0.860	-0.309	0.9997

TEST NO. = 34
FLOW RATE = 3.0
NaOH CONC = 1.0
PRESSURE = 70.1
GAS TRANSMISSION = 1.021E-3

#	X	Y
1	0.0	1.2
2	0.5	2.6
3	2.0	6.9
4	4.0	13.5
5	6.0	19.7
6	8.0	26.2
7	10.0	31.8
8	14.0	44.7
9	16.0	51.9
10	18.0	57.0
11	20.0	63.4

gradient	X-intercept	Y-intercept	correlation
3.130	0.964	-0.308	0.9999

TEST NO. = 36
FLOW RATE = 3.5
NaOH CONC = 1.0
PRESSURE = 70.1
GAS TRANSMISSION = 1.148E-3

#	X	Y
1	0.0	1.2
2	0.5	2.0
3	2.0	6.6
4	4.0	12.5
5	6.0	18.9
6	8.0	25.0
7	10.0	30.3
8	12.0	36.8
9	14.0	42.6
10	16.0	48.5
11	18.0	53.9
12	20.0	60.6

gradient	X-intercept	Y-intercept	correlation
2.977	0.830	-0.279	0.9999

TEST NO. = 37
FLOW RATE = 4.0
NaOH CONC = 1.0
PRESSURE = 70.1
GAS TRANSMISSION = 1.092E-3

#	X	Y
1	0.0	1.4
2	0.5	2.7
3	2.0	7.3
4	4.0	13.5
5	6.0	19.6
6	8.0	25.5
7	10.0	31.9
8	12.0	37.6
9	14.0	43.4
10	16.0	50.1
11	18.0	55.6
12	20.0	61.7

gradient	X-intercept	Y-intercept	correlation
3.023	1.357	-0.449	1.0000

TEST NO. = 38
FLOW RATE = 4.0
NaOH CONC = 1.0
PRESSURE = 70.1
GAS TRANSMISSION = 1.109E-3

#	X	Y
1	0.0	1.1
2	0.5	5.6
3	2.0	18.6
4	4.0	37.0
5	6.0	54.2
6	8.0	70.2
7	10.0	88.2
8	12.0	104.6
9	14.0	119.9
10	16.0	136.4
11	18.0	150.7
12	20.0	163.4

gradient	X-intercept	Y-intercept	correlation
8.239	3.294	-0.400	0.9993

TEST NO. = 39
FLOW RATE = 3.5
NaOH CONC = 1.0
PRESSURE = 67.4
GAS TRANSMISSION = 1.085E-3

#	X	Y
1	0.0	1.1
2	0.5	5.3
3	2.0	18.7
4	4.0	39.0
5	6.0	55.5
6	8.0	74.3
7	10.0	93.1
8	12.0	112.4
9	14.0	124.9
10	16.0	142.0

gradient	X-intercept	Y-intercept	correlation
8.923	1.940	-0.217	0.9993

TEST NO. = 40
FLOW RATE = 3.5
NaOH CONC = 1.0
PRESSURE = 67.4
GAS TRANSMISSION = 1.175E-3

#	X	Y
1	0.0	1.1
2	0.5	5.2
3	2.0	19.0
4	4.0	38.5
5	6.0	57.4
6	8.0	75.6
7	10.0	93.0
8	12.0	111.6
9	14.0	127.7
10	16.0	145.6

gradient	X-intercept	Y-intercept	correlation
9.080	1.641	-0.181	0.9998

TEST NO. = 41
FLOW RATE = 3.5
NaOH CONC = 1.0
PRESSURE = 67.4
GAS TRANSMISSION = 1.196E-3

#	X	Y
1	0.0	1.3
2	0.5	6.1
3	2.0	20.7
4	4.0	40.9
5	6.0	59.3
6	8.0	78.4
7	10.0	98.1
8	12.0	116.6
9	14.0	132.5
10	16.0	151.0
11	18.0	165.0
12	20.0	173.7

gradient	X-intercept	Y-intercept	correlation
8.946	4.587	-0.513	0.9978

TEST NO. = 42
FLOW RATE = 3.5
NaOH CONC = 1.0
PRESSURE = 69.1
GAS TRANSMISSION = 1.149E-3

#	X	Y
1	0.0	1.3
2	0.5	5.2
3	2.0	18.7
4	4.0	37.9
5	6.0	54.1
6	8.0	72.6
7	10.0	89.8
8	12.0	104.9
9	14.0	122.4
10	16.0	141.7
11	18.0	155.5

gradient	X-intercept	Y-intercept	correlation
8.638	2.030	-0.235	0.9997

TEST NO. = 43
FLOW RATE = 3.5
NaOH CONC = 1.0
PRESSURE = 69.3
GAS TRANSMISSION = 1.106E-3

#	X	Y
1	0.0	1.2
2	0.5	6.0
3	2.0	21.1
4	4.0	41.1
5	6.0	62.0
6	8.0	82.3
7	10.0	99.5
8	12.0	119.6
9	14.0	135.1
10	16.0	154.0
11	18.0	175.4

gradient	X-intercept	Y-intercept	correlation
9.605	2.551	-0.266	0.9996

TEST NO. = 44
FLOW RATE = 3.5
NaOH CONC = 1.0
PRESSURE = 69.1
GAS TRANSMISSION = 1.234E-3

#	X	Y
1	0.0	1.3
2	0.5	5.3
3	2.0	17.8
4	4.0	35.7
5	6.0	52.5
6	8.0	70.3
7	10.0	87.5
8	12.0	104.3
9	14.0	120.8
10	16.0	135.9

gradient	X-intercept	Y-intercept	correlation
8.509	1.448	-0.170	0.9999

TEST NO. = 45
FLOW RATE = 3.5
NaOH CONC = 1.0
PRESSURE = 69.3
GAS TRANSMISSION = 1.090E-3

#	X	Y
1	0.0	1.3
2	0.5	5.3
3	2.0	19.4
4	4.0	39.1
5	6.0	59.0
6	8.0	77.8
7	10.0	97.3
8	12.0	117.4
9	14.0	136.0
10	16.0	152.1
11	18.0	163.3

gradient	X-intercept	Y-intercept	correlation
9.330	2.147	-0.230	0.9989

TEST NO. = 46
FLOW RATE = 3.5
NaOH CONC = 1.0
PRESSURE = 69.3
GAS TRANSMISSION = 1.195E-3

#	X	Y
1	0.0	1.3
2	0.5	2.8
3	2.0	17.9
4	4.0	37.5
5	6.0	58.8
6	8.0	77.7
7	10.0	96.2
8	12.0	114.1
9	14.0	132.9
10	16.0	145.8
11	18.0	168.3
12	20.0	178.9

gradient	X-intercept	Y-intercept	correlation
9.161	1.658	-0.181	0.9989

TEST NO. = 47
FLOW RATE = 4.0
NaOH CONC = 1.0
PRESSURE = 69.3
GAS TRANSMISSION = 1.173E-3

#	X	Y
1	0.0	1.5
2	0.5	6.3
3	2.0	21.7
4	4.0	43.9
5	6.0	65.2
6	8.0	85.6
7	10.0	106.2
8	12.0	129.0
9	14.0	144.5
10	16.0	161.6
11	18.0	177.3
12	20.0	187.9

gradient	X-intercept	Y-intercept	correlation
9.669	5.189	-0.537	0.9973

TEST NO. = 48
FLOW RATE = 3.0
NaOH CONC = 1.0
PRESSURE = 69.3
GAS TRANSMISSION = 1.238E-3

#	X	Y
1	0.0	1.7
2	0.5	6.0
3	2.0	20.3
4	4.0	40.8
5	6.0	60.1
6	8.0	78.0
7	10.0	97.0
8	12.0	115.8
9	14.0	132.8
10	16.0	151.1
11	18.0	166.9
12	20.0	183.7

gradient	X-intercept	Y-intercept	correlation
9.180	3.319	-0.362	0.9996

TEST NO. = 49
FLOW RATE = 3.0
NaOH CONC = 1.0
PRESSURE = 69.3
GAS TRANSMISSION = 1.176E-3

#	X	Y
1	0.0	1.4
2	0.5	6.0
3	2.0	21.5
4	4.0	42.1
5	6.0	63.3
6	8.0	84.1
7	10.0	103.9
8	12.0	123.9
9	14.0	140.3
10	16.0	156.3
11	18.0	179.9
12	20.0	194.7

gradient	X-intercept	Y-intercept	correlation
9.758	3.265	-0.335	0.9993

TEST NO. = 50
FLOW RATE = 3.0
NaOH CONC = 1.0
PRESSURE = 69.3
GAS TRANSMISSION = 1.250E-3

#	X	Y
1	0.0	2.2
2	0.5	5.5
3	2.0	20.7
4	4.0	39.5
5	6.0	59.4
6	8.0	77.2
7	10.0	96.4
8	12.0	115.1
9	14.0	134.9
10	16.0	147.9
11	18.0	164.2
12	20.0	179.2

gradient	X-intercept	Y-intercept	correlation
9.028	3.720	-0.412	0.9990

TEST NO. = 51
FLOW RATE = 2.5
NaOH CONC = 1.0
PRESSURE = 69.9
GAS TRANSMISSION = 1.146E-3

#	X	Y
1	0.0	1.5
2	0.5	6.3
3	2.0	21.5
4	4.0	43.0
5	6.0	63.7
6	8.0	84.3
7	10.0	103.0
8	12.0	122.1
9	14.0	141.1
10	16.0	164.0
11	18.0	172.7
12	20.0	191.6

gradient	X-intercept	Y-intercept	correlation
9.650	4.037	-0.418	0.9987

TEST NO. = 52
FLOW RATE = 2.5
NaOH CONC = 1.0
PRESSURE = 69.9
GAS TRANSMISSION = 1.225E-3

#	X	Y
1	0.0	1.2
2	0.5	6.2
3	2.0	22.3
4	4.0	43.9
5	6.0	65.8
6	8.0	86.8
7	10.0	108.9
8	12.0	130.0
9	14.0	149.7
10	16.0	169.0
11	18.0	189.9

gradient	X-intercept	Y-intercept	correlation
10.535	1.842	-0.175	0.9999

TEST NO. = 53
FLOW RATE = 2.5
NaOH CONC = 1.0
PRESSURE = 69.9
GAS TRANSMISSION = 1.338E-3

#	X	Y
1	0.0	2.0
2	0.5	5.6
3	2.0	19.6
4	4.0	36.8
5	6.0	54.5
6	8.0	72.3
7	10.0	89.8
8	12.0	108.7
9	14.0	125.5
10	16.0	141.8
11	18.0	157.0
12	20.0	171.0

gradient	X-intercept	Y-intercept	correlation
8.613	2.738	-0.318	0.9996

TEST NO. = 54
FLOW RATE = 2.0
NaOH CONC = 1.0
PRESSURE = 69.9
GAS TRANSMISSION = 1.094E-3

#	X	Y
1	0.0	1.2
2	0.5	4.9
3	2.0	19.1
4	4.0	38.3
5	6.0	58.3
6	8.0	76.8
7	10.0	93.9
8	12.0	112.6
9	14.0	130.3
10	16.0	148.0
11	18.0	163.4
12	20.0	177.6

gradient	X-intercept	Y-intercept	correlation
8.992	2.561	-0.285	0.9994

TEST NO. = 55
FLOW RATE = 2.0
NaOH CONC = 1.0
PRESSURE = 69.9
GAS TRANSMISSION = 1.142E-3

#	X	Y
1	0.0	1.5
2	0.5	5.6
3	2.0	19.5
4	4.0	39.4
5	6.0	59.0
6	8.0	77.8
7	10.0	98.3
8	12.0	115.9
9	14.0	135.0
10	16.0	151.5
11	18.0	169.3
12	20.0	184.1

gradient	X-intercept	Y-intercept	correlation
9.299	2.449	-0.263	0.9995

TEST NO. = 56
FLOW RATE = 4.0
NaOH CONC = 1.0
PRESSURE = 69.9
GAS TRANSMISSION = 1.181E-3

#	X	Y
1	0.0	1.7
2	0.5	6.8
3	2.0	24.1
4	4.0	44.9
5	6.0	68.5
6	8.0	91.0
7	10.0	110.8
8	12.0	130.7
9	14.0	151.1
10	16.0	168.7
11	18.0	186.3

gradient	X-intercept	Y-intercept	correlation
10.397	3.968	-0.382	0.9992

TEST NO. = 57
FLOW RATE = 4.0
NaOH CONC = 1.0
PRESSURE = 69.9
GAS TRANSMISSION = 1.320E-3

#	X	Y
1	0.0	1.3
2	0.5	5.7
3	2.0	20.5
4	4.0	41.9
5	6.0	60.6
6	8.0	80.7
7	10.0	99.5
8	12.0	118.0
9	14.0	135.3
10	16.0	152.9
11	18.0	169.2

gradient	X-intercept	Y-intercept	correlation
9.431	2.916	-0.309	0.9995

TEST NO. = 59
FLOW RATE = 4.0
NaOH CONC = 1.0
PRESSURE = 69.3
GAS TRANSMISSION = 1.208E-3

#	X	Y
1	0.0	2.6
2	0.5	7.1
3	2.0	21.5
4	4.0	41.8
5	6.0	61.7
6	8.0	80.7
7	10.0	101.4
8	12.0	119.8
9	14.0	137.4
10	16.0	153.1
11	18.0	172.5
12	20.0	187.8

gradient	X-intercept	Y-intercept	correlation
9.378	4.260	-0.454	0.9994

TEST NO. = 58
FLOW RATE = 4.0
NaOH CONC = 1.0
PRESSURE = 69.3
GAS TRANSMISSION = 1.201E-3

#	X	Y
1	0.0	0.5
2	0.5	5.3
3	2.0	20.2
4	4.0	38.9
5	6.0	58.4
6	8.0	77.8
7	10.0	96.2
8	12.0	116.0
9	14.0	133.8
10	16.0	152.4
11	20.0	184.5

gradient	X-intercept	Y-intercept	correlation
9.337	1.848	-0.198	0.9996

TEST NO. = 60
FLOW RATE = 2.0
NaOH CONC = 1.0
PRESSURE = 68.9
GAS TRANSMISSION = 1.203E-3

#	X	Y
1	0.0	1.7
2	0.5	5.1
3	2.0	20.4
4	4.0	40.9
5	6.0	61.4
6	8.0	78.1
7	10.0	99.9
8	12.0	115.7
9	14.0	135.0
10	16.0	152.1
11	18.0	168.7
12	20.0	174.2

gradient	X-intercept	Y-intercept	correlation
9.055	4.381	-0.484	0.9975

TEST NO. = 61
FLOW RATE = 2.5
NaOH CONC = 1.0
PRESSURE = 69.3
GAS TRANSMISSION = 1.160E-3

#	X	Y
1	0.0	1.0
2	0.5	5.2
3	2.0	19.9
4	4.0	39.5
5	6.0	58.2
6	8.0	76.2
7	10.0	97.1
8	12.0	115.1
9	14.0	131.0
10	16.0	147.3
11	18.0	163.8
12	20.0	177.1

gradient	X-intercept	Y-intercept	correlation
8.982	3.241	-0.361	0.9990

TEST NO. = 62
FLOW RATE = 3.0
NaOH CONC = 1.0
PRESSURE = 69.3
GAS TRANSMISSION = 1.150E-3

#	X	Y
1	0.0	1.0
2	0.5	4.9
3	2.0	18.2
4	4.0	37.1
5	6.0	55.6
6	8.0	73.2
7	10.0	92.3
8	12.0	110.5
9	14.0	126.5
10	16.0	145.0
11	18.0	160.5
12	20.0	175.9

gradient	X-intercept	Y-intercept	correlation
8.874	1.677	-0.189	0.9997

TEST NO. = 63
FLOW RATE = 4.0
NaOH CONC = 1.0
PRESSURE = 69.6
GAS TRANSMISSION = 1.132E-3

#	X	Y
1	0.0	1.3
2	0.5	4.6
3	2.0	18.6
4	4.0	37.0
5	6.0	54.3
6	8.0	74.4
7	10.0	89.9
8	12.0	109.3
9	14.0	126.1
10	16.0	142.2
11	18.0	156.2
12	20.0	174.5

gradient	X-intercept	Y-intercept	correlation
8.723	2.042	-0.234	0.9996

TEST NO. = 64
FLOW RATE = 2.0
NaOH CONC = 1.0
PRESSURE = 69.6
GAS TRANSMISSION = 1.112E-3

#	X	Y
1	0.0	1.0
2	0.5	4.8
3	2.0	18.5
4	4.0	36.2
5	6.0	54.0
6	8.0	71.9
7	10.0	88.4
8	12.0	106.7
9	14.0	121.9
10	16.0	138.8
11	18.0	153.8
12	20.0	171.0

gradient	X-intercept	Y-intercept	correlation
8.531	2.032	-0.238	0.9997

TEST NO. = 65
FLOW RATE = 2.5
NaOH CONC = 1.0
PRESSURE = 69.6
GAS TRANSMISSION = 1.088E-3

#	X	Y
1	0.0	2.4
2	0.5	6.9
3	2.0	22.1
4	4.0	42.2
5	6.0	61.2
6	8.0	80.8
7	10.0	100.5
8	12.0	117.6
9	14.0	137.2
10	16.0	152.7
11	18.0	170.4

gradient	X-intercept	Y-intercept	correlation
9.407	3.877	-0.412	0.9996

TEST NO. = 67
FLOW RATE = 4.0
NaOH CONC = 1.0
PRESSURE = 68.5
GAS TRANSMISSION = 1.219E-3

#	X	Y
1	0.0	1.2
2	0.5	4.6
3	2.0	17.9
4	4.0	36.6
5	6.0	54.0
6	8.0	71.2
7	10.0	88.3
8	12.0	104.9
9	14.0	123.6
10	16.0	139.9
11	18.0	155.6

gradient	X-intercept	Y-intercept	correlation
8.658	1.296	-0.150	0.9999

TEST NO. = 66
FLOW RATE = 3.0
NaOH CONC = 1.0
PRESSURE = 69.6
GAS TRANSMISSION = 1.104E-3

#	X	Y
1	0.0	1.2
2	0.5	5.0
3	2.0	17.8
4	4.0	35.3
5	6.0	51.1
6	8.0	67.5
7	10.0	84.8
8	12.0	99.8
9	14.0	115.5
10	16.0	130.9
11	18.0	145.4
12	20.0	159.2

gradient	X-intercept	Y-intercept	correlation
7.982	2.626	-0.329	0.9996

TEST NO. = 68
FLOW RATE = 2.0
NaOH CONC = 1.0
PRESSURE = 68.5
GAS TRANSMISSION = 1.034E-3

#	X	Y
1	0.0	1.4
2	0.5	5.3
3	2.0	18.0
4	4.0	34.8
5	6.0	50.9
6	8.0	68.9
7	10.0	84.5
8	12.0	100.5
9	14.0	115.4
10	16.0	133.7
11	18.0	145.7
12	20.0	158.5

gradient	X-intercept	Y-intercept	correlation
8.003	2.774	-0.347	0.9994

TEST NO. = 69
FLOW RATE = 2.5
NaOH CONC = 1.0
PRESSURE = 68.5
GAS TRANSMISSION = 1.037E-3

#	X	Y
1	0.0	1.0
2	0.5	5.7
3	2.0	20.6
4	4.0	39.6
5	6.0	58.8
6	8.0	79.1
7	10.0	97.7
8	12.0	118.4
9	14.0	134.6
10	16.0	152.2
11	18.0	173.6

gradient	X-intercept	Y-intercept	correlation
9.552	1.531	-0.160	0.9998

TEST NO. = 70
FLOW RATE = 3.0
NaOH CONC = 1.0
PRESSURE = 68.5
GAS TRANSMISSION = 1.238E-3

#	X	Y
1	0.0	1.3
2	0.5	5.3
3	2.0	20.1
4	4.0	39.4
5	6.0	60.5
6	8.0	79.0
7	10.0	97.1
8	12.0	116.3
9	14.0	136.0

gradient	X-intercept	Y-intercept	correlation
9.642	1.139	-0.118	0.9999

TEST NO. = 71
FLOW RATE = 4.0
NaOH CONC = 1.0
PRESSURE = 68.5
GAS TRANSMISSION = 1.249E-3

#	X	Y
1	0.0	1.5
2	0.5	4.5
3	2.0	17.2
4	4.0	35.0
5	6.0	52.8
6	8.0	70.8
7	10.0	88.4
8	12.0	105.9
9	14.0	122.6
10	16.0	141.1
11	18.0	159.5
12	20.0	172.2

gradient	X-intercept	Y-intercept	correlation
8.719	0.669	-0.077	0.9998

TEST NO. = 72
FLOW RATE = 2.0
NaOH CONC = 1.0
PRESSURE = 68.5
GAS TRANSMISSION = 1.130E-3

#	X	Y
1	0.0	1.8
2	0.5	5.5
3	2.0	19.9
4	4.0	40.2
5	6.0	58.7
6	8.0	78.9
7	10.0	97.4
8	12.0	115.2
9	14.0	132.0
10	16.0	150.3
11	18.0	165.8
12	20.0	180.2

gradient	X-intercept	Y-intercept	correlation
9.093	3.424	-0.377	0.9992

TEST NO. = 73
FLOW RATE = 2.5
NaOH CONC = 1.0
PRESSURE = 68.7
GAS TRANSMISSION = 1.175E-3

#	X	Y
1	0.0	1.6
2	0.5	5.4
3	2.0	19.6
4	4.0	38.8
5	6.0	57.1
6	8.0	74.7
7	10.0	93.8
8	12.0	111.4
9	14.0	128.0
10	16.0	144.7
11	18.0	161.3
12	20.0	177.1

gradient	X-intercept	Y-intercept	correlation
8.861	2.861	-0.323	0.9996

TEST NO. = 74
FLOW RATE = 3.0
NaOH CONC = 1.0
PRESSURE = 68.7
GAS TRANSMISSION = 1.145E-3

#	X	Y
1	0.0	1.6
2	0.5	4.8
3	2.0	17.7
4	4.0	35.8
5	6.0	53.5
6	8.0	69.5
7	10.0	87.8
8	12.0	103.9
9	14.0	121.5
10	16.0	137.9
11	18.0	150.2
12	20.0	164.2

gradient	X-intercept	Y-intercept	correlation
8.311	2.499	-0.301	0.9993

TEST NO. = 75
FLOW RATE = 2.0
NaOH CONC = 1.0
PRESSURE = 68.7
GAS TRANSMISSION = 1.074E-3

TEST NO. 1 - 22 SCI-MED SILICONE RUBBER

#	X	Y
1	0.0	0.7
2	0.5	0.8
3	2.0	1.3
4	4.0	1.8
5	6.0	2.2
6	8.0	2.5
7	10.0	2.9
8	12.0	3.4
9	14.0	3.6
10	16.0	3.9
11	18.0	4.5
12	20.0	4.8

gradient	X-intercept	Y-intercept	correlation
0.200	0.856	-4.278	0.9965

TEST NO. = 1
FLOW RATE = 2.5
NaOH CONC = 1.0
PRESSURE = 68.8
GAS TRANSMISSION = 2.583E-5

#	X	Y
1	0.0	0.9
2	0.5	1.0
3	2.0	1.3
4	4.0	2.0
5	6.0	2.4
6	8.0	3.0
7	12.0	4.0
8	14.0	4.8
9	16.0	5.3
10	18.0	5.9
11	20.0	6.4

gradient	X-intercept	Y-intercept	correlation
0.279	0.815	-2.919	0.9992

TEST NO. = 3
FLOW RATE = 3.5
NaOH CONC = 1.0
PRESSURE = 68.8
GAS TRANSMISSION = 3.599E-5

#	X	Y
1	0.0	1.3
2	2.0	1.4
3	4.0	2.0
4	6.0	2.5
5	8.0	3.0
6	10.0	3.6
7	12.0	4.1
8	14.0	4.8
9	16.0	5.3
10	18.0	5.9
11	20.0	6.2

gradient	X-intercept	Y-intercept	correlation
0.264	1.005	-3.804	0.9971

TEST NO. = 2
FLOW RATE = 3.0
NaOH CONC = 1.0
PRESSURE = 68.8
GAS TRANSMISSION = 3.407E-5

#	X	Y
1	0.0	1.1
2	2.0	1.4
3	4.0	1.7
4	6.0	2.2
5	8.0	2.7
6	10.0	3.0
7	12.0	3.3
8	16.0	4.5

gradient	X-intercept	Y-intercept	correlation
0.209	0.971	-4.643	0.9942

TEST NO. = 4
FLOW RATE = 4.0
NaOH CONC = 1.0
PRESSURE = 67.7
GAS TRANSMISSION = 2.742E-5

#	X	Y
1	0.0	1.4
2	2.0	1.4
3	4.0	1.9
4	6.0	2.3
5	8.0	2.7
6	10.0	3.1
7	12.0	3.5
8	16.0	4.2
9	20.0	5.1

gradient	X-intercept	Y-intercept	correlation
0.192	1.178	-6.129	0.9965

TEST NO. = 5
FLOW RATE = 4.0
NaOH CONC = 1.0
PRESSURE = 67.7
GAS TRANSMISSION = 2.520E-5

#	X	Y
1	0.0	1.2
2	0.5	1.7
3	4.0	2.1
4	6.0	2.7
5	10.0	3.3
6	12.0	3.7
7	14.0	4.2
8	16.0	4.5
9	18.0	5.2

gradient	X-intercept	Y-intercept	correlation
0.203	1.364	-6.723	0.9943

TEST NO. = 6
FLOW RATE = 4.0
NaOH CONC = 1.0
PRESSURE = 69.0
GAS TRANSMISSION = 2.609E-5

#	X	Y
1	0.0	1.4
2	0.5	1.4
3	2.0	1.7
4	4.0	2.1
5	6.0	2.6
6	10.0	3.2
7	12.0	3.9
8	16.0	4.7
9	18.0	4.8

gradient	X-intercept	Y-intercept	correlation
0.201	1.337	-6.652	0.9965

TEST NO. = 7
FLOW RATE = 4.0
NaOH CONC = 1.0
PRESSURE = 69.0
GAS TRANSMISSION = 2.585E-5

#	X	Y
1	0.0	1.4
2	0.5	1.6
3	4.0	2.5
4	6.0	3.0
5	8.0	3.6
6	10.0	4.3
7	12.0	4.7
8	14.0	5.2
9	16.0	5.9
10	18.0	6.4
11	20.0	6.9

gradient	X-intercept	Y-intercept	correlation
0.276	1.415	-5.126	0.9995

TEST NO. = 8
FLOW RATE = 4.0
NaOH CONC = 1.0
PRESSURE = 69.0
GAS TRANSMISSION = 3.550E-5

#	X	Y
1	0.0	1.2
2	2.0	1.4
3	4.0	1.9
4	6.0	2.2
5	8.0	2.5
6	10.0	3.1
7	12.0	3.4
8	14.0	3.7
9	16.0	4.0
10	18.0	4.5
11	20.0	4.9

gradient	X-intercept	Y-intercept	correlation
0.187	1.114	-5.961	0.9981

TEST NO. = 9
FLOW RATE = 2.0
NaOH CONC = 1.0
PRESSURE = 68.7
GAS TRANSMISSION = 2.414E-5

#	X	Y
1	0.0	1.6
2	2.0	2.1
3	4.0	2.3
4	6.0	2.8
5	8.0	3.2
6	10.0	3.8
7	12.0	4.3
8	14.0	4.8
9	16.0	5.5
10	18.0	5.9
11	20.0	6.5

gradient	X-intercept	Y-intercept	correlation
0.247	1.418	-5.735	0.9966

TEST NO. = 10
FLOW RATE = 3.0
NaOH CONC = 1.0
PRESSURE = 68.7
GAS TRANSMISSION = 3.195E-5

#	X	Y
1	0.0	1.4
2	2.0	1.6
3	4.0	2.1
4	6.0	2.5
5	8.0	2.8
6	12.0	3.9
7	14.0	4.4
8	16.0	4.9
9	18.0	5.3
10	20.0	5.7

gradient	X-intercept	Y-intercept	correlation
0.225	1.205	-5.347	0.9978

TEST NO. = 11
FLOW RATE = 3.5
NaOH CONC = 1.0
PRESSURE = 68.7
GAS TRANSMISSION = 2.913E-5

#	X	Y
1	0.0	0.8
2	2.0	1.7
3	4.0	2.4
4	6.0	2.8
5	8.0	3.7
6	10.0	4.2
7	12.0	4.9
8	14.0	5.3
9	16.0	6.0
10	18.0	6.7
11	20.0	7.1

gradient	X-intercept	Y-intercept	correlation
0.311	1.032	-3.314	0.9980

TEST NO. = 12
FLOW RATE = 4.0
NaOH CONC = 1.0
PRESSURE = 69.0
GAS TRANSMISSION = 4.005E-5

#	X	Y
1	0.0	1.3
2	2.0	1.6
3	4.0	2.1
4	6.0	2.7
5	8.0	3.2
6	10.0	3.6
7	12.0	4.3
8	14.0	4.7
9	16.0	5.4
10	18.0	5.9
11	20.0	6.5

gradient	X-intercept	Y-intercept	correlation
0.265	1.109	-4.192	0.9985

TEST NO. = 13
FLOW RATE = 3.0
NaOH CONC = 1.0
PRESSURE = 69.0
GAS TRANSMISSION = 3.403E-5

#	X	Y
1	0.0	1.5
2	2.0	1.6
3	4.0	1.9
4	6.0	2.4
5	8.0	2.7
6	10.0	3.1
7	12.0	3.5
8	14.0	3.8
9	16.0	4.2
10	18.0	4.6
11	20.0	5.1

gradient	X-intercept	Y-intercept	correlation
0.184	1.286	-6.988	0.9970

TEST NO. = 14
FLOW RATE = 4.0
NaOH CONC = 1.0
PRESSURE = 69.0
GAS TRANSMISSION = 2.368E-5

#	X	Y
1	0.0	0.8
2	2.0	1.5
3	4.0	1.8
4	6.0	2.4
5	8.0	2.8
6	10.0	3.4
7	12.0	4.1
8	14.0	4.6
9	16.0	4.9
10	18.0	5.4
11	20.0	6.2

gradient	X-intercept	Y-intercept	correlation
0.262	0.827	-3.160	0.9979

TEST NO. = 15
FLOW RATE = 2.0
NaOH CONC = 1.0
PRESSURE = 69.0
GAS TRANSMISSION = 3.368E-5

#	X	Y
1	0.0	1.0
2	2.0	1.4
3	4.0	1.7
4	6.0	2.0
5	8.0	2.5
6	10.0	3.0
7	12.0	3.4
8	14.0	3.6
9	16.0	4.1
10	18.0	4.7
11	20.0	5.1

gradient	X-intercept	Y-intercept	correlation
0.205	0.909	-4.444	0.9973

TEST NO. = 16
FLOW RATE = 3.0
NaOH CONC = 1.0
PRESSURE = 69.0
GAS TRANSMISSION = 2.631E-5

#	X	Y
1	0.0	1.0
2	2.0	1.7
3	4.0	2.4
4	6.0	2.8
5	8.0	3.4
6	10.0	3.8
7	12.0	4.5
8	14.0	5.0
9	16.0	5.5
10	18.0	5.8
11	20.0	6.6

gradient	X-intercept	Y-intercept	correlation
0.269	1.173	-4.358	0.9980

TEST NO. = 17
FLOW RATE = 2.0
NaOH CONC = 1.0
PRESSURE = 70.3
GAS TRANSMISSION = 3.397E-5

#	X	Y
1	0.0	1.0
2	2.0	1.7
3	4.0	2.4
4	6.0	2.9
5	8.0	3.5
6	10.0	4.1
7	12.0	4.7
8	14.0	5.2
9	16.0	5.9
10	18.0	6.4
11	20.0	7.1

gradient	X-intercept	Y-intercept	correlation
0.298	1.100	-3.689	0.9996

TEST NO. = 18
FLOW RATE = 3.0
NaOH CONC = 1.0
PRESSURE = 71.3
GAS TRANSMISSION = 3.712E-5

#	X	Y
1	0.0	1.6
2	2.0	1.7
3	4.0	2.0
4	6.0	2.3
5	8.0	2.6
6	10.0	3.3
7	12.0	3.6
8	14.0	3.9
9	16.0	4.4
10	18.0	4.7
11	20.0	5.1

gradient	X-intercept	Y-intercept	correlation
0.186	1.341	-7.213	0.9944

TEST NO. = 19
FLOW RATE = 2.0
NaOH CONC = 1.0
PRESSURE = 71.3
GAS TRANSMISSION = 2.314E-5

#	X	Y
1	0.0	1.8
2	2.0	2.1
3	4.0	2.5
4	6.0	3.2
5	8.0	3.7
6	10.0	4.3
7	12.0	4.9
8	14.0	5.5
9	16.0	6.0
10	18.0	6.7
11	20.0	7.4

gradient	X-intercept	Y-intercept	correlation
0.285	1.523	-5.343	0.9977

TEST NO. = 20
FLOW RATE = 3.0
NaOH CONC = 1.0
PRESSURE = 71.3
GAS TRANSMISSION = 3.548E-5

#	X	Y
1	0.0	1.4
2	2.0	1.8
3	4.0	2.2
4	6.0	2.5
5	8.0	2.8
6	10.0	3.3
7	12.0	3.7
8	14.0	4.1
9	16.0	4.5
10	18.0	4.9
11	20.0	5.7

gradient	X-intercept	Y-intercept	correlation
0.204	1.314	-6.437	0.9957

TEST NO. = 21
FLOW RATE = 2.0
NaOH CONC = 1.0
PRESSURE = 71.3
GAS TRANSMISSION = 2.541E-5

#	X	Y
1	0.0	1.6
2	2.0	2.2
3	4.0	2.5
4	6.0	2.8
5	8.0	3.1
6	10.0	3.6
7	12.0	4.1
8	14.0	4.4
9	16.0	4.7
10	18.0	5.2
11	20.0	5.5

gradient	X-intercept	Y-intercept	correlation
0.192	1.686	-8.771	0.9981

TEST NO. = 22
FLOW RATE = 3.0
NaOH CONC = 1.0
PRESSURE = 71.3
GAS TRANSMISSION = 2.393E-5